



WEST INDIAN JOURNAL OF ENGINEERING

Editorial.....	2
Formalising the National Innovation System in a Developing Country	4
A Case Study for Improving Maintenance Planning of Centrifugal Pumps Using Condition-Based Maintenance	17
Analysis and Development of Innovative Engineering Programmes.....	25
A Review of Caribbean Geothermal Energy Resource Potential	37
An Analysis of the Use of Hydraulic Jet Pumps, Progressive Cavity Pumps and Gas Lift as Suitable Artificial Lift Methods for Heavy Oil Production in East Soldado Reservoirs, Offshore the Southwest Coast of Trinidad	44
Physicochemical and Functional Properties of Starch from Ackee (<i>Blighia sapida</i>) Seeds	54
Investigating the Impact of Deformation on a 3D-printed Antenna in Biomedical Systems	66
Driver Gap Acceptance Behaviour at Roundabouts in Trinidad and Tobago	77
Microwave Drying of West Indian Bay Leaf (<i>Pimenta racemosa</i>)	87
Electrical Engineering and the New SI Definitions	96

Published by:
Faculty of Engineering, The University of the West Indies
St Augustine, Trinidad and Tobago, West Indies

WEST INDIAN JOURNAL OF ENGINEERING

The WIJE Editorial Office

Faculty of Engineering, The University of the West Indies, St Augustine
The Republic of Trinidad and Tobago, West Indies
Tel: (868) 662-2002, ext. 83459; Fax: (868) 662-4414;
E-mail: uwije@sta.uwi.edu
Website: <http://sta.uwi.edu/eng/wije/>

The West Indian Journal of Engineering, WIJE (ISSN 0511-5728) is an international journal which has a focus on the Caribbean region. Since its inception in September 1967, it is published twice yearly by the Faculty of Engineering at The University of the West Indies (UWI) and the Council of Caribbean Engineering Organisations (CCEO) in Trinidad and Tobago. WIJE aims at contributing to the development of viable engineering skills, techniques, management practices and strategies relating to improving the performance of enterprises, community, and the quality of life of human beings at large. Apart from its international focus and insights, WIJE also addresses itself specifically to the Caribbean dimension with regard to identifying and supporting the emerging research areas and promoting various engineering disciplines and their applications in the region.

The Publications and Editorial Board

Professor Edwin I. Ekwue, Chairman (Dean, Faculty of Engineering), *UWI*; E-mail: Edwin.Ekwue@sta.uwi.edu
Professor Boppana V. Chowdary, Vice-Chairman (Deputy Dean, R&PG Affairs), *UWI*; E-mail: Boppana.Chowdary@sta.uwi.edu
Professor Stephan J.G. Gift, Member (Immediate Past Chairman), *UWI*; E-mail: Stephan.Gift@sta.uwi.edu
Professor Kit Fai Pun, Member (Editor), *UWI*; E-mail: KitFai.Pun@sta.uwi.edu
Professor Winston A. Mellowes, Member (Immediate Past Editor), *UWI*; E-mail: wamello@yahoo.com
Dr. Jacqueline Bridge, Member (Mechanical & Manufacturing Engineering), *UWI*; Jacqueline.Bridge@sta.uwi.edu
Dr. Michael Sutherland, Member (Geomatics Engineering and Land Management), *UWI*; E-mail: Michael.Sutherland@sta.uwi.edu
Dr. Fasil Muddeen, Member (Electrical & Computer Engineering), *UWI*; E-mail: Fasil.Muddeen@sta.uwi.edu
Dr. Raffie Hosein, Member (Chemical Engineering), *UWI*; E-mail: Raffie.Hosein@sta.uwi.edu
Dr. Trevor A. Townsend, Member (Civil & Environmental Engineering), *UWI*; E-mail: Trevor.Townsend@sta.uwi.edu

International Editorial Advisory Committee

Professor Andrew K.S. Jardine, *University of Toronto, Toronto, Canada*; E-mail: jardine@mie.utoronto.ca
Professor Andrew Wojtanowicz, *Louisiana State University, Louisiana, USA*; E-mail: awojtan@lsu.edu
Professor Clive E. Davies, *Massey University, Palmerston North, New Zealand*; E-mail: C.Davies@massey.ac.nz
Professor John Yilin Wang, *The Pennsylvania State University, Pennsylvania PA, USA*; E-mail: john.wang@psu.edu
Professor Joseph K. Ssegawa, *University of Botswana, Gaborone, Africa*; E-mail: ssegawaj@mopipi.ub.bw
Professor Marehalli G. Prasad, *Stevens Institute of Technology, Hoboken, New Jersey, USA*; E-mail: mprasad@stevens.edu
Professor Nageswara Rao Posinasetti, *University of Northern Iowa, Cedar Falls IA, USA*; E-mail: Posinasetti.Rao@uni.edu
Professor Prasanta Kumar Dey, *Aston University, Birmingham, UK*; E-mail: p.k.dey@aston.ac.uk
Professor Richard Hobbs, *University of Durham, Nuffield, Durham, U.K.*; E-mail: r.w.hobbs@durham.ac.uk
Professor V.M. Rao Tummala, *Eastern Michigan University, Ypsilanti MI, USA*; E-mail: rao.tummala@emich.edu
Professor Wach Grant, *Dalhousie University, Halifax, Nova Scotia, Canada*; E-mail: Grant.Wach@Dal.Ca
Dr. Albert H.C. Tsang, *The Hong Kong Polytechnic University, Kowloon, Hong Kong, China*; E-mail: albert.tsang@polyu.edu.hk
Dr. Henry Lau, *University of Western Sydney, Parramatta Campus, Sydney, Australia*; E-mail: H.Lau@uws.edu.au
Dr. Jeffery A. Jones, *University of Warwick, Coventry, UK*; E-mail: J.A.Jones@Warwick.ac.uk
Dr. Kiran Tota-Maharaj, *University of the West of England (UWE), Bristol, U.K.*; E-mail: Kiran.Tota-Maharaj@uwe.ac.uk
Dr. Kwai-Sang Chin, *City University of Hong Kong, Kowloon, Hong Kong, China*; E-mail: mekschin@cityu.edu.hk
Dr. Morris Abraham G. Ezra, *Universiti Tunku Abdul Rahman, Kajang, Selangor Malaysia*; E-mail: ezram@utar.edu.my

Editorial Sub-Committee

Professor Kit Fai Pun, Chairman and Editor (Office of Industrial Engineering), *UWI*; E-mail: KitFai.Pun@sta.uwi.edu
Dr. Chris Maharaj, Vice Chair (Mechanical & Manufacturing Engineering), *UWI*; E-mail: Chris.Maharaj@sta.uwi.edu
Mr. Kevon Andrews, Member (Electrical & Computer Engineering), *UWI*; E-mail: Kevon.Andrews@sta.uwi.edu
Ms. Crista Mohammed, Member (Electrical & Computer Engineering), *UWI*; E-mail: Crista.Mohammed@sta.uwi.edu
Mrs. Marlene Fletcher-Cockburn, Member (Outreach Office), *UWI*; E-mail: Marlene.Fletcher-Cockburn@sta.uwi.edu
Mrs. Paula Wellington-John, Member (Systems Laboratory), *UWI*; E-mail: Paula.John@sta.uwi.edu

To order subscriptions or report change of address, simply fill in the required information on the Subscription Order Form provided at the back of the Journal or downloaded from the WIJE website, and/or write to: The Editor-in-Chief, The Editorial Office, West Indian Journal of Engineering, c/o Block #1, Faculty of Engineering, The University of the West Indies, St Augustine, Trinidad and Tobago, West Indies. Fax: (868) 662 4414; Emails: uwije@sta.uwi.edu; KitFai.Pun@sta.uwi.edu

WEST INDIAN JOURNAL OF ENGINEERING



Volume 42 • Number 2
(ISSN 0511-5728) • January 2020

The Editorial Office
West Indian Journal of Engineering
Faculty of Engineering
The University of the West Indies
St Augustine
The Republic of
Trinidad and Tobago
West Indies
Tel: (868) 662-2002, ext. 83459
Fax: (868) 662-4414
E-mails: uwije@sta.uwi.edu;
KitFai.Pun@sta.uwi.edu
Website:
<http://sta.uwi.edu/eng/wije/>

Editor-in-Chief:
Professor Kit Fai Pun

The Publication and Editorial Board of the *West Indian Journal of Engineering*, WIJE (ISSN 0511-5728) shall have exclusive publishing rights of any technical papers and materials submitted, but is not responsible for any statements made or any opinions expressed by the authors. All papers and materials published in this Journal are protected by Copyright. One volume (with 1-2 issues) is published annually in July and/or January in the following year. Annual subscription to the forthcoming Volume (2 Issues): US\$15.00 (Local subscription); and US\$25.00 (By airmail) or equivalent in Trinidad and Tobago Dollars. Orders must be accompanied by payment and sent to The Editorial Office, The West Indian Journal of Engineering, Block 1, Faculty of Engineering, UWI, Trinidad and Tobago. Copyright and Reprint Permissions: Extract from it may be reproduced, with due acknowledgement of their sources, unless otherwise stated. For other copying, reprint, or reproduction permission, write to The Editorial Office, WIJE. All rights reserved. Copyright© 2020 by the Faculty of Engineering, UWI. Printed in Trinidad and Tobago. Postmaster: Send address changes to The Editorial Office, The West Indian Journal of Engineering, Faculty of Engineering, UWI, Trinidad and Tobago, West Indies; Printed in Trinidad and Tobago.

- 2 **Editorial**
- 4 **Formalising the National Innovation System in a Developing Country**
by Shellyanne Wilson, Chris S. Maharaj, and Rean Maharaj
- 17 **A Case Study for Improving Maintenance Planning of Centrifugal Pumps Using Condition-Based Maintenance**
by Chanan S. Syan, Geeta Ramsoobag, Kavisha Mahabir, and Vikash Rajnauth
- 25 **Analysis and Development of Innovative Engineering Programmes**
by Sarim Al-Zubaidy, Andrew Ordys, and Eugene D. Coyle
- 37 **A Review of Caribbean Geothermal Energy Resource Potential**
by Randy Koon Koon, Sheldon Marshall, Dawin Morna, Randy McCallum, and Masaō Ashtine
- 44 **An Analysis of the Use of Hydraulic Jet Pumps, Progressive Cavity Pumps and Gas Lift as Suitable Artificial Lift Methods for Heavy Oil Production in East Soldado Reservoirs, Offshore the Southwest Coast of Trinidad**
by Raffie Hosein, and Amrit S. Balgobin
- 54 **Physicochemical and Functional Properties of Starch from Ackee (*Blighia sapida*) Seeds**
by O'Neil Falloon, Saheeda Mujaffar, and Donna Minott
- 66 **Investigating the Impact of Deformation on a 3D-printed Antenna in Biomedical Systems**
Jeevan Persad and Sean Roche
- 77 **Driver Gap Acceptance Behaviour at Roundabouts in Trinidad and Tobago**
by Khary Leighton Campbell and Trevor A. Townsend
- 87 **Microwave Drying of West Indian Bay Leaf (*Pimenta racemosa*)**
by Saheeda Mujaffar, and Shari Bynoe
- 96 **Electrical Engineering and the New SI Definitions**
by Fasil Muddeen

Editorial

About This Issue

This Volume 42 Number 2 includes ten (10) research/technical articles. The relevance and usefulness of respective articles are summarised below.

S. Wilson, C.S. Maharaj, and R. Maharaj, “Formalising the National Innovation System in a Developing Country”, employed system dynamics to examine the policy initiative and contributed to the formalising a NIS for small developing countries that operate largely in low-technology sectors. A case study approach was adopted, detailing the steps for formalising a NIS in a developing country, the Republic of Trinidad and Tobago (T&T). It was advocated that the design of the system must account for three key elements: namely, the actors, the interactions among the actors and the intended innovation output.

In the article, “A Case Study for Improving Maintenance Planning of Centrifugal Pumps Using CBM”, **C.S. Syan et al.**, investigated the adoption of CBM approach for CP maintenance as compared to the current practices of a leading offshore company in Trinidad and Tobago (T&T). A test programme was simulated, and vibration data for the CPs was utilised to develop the P-F curve for pump failure as a result of faulty bearings. The tests demonstrated the possibility for improved fault classification and data driven maintenance planning with a CBM best practice approach. Future work will investigate the ability of enhanced Artificial Intelligent (AI) techniques to improve the classification accuracies in the face of more complex operational conditions.

S. Al-Zubaidy, A. Ordys, and E.D. Coyle, “Analysis and Development of Innovative Engineering Programmes”, focused on the level of interaction between engineering disciplines, meeting requirements for professional accreditation and meeting requirements for the skilled work-force in the place of implementation. In line with the standards of the UK Engineering Council, the design of curricula had to encompass a number of elements, and demonstrate that they are safeguarding the quality requirements of the professional engineering institutions. In this paper, some metrics are proposed, based on fuzzy logic approach to establish membership functions for measuring interaction between the programmes, and the emphasis of the programmes on particular aspects of engineering learning outcomes.

R. Koon Koon et al., “A Review of Caribbean Geothermal Energy Resource Potential”, presented quantitative findings as to the potential power production, economic and environmental savings through which geothermal energy development can bring to each respective nation in the Caribbean. An estimated 184.49 MW of geothermal capacity can be absorbed into the national energy mix, displacing 855,600 barrels of oil (bbls) importation, resulting in approximately 1.1 million

tonnes of carbon dioxide (tCO₂) emissions being avoided per year. In this paper, an inter-island grid connection approach is presented to tackle large-scale energy projects to attract financial investors in an effort to combat the upfront challenges associated with geothermal energy development.

In the fifth article, “An Analysis of the Use of Hydraulic Jet Pumps, Progressive Cavity Pumps and Gas Lift as Suitable Artificial Lift Methods for Heavy Oil Production in East Soldado Reservoirs, Offshore the Southwest Coast of Trinidad”, **R. Hosein and A.S. Balgobin**, developed models for the currently installed gas lift and PCP configurations and then optimised to determine the best oil lifting capabilities for these two systems. A lift score analysis between PCP pumps and hydraulic jet pumps was also conducted by comparing lifting potential, installation cost and time, rig vs. non-rig intervention for the installation; and ease of operation and optimisation. The results from this analysis indicate that using hydraulic jet pumps would be a more cost-effective oil lift system compared to PCP pumps. This lift score can also be used as a guide to effectively optimise artificial lift systems for other oil wells from the field.

O. Falloon, S. Mujaffar, and D. Minott, “Physicochemical and Functional Properties of Starch from Ackee (*Blighia sapida*) Seeds”, investigated the physicochemical and functional properties of isolated ackee seed starch. Solubility, swelling power, water absorption, oil absorption and extent of syneresis of the starch were measured and hypoglycin content was determined by reversed phase HPLC. Pasting, thermal properties, crystalline pattern, granule morphology and gel texture were determined, and the gelatinised starch used to prepare retrograded resistant starch. Ackee starch had a high setback, high syneresis, produced opaque pastes and formed a hard gel texture. Based on the properties, the starch may be suitable in manufacturing of noodles and to produce retrograded resistant starch and may have applications in fat replacers, dusting/face powders and bioplastics.

J. Persad and S. Rocke, “Investigating the Impact of Deformation on a 3D-printed Antenna in Biomedical Systems”, investigated the Radio frequency (RF) characteristics of a flexible Planar Inverted-F Antenna (PIFA) antenna intended for biomedical applications. Using a traditional PIFA antenna structure on a Nylon substrate, simulations facilitated investigation of the impact of the mechanical deformations on antenna performance, through consideration of the impact of flexibility on the reflection coefficient, transmission frequency and radiation patterns between 700MHz and 4GHz. Results demonstrated good stability on the antennas resonant frequency and physical resilience. This provides valuable insights for those interested in deploying flexible antenna structures for wearable antenna

and RF sensor applications

In the eighth article, “Driver Gap Acceptance Behaviour at Roundabouts in Trinidad and Tobago”, **K.L. Campbell** and **T.A. Townsend**, investigated the gap acceptance behaviour of motorists to determine the critical gap in Trinidad and Tobago (T&T). The estimated critical gaps were compared with values commonly used in the Highway Capacity Manual (HCM), so as to determine the effect on estimated intersection capacity. The results indicated that the critical gap values would differ significantly from the United States (US) default values (as one of the standards adopted by T&T), which therefore would affect the estimated capacity of the roundabouts. It was argued that the published values from the HCM were significantly higher than the values obtained, indicating that the estimated capacities using the default US values would underestimate the existing capacities in T&T.

S. Mujaffar and **S. Bynoe**, “Microwave Drying of West Indian Bay Leaf (*Pimenta racemosa*)”, investigated the effect of microwave power (200, 500, 700 and 1000W) on the drying behaviour of West Indian Bay leaf. The results show the clear potential for microwave drying as a rapid drying method of drying bay leaves. Microwave power level had a significant impact on the drying rates and quality of dried samples. An increase in power level resulted in increased drying rates, with browning and the risk of scorching increasing at 1000W power. Drying at 200W power level was unfavourable in terms of low drying rates and leaf quality. The drying data was successfully analysed through the determination of drying rate constants (k) and moisture diffusivity values (D_{eff}), and the Verma and Jena and Das models best fit the data for leaves dried at 500W and 700W, respectively.

F. Muddeen, “Electrical Engineering and the New SI Definitions”, reviewed the new definitions of Systeme International des Unites or SI system. These new definitions marked a substantial change from the previous ones and would have a considerable impact on the realisation of the various units and in particular the kilogram. Seven of these units directly relate to the units of measure used in Electrical Engineering. In this paper, the author examined how the fundamental units of electrical engineering be realised from the definitions, and also looked into the impact of these changes on the uncertainty of measurement of electrical units and discussed the role of the new Volt, Ohm and Ampere in the realisation of the new kilogram.

On behalf of the Editorial Office, we gratefully acknowledge all authors who have made this special issue possible with their research work. We greatly appreciate the voluntary contributions and unfailing support that our reviewers give to the Journal.

Our reviewer panel is composed of academia, scientists, and practising engineers and professionals from industry and other organisations as listed below:

- **Dr. Abrahams Mwasha**, The University of the West

Indies (UWI), Trinidad & Tobago (T&T)

- **Dr. Albert H.C. Tsang**, Hong Kong Polytechnic University, Hong Kong (HK)
- **Professor Andrew Jupiter**, UWI, T&T
- **Dr. Cavelle Motilal**, Engineer at Government, T&T
- **Mr. Christian Virgil**, College of Science, Technology and Applied Arts of Trinidad and Tobago, T&T
- **Ms. Crista Mohammed**, UWI, T&T
- **Professor Diego Carro-Lopez**, Universidade da Coruna, Spain
- **Dr. Fasil Muddeen**, UWI, T&T
- **Professor Garth A. Myers**, Trinity College, Hartford, Connecticut, USA
- **Dr. Graham A. Ryan**, Seismic Research Centre, UWI, T&T
- **Dr. Graham King**, UWI, T&T
- **Dr. Haydn I. Furlonge**, Brunei National Petroleum Company, T&T
- **Dr. Judith Ephraim**, The Organisation of Eastern Caribbean States, Saint Lucia
- **Mr. Kamel Singh**, IAL Engineering Services Ltd., T&T
- **Professor Kit Fai Pun**, UWI, T&T
- **Mr. Lacey Williams**, Caritrans Limited, T&T
- **Ms Man Yin Rebecca Yiu**, UWI, T&T
- **Dr. Marcia Nathai-Balkissoon**, UWI, T&T
- **Dr. Kameswara Musti**, Namibia University of Science and Technology, Windhoek, Namibia
- **Dr. Paul Aiken**, Faculty of Engineering, UWI, Jamaica
- **Dr. Phibert Morris**, Softcom Limited, T&T
- **Dr. Prince Jeya Lal Lazar**, KCG College of Technology, Chennai, India
- **Dr. Rae Julien Furlonge**, L F Systems Limited, T&T
- **Professor Ramadhansyah Putra Jaya**, Universiti Teknologi Malaysia, Johor, Malaysia
- **Professor Emeritus Richard Dawe**, UWI, T&T
- **Dr. Stephen Giblin**, International Bureau of Weights and Measures, BIPM, UK
- **Dr. Terrence Lalla**, UWI, T&T
- **Dr. Ts. Morris Abraham G. Ezra**, Universiti Tunku Abdul Rahman, Selangor, Malaysia
- **Professor Wach Grant**, Dalhousie University, Halifax, Canada
- **Dr. Wanchai Asvapoositkul**, King Mongkut's University of Technology, Bangkok, Thailand
- **Dr. Winny Routray**, McGill University, Quebec, Canada
- **Dr. Zulfiqar Ali**, College of Engineering, City University of Hong Kong, HK

The views expressed in articles are those of the authors to whom they are credited. This does not necessarily reflect the opinions or policy of the Journal.

KIT FAI PUN, *Editor-in-Chief*

Faculty of Engineering,
The University of the West Indies,
St Augustine, Trinidad and Tobago, West Indies

January 2020

Formalising the National Innovation System in a Developing Country

Shellyanne Wilson^a, Chris S. Maharaj^{b,Ψ}, and Rean Maharaj^c

^aDepartment of Management Studies, The University of the West Indies, St. Augustine, Trinidad and Tobago, West Indies; Email: Shellyanne.Wilson@sta.uwi.edu

^bDepartment of Mechanical and Manufacturing Engineering, The University of the West Indies, St. Augustine, Trinidad and Tobago, West Indies; Email: chris.maharaj@sta.uwi.edu

^cProcess Engineering Department, The University of Trinidad and Tobago, Point Lisas Industrial Estate, Couva, Trinidad and Tobago, West Indies; Email: rean.maharaj@utt.edu.tt

^Ψ Corresponding Author

(Received 11 February 2019; Revised 4 May 2019; Accepted 26 September 2019)

Abstract: Since the introduction of the National Innovation System (NIS) concept, most of the research has focused on innovation capabilities and economic development of developed countries. The paper contributes to the NIS literature for small developing countries that operate largely in low-technology sectors. A case study approach was adopted, detailing the steps for formalising a NIS in a developing country, The Republic of Trinidad and Tobago (T&T). System dynamics is used to examine the policy initiative. For the formalisation of the NIS in T&T, the design of the system must account for all three elements of innovation systems: the actors, the interactions among the actors and the intended innovation output. Policy makers in developing countries must consider their local context when specifying the innovative activity of the NIS. In measuring the success of innovation policies targeting small and medium-sized enterprises (SMEs), financial and non-financial measures should be used.

Keywords: National Innovation System; Developing Country; Economic Diversification; Small Business Innovation

1. Introduction

A nation's competitiveness depends on the capacity of its industry to innovate and upgrade (Porter, 1990). The concept of the National Innovation System (NIS) or National System of Innovation (NSI) has gained prominence as a conceptual framework for analysing technological change, which is viewed as a pillar for the long-term economic development of a nation (Liu, Lu, and Ho, 2014; Lundvall, 2010; Nelson, 1993; Teixeira, 2014). Understanding the linkages amongst institutions and agencies is critical to boosting a country's innovative performance (OECD, 1997). NIS concept benchmarks can be used to measure the innovation capacity and potential of the country (Marx and Brunner, 2013). The NIS concept is highly touted as a mechanism that can enhance a country's overall competitiveness. Not surprisingly, there is burgeoning interest among economists and policy makers in the potential of the NIS to transform the economies of developing countries, with examples of researchers, such as Attia (2015) focussing on African countries and Delvenne and Thoreau (2012) focusing on Latin American countries.

Trinidad and Tobago (T&T) is one such economy, where the establishment of the National Innovation System for Trinidad and Tobago (NISTT) is viewed as a means of achieving economic restructuring. According to the Ministry of Planning and the Economy (2011), the core focus of the NISTT is to facilitate economic

diversification through the promotion of R&D driven innovation. It will support the ideas of individuals and companies. The NISTT will develop and implement a holistic and competitive innovation policy to transform the economy by gradually shifting our economic dependence away from hydrocarbons. This will require the increase in R&D investment to at least 3% of our GDP over the next ten years to generate new products, services and processes. This will improve T&T's Global Competitiveness and Innovation Rank which is a critical indicator of development.

Policy makers, however, face a variety of challenges when they attempt to develop and implement innovation systems. One particular challenge lies in the very conceptualisation of the systems which would be largely informed by examples reported in the NIS literature. But, as researchers such as Varblane, Dyker, and Tamm (2007) warned, attempts to replicate a successful NIS model in another country without making the necessary adaptations for country-specific characteristics would likely lead to failure. A second significant challenge facing policy makers is the identification of the indicators to determine the efficacy of the established national innovation policy (Casanova, Cornelius, and Dutta, 2018). These NIS development and implementation challenges are further pronounced in developing countries. The literature does not offer much guidance, as a review of the literature in this area shows

that research has mainly focused on analysing the NIS in developed countries, with even fewer studies analysing developing countries, such as Korea, Taiwan and Singapore. These developing countries are unique as their policies are relatively aggressive, as they seem to be focussed on catching up with developed countries (Intarakamnerd, Chairatana, and Tangchitpiboon, 2002; Wong, 1999). Even in investigating the appropriateness of a NIS to a developing country, the focus has been on what Intarakamnerd et al. (2002) referred to as ‘learning intensive’, speaking to the country’s ability to not only use and operate technology, but also its ability to acquire and assimilate technology; reverse engineer and upgrade technology; and perform research and technology development. Likewise, Lundvall (2007) notes that research on NIS typically focusses on mature, well-developed innovation systems, largely found in developed countries. There is a dearth of research on developing countries, such as Trinidad and Tobago, that are not learning intensive.

Even further, as highlighted by Golichenko (2016), the NIS literature does not focus explicitly on the entrepreneurs operating as micro or small and medium sized (MSME) enterprises. This limited attention on MSMEs in the NIS literature is a glaring deficit since research has shown that small enterprises innovate differently from large firms. Small enterprises are often plagued by many barriers to innovation; and are less able to dedicate resources to research and development, updating technologies and conducting market research (Todtling and Kaufmann, 2002). As a result of these characteristics, Todtling and Kaufmann (2002) argued that small enterprises can overcome their innovation challenges by relying on external resources and partners, which speaks directly to the interactivity and networks of the NIS concept.

This paper seeks firstly to contribute to our understanding of the nascent stages of the establishment of a NIS in a developing country by exploring T&T as a

case study. Secondly, the paper examines how the interactions among a state agency, a university and a small entrepreneur lead to institutional capacity building as described by Watkins et al. (2015).

The paper proceeds as follows. Section 2 provides an overview of the literature on the NIS approach, and describes specific issues relating to national innovation systems in developing countries. Section 3 presents the research methodology adopted for this study. Section 4 reports on the case study of the formalisation of the NIS in T&T and details a state sponsored innovation promotion initiative. Section 5 presents the results of the innovation promotion initiative. Section 6 discusses the findings. Section 7 concludes the paper.

2. Literature Review

2.1 Overview of National Innovation Systems

The Organisation for Economic Co-operation and Development's (OECD) (1997) report on National Innovation Systems quoted five NIS definitions, shown in Table 1, from early seminal papers on the topic from the 1980s and the 1990s. Even after 20 years since this popular OECD publication, the more recent journal articles often rely on these definitions or on their main premise; which implies that within the research community, there is general acceptance of what is meant by the term ‘national innovation system’.

The information presented within the definitions in Table 1 shows at least three critical elements which are highlighted in Table 2. The first four definitions refer specifically to the actors or institutions that comprise the NIS. In the fifth definition as given by Lundvall (2010) instead refers to ‘elements and relationships’. Secondly, four of the five definitions refer to the relationships among the said actors. Thirdly, all five definitions address the issue of the innovative activity, by highlighting the existence of new knowledge, learning or technologies.

Table 1. Seminal NIS Definitions

NIS Definitions
<i>Freeman (1987) - The network of institutions in the public and private sectors whose activities and interactions initiate, import, modify and diffuse new technologies.”</i>
<i>Lundvall (1992) - The elements and relationships which interact in the production, diffusion and use of new, and economically useful, knowledge ... and are either located within or rooted inside the borders of a nation state.”</i>
<i>Nelson (1993) - A set of institutions whose interactions determine the innovative performance ... of national firms.”</i>
<i>Patel and Pavitt (1994) - The national institutions, their incentive structures and their competencies that determine the rate and direction of technological learning (or the volume and composition of change generating activities) in a country.”</i>
<i>Metcalfe (1997) - A system of interconnected institutions to create, store and transfer the knowledge, skills and artefacts which define new technologies.”</i>

Source: Adapted from OECD (1997)

Table 2. Elements of the Seminal NIS Definitions

NIS Definitions	Actors	Relationships among the Actors	Innovative Activity
Freeman (1987) <i>The network of institutions in the public and private sectors whose activities and interactions initiate, import, modify and diffuse new technologies."</i>	<i>The network of institutions in the public and private sectors</i>	<i>Activities and interactions</i>	<i>Initiate, import, modify and diffuse new technologies."</i>
Lundvall (1992) <i>The elements and relationships which interact in the production, diffusion and use of new, and economically useful, knowledge ... and are either located within or rooted inside the borders of a nation state."</i>	<i>The elements and relationships</i>	<i>Interact</i>	<i>The production, diffusion and use of new, and economically useful, knowledge</i>
Nelson (1993) <i>A set of institutions whose interactions determine the innovative performance ... of national firms."</i>	<i>A set of institutions</i>	<i>Interactions</i>	<i>Innovative performance</i>
Patel and Pavitt (1994) <i>The national institutions, their incentive structures and their competencies, that determine the rate and direction of technological learning (or the volume and composition of change generating activities) in a country."</i>	<i>The national institutions</i>	---	<i>The rate and direction of technological learning (or the volume and composition of change generating activities)</i>
Metcalfe (1997) <i>A system of interconnected institutions to create, store and transfer the knowledge, skills and artefacts which define new technologies."</i>	<i>A system of ... institutions</i>	<i>Interconnected</i>	<i>Create, store and transfer the knowledge, skills and artefacts which define new technologies."</i>

Source: Adapted from OECD (1997)

2.1.1 The Actors in the NIS

There are varying typologies regarding the actors making up the NIS. In one typology, the university, industry and government make up the three actors of the triple helix model (see Figure 1). They interact with each other, contributing to the innovative activity in knowledge-based societies (Etzkowitz and de Mello, 2003). In this model, the university’s role includes conducting research and commercialising research outputs, and also educating and training people; industry’s role is to convert ideas and inventions; while government’s role is to formalise policies and provide funding (Datta and Saad, 2011).

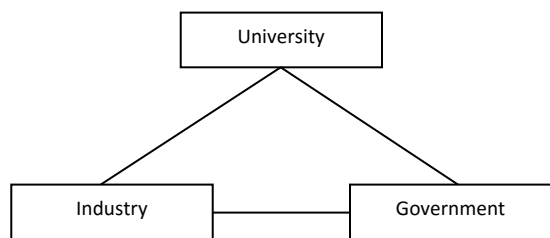


Figure 1. Typology 1 detailing Three NIS Actors

In another typology, authors such as Sakarya (2011) identified six actors comprising the NIS: public and private innovative firms; non-profit public or semi-private research institutions; the scientific system made up of universities and research institutions; supporting and bridge institutions; financing institutions; policy-making, implementing and assessing institutions. The inter-relationship among these factors is shown in Figure 2.

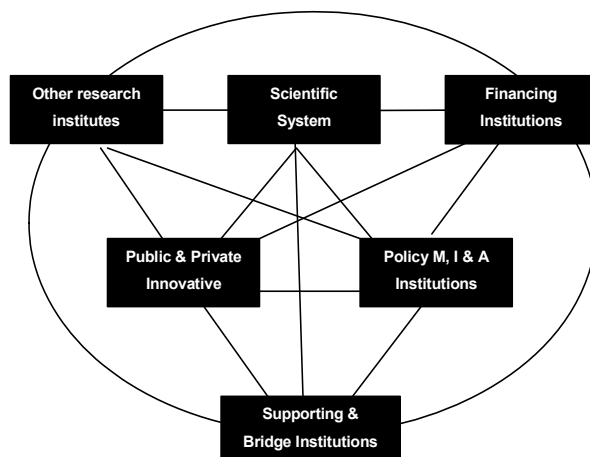


Figure 2. Typology 2 detailing Six (6) NIS Actors

The typology in Figure 2 is also seen in research by Gododze (2016), who described the NIS as a socio-economic system made up of actors, such as companies; research and academic organisations; public administrations; professional mediators; and other formal and informal institutions.

There are both similarities and differences in the narrow and moderate typologies. In terms of the similarities, public and private innovative firms, and the scientific system identified by Sakarya (2011) mirror the industry and university identified in the triple helix model. Likewise, policy making, implementing and assessing institutions identified by Sakarya (2011) bear much similarity to the government actor identified in the triple helix model. With respect to the differences, the research institutions can be viewed as complementary to

the university, whilst recognising that there are several other institutions, not be classified as universities, conducting and disseminating research. The supporting and bridging institutions identified by Sakarya (2011) as institutions that provide services such as laboratory testing and standards setting are important additions, especially as these firms are most often certifying various regulatory dimensions of the innovative products. Lastly in addition to government's financial input in innovation as highlighted in the triple helix model, institutions like venture capital firms also play essential roles in terms of providing the critically required financing for innovation.

A more detailed typology identified by Roos, Fernstrom, and Gupta (2005) reveals 12 NIS 'constituents'. This is shown in Table 3. In this model, the NIS is described as comprising all economic, political and other social institutions involved in innovative activities, specifically universities and research bodies, financial systems, monetary policies and the international organisation of private firms. In the same light, Acs et al. (2017) provided a highly comprehensive view of the actors of the NIS, by identifying scientific and technological institutions, the education, research, apprenticeship, and training system, the financial system, the intellectual property rights system, the tax system, the structure of the industry and labour market, individual and firm level incentives, and other systems.

The model by Roos et al. (2005) offers greater details than the typologies shown in Figures 1 and 2. For instance, the 'government' actor in Typology 1 and the 'policy making, implementing and assessing institutions' in Typology 2 are reflected in constituents 11 and 12, 'Rewards/Incentives' and 'Government Policy, Funding and Procurement Institutions'. Noteworthy distinctions from the Typologies 1 and 2 are the inclusion of the role

of 'People and Culture', 'Public Good' and 'Domestic and International Customers'.

2.1.2 The Relationships among the Actors in the NIS

The relationships among the actors in the NIS concern their interactions with institutions and policies (Liu and White, 2001). These interactions in the NIS have been related to a number of different 'flows' among the actors making up the NIS. These flows include knowledge flows, financial flows, human flows, and regulation flows (Niosi, 2002). Of the four flows identified by Niosi (2002), knowledge flows, referred to as 'the lifeblood of the system' (Golden, Higgins, and Lee, 2003) predominate in the literature. For example, according to OECD (1997), assessing a NIS is based on the measurement of the following types of knowledge flows:

- Joint research activities and other technical collaborations.
- Co-patenting, co-publications and informal linkages.
- Diffusion of knowledge and technologies and diffusion through machinery and equipment.

Financial flows also feature significantly in the NIS literature. For example, Roos et al. (2005) explain Finland's NIS, and detail the range of public and private capital providers that supply funding and financing for research projects, training projects, technology transfer and foreign venture capital funds. Similarly, in describing Sweden's NIS, Roos et al. (2005) identify the agencies and their respective roles in providing seed financing, research and development (R&D) funding, and loans.

Human flows among universities, firms and government laboratories are important in the NIS. Human flows and knowledge flows are highly interrelated, as humans are viewed as the 'bearers of tacit knowledge and know-how' (Niosi, 2002), and knowledge is viewed as being embodied in humans.

Table 3. NIS Constituents Identified by Roos et al. (2005)

	NIS Constituents	Description
1	People and Culture	Education levels; Innovative / Creative; Risk Tolerance; Entrepreneurship; Attitudes to Science and Technology
2	Education	Teaching; Higher Degrees; Tertiary; Workforce Development; Vocational and Educational Training; Primary and Secondary
3	Public and Non-Profit R&D	University, Government R&D; Non-Profit and Private Research
4	Public Good	Health and Medical, Environment; Art and Culture; Defence; Space
5	Linkages	Technology Transfer; Cooperative Research; Incubators; Technology Diffusion; Innovation Awareness; Conferences
6	Clusters	Cluster Networks; MNCs, Large Companies, SMEs; Emerging Exporters; Innovative Companies; R&D Performing Firms; Start-ups / Spinoffs; Industry Bodies; Advisor Services; Investors; Creditors
7	Domestic and International Customers	Leading Customers; Direct Customers; End users / Stakeholders; Government Procurement; International Customers
8	International Links and Infrastructure	R&D and Business Links; Recruit and Retain Companies; Imports / Exports and Infrastructure (Physical and Information)
9	Intellectual Policy	Patents, etc.
10	Risk Finance	Retained Earnings; VC, Debt, Equity, Grants
11	Rewards / Incentives	Tax Rates; R&D breaks; Capital Gain Tax Options
12	Government Policy, Funding and Procurement Institutions	Education Funding Bodies; R&D Funding Bodies; Science, Technology and Innovation Policy Advisory Bodies; Standards; Regulations; Contract Legal System; Fiscal and Tax Policy; Trade / Tariff and Procurement Policies; Federal and Regional Decision-Making Processes

(OECD, 1997). Hence, personnel mobility, where technical personnel move within and between the public and private sector, is one type of flow used to measure and assess NIS (OECD, 1997).

Regulation flows, identified as moving outward from government agencies, typically take the form of policy instruments, and its primary purpose is to stimulate the formation of the innovation system. These policies often relate to factors such as regulations, taxes, financing, competition, and intellectual property that create and enhance innovation opportunities (Metcalfe and Ramlogan, 2008)

2.1.3 Innovative Activity in the NIS

Innovative activity is considered the output of the NIS. There is, however, some debate in the NIS literature relating to how narrowly or how broadly 'innovation' should be defined. As the NIS is viewed as a means of creating and developing a knowledge-based economy, the argument for a narrow definition of innovative activity is based on innovation being the result of 'knowledge-intensive activity', that is 'more science-intensive', 'more technology-intensive' and 'more skills-intensive' (OCED, 1999). According to OCED (1999), innovation in a knowledge-based economy is 'the creative use of various forms of knowledge': technical knowledge, scientific knowledge, and production and engineering knowledge. In this regard, output and input indicators of innovative activity would include metrics such as R&D expenditure, R&D researchers, FDI outflows, high technology exports, technology fees received and registered patents in the US (Singh, 2004).

Those in support of taking a broad view of innovative activity in the NIS often refer to definitions found in mainstream innovation research, where innovation is viewed as the process involved in the search for, discovery, experimentation, development, imitation and adoption of new products, production processes and organisational setups (Dosi, 1988). Whilst acknowledging the inextricable link between the NIS and knowledge-based economy, proponents for the broader view such as Lundvall (2007) note that although there is a bias towards high-technology industries and the science-technology-innovation (STI) mode, there should also be recognition that innovative activity also occurs in low-technology industries and via the doing-using-interacting (DUI) mode of innovation.

2.2 NIS in Developing Economies

Since innovation is viewed as one of the main ways through which both firms and countries can achieve and maintain competitiveness, the premise of the NIS is inextricably linked to economic growth and development. The role of the NIS in developed countries is however quite different from its intended role in developing countries (Feinson, 2003). Whereas for developed countries, the NIS allows for continuing to

develop and enhance competitiveness, for developing countries, the NIS's intended role is much urgent, in that its goal is to provide these countries with a means of 'catching up' with the type of economic independence experienced by the developed countries. For developing countries, objectives of NIS have been identified as poverty reduction and improved income distribution (Attia, 2015), and overall economic health (Bartels et al., 2012).

The NIS literature therefore makes a point of distinguishing between the characteristics of developed countries and developing countries. According to Varblane et al. (2007), the concept of the NIS was based on developed economies, which typically have high income levels, strong knowledge bases, well-functioning market systems, and strong institutional and infrastructural support for innovation. Developing countries, on the other hand, are characterised by being just the opposite in terms of income level, knowledge base, market-structure, and support for innovation. In light of these characteristics the study of the role of the NIS in developing economies has centred largely on the need to build up the indigenous science and technology base (OECD, 1999), bearing in mind related issues such as the path-dependent nature of economic development; degree of technological absorptive capacity; geographic and cultural proximity to leading technology countries; underestimation of the role of public policy in the development of an NIS and potential institutional, social and cultural obstacles to innovation (Intarakamnerd et al., 2002; Varblane et al., 2007).

Of the above stated issues critical to NIS in developing countries, perhaps the most referred to as 'the degree of technological absorptive capacity'. For example, Feinson (2003) reported that '...successful economic and industrial development is intimately linked to a nation's capacity to acquire, absorb and disseminate modern technologies'. In this study, Feinson (2003) stresses that far more than simply acquiring technology, there must also be a 'command' of this technology, where there must be an understanding of 'how' and 'why' the technology works. The ability to learn, both in terms of 'passive learning' and 'active learning' therefore has become a focal point for the development of NIS in developing economies.

3. Research Methodology

This research seeks to contribute to the understanding of the formalisation of NIS in developing countries, and to explore the impact of policy initiatives designed to promote innovation in small companies. For the formalisation aspect, the design of the NIS and the steps taken for its implementation are detailed via the reporting of secondary data. For the policy initiative, an inductive approach is adopted, whereby the research utilises a case study design, set in T&T, to study an innovation promotion initiative that involved multiple

NIS actors. The research question posed is: *Can a small business innovate with the assistance of an innovation program in the absence of a NIS?*

Primary data was collected via interviews with the owners of a small manufacturing company, the case company enrolled in the innovation programme initiative, programme facilitators and administrators; and participant observations of the two assigned mentors. Secondary data was collected via documentation from the case company, state agency and state university; and institutional websites.

Data analysis was achieved via a system dynamics approach, as described by Sterman (2000). To represent the NIS, Stock and Flow Diagrams (SFD) are used, where stocks represent accumulations, and flows represent the rate of change of the accumulations. Causal loops are also used to show the relationships among variables, where a positive or reinforcing loop indicates the change of one variable leading to a change in the same direction for the second variable; while a negative or balancing loop indicates the change in one variable leading to a change in the opposite direction for the second variable. Vensim PLE software was used for the creation of the diagram.

4. Case Study

Trinidad and Tobago, a twin-island republic located in the Caribbean with a population of 1.369 million persons, is described by the World Bank as a high-income non-OECD country, with a 2017 GDP figure of 22.08 billion USD (www.worldbank.org). In 2017, the country’s GDP contributions included 19.6% from the mining and quarrying sector, 19.1% from the manufacturing sector, 6.6% from the financial and insurance industry, and 0.4% from the agriculture, forestry and fishing sector (MoF, 2018).

Because of the country’s heavy dependence on its oil and gas sectors, the need for diversification has been long touted (Khadan and Ruprah, 2016). However, diversification efforts have not resulted in positive results. The formalisation of the NIS in the last decade represents yet another attempt at the country’s diversification efforts.

4.1 Formalisation of the NIS in T&T

The formalisation of the NIS in T&T entailed two main iterative steps, namely, the design of the NIS and the implementation of the NIS.

4.1.1 Design of the NIS

A draft National Innovation System of Trinidad and Tobago (NISTT) was established in the fourth quarter of 2010, with the main aim of diversifying the oil and gas driven economy of T&T, through the combination of investment and innovation. The management of the NISTT falls under a Council of Ministers, led by the Prime Minister, and is made up of eight other

government ministers as shown in Figure 3. Further management support is provided by the Economic Development Board (EDB) and the Council for Innovation and Competitiveness (CIC), whose roles include policy identification and advisory support for short-term economic improvement and longer-term economic strategic management; and consultation with stakeholders.

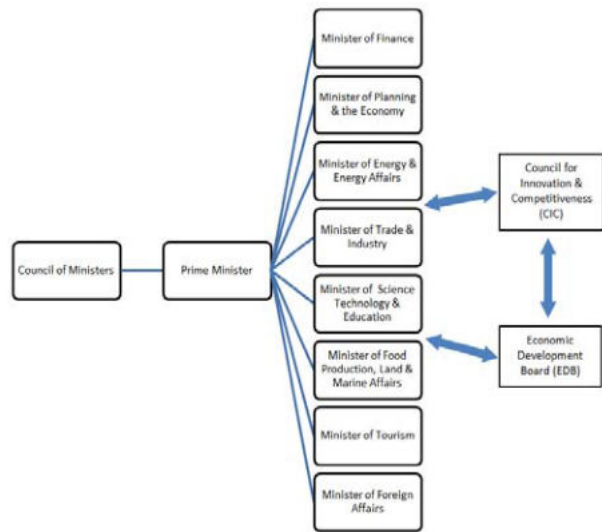


Figure 3. Draft NISTT Management Structure

Moreover, using an Innovation Diamond, the NISTT was designed to comprise 5 main actors (see Figure 4). The learning and R&D systems in the Innovation Diamond include the two state-sponsored universities, The University of Trinidad and Tobago (UTT) and The University of the West Indies (UWI). The planned focus and function of each of the five NISTT actors are detailed below in Table 4.

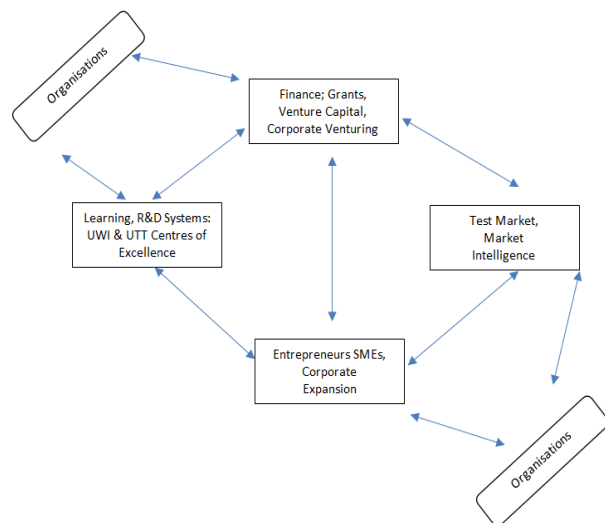


Figure 4. Draft NISTT Innovation Diamond

Table 4. Focus and Function of the NISTT Actors

NISTT Actors	Planned Focus	Function
Learning, R&D Systems: Centre of Excellences	Identification of technologies and sectors for growth and development	<ul style="list-style-type: none"> To create and diffuse knowledge <ul style="list-style-type: none"> To foster technology transfer
Finance; Grants, Venture Capital and Corporate Venturing	Financing for Innovation	<ul style="list-style-type: none"> To incubate new and developing SMEs To provide grants for: <ul style="list-style-type: none"> R&D Proof of concept To provide finance support for innovative SMEs via: <ul style="list-style-type: none"> Venture capital Government Economic Development Bonds
Test Market, Marketing and Market Development	Supporting services	<ul style="list-style-type: none"> To support product / service and process development
Entrepreneurs, SMEs, Corporate Expansion	Cluster formation	<ul style="list-style-type: none"> To provide support for growth of SMEs To facilitate formation of clusters
Organisations	Networking	<ul style="list-style-type: none"> To facilitate overall growth of all actors comprising the NISTT

4.1.2 Implementation of the NISTT

For the implementation of the draft NISTT, two main activities were undertaken. The first activity was a series of five sessions, which was attended by over 800 people. The objective of these sessions was to inform the population of the planned NISTT; to obtain buy-in; to receive feedback about the draft plans for the NISTT; and to brainstorm for economic and social development ideas. The second activity was a foresighting exercise involving experts, who were asked to project 15 to 20 years in the future, to determine the key areas and technologies for potential investment (<http://pesrga.gov.tt/>). The draft NISTT was never implemented. Subsequent to this, a National Innovation Policy was crafted and is currently awaiting governmental approvals.

4.2 Innovation Promotion Initiative for SMEs: A Case Study

4.2.1 Introduction to the Innovation Promotion Initiative: The INSTIL Innovation Programme

In T&T, the Business Development Company (BDC), established in 2002, was formed with the mandate of enterprise development for T&T. Its suite of services included Consultancy Services, Export Certification, Financial Support Services, International Business Promotion Support Services, Trade Assistance, and Training and Business Advisory Services (<http://www.bdc.co.tt>). BDC, alongside contracted innovation management companies, Dolmen, based in Ireland (Dolmen, 2011) and the NEXT Corporation (NEXT Corporation, 2008), designed ‘INSTIL Innovation’ as a 12-month programme for SMEs, with the intended aims of the SMEs introducing new processes to improve their efficiency and productivity, and creating new products and services for local and export markets (BDC, 2011). The INSTIL Innovation programme’s main features included mentorship, workshops, and access to state-supported institutions and programmes. In T&T, companies are defined as in Table 5 (MoEDFA, 2001).

Table 5. Definitions of Firms in T&T

Category	Number of Employees	Assets (TTD) ¹	Sales (TTD)
Micro	< 6	< 250 K	<250 K
Small	6 - 25	250 K – 1,500 K	250 K – 5,000 K
Medium	25 - 50	1,500 K – 5,000 K	5,000 K -10,000 K

¹ \$1TTD = \$0.15 USD

In terms of the mentorship, two mentors were assigned to each SME participating in the programme. Mentors were identified from local universities and other state agencies that provide research and business support. The mentors were required to attend the workshops held by the BDC, NEXT Corporation, and Dolmen; and had the responsibility of guiding and advising the SME’s innovation process. The mentors’ primary purpose was to ensure that outside of the workshops, continuous communication and feedback were maintained with the SMEs with respect to ensuring that innovation targets were on their way to being met.

The second feature comprised six workshops. The timing and focus of each workshop are given in Figure 5.

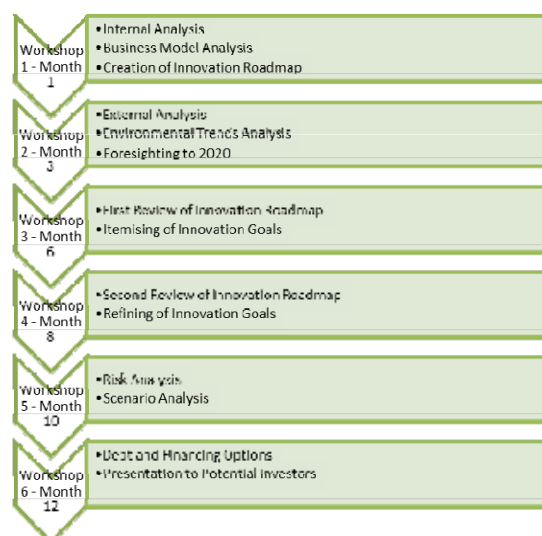


Figure 5. INSTIL Innovation Workshops Timing and Focus

In terms of access to state supported institutions and programmes, the BDC facilitated access to a number of state institutions and programmes aimed at providing the SMEs participating in the INSTIL programme technical, financial, and business support. For example, the University of Trinidad and Tobago (UTT) was poised to provide technical support. The Metal Industry Company Ltd (MIC) was engaged to provide engineering services (MIC, 2011). The Research and Development Facility (RDF) administered by the BDC, offered research and development funding, via a grant, where the maximum funding for a single company project is TT\$500,000 (BDC, 2008).

4.2.2 Introduction to the Case Company – Alpha Manufacturing Limited

Alpha Manufacturing Limited (name changed for anonymity purposes) is a small manufacturing business, with fewer than 15 employees, that makes soft-case products for the musical instrument industry. Alpha was very successful for the first 12 years of operation in terms of sales, both locally and internationally. However, with the global financial downturn in 2008, revenues dropped sharply and the company struggled to maintain its financial commitments and obligations. The owners had very little formal business training but they had innovative ideas for the storage, transport and protection of musical instruments. Their competitive advantage was identified as quality and responsiveness. In their 14th year of operation Alpha joined the INSTIL Innovation program.

4.2.3 Alpha Manufacturing Limited and the INSTIL Innovation Programme

1) The Mentors

The two mentors assigned to Alpha Manufacturing Limited were two faculty members of the Design and Manufacturing section of a state-funded university, The University of Trinidad and Tobago (UTT, 2011a). Of major relevance to the INSTIL Innovation programme was The Industrial Innovation, Entrepreneurship, and Management (IEM) 1-year Master of Science (MSc) programme. The IEM programme was developed through a partnership established with the Institute for Manufacturing at The University of Cambridge. Students in this programme undertake a series of interconnected modules. Modules comprise a two-week teaching period followed by a project for which students are located in an industry/manufacturing plant to solve a real problem (UTT, 2011b). The intent was for the IEM students to be assigned to Alpha during the relevant modules during the course of the INSTIL programme.

2) The Workshops

At the launch of the INSTIL Innovation programme, an innovation scorecard evaluation was done for Alpha. This scorecard rated Alpha and its owners with regards

to awareness and practice of innovation and associated strategies.

Workshop 1: Alpha's vision was to be the largest manufacturer of cases for a particular musical instrument, by providing high quality products through efficient production processes. Objectives were to actively pursue and capture new markets, to extend the company product line and quality, and to put in place adequate and reliable machinery. Alpha expected to achieve goals that were spread over a 12-month time frame. These goals included:

- Three new products which could be brought to market in three, six, and nine months, respectively.
- A new manufacturing process in 12 months.
- A new brand in two months.
- Communications improvement including promotions, advertisements, and website restructuring.

Workshop 2: The external analysis considered trends that would impact Alpha's business, which included rising energy prices, a global aging population and on-line shopping. Based on these trends, Alpha was challenged to think about the trends leading up to the year 2020 and the changes that would be required to their existing business model and value chain.

Workshop 3: The first review of the innovation roadmap identified a number of challenges to Alpha's innovation roadmap, where the major concern was the company's limited resources to simultaneously run the business and execute the innovation goals. The itemised innovation goals were:

- An increase in one-to-one marketing with two to three days a week dedicated to this activity. To achieve this goal, expedited training and restructuring of staff and Alpha, respectively, were required.
- A new layout plan for Alpha's premises as the existing one was not optimised for production and customer walk-ins.
- Sourcing of items for new product development, name and product rebranding, and website revamping.

Workshop 4: Alpha's progress was discussed and documented as follows:

- The one-to-one marketing of two to three days per week was not achieved due to time constraints. However, due to expedited training of staff, a one-to-one marketing push of two days per week was achieved.
- The new layout plan for Alpha's premises was still in the brainstorming stages. However, workflow processes were formally documented to aid in the new layout plan.

- Product rebranding was achieved with Alpha placing labels on their products for the first time.
- A new product name was established that was short and memorable.
- Marketing brochures were developed.
- Discussions were initiated with website developers for website rebranding. For on-line sale transactions, the intent was to utilise the BDC's website portal as the BDC have developed a facility to assist with this.
- New product development was also achieved with Alpha sourcing new materials for their cases and formally establishing different product lines that relate to different pricing strategies.

The roadmap to Month 12 was refined as follows:

- Continuing the training of staff to allow the leadership to focus on one-to-one marketing.
- Increasing manufacturing capabilities by considering outsourcing of certain aspects of manufacture, and also identifying bottlenecks in production with the aim of improvements.
- Finalising prices of new product lines.
- Finishing website development so that the new one is clear in communication, usable, and supports customer customisation of case components.

Workshop 5: The Business as Usual (BAU) scenario was determined to be a risk in itself as the wants and needs of a customer continue to change with time. The risk in innovation for Alpha was identified as:

- Customer/market (determining the unmet needs),
- Financial (loans required to support the innovation process),
- Opportunity (which product/service ideas to focus on),
- Income (loss of income during the innovation process),
- Country (security, stability, cultural stigma with respect to innovation),
- People (trusting others), and
- Event (predictable and unpredictable changes in the business playing field).

The BAU and Innovative Business Financial scenarios were identified for Alpha. From this, a risk management plan for Alpha's new products was generated.

Workshop 6: This workshop brought an end to the programme and discussed funding issues and the presentation of business innovation plans to potential financiers. Additionally, goals for Yr. 4 were established as was done in the first workshop. Alpha's new goals included:

- Hard case commissioning and production.
- Increase in sales of existing products by 15%.

- Introduction of outsourced accessories with the overall intent of becoming a 'one-stop shop' for the musical instrument.
- Continued R&D into new products that can satisfy unmet needs in the musical industry.

Alpha accessed the following institutions and programmes:

- Technical support of the UTT through the IIEM programme for product development, name and product rebranding, and website revamping.
- Research and development grant funding through the RDF of the BDC for product development, where as a small business, Alpha contributed 30% and the RDF contributed 70%.
- Engineering services of MIC for new product development to determine a new material and novel fabrication techniques for manufacture of hard carry cases.

5. Results of the INSTIL Innovation Programme

The analysis centres on the development of a simulation model, as described by Sterman (2000). The model is represented by the conceptual design of the INSTIL programme. The programme was designed to facilitate product and process innovation training for SMEs, to be achieved via the six innovation workshops and the mentorship programme, and, by extension, access to state agencies and programmes. This combination was expected to encourage a culture of innovation in the INSTIL participant companies, evidenced by the introduction of new products and new processes, that would ultimately lead to increased company performance, and overall improved SME performance.

INSTIL Innovation was an initiative of the BDC, a state agency financed by public funds. The workshops provided formal training for both product and process innovation, which was expected to lead to increased rates of innovation by the INSTIL company participants. The mentorship element, evidenced by the mentorship meetings, provided business support, where the frequency of meetings depended on the INSTIL participant's need for support. The business support provided by the mentor was expected to contribute to the decisions and actions by the INSTIL participant, which were then expected to lead to increased rates of innovation. The mentors were selected from a wide pool of candidates, inclusive of university faculty. The university faculty members were expected to not only lend business and technical expertise, but also to facilitate the INSTIL company participants' usage of and access to university facilities.

Product innovation was expected to lead to increased product offerings to the customers, increasing overall product attractiveness, therefore leading to increased sales. Similarly, process innovation was

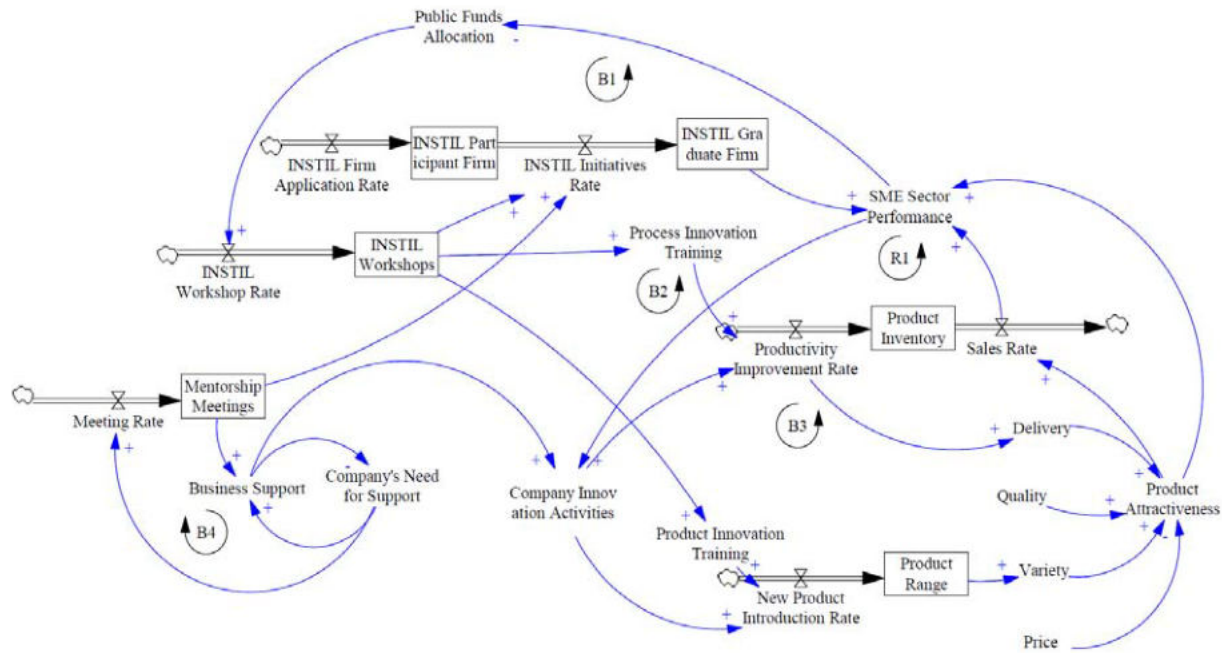


Figure 6. Conceptual System Dynamics Model of the INSTIL Programme

Table 6. Description of Selected Feedback Loops

Feedback Loop	Description
B1	This balancing loop shows the premise of the INSTIL programme, where public funds are utilised to run the INSTIL workshops, to produce INSTIL graduate firms. These graduate firms will increase overall SME performance, and hence, public funds allocated to this INSTIL programme will be reduced.
B2	This balancing loop focuses on the process innovation training. This training leads to increased product attractiveness, which positively impacts sales rate and SME performance. The higher SME performance will lead to a reduction in public funds allocated to the programme.
B3	This balancing loop is similar to the B2 loop, but with the the focus being on product innovation training. This training leads to increased product attractiveness, which positively impacts sales rate and SME performance. The higher SME performance will lead to a reduction in public funds allocated to the programme.
B4	This balancing loop considers the role of the mentors in providing business support. As the need for business support increases, the meeting rate increases, and provides increased business support, which in turn decreases the need for business support.
R1	This reinforcing loop considers the company’s innovation activities, which have a positive impact on product attractiveness and sales rate and SME performance. Increased SME performance will have a positive impact on the company’s innovation activities

expected to lead to increased productivity, and then increase product inventory. Increased product inventory should have led to the company’s ability to better meet delivery requirements, thus, increasing product attractiveness, and increased sales rate. Figure 6 shows the resultant model for the INSTIL programme, and Table 6 provides a description of selected feedback loops.

6. Discussion

The discussion firstly explores the issue of the formalisation of the NISTT, and then considers Alpha in the INSTIL Innovation programme. The nascent stages of the NISTT indicated that the main actors found in mature NISs are present in T&T. However, the existence of the individual actors does not automatically lead to a

functioning NIS. In examining the implementation of the NISTT, there was no evidence of measures put in place to develop and strengthen the relationships among the NIS actors. With the literature identifying these interactions as ‘flows’, with ‘knowledge flows’ described as ‘the lifeblood of the NIS’ (Golden, Higgins, and Lee, 2003), the absence of concrete steps to develop these relationships could be viewed as a major shortcoming in the implementation of the NISTT.

Similarly, the implementation of NISTT never specified the type of NIS innovative activity that would be the desired output. So, while the NISTT specifies the Centres of Excellence with a planned focus of identifying technologies and sectors for growth and development, the business landscape of T&T is characterised by low-technology industries. Moreover,

the indigenous science and technology base, degree of technological absorptive capacity, and potential institutional, social and cultural obstacles to innovation needed to be carefully considered to implement a well-functioning NIS.

These observations about the NISTT reflect the findings of the study conducted by Guinet (2014) who analysed T&T's National Innovation Ecosystem. It was found that the main types of institutions and actors typically found in more mature systems are present, but they are too small, lack maturity and engagement and are incoherent with respect to the strong inner dynamics of a functioning innovation system. Moreover, Guinet (2014) found that the local National Innovation Ecosystem lacks sufficient public and private investment in research and development and innovation, collaboration between academia and industry, governance arrangements, innovation readiness of the private sector firms.

The INSTIL Innovation programme brought together the main elements of the NIS. The actors included private SMEs, universities, supporting institutions, financing institutions, and the policy-making, implementing and assessing institutions. In addition to the actors, the INSTIL Innovation programme was designed to facilitate and encourage the interactions of the actors via knowledge flows, financial flows and regulation flows. Lastly, the INSTIL Innovation programme clearly specified the innovative activity that was the expected output. In essence, therefore, the INSTIL Innovation programme is a microcosm of an innovation system in terms of its design and intent.

The success of the INSTIL Innovation programme, however, was not easily discerned. On the one hand, Alpha, a small manufacturing company with a desire to innovate, was able to benefit from formalised training, which resulted in new production processes, new products, and new marketing strategies. Alpha was able to access services from the UTT, MIC, and the BDC for these innovations. However, on the other hand, the financial impact of the programme, in the case of Alpha, was not overwhelming.

Alpha's revenue compared to T&T's manufacturing GDP is given in Figure 7, noting that the company's entry into the INSTIL Innovation Programme began in Year 2. The company's revenue appears to track GDP, with both peaking in Year 5. With respect to Alpha's profit compared to revenue, Figure 8 reveals a higher profit margin on Year 4 and the years prior. Part of the reason for Alpha's reduction in profit outlays was due to investment in the innovation process and some of the outlays in meeting the INSTIL Innovation programme goals.

Again, the results of the case study mirror the existing literature. As a small enterprise Alpha does not have the resources to commit to a well-defined innovation strategy. The resource limitations include human resource as the management of the company is heavily involved in day-to-day operations, as well as

financial resources to pursue research and development and market research, as described by Todtling and Kaufmann (2002). Without the external resources provided by the INSTIL programme, Alpha would not have been able to overcome many of the challenges of new product development, process and market innovation.

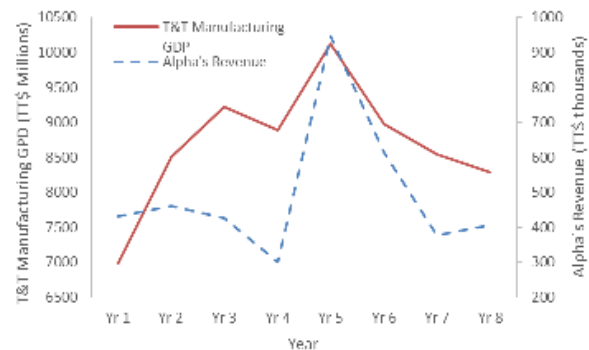


Figure 7. T&T's Manufacturing GDP compared to Alpha's revenue

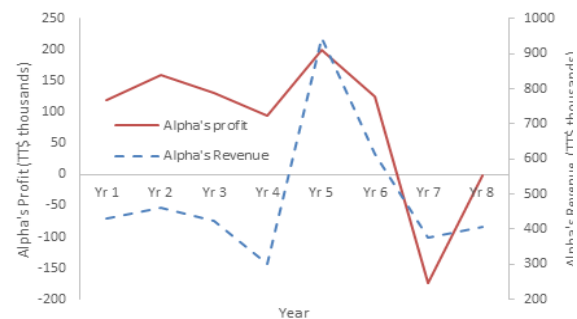


Figure 8. Alpha's profit compared to revenue

7. Conclusions

The paper examines the formalisation of the National Innovation System of T&T and efficacy of a state-led innovation promotion initiative. The examination of the NISTT showed that in designing a National Innovation System, policy makers must not only consider the actors making up the system, but they must also carefully craft mechanisms for the interactions among the actors to ensure there are knowledge, financial, human and regulation flows. Without these interactions, the NIS will not be a well-functioning system. Additionally, policy makers need also consider the historical, current and future contexts of a country in specifying the intended outcomes of the NIS. Without considering a country's context, despite efforts of pulling together the necessary NIS actors, the system will be unable to produce the intended output.

The examination of the INSTIL Innovation programme showed that even when programmes are well-designed, reflecting all elements of a NIS, success,

at least in the short term, and measured in financial terms, is not guaranteed. For SMEs operating in developing countries (such as T&T) that engage in low-technology sectors, external support is invaluable. While financial measures of success would be a key indicator of the efficacy of innovation policy, payback periods may be lengthy, and so, non-financial measures of success could be useful in the short-term.

Acknowledgements:

The authors wish to acknowledge the participants of the Instil Innovation programme, including the workshop facilitators, mentors and business participants. Specifically, we would like to thank Sean McNulty, Ian Ivey, Tricia Ramoutar Soo-Han, Michelle Britto, and Meghnath Gosein.

References:

- Acs, Z., Audretsch, D., Lehmann, E., and Licht, G. (2017). "National systems of innovation", *The Journal of Technology Transfer*, Vol.42, No.5, 997-1008.
- Attia, A. (2015), "National innovation systems in developing countries: Barriers to university-industry collaboration in Egypt", *The International Journal of Technology Management and Sustainable Development*, Vol.14, No.2, 113-124.
- Bartels, F., Hinrich, V., Lederer, S., and Bachtrog, C. (2012), "Determinants of national innovation systems: Policy implications for developing countries", *Innovation: Management: Policy and Practice*, Vol.14, No.1, 2-18.
- BDC (2008), *The Research and Development Facility (RDF)*, Business Development Company Limited, Retrieved May 19, 2011, from BDC Business Solutions: <http://www.bdc.co.tt/bbs?page=57>
- BDC (2011), *BDC Instil Innovation*, Business Development Company Ltd. Retrieved May 19, 2011, from <http://www.bdc.co.tt/bbs.php?page=115>
- Casanova, L., Cornelius, P., and Dutta, S. (2018), "Global innovation competitiveness: How emerging economies compare", In: *Financing Entrepreneurship and Innovation in Emerging Markets*, Academic Press, London, p. 31-67
- Datta, S., and Saad, M. (2011), "University and innovation systems: The case of India", *Science and Public Policy*, Vol.38, No. 1, pp.7-17.
- Delvenne, P., and Thoreau, F. (2012), "Beyond the 'Charmed Circle' of OECD: New directions for studies of national innovation systems", *Minerva: A Review of Science, Learning and Policy*, Vol.50, pp.205-219.
- Dolmen (2011), *Dolmen Innovation and Design Consultants*, Retrieved May 19, 2011, from Welcome: <http://www.dolmen.ie/home.htm>
- Dosi, G. (1988), "Sources, procedures, and microeconomic effects of innovation", *Journal of Economic Literature*, Vol. 26, No.3, pp.1120-1171.
- Etzkowitz, H., and de Mello, J. (2003), "The rise of the triple helix culture", *International Journal of Technology Management and Sustainable Development*, Vol.2, No.3, pp.159-171.
- Feinson, S. (2003), *National Innovation Systems: Overview and Country Cases*, Rockefeller Foundation, New York
- Gogodze, J. (2016), "Mechanisms and functions within a national innovation system", *Journal of Technology Management and Innovation*, Vol.11, No.4, pp.12-21.
- Golden, W., Higgins, E., and Lee, S. (2003), "National innovation systems and entrepreneurship", Retrieved July 8, 2011, from Centre for Innovation and Structural Change (CISC) Working Paper No.8. Galway, National University of Ireland, Ireland, www.nuigalway.ie
- Golichenko, O. (2016), "The national innovation system: From concept to research methodology", *Problems of Economic Transition*, Vol.58, No.5, pp.463-481.
- Guinet, J. (2014), *Assessment of the National Innovation Ecosystem of Trinidad and Tobago: Final Report*, IADB, Washington, DC
- Intarakamnerd, P., Chairatana, P., and Tangchitpiboon, T. (2002), "National innovation system in less successful developing countries: The case of Thailand", *Research Policy*, Vol.31, Nos.8-9, pp.1445-1457.
- Khadan, J., and Ruprah, I. (2016), "Diversification in Trinidad and Tobago: Waiting for Godot?" October, Retrieved from <https://publications.iadb.org/en/publication/12562/diversification-trinidad-and-tobago-waiting-godot>
- Liu, J., Lu, W., and Ho, M. (2014), "National characteristics: Innovation systems from the process efficiency perspective", *R&D Management*, Vol.45, No.4, pp.317-338.
- Liu, X., and White, S. (2001), "Comparing innovation systems: A framework and application to China's transitional context", *Research Policy*, Vol.30, pp.1091-1114.
- Lundvall, B.-A. (2007), "National innovation systems: Analytical concept and development tool", *Industry and Innovation*, Vol.14, No.1, pp.95-119.
- Marx, C., and Brunner, C. (2013), "Analysing and improving the national innovation system of highly developed countries: The case of Switzerland", *Technological Forecasting and Social Change*, Vol.80, No.6, pp.1035-1049
- MDCum (2011), *Business Solutions and Beyond*, Retrieved May 19, 2011, from <http://www.mdc-um.com/index.html>
- Metcalf, S., and Ramlogan, R. (2008), "Innovation systems and the competitive process in developing economies", *The Quarterly Review of Economics and Finance*, Vol.48, pp.433-446.
- MIC (2011), *Engineering Services*, Metal Industry Company Limited, Retrieved May 19, 2011, from <http://www.mic.co.tt/home/engineering/engineering-services.html>
- MoEDFA (2001), *Enterprise Development Policy and Strategic Plan for Trinidad and Tobago 2001-2005: Forging a Competitive Economy Through Partnership*, Ministry of Enterprise Development and Foreign Affairs, Retrieved from http://www.sice.oas.org/ctyindex/TTO/INDPolicy_e.pdf
- MoF (2018), *Review of the Economy 2018*, Retrieved from <https://www.finance.gov.tt/wp-content/uploads/2018/10/Review-Of-The-Economy-2018.pdf>
- Ministry of Planning and the Economy (2011), Ministry of Planning and the Economy, Retrieved July 8, 2011, from <http://pesrga.gov.tt/>
- Next Corporation (2008), *NEXT*, Retrieved May 19, 2011, from http://www.nextcorporation.net/who_we_are
- Niosi, J. (2002), "National systems of innovations are 'X-efficient' (and X-effective). Why some are slow learners", *Research Policy*, Vol.31, pp.291-302.
- OECD (1997), *National Innovation Systems*, Organisation for Economic Co-operation and Development, Paris
- OECD (1999), *Managing National Innovation Systems*, Organisation for Economic Co-operation and Development, Paris
- Porter, M. (1990), "The competitive advantage of nations", *Harvard Business Review*, March - April, pp.73-93.
- Roos, G., Fernstrom, L., and Gupta, O. (2005), *National Innovation Systems: Finland, Sweden and Australia. Compared Learnings for Australia*, Intellectual Capital Serviced Ltd., London
- Sakarya, A. (2011), "Institutions' and initiatives' role in Turkey's national innovation system", *International Business and Economics Research Journal*, Vol.10, pp.29-39.

- Singh, L. (2004), "Globalisation, national innovation systems and response of public policy", *International Journal of Technology Management and Sustainable Development*, Vol.3, No.3, pp.215-231.
- Sterman, J. (2000), *Business Dynamics: Systems Thinking and Modeling for a Complex World*, McGraw-Hill, Boston
- Teixeira, A. (2014), "Evolution, roots and influence of the literature on national systems of innovation: A bibliometric account", *Cambridge Journal of Economics*, Vol.38, No.1, pp.181-214.
- Todtling, F., and Kaufmann, A. (2002), "SMEs in regional innovation systems and the role of innovation support: The case of Upper Austria", *Journal of Technology Transfer*, Vol.27, No.1, pp.15-26.
- UTT (2011a), *Design and Manufacturing*, The University of Trinidad and Tobago, Retrieved May 19, 2011, from <http://u.tt/index.php?design=1>
- UTT (2011b). IEM programme, The University of Trinidad and Tobago, Retrieved May 19, 2011, from http://u.tt/index.php?design=1&page_key=595
- Varblane, U., Dyker, D., and Tamm, D. (2007), "How to improve the national innovation systems of catching-up economies?" *TRAMES*, Vol.11 (61/56), No.2, pp.106-123.
- Varblane, U., Dyker, D., Tamm, D., and Von Tunzelmann, N. (2007), "Can the national innovation systems of the new EU Member States be improved?" *Post-communist Economies*, Vol.19, No.4, pp.399-416
- Watkins, A., Papaioannou, T., Mugwagwa, J., and Kale, D. (2015), "National innovation systems and the intermediary role of industry associations in building institutional capacities for innovation in developing countries: A critical review of the literature", *Research Policy*, Vol.44, No.8, pp.1407-1418.

Authors' Biographical Notes:

Shellyanne Wilson is Lecturer of the Department of Management Studies at The University of the West Indies (UWI), Trinidad and Tobago. Dr. Wilson is a graduate of The UWI, where she read for

a B.Sc. in Chemistry and Management, and a M.Sc. in Production Management. She completed her PhD at the Institute for Manufacturing (IfM), Cambridge University, in Manufacturing Strategy. Her research interests include operations strategy, competitiveness and value chain analysis. In the Department of Management Studies, she lectures Production and Operations Management, Operations Planning and Control, Supply Chain Management and Business Strategy and Policy. Prior to joining academia, Dr. Wilson worked in the manufacturing sector in areas of Quality Management and Manufacturing Management.

Chris S. Maharaj is Senior Lecturer in the Department of Mechanical and Manufacturing Engineering at The University of the West Indies (UWI). He holds BSc and MSc qualifications in Mechanical Engineering and Engineering Management respectively from the UWI. He started his career as a Mechanical Engineer in Condition Monitoring and Inspection, working in the industry. He later went on to pursue his PhD at Imperial College London in Mechanical Engineering. His present teaching and research interests are in alternative use of waste materials, mechanical design optimisation, failure analysis, component life assessment, asset management, innovation management, and enhancing student motivation.

Rean Maharaj holds a Bachelors (B.Sc.) Degree in Chemistry, specialising in Analytical Chemistry at The University of the West Indies (UWI), St. Augustine, a Masters of Philosophy (M.Phil.) degree in the field of Applied Physical Chemistry (UWI) and a PhD. Degree in Process and Utilities Engineering from The University of Trinidad and Tobago (UTT). After starting his career as an application chemist in industry and serving as a Forensic Analyst for many years, Dr. Maharaj is currently an Associate Professor in Process Engineering at UTT. His research interest is mainly based in the applied chemistry/materials science area including cement and asphalt technology.

■

A Case Study for Improving Maintenance Planning of Centrifugal Pumps Using Condition-Based Maintenance

Chanan S. Syan ^{a,Ψ}, Geeta Ramssoobag ^b, Kavisha Mahabir ^c and Vikash Rajnauth ^d

^{a,b,c} Department of Mechanical and Manufacturing Engineering, The University of the West Indies, St. Augustine Campus, Trinidad and Tobago, West Indies;

^a Email: Chanan.Syan@sta.uwi.edu

^b Email: geeta.ramssoobag@my.uwi.edu

^c Email: kavisha.mahabir@my.uwi.edu

^d KVR Energy Limited, Samaroo Road East, Aranguez, Trinidad and Tobago, West Indies;
Email: Vikash.rajnauth@kvrel.com

^Ψ Corresponding Author

(Received 25 February 2019; Revised 30 July 2019; Accepted 27 September 2019)

Abstract: Centrifugal Pumps (CPs) are one of the most widely used industrial assets globally. Condition-based maintenance (CBM) is one of the maintenance strategies applied for monitoring the operational conditions of CPs. Use of CBM has resulted in improvements in CP performance. However, CBM practice for maintenance planning is suboptimal. This work presents a case study which utilises a CBM approach for monitoring CPs as part of a safety critical Fire Water System aboard an Offshore Production Platform. A CBM approach for CP maintenance was researched, and the best practice identified. This was compared to the practices of the offshore company, and the deficiencies in application and data collection observed. A test programme was simulated which would represent the company's operations. Subsequently, data was collected to assess the ability of CBM to identify various failures for CPs. Vibration data for the CPs was utilised to develop the P-F curve for pump failure as a result of faulty bearings. The results were then used for establishing potential inspection activities. In cases where a single fault was studied, a classification accuracy of 100% was attained from the test programme. In cases where multiple faults were studied, a classification accuracy of 67% was attained. An overall classification accuracy of 76.5% was attained. Furthermore, a P-F interval of five months was obtained, implying that inspections should be performed every two or three months for the bearings compared with the current schedule of one month. The tests demonstrated the possibility for improved fault classification and data driven maintenance planning when a CBM best practice approach is implemented effectively. Future work will investigate the ability of enhanced Artificial Intelligent (AI) techniques to improve the classification accuracies in the face of more complex operational conditions.

Keywords: Condition Based Maintenance, Centrifugal Pumps, Vibration Analysis, Failure Modes, Effects and Criticality Analysis, PF Curve

1. Introduction

Centrifugal Pumps (CPs) are one of the most widely utilised assets in a number of industries globally. These assets are ubiquitous in safety critical systems such as those in Offshore Oil and Gas Production which require high levels of availability and reliability (Farokhzad, 2013; Mahalik et al., 2012). With technological advancements, Condition-based maintenance (CBM) has emerged as the most prevalent type of Preventive Maintenance (PM) activity that is used for CPs. In CBM sensor technology is utilised to monitor the condition of assets and thereby detect failures before they occur (Moubray, 1997; Beebe, 2004). CBM monitors a measured asset condition to determine deterioration with time. It therefore allows for appropriate action to avoid catastrophic failures of CPs. One popular measureable quantity monitored includes equipment vibration.

Vibration Analysis (VA) is a CBM technique which measures the vibration levels present with various forms of asset condition (Farokhzad, 2013). The ability of VA to detect a wide range of equipment faults makes it perhaps the most versatile and thus widely applied CBM technique for monitoring most rotational equipment.

While the application of CBM techniques to dynamic equipment is no new task, many organisations fail to realise the full benefits since the execution of a complete CBM best practice approach is not always adhered to. There have also been reports of defects such as cracks, gear defects and other bearing and electrical faults remaining undetected (Mahalik et al., 2012). Current VA methods are unable to detect all incipient faults and therefore there is still a need for frequent Corrective Maintenance (CM) (Albraik et al., 2012). Furthermore, Albraik et al. (2012) and Wang and Gao

(2006) have indicated that vibration levels are dependent on operating parameters such as flow rate, suction pressure, output pressure, drive power, speed, bearing temperatures and others. In some cases, if the CBM approach is not implemented with a full understanding of these conditions, faults may be misclassified. These factors have resulted in the need to investigate whether a properly implemented CBM best practice approach can improve the fault diagnosis and aid maintenance of CPs.

The aim of this work is to improve the maintenance planning process as applied to CPs by utilising a CBM approach. To achieve the aim, the steps of a CBM best practice approach were determined through extensive literature research and compared to industry practice at a collaborating offshore oil and gas company. The gaps in the implementation process were noted and an experimental study was designed and applied to evaluate the extent to which the best practice approach, if properly implemented, can lead to efficient and effective maintenance planning.

In Section 2, this paper describes the common maintenance practices that are employed for CPs. This includes the currently applied CBM approach and the techniques which are applied. Section 3 outlines the research process including the data collection design and analysis process. Section 4 presents and discusses the results. Finally, Section 5 provides concluding remarks and suggestions for future work.

2. Maintenance Practices for CPs

Generally, there are two (2) main types of maintenance which are performed for CPs. These include Corrective Maintenance performed when unplanned breakdown occurs, and Preventive Maintenance. With the dawn of the Information and Communications Technology (ICT) tools, CBM inspections, a type of PM, have become ubiquitous the globe. Figure 1 illustrates the percentage of CBM techniques which have been applied for monitoring pump operation including lubrication analysis, infrared thermography and motor current signature analysis.

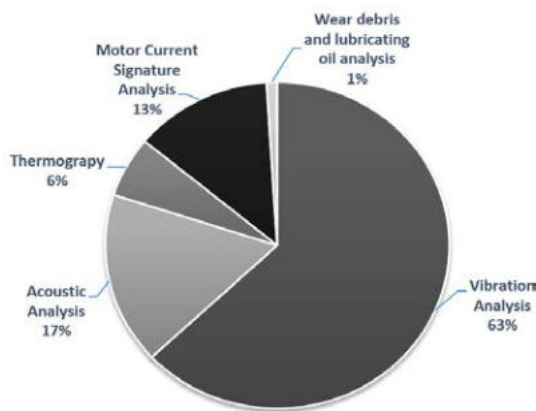


Figure 1. CBM Technologies Applied to CPs in the Literature

However, the most common type of CBM techniques includes Vibration Analysis (VA) (Beebe, 2004). This is because VA is the most versatile of all techniques and it is adaptively useful at detecting a wide range of common failure modes that exist not only for CPs but for most rotating equipment.

2.1 CBM Approach for Fault Diagnosis of CPs

The basic CBM approach is conceived as having three (3) steps including Data Acquisition, Data Processing and Maintenance Decision-Making (Jardine et al., 2006). Over the years, authors have proposed variations to this general approach. Lebold et al. (2003) suggest seven modules in the CBM process including, Data Acquisition, Data Manipulation, Condition Monitoring, Health Assessment, Prognostics, Automatic Decision Reasoning and Human Computer Interface. Mohsen (2017) suggests four phases of CBM including Data Processing, Diagnostics, Prognostics and Maintenance Operation.

In addition to these commonly applied stages, past applications of the CBM approach to CPs included proper definitions of the system boundaries and significant failure analysis. Failure analysis is a critical aspect prior to implementation of CBM since an abundance of different failures are possible for these assets. Although this is the case, researchers and practitioners note that only some of these failures are highly critical and require significant focus over others. Thus, failure analysis is essential in determining these failures prior to testing the capability of CBM for detection of incipient failures (Selvakumar and Natarajan, 2015).

2.2 Failure Analysis of CPs

CPs consist of many interconnected components which may fail in numerous ways. Each failure can impact the overall operation of the CP differently. Since maintenance resources must be wisely distributed, a Failure Mode, Effects and Criticality Analysis (FMECA) aids in scoping the analysis to only include those failure modes which are most critical for pump operation. Several common failure mechanisms are noted in the literature as pertaining to CPs, including unbalance, misalignment, bearing failure, seal failure, resonance, bent shaft, blade pass, vane pass vibrations, and cavitation (Mahmood, 2011).

Due to the large number of possible failure modes it is impractical to use Condition Monitoring for testing the ability of CBM to detect all of them. In such cases, techniques have been proposed and utilised which have aided practitioners and the authors to narrow these failure modes to a much more manageable level that can be tested. The Pareto technique (20/80) is an effective method which can be used to narrow the scope of these failure modes. It involves of acquiring data for each failure mode such as frequency of occurrence and

plotting this data (in descending order) against the failure modes. The method is hinged on the basis of 20% of critical failure modes which causes 80% of failures. The modes can then be extracted from the graphical plot. Bejger et al. (2012) and Sheikh et al. (2002) have illustrated the use of Pareto for such analyses.

Besides, several commonly applied techniques have been identified for performing failure analysis. These included FMECA, Root Cause Analysis (RCA), Fault Tree Analysis (FTA), the 5 Whys and Weibull Analysis. The most popularly applied technique was found to be FMECA, appearing in 55% of all reviewed studies.

FMECA has the capability of examining potential failure modes as well as functional failures within a system and is able to analyse failure causes and effects, identify potential weak critical areas, and propose improvement measures (Ravi Sankar and Bantwal, 2001). FMECAs can be both qualitative and quantitative in its examination of systems faults. Quantitative methods make use of a Risk Priority Number (RPN) which is the product of the occurrence, severity, and detection of the failure mode. Mathematically, this is formulated as:

$$\text{RPN} = \text{Occurrence} \times \text{Severity} \times \text{Detection} \quad (1)$$

Singh and Suhane (2015) applied a quantitative FMECA to examine CP faults and found the most critical (highest RPN) components to be bearings, the mechanical seal, impeller and shaft. Utilisation of the FMECA allowed for improvements in the selection of maintenance strategies. This meant an increase in the overall profit by 36.74% per year through reductions in labor, downtime and part replacement costs.

3. Research Framework

This research was guided by the framework as developed and illustrated in Figure 2. It was developed subsequent to the literature research which identified the necessary factors such as data requirements and the application setting for CBM. The framework begins by determining and comparing the steps in CBM that are proposed as part of best practice as opposed to that implemented in the industry. This would indicate shortfalls in the maintenance system.

3.1 Determine the Steps in a CBM Best Practice Approach

The literature research involved the initial gathering of publications within eighteen (18) years from 2000-2018. These included sources such as journal and conference papers, PhD and Masters theses and books. The publication search focused on finding work related to the following title areas 'Vibration Analysis', 'Centrifugal Pumps', and 'CBM Approach'.

A total of fifty (50) publications were eventually obtained which were found to be relevant and current. Over the years, several authors have proposed variations to the CBM approach that have been applied to

maintenance of CPs as discussed in Section 2. In this study, the analysis of reviewed literature has highlighted the following steps in the CBM approach that have been adopted for testing and validation purposes. These are depicted in Figure 3.

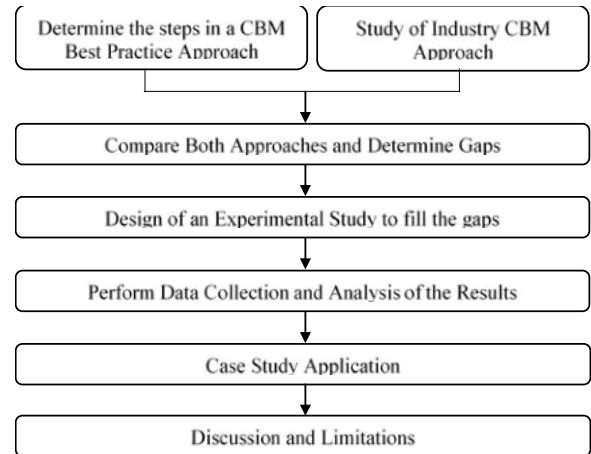


Figure 2. The Research Process Stages Adopted in this Study

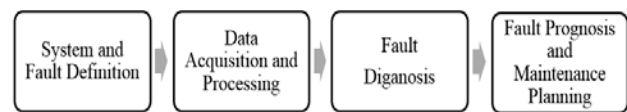


Figure 3. Steps of the CBM Approach

3.1.1 System and Fault Definition

The first step in the approach involves System and Fault Definition. One application of CPs involves utilisation as part of a Fire Water Pump (FWP) safety system for most offshore platforms (Pettersen, 2009). In this work, the operation of CPs in this context was investigated since pump vibration data from an offshore oil and gas company will also be available for further collection and analysis purposes. The typical CP system comprises of a driver-driven series configuration with the driver unit being an electric motor in most cases which drives the pump. Failures of either the driver or driven units result in complete failure and downtime of the entire system and thus the boundaries that were assigned for the current study include both the motor and pump units.

As mentioned in the literature research, it is often impractical to test and examine the effectiveness of CBM for detection of all potential failure modes of CPs because of their abundance. Thus, in step two, techniques were used to determine the most critical failure modes for the current study. The first included a Pareto 20/80 as identified in literature to be useful when identifying the few most critical failure modes which contribute to 80% of the failures. The Offshore Reliability Data Handbook (OREDA, 2002) lists a total

of 16 critical failure modes for CPs as spurious stop, external leakage-process medium, overheating, vibration, external leakage-utility medium, low output, breakdown, parameter deviation, high output, other, structural deficiency, noise, internal leakage, failure to start on demand, failure to stop on demand and erratic output. These were utilised in the Pareto Analysis to identify the most critical failure modes. Subsequently, to effectively rank the criticality of these failures modes and identify faults which should be the focus of experimental testing, a quantitative FMECA technique was implemented. Figure 3 illustrates the process of Failure Analysis used. It illustrates the scoping of all failures for CPs down to 5 CP faults with the highest RPN values.

3.1.2 Data Acquisition and Processing

Collection of the right data types is of paramount importance for such an application, since the ability of CBM to monitor faults with sufficient time before failure depends on the nature of the data collected. The selection of appropriate data collection instrumentation, allocation of data collection points and directions are all critical decisions for this stage.

3.1.3 Fault Diagnosis

In this study, time and frequency signal analysis was performed on the raw data to aid in detection of the faults. A classification accuracy performance metric was calculated and utilised to determine the accuracy of CBM for fault detection. This metric is estimated only to illustrate the effectiveness of the current detection methods with respect to all the faults considered.

3.1.4 Fault Prognosis and Maintenance Planning

The P-F interval curve as defined in literature was constructed using a combination of theoretical and practical data. The data obtained from the P-F interval curve aids in planning inspection intervals for the asset.

3.2 Study of Industry CBM Approach

The literature research was conducted alongside the study of CP operation aboard an Offshore Production platform utilised as part of a fire water safety system. In the industry however, it was found that while the infrastructure for CBM implementation is in place, not all the stages of a CBM Best Practice are followed. Instead CBM is used simply to indicate that CP components are approaching an alarm limit of wear and degradation. Such alarm limits are typically established by experienced personnel over time who were able to identify marginal vibration levels beyond which failure was imminent.

3.3 Compare Both Approaches and Determine Gaps

Subsequent to understanding the approaches proposed as 'Best Practice', and those used in the industry, both were

compared and analysed to identify areas for improvement. These are:

- Since CBM was not employed in the initial stages of CP operation, initial baseline data is missing for certain components.
- The failure vibration frequencies for certain components are missing, and as such faults in such cases remain undetected until it is too late.
- While data were used to create alarm limits which dictate repair or replacement points for CP components, they are not used further for fault prognosis and maintenance planning.

3.4 Design of an Experimental Study to close the gaps

An experimental procedure was subsequently designed for appropriate data to be collected and for validation of the best practice approach. The factors which influenced the experimental test size are listed in Table 1. Other factors which did not affect the number of experiments conducted but were considered for each test includes the number of lines, resolution, frequency span and window type.

Table 1. The Controlled Parameters in the Experiments

Parameters	Designed Values
Operating speeds	25Hz, 40Hz and 55Hz
Measurement/Transducer location	Vertical, Horizontal, Axial
Number of Experimental Trials/ test	3

The testing procedure was performed in two phases. The first phase tested the capability of the CBM approach to detect a single fault at a point in time. The system was set up in five (5) different configurations each consisting of a single fault. Each faulted setting was labelled as unknown faults 1-5. The second phase tested the ability of the CBM approach to detect multiple failures within the system which is not uncommon in the industry. The system was set up in three different configurations with each consisting of multiple faults. In addition, a baseline test for the system as it exists in 'good working condition' was also included in the procedure.

This resulted in a total of nine (including one baseline setting and eight faulted settings) settings of the system for which data were collected. Considering the factors of operating speed, measurement directions and number of replications, the total number of trials conducted to collect data was calculated as:

$$3 \text{ replications} \times 3 \text{ measurement directions} \times 3 \text{ operating speeds} \times 9 \text{ experiments} = 243 \text{ tests.}$$

3.5 Perform Data Collection and Analyze the Results

To collect data for testing s, an experimental test rig namely the Machinery Fault Simulator (MFS) was utilised. For this experimental apparatus set-up (to be similar to a practical pump set-up in industry),

modifications were made to the MFS system. For the purpose of this investigation, the accelerometer was mounted via a magnet at the horizontal and vertical locations on the bearing centerline to sense vibrations from radial forces. In the case of vibrations from axially-directed forces, the accelerometer was placed in the axial direction. The VibExpert II Data Analyser was utilised to collect data from the test rig and transmit to the PC. OMNITREND software was utilised for the data collection process (Pruftechnik, 2017).

3.6 Case Study Application

The procedure was subsequently applied to establish the PF curve for a practical case study. Data were obtained from a collaborating company for motor bearings in two (2) firewater pumps A and B, where pump A is the stand-by pump that remains inactive unless otherwise switched on. This type of inspection used vibration analysis techniques to measure the RMS velocity of motors A and B over a period of time. The operating speed of the pump was recorded as 3,500 rpm. Using practical RMS velocity data for the inspection of motor bearings experimental RMS velocity data via the MFS system, the P-F curve was plotted to determine the point of potential failure (P) and hence the P-F interval.

The results were gathered and analysed to assess the effectiveness of the CBM approach for fault classification.

4. Results and Findings

4.1 Failure Analysis

From the Pareto analysis, the most severe and frequent failure modes (refer to Figure 4) were found to be vibration, overheating, external leakage-process medium, failure to start on demand and spurious stops. Consequently, these five failure modes were further analysed in a FMECA. From the FMECA, most critical causes of failure are misalignment, imbalance, defective bearings, cavitation and mechanical looseness.

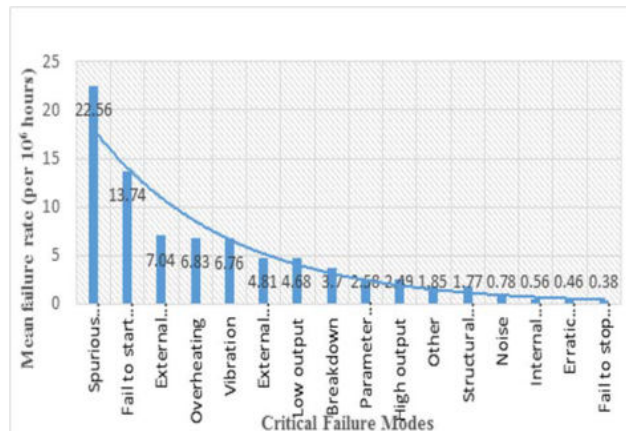


Figure 4. Pareto plot for CP Failure Modes

4.2 Singular Fault Testing

The vibration spectrum obtained from measurements in three perpendicular directions at each operating speed were obtained and then analysed. Key frequencies for faults pertaining to bearing and gearbox failures were calculated, and their presence was used as indication of specific types of fault in the system.

Figures 5 and 6 show some of these results. For an operating speed of 25Hz, the vibration spectrum in Figure 5 shows high axial vibration at 1X, 2X and 3X, indicating angular misalignment. At higher operating speeds, the machine tended to produce stronger vibrations. This is also the case when the system operates at 40 Hz and 55 Hz. The spectrum showed a high increase the RMS velocity from 4.88 mm/s to 5.64 mm/s at 1X followed by a small 2X and 3X peak.

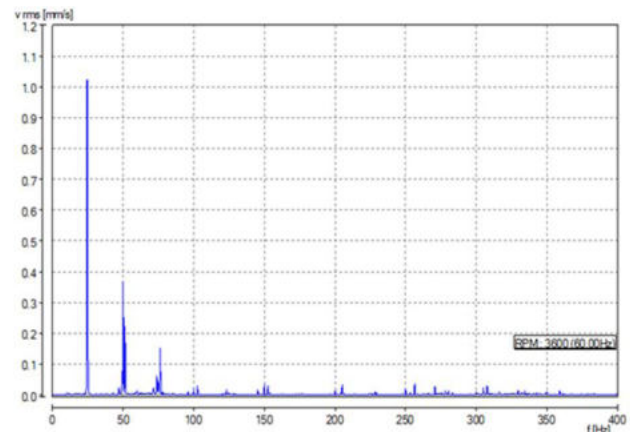


Figure 5. Vibration Spectrum in the Axial Direction at an Operating Speed of 25Hz Depicting the Presence of Angular Misalignment in the Motor

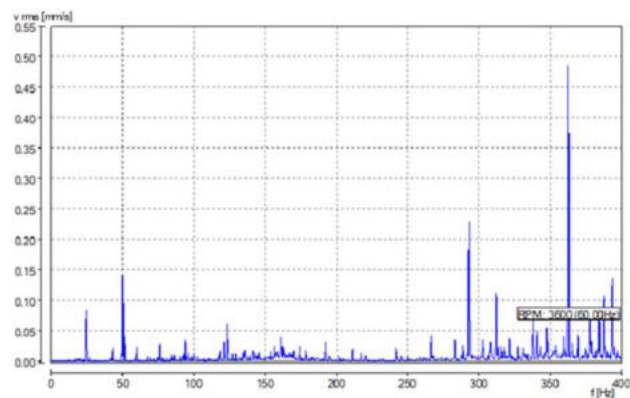


Figure 6. Vibration spectrum for the vertical direction at an operating speed of 25Hz depicting the presence of inner and outer race bearing defect with respect to the motor

The vibration spectrum for vertical measurements at an operating speed of 25Hz shows the inner race defect frequency (BPFI) and its multiples, as well as the four times the outer race defect frequency (BPFO) (See

Figure 6). This indicates a bearing defect with respect to the inner and outer races of the bearing. At an operating speed of 40Hz, the defective rolling element frequency (BSF) and its multiples are visible on the vibration spectrum in the radial directions. The defective rolling element frequency and its multiples are also visible in the vibration spectrum for the radial directions at an operating speed of 55 Hz.

Phase 1 of the testing and validation investigated singularly tested faults. Table 2 lists the results for these tests. Root Mean Square (RMS) velocities and Fast Fourier Transform (FFT) analysis were utilised to diagnose the faults. The Table lists the predicted and true faults allowing for comparison. The results show a total classification accuracy of 100% for this phase of testing.

Table 2. Results Obtained for Phase 1 of the Testing and Validation for Singular Faults

Fault #	Predicted Fault(s)	True Fault(s)
1	Inner race bearing defect with respect to motor	Inner race bearing defect with respect to motor
2	Angular misalignment of shaft	Angular misalignment of shaft
3	Defective rolling element bearings (motor)	Defective rolling element bearings (motor)
4	Cavitation in pump	Cavitation in pump
4	Unbalanced motor	Unbalanced motor
5	Bowed rotor which may have been caused by a broken rotor bar	Broken rotor bar in motor

Classification Accuracy: 100%

4.3 Multiple Fault Testing

The second phase of tests involved combinations of up to four (4) faults within a single run. The classification accuracy attained was 67%. The results are shown in Table 3.

Table 3. Results Obtained from Combinational Fault Testing

Fault #	Predicted Fault(s)	True Fault(s)
6	Bowed rotor which may have been caused by a broken rotor bar	Broken rotor bar in motor
	Unable to Detect Fault	Misalignment between pump and motor
7	Base plate of pump loose	Base plate of pump loose
	Cavitation in pump	Cavitation in pump
	Defective rolling element bearings (motor)	Defective rolling element bearings (motor)
	Unable to Detect Fault	Misalignment between pump and motor
8	Unable to Detect Fault	Defective blade fan in motor
	Cavitation in pump	Cavitation in pump
	Unbalanced motor	Unbalanced motor
	Unable to Detect Fault	Defective blade fan in motor
	Base plate of pump loose	Base plate of pump loose

Classification Accuracy: 76.5 %

It is noted although that misalignment and defective blade fans were the two faults that were undetected in cases where others within the combination were found. From both phases 1 and 2 of testing, the final overall classification accuracy was 76.5%.

4.4 P-F Interval Determination

One of the key steps subsequent to fault diagnosis is utilising the machine condition covariate data to aid in fault prognosis and maintenance planning efforts. To illustrate that this was possible, vibration condition data were collected from the organisation for the CPs operation for a period of twelve (12) months. The operational speed provided was 3,500 RPM.

To develop the P-F curve required, the baseline and fault condition readings would be required. Since vibration analysis began on the CP system only subsequent to a few years of pump operation, precise vibration readings with respect to the ‘Good Operating Condition’ were not stored. Data records of vibration readings were not specified for a ‘roller element bearing failure condition’. To obtain this data for the P-F curve, the MFS was set up to operate at 3,500 RPM (the same running speed as the CPs in the industry) and the vibration condition readings observed under ‘good working condition’ and ‘a roller element bearing faulted condition’. These readings were plotted on P-F curve shown in Figure 7.

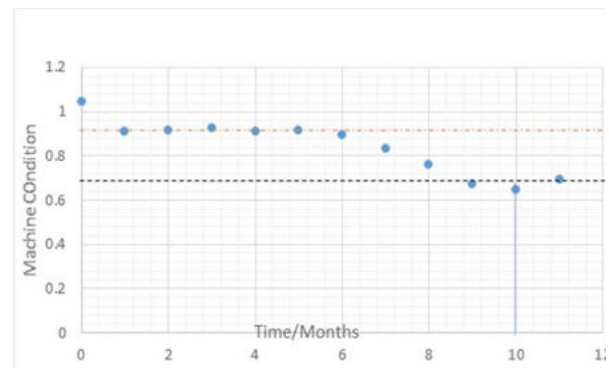


Figure 7. The PF Curve for Motor A

The theoretical baseline and failure condition readings were superimposed on the trending data obtained from the organisation. The baseline conditions and faulted conditions were obtained from the experimental study as well as projected baseline and machine fault conditions for the company. Although these values were close, there were slight differences as shown in Figure 7.

These differences can be attributable to the difference in operating conditions, since the MFS produced values in a relatively controlled environment as opposed to the industrial setting. The motor-pump system used at the company had different specifications and capacity and the operating environment itself was different. The

general baseline readings observed from the company data was found to be 1.1 mm/s. This is 0.14 mm/s greater than 0.96 mm/s found from the experimental study.

The machine fault condition for a roller element bearing fault from the organisation data was found to be 1.55 mm/s, while 1.44 mm/s was obtained from the theoretical tests. With the general curve plotted, it was noted that the deterioration condition for the roller element faulted bearings began at 1.12 mm/s. This was taken as the potential failure point P and thus the P-F interval calculated as 5 months. This implies that from this potential failure point P, the company can then plan maintenance inspections to a suitable interval to avoid corrective maintenance on the bearing.

As a rule of thumb the inspection interval is utilised as half or one-third of the P-F interval in some cases (e.g., Blann, (2013), and Moubray (1997)). The results illustrate that the organisation should perform inspections on the bearings every two or three months. Currently, inspections are done on a monthly basis. Considering the cost of inspections, there could be a potential cost savings..

5. Conclusions

The benefits of applying a CBM Best Practice approach have been well reported in the literature. Although this is the case, many companies fail to realise these benefits due to improper application of the approach. This study sought to investigate improvements in fault diagnosis and maintenance planning when a CBM approach is applied to CPs. Initially, the steps in the best practice approach were identified from the literature, and compared with that applied to a set of CPs used in the fire water system aboard an offshore production platform. Subsequently, the gaps were found, and an experimental procedure designed and implemented to fill these gaps and illustrate the applicability and benefits of applying the approach in full.

Although the CBM data was collected by the organisation, it is not always analysed in a manner which would facilitate efficient fault diagnosis and maintenance planning. The experimental tests produced data which would aid fault diagnosis capabilities for prognostic decisions of CPs.

A fault classification accuracy (FCA) of 100% was obtained for fault diagnosis of singular faults, 67% for multiple combinations of faults and an overall Classification Accuracy of 76.5%. In addition, the P-F curve for the FWP motor was obtained from which a PF interval of 6 months was attained. This could potentially be utilised to plan maintenance activities for the motor. It should be noted that the classification accuracy is based on the number of trials undertaken in this study which were three (3) trials per failure for this work.

The work performed has introduced several key innovative contributions:

1. The use of two failure analysis techniques including a Pareto technique and a FMECA for determination of the most prevalent failure modes and ranking the criticality of those faults. Although the failure analysis technique has been applied extensively in the past, the combination of Pareto and FMECA proved to appropriately scope the large numbers of failures and allow for focusing of the experimental testing procedure whilst maintaining the effectiveness of the CBM approach.
2. The approach was tested using two phases. The second phase incorporated multiple combinations of faults which allowed for a much more realistic representation of the work conducted.
3. The approach has uniquely combined both the theoretical data and practically collected industry data to plot the PF interval curve which can aid the company in planning maintenance in a much more evidence-based manner.
4. While the current method represents a pragmatic approach towards P-F interval estimation, the method is best suited for cases where the uncertainty in the P-F interval of failures is negligible. It should be noted that alternative methods such as the use of Proportional Hazards Modeling (PHM) in combination with covariate data and Delay-Time models could be utilised when this uncertainty cannot be ignored.

The use of other vibration analysis techniques such as phase analysis and orbital analysis could potentially increase the classification accuracy from 76.5 % significantly. As a result, future work could investigate 1) the use of a combination of vibration techniques in fault diagnosis of other types of pumps, turbines or generators, 2) the use of oil and acoustic analysis in pump maintenance, and 3) the vibration and flow in cavitation in pumps.

References:

- Albraik, A., Althobiani, F., Gu, F., and Ball, A. (2012), "Diagnosis of centrifugal pump faults using vibration methods", *Journal of Physics: Conference Series*, Vol. 364, No. 1, pp. 012139.
- Beebe, R.S. (2004), *Predictive Maintenance of Pumps Using Condition Monitoring*, Elsevier
- Bejger, A., Ski, S.B., and Ska, K.G. (2012), "Application of the Pareto analysis for the description of faults and failures of marine medium power engines with self-ignition", *Seizure - European Journal of Epilepsy*, Vol.1, No.2, pp.3.
- Farokhzad, S. (2013), "Vibration based fault detection of centrifugal pump by fast fourier transform and adaptive neuro-fuzzy inference system", *Journal of Mechanical Engineering and Technology*, Vol.1, No.3, pp.82-87.
- Jardine, A.K.S, Lin, D. and Banjevic, D. (2006), "A review on machinery diagnostics and prognostics implementing condition-based maintenance", *Mechanical Systems and Signal Processing*, Vol.20, No.7, pp.1483-1510.
- Lebold, M., Reichard, K., and Boylan, D. (2003), "Utilising DCOM in an open system architecture framework for machinery monitoring and diagnostics", *Proceedings of IEEE Aerospace*

- Conference, Big Sky, MT USA, March, DOI: 10.1109/AERO.2003.1235237.
- Mahalik, N., Dastidar, S.G. and Mohanty, A.R. (2012), "Fault detection in a centrifugal pump using vibration and motor current signature analysis", *International Journal of Automation and Control*, Vol.6, No.3/4, pp. 261-276.
- Mahmood, S.T. (2011), *Use of Vibrations Analysis Technique in Condition Based Maintenance*, Master's Thesis (unpublished), Royal Institute of Technology, Sweden.
- Mohsen, A. (2017), *Condition Based Maintenance*, Thesis (unpublished), Future University, Egypt.
- Moubray, J. (1997), *Reliability-centered Maintenance*, Industrial Press Inc.
- Oreda (2002), *Oreda Reliability Data Handbook*, DNV, Oslo, Norway.
- Pettersen, M.N. (2009), *Reliability Analysis of Fire Water Systems on Offshore Installations*, Institutt for matematiske fag.
- Pruftechnik. (2017). "OMNITREND" available at: https://www.pruftechnik.com/products/condition-monitoring-systems/condition-monitoring-software/omnitrend.html?adtype=Allg_Moni&addate=20160831&gclid=Cj0KCQjwuLPnBRDjARIsACDzGL3MqC27FCnjq5Y0gt5ATkUiqpsDGxPlvm4SqiFnRiXIYmIe8D5zuAUaAjUvEALw_wcB. Accessed on February 1st 2016.
- Ravi Sankar, N., and Prabhu, B.S. (2001), "Modified approach for prioritisation of failures in a system failure mode and effects analysis", *International Journal of Quality and Reliability Management*, Vol.18, No.3, pp.324-336.
- Selvakumar, J., and Natarajan, K. (2015), "Failure analysis of centrifugal pumps based on survey", *ARPJ Journal of Engineering and Applied Sciences*, Vol.10, No.4, pp.1960-1965.
- Sheikh, A.K., Younas, M., and Al-Anazi, D.M. (2002), "Weibull analysis of time between failures of pumps used in an oil refinery", *Proceedings of the 6th Saudi Engineering Conference, KFUPM*, Dhahran, vol. 4, pp. 475-491.
- Singh, D. and Suhane, A. (2015), "Study of centrifugal pump using failure modes effect and critical analysis based on fuzzy cost estimation: A case study", *International Journal of Science and Research*, Vol. 4, No. 7, pp 19-22.
- Wang, L., and Gao, R.X. (2006), *Condition Monitoring and Control for Intelligent Manufacturing*, Springer Science and Business Media.

Authors' Biographical Notes:

Chanan S. Syan graduated from the University of Bradford, United Kingdom (UK) in 1983 with a BEng (Hons) in Mechanical Engineering. In 1988, he obtained a doctorate from the University of Hull, UK in Artificial Intelligence in Design for Manufacture. He has over 13 years of industrial experience and over 30 years in academia at various levels. At present, he is Professor of Production Engineering and Management of the Department of Mechanical and Manufacturing Engineering at The University of the West Indies, St. Augustine, Trinidad and Tobago. Professor Syan teaches Robotics and Automation, Research Methods, Engineering Asset Management, and Manufacturing Management. His research specialisations include brain computer interface (BCI), design and manufacture, asset management, AI and automation. He is the leader of the BCI, Robotics and Automation research groups and associated laboratories in the Department.

Geeta Ramsoobag is a PhD student at the Department of Mechanical and Manufacturing Engineering, Faculty of Engineering, The University of the West Indies, St. Augustine, Trinidad and Tobago. She currently holds a BSc in Mechanical Engineering (Hons) from The UWI. Her areas of research include engineering asset management, reliability engineering and maintenance optimisation.

Kavisha Mahabir graduated from The University of the West Indies, St. Augustine, Trinidad and Tobago in 2018. She holds a BSc in Mechanical Engineering. Her research work is in Condition Based Maintenance.

Vikash Rajnauth is the Owner and Managing Director of KVR Energy Limited, providing service and support for Energy and related Industries. His experience and expertise is in Engineering Asset Management, Mr. Rajnauth has over 18 years of experience in industry as senior manager with various organisations including local and international experience at defense and security, petrochemical, oil and gas, manufacturing, maritime, food and beverage, and chemical facilities.

■

Analysis and Development of Innovative Engineering Programmes

Sarim Al-Zubaidy ^{a,ψ}, Andrew Ordys ^b, and Eugene D. Coyle ^c

^aThe University of Trinidad and Tobago O'Meara Campus, Arima, Trinidad and Tobago, West Indies;
E-mail: sarim.alzubaidy@utt.edu.tt

^bWarsaw University of Technology, Faculty of Mechatronics, 02-525 Warszawa, Poland;
E-mail: andrzej.ordys@pw.edu.pl

^cMilitary Technological College, Muscat, Oman E-mail: Eugene.coyle@mtc.edu.om

^ψ Corresponding Author

(Received 11 March 2018; Revised 20 September 2019; Accepted 11 October 2019)

Abstract: This paper presents a method of analysis and, potentially, design of innovative engineering programmes, mainly focusing on the level of interaction between engineering disciplines, meeting requirements for professional accreditation and meeting requirements for the skilled work-force in the place of implementation. The programmes are in line with the standards of the UK Engineering Council. Hence, design of curricula had to encompass a number of elements, and demonstrate that they are safeguarding the quality requirements of the professional engineering institutions. The core building construct is outlined. The proposition is developed that sharing components of engineering programmes of study across diverse disciplines is beneficial in preparing students for engineering of the future. Some metrics are proposed, based on fuzzy logic approach to establish membership functions for measuring interaction between the programmes, and the emphasis of the programmes on particular aspects of engineering learning outcomes. It is demonstrated how such metrics can be used in designing and analysis of modern engineering programmes. Furthermore, to exemplify the proposed approach, the paper outlines the methodology of establishing and analysing the link between academic contents and practical “shop-floor” skills, both of which are required from engineers in modern industry. It is felt that the approach used and the experiences gained may assist academics who are considering establishing similar or related type programmes of study and may also be of value to institutions undergoing transformation.

Keywords: Professional Engineering Competencies, System based curriculum design, Mapping of learning outcomes, Curriculum design, Workshop skills

1. Introduction

It is widely accepted that France, through the creation of technical institutes in the eighteenth century, formalised the engineering disciplines. The first institute, the Ecole Polytechnique was established in Paris in 1794 (Bugliarello, 1991). It is therefore justifiable to conclude that all engineering disciplines, in the time of little knowledge generation, have started from a single discipline namely military engineering as documented by Encyclopaedia Britannica (Encyclopaedia Britannica, 1779). Figure 1 shows a schematic approximation of the historical evolution of engineering disciplines as suggested by Tadmor (2006).

As knowledge in general, and particularly engineering knowledge, began to accumulate in the following years, decades and centuries, and in order to equip professionals with the appropriate total sum of skills and specific discipline knowledge, engineering education tended to continuously diverge. One may argue that the basic/fundamental disciplines of engineering are: Civil, Mechanical, Electrical and Chemical. However, as time progressed, many sub-disciplines emerged and eventually became disciplines in

their own right, for example Electronic Engineering, Computer Engineering and Manufacturing Engineering.

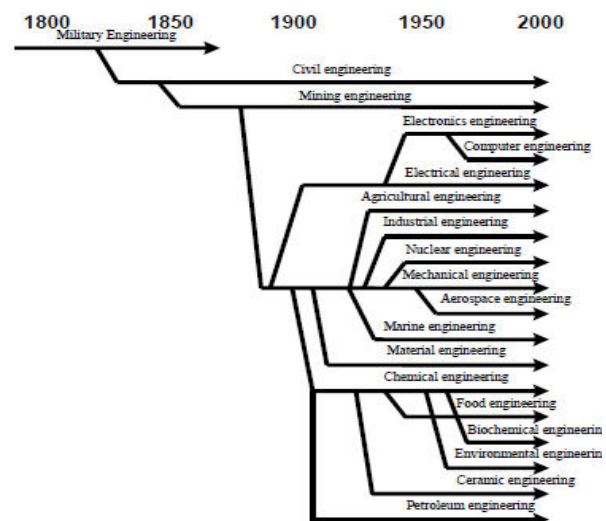


Figure 1: Branching of Engineering through time
Source: Abstracted from Tadmor (2006)

As those emerging disciplines tried to find their own identities, this was accompanied by vanishing commonalities not only between engineering and non-engineering disciplines, but also between the engineering disciplines themselves. At a point in time, these disciplines appeared to be self-contained as if not affected by the larger body of knowledge. This was noticeable until the middle of the twentieth century (Rugarcia et al, 2000).

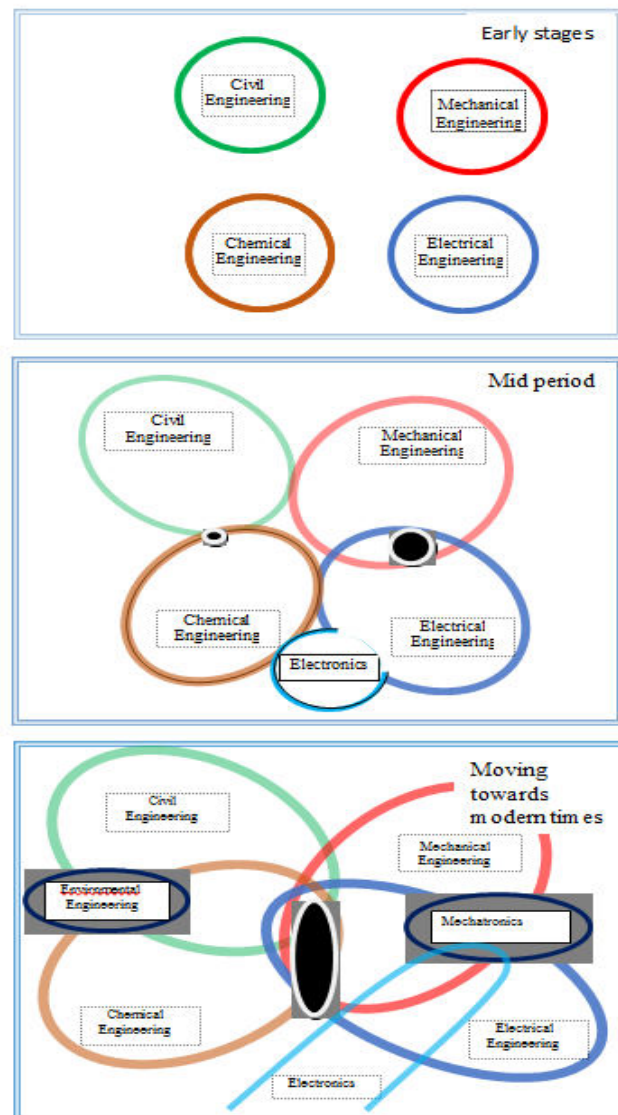
Today however, engineers do not work in isolation, but they work in the context of enterprises, cultures and communities, which represents divergent interests and perspectives. If one accepts that engineering education in the twentieth century developed based on the emerging science revolution, which led to science based curricula, then it is notable that the twenty-first century now sees the fusion of science and technology which will not only blur the difference between engineering disciplines but also between science and engineering.

In the past few decades, there has been an increasing demand for the integration of engineering education. This is accompanied by increased awareness of the vital importance of multi-disciplinary, socio-cultural and economic development, which young, successful, emerging engineers will encounter. At the same time, higher education is facing challenges, including new technologies changing the ways in which knowledge is produced, accessed, disseminated, managed, and controlled. Cultures and societies have become increasingly knowledge-based so that higher learning and research now act as essential components of cultural, socio-economic and environmentally sustainable development of individuals, communities and nations.

Consequently, the picture of contemporary engineering is a dynamic one, changing at a fast pace. To illustrate the changes, the authors propose a graphical representation as presented in Figure 2. It attempts to demonstrate the engineering disciplines with the progression of time. Discipline specialisations have matured and expanded with time and have, in part, overlapped with neighbouring disciplines (Mechanical, Electrical, Civil, Chemical Engineering), resulting in some instances, in the creation of newly formed disciplines, such as Mechatronics.

In the dynamic world of today such disciplines are not necessarily self-contained, as was the case in the past. Instead, they all draw from the increasingly common and expanding base of knowledge and tools (often software related) to solve engineering design problems. Therefore, even if new disciplines are created and named, they substantially overlap with other (old and new) disciplines.

In this article, the authors combine their amalgamated experience from working in engineering higher education institutions in different countries, to discuss aspects of analysis and design of modern engineering curricula, in particular through exploration of synergies between different engineering programmes.



Black spots indicate clusters for potential new disciplines being created.

Figure 2. Evolution and expansion of engineering disciplines over time, from earlier to later

To illustrate the concept, a proposed degree programme in Automotive Engineering is presented. The context is that of an Engineering Faculty/School comprising a number of programmes: Civil Engineering, Electronic Engineering (with focus on Avionics), Petroleum Engineering, and Automotive Engineering.

In setting out to create a new suite of engineering programmes or in revising an existing one, the attention is focused on:

- Accreditation of an engineering degree programme: successful accreditation will ensure that the programmes developed have been designed to meet the highest standards set by the engineering professions. In this paper, the authors focus on professional accreditation with the Engineering Council United Kingdom (UK), in order to afford

students in turn the opportunity to become registered incorporated (IEng), and later Chartered (CEng) engineers.

- Resource implications: In particular, the number of staff required to teach and the facilities (including laboratories and workshops) which are needed. This closely linked to the number of units of study (modules) to be attributed to a given programme.
- Needs of industry in the region of implementation of the programme: Which engineering disciplines are considered; also, which specific sub-disciplines and specific practical skills (e.g. in relation to particular technical equipment) are required.

Towards achieving the goal of satisfying the standards of professional accreditation, the requirements are set out in the document the UK-SPEC Standard for Professional Engineering Competence (UK-SPEC, 2014). The UK-SPEC requires achievement of five *Specific learning outcomes* and four *General learning outcomes*. The specific learning outcomes, as required by Engineering Council UK (ECUK, 2014) are briefly summarised below:

- Science and Mathematics (SM): Graduates are required to possess knowledge and understanding of underpinning scientific principles and methodology, thus attaining the mathematical and statistical methods necessary for their education in their engineering discipline (and beyond).
- Engineering Analysis (E): The requirement is that graduates be able to apply engineering principles, quantitative and computational methods to solve engineering problems. *Ability to use a system approach is noted herein.*
- Design (D): Focus is on the ability of developing a viable product or system to satisfy product specification. The graduates should be able to consider business needs, customer needs, product aesthetics and environmental impact. Further, they should be able to effectively explain their work to non-experts.
- Economic, legal, social, ethical and environmental context (S): It is necessary that engineering graduates be aware of environmental and societal impacts that engineering activities may impose, and are able to manage those impacts accordingly.
- Engineering practice (P): Students should encounter elements of practical engineering work while studying, prior to entering the engineering workforce as graduate professionals.

The detailed list of Learning Outcomes related to each of the above areas (from ECUK, 2014) is provided in the Appendix-1.

Reflecting on the aforementioned “specific” learning outcomes it is difficult to escape a conclusion that, although there will be components (competencies) which are specific to an engineering discipline nevertheless many components will be common across most (if not

all) disciplines. It has been recognised that commonality in “Design” can be particularly beneficial. Through focused education in design, clear emphasis is placed on integration of combined engineering and non-engineering considerations through implementation of a system’s based approach. The area wherein is potential for least overlap is perhaps “Engineering Practice”. This may only be achieved through practice in the selected discipline, often associated with specialist laboratory and/or workshop experience.

The UK-SPEC General Learning Outcomes (GT) cover, in summary, specific areas of personal development such as (i) Problem solving, communication skills, use of IT facilities, (ii) Planned self-learning (Continuous Professional Development (CPD)), (iii) Being able to plan and carry out a personal programme of work, (iv) Exercising personal responsibility.

Many of the learning outcomes (including design, economic, legal, social, environmental and ethical considerations) augment the requirements expected of today’s engineering graduates. These requirements are sometimes grouped holistically under the umbrella of “General or Transferrable Skills”.

The authors passionately believe that, of these general skills, the ability to embed the concept of student (and graduate) self-learning, is a critically important aspect in engineering (and other) programme designs. In doing so, it is vitally important that programmes be designed for accreditation at Honours level, thus including a substantial project work. An important point to bear in mind is that the “weighting given to different areas of the above will vary according to the nature and aims of the programme”, i.e. not every outcome will be covered by the same number of modules.

Both the Professional Engineering Institutions and Engineering Council UK encourage the accreditation of innovative engineering programmes to reflect the new delivery and content. It is postulated that an emphasis should be placed on a system approach and on inter-disciplinarity. Furthermore, it is proposed that this could be effectively achieved only via a holistic system based design of curriculum with substantial overlaps between the engineering degree disciplines.

The authors accept that a counter argument may be made that the ECUK learning outcomes could be delivered by developing and operating engineering programmes separately for each discipline, without inclusion of overlap. However, it is our belief that such an approach would be not effective in terms of utilisation of resources. Moreover, and more importantly, it will not be effective in terms of preparing the students for the engineering world of the future, wherein interdisciplinarity and a systems based approach to engineering education is expected to predominate.

Towards meeting the local industrial requirements, a fundamental tenet of programme design is that of Engineering Practice. Often engineering practice is

linked solely to laboratory and/or workshop experience of the related discipline of study. Hence, it is expected to differ from discipline to discipline and, even within one engineering discipline it will depend strongly on the localisation where the programme is implemented.

2. General Set-up of the Curriculum

The curriculum presented here refers to an exemplar programme, which has been created based on the authors' amalgamated knowledge and experience of different engineering colleges and universities. Its development is based on the *systems approach*. The core building-blocks of the degree programmes are as follows:

- *Problem-centric learning*: This is an approach in which students tackle a carefully constructed set of 'problems', generally engineering projects of growing scale and complexity.
- *The 'upside-down' curriculum*: This approach moves material on engineering applications to the earlier stages of education in order to motivate, more strongly, the students' interest in fundamental mathematics and science that can otherwise seem dry and indigestible.
- *Mathematics in context*: The teaching of engineering mathematics by engineers and presented in an 'applied' setting, rather than by mathematicians in a more rigorous 'proof-oriented' style that is ultimately less accessible.
- *Design orientation*: Many engineering programmes place a substantial emphasis on analysis, but creative synthesis, that is design, is a central, perhaps defining activity in engineering and must be central to a curriculum. Engineering students need design experience and in particular should, from an early stage, be working on 'real problems' with 'real customers' and in interdisciplinary teams, such as they would experience in the workplace.
- *Combining simulation, and laboratory*: The use of sophisticated simulation has transformed engineering education; however, there is no substitute for laboratory and practical training facilities. Many training organisations and their industrial partners find there is a need to develop and combine the theoretical learning with practical application. The addition of country-specific competences and the need for multi-skilling requires the introduction of innovative approaches that blend with theoretical delivery and utilising virtual learning or simulation platforms that safely and logically lead the student to real time applications in laboratories and workplaces.

The above are all connected through the central themes of *safety and sustainability*, *transferable skills development* and *management and entrepreneurship*. The approach to teaching and learning in all engineering programmes is one based on engineering systems

combined with engineering practice. Such an approach will inculcate in the students an understanding of the impacts and consequences of engineering decisions on issues of safety management, economics and environmental pollution.

3. Analysis of the Resulting Curriculum Set-up

3.1 Meeting the Requirements for Professional Accreditation: ECUK Learning Outcomes

Documentation to demonstrate that the designed programmes meet the outcomes as set out in Section 2 above, requires completion of a learning outcomes matrix. This document is crucial to demonstrating that the programme meets all the required learning outcomes. The matrix lists all the modules (units of teaching) covered by a programme of study and all ECUK learning outcomes (generic and specific). For each module, the matrix specifies wherein it contributes towards a specific learning outcome, by means of a "tick" at the appropriate cross-section of module and learning outcome in the matrix. The "tick" is therefore interpreted as a statement: "a given module belongs to the set of modules supporting a given Learning Outcome". Working with variety of academics in different countries the authors encountered different approaches to filling-in the output standard matrix. Some people tend to be quite conservative in their judgement and only tick a given learning outcome for their module if it is fully covered.

A problem with this approach is that a substantial amount of information about modules contributing to a specific learning outcome would be lost. For illustration, say a Learning Outcome: *E2. Ability to identify, classify and describe the performance of systems and components through the use of analytical methods and modelling techniques* (see Appendix 1) is covered in two modules: one focusing on analytical methods and another focusing on modelling techniques. A "conservative" academic would not tick any of those modules against the Learning Outcome E2, because none of them is realising it fully. However, those two together would fully address the requirements of this particular learning outcome.

On the other hand, some academics tend to be liberal / generous with their assessment. Taking for illustration the same Learning Outcome E2, a module can only address "ability to identify the performance of components" and still receive a "tick". Theoretically, there is nothing wrong with such approach, as long as the rest of the Learning Outcome E2 is covered somewhere else in the programme of study. (The task of the accrediting body would therefore be to verify such full coverage, based on the detailed contents of module's delivery and assessment). However, a vital information about the function and position of a given module in the bigger picture of the programme of study would be lost of at least diluted.

Therefore, it has to be appreciated that the numerical

analysis of how the ECUK learning outcomes are met, is, by its nature not an absolute or precise science and carries a degree of subjectivity. The reason for this is that a given learning outcome is generally only partially fulfilled in any given module. Taking another example: in addition to dedicated modules in higher mathematics, underpinning of mathematical concepts is normally also addressed via more generic engineering modules, including Control Systems, Signal Processing, and Thermodynamics. A question may be posed: to what extent a given module meets the requirements of a specific learning outcome? Such a question, and analysis based on answer to it, could be useful in programme design or re-design, by allocating weight of different modules to different learning outcomes. Possible answers may be: *not at all, to a small extent, partially, almost completely, or fully*. In assigning numerical values to this questionnaire a fuzzy logic tool may be applied.

Zimmermann (2000) and Meier et al. (2008) apply a fuzzy classification which the authors have adapted here to analyse the above proposition. In this approach, ϵ an element x is classified as belonging to a set Λ with a degree of membership, called membership function μ .

$$\mu_{\Lambda}(x) := c \text{ where } c \in (0,1) \quad (1)$$

This is in contrast to “crisp” classification where:

$$1_{\Lambda}(x) := \begin{cases} 1 & \text{if } x \in \Lambda \\ 0 & \text{if } x \notin \Lambda \end{cases} \quad (2)$$

In fuzzy classification, for individual members, the value of the membership function may vary between 0 and 1. Considering as elements the *modules* on the programme of study, the membership functions are subjectively assigned to each module, in terms of “belonging” to a given Learning Outcome (set Λ_i).

Table 1 provides an example of fuzzy classification performed for one programme of study: Automotive Engineering. The programme has 23 modules (elements). All modules, except for the final project, have the credit value of 20 credits each whereas the final project module has a credit value of 40 credits. Hence, the total number of credits for Diploma in Higher Education is 360 and for Bachelor (honours) in Engineering (BEng) is 480 credits. The modules are as follows:

Level 3 (Engineering Foundation):

- Algebra and Geometry
- Engineering Physics
- Electrical Engineering
- Engineering Materials
- Engineering Systems Design 1
- Introduction to Electrical Machines

Level 4:

- Engineering Mathematics
- Engineering Systems Design 2
- Environmental Engineering
- Thermodynamic Systems
- Thermal Systems Engineering 1
- Mechanical Systems

Level 5 (Diploma in Higher Education):

- Safety Engineering
- Group Design Project
- Engine and Transmission
- Thermal Systems Engineering 2
- Vehicle Chassis and Aerodynamics
- Engine Management Systems

Level 6 (Bachelor of Engineering - Honours):

- Engineering Management
- Individual Project (double module)
- Engineering Maintenance
- Advanced Vehicle Design
- Alternative Energy Systems

The fuzzy membership functions of those modules are assigned for 32 learning outcomes (32 sets Λ_i $i = 1, \dots, 32$). The assignment has been performed by analysing the module descriptor for each module and by inspecting the format of its delivery. The detailed description of those learning outcomes, which comes from the specification of the UK Engineering Council (UK-SPEC, 2014; ECUK, 2014), is provided in Appendix 1.

As an example, to illustrate this approach, take Learning Outcome: *SM2. Knowledge and understanding of mathematical and statistical methods necessary to underpin their education in their engineering discipline and to enable them to apply mathematical and statistical methods, tools and notations proficiently in the analysis and solution of engineering problems*, in the module: *Thermodynamic Systems*. Analysis of the delivery plan of this module shows that 10% of time is devoted to enhancing students’ knowledge and understanding of mathematical methods (partial differential equations) and further 20% to application of those methods to solutions of engineering problems. Statistical methods are only mentioned (5%). More importantly, and consistent with the analysis above, inspecting the assessment of the module reveals that approximately 20% of the marks which can be obtained are related to mathematical skills whereas the remaining 80% can be linked to other aspects/knowledge covered in the module. Hence, the value of membership function has been assigned as 0.2. It has to be stressed again that such assignment carries a substantial degree of subjectivity – hence fuzzy-set approach.

Nevertheless, is more accurate than “zero” or “one”. The next step is to combine the learning outcomes into groups, as specified by ECUK. This can mean for example that the sets: SM1, SM2, SM3 are added together to form a single set: Science and Mathematics. The membership of each element in this new set (sum of three) is defined, according to Fuzzy logic rules, using the Max function (x OR $y = \text{maximum}(\text{truth}(x), \text{truth}(y))$). Hence:

$$\begin{aligned} & (x \in \Lambda_1) \text{ OR } (x \in \Lambda_2) \text{ OR } (x \in \Lambda_3) = \\ & \text{Max} \{ (\mu_{\Lambda_1}(x)), (\mu_{\Lambda_2}(x)), (\mu_{\Lambda_3}(x)) \} \end{aligned} \quad (3)$$

In the final stage, the modules are grouped into three sub-sets with respect to their sharing status. “Sharing” identifies the modules as: shared with all other departments (A), shared with some other departments (S), and not shared (N). For each sub-set of modules, the membership function in a given Learning Outcome is calculated as an average (rather than a maximum) of the individual members functions. The result is then defuzzified by scaling the membership functions to the range 0:100%.

Figure 3 shows the percentage contribution to Learning Outcomes by modules which are: Department specific, shared with other Departments, not shared. It should be emphasised that this is an illustration and it is for the Automotive Engineering specialisation only. However, from the authors’ experience, and from other departments’ specialisations at different institutions, similar shared trends emerge.

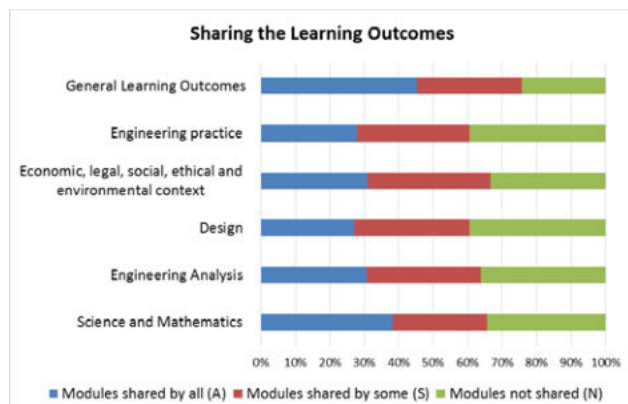


Figure 3. Assessment of contribution to learning outcomes by the modules: shared by all (common) shared by some, and not shared

Another representation of the same data is shown in Figure. 4. In this instance no scaling has been applied, hence the bar-chart places emphasis of the programme towards particular aspects of ECUK Learning Outcome objectives. As can be seen, this example is of a programme with a substantial component of Engineering Practice.

- Science and Mathematics: The underpinning knowledge is mainly achieved in common modules such as Algebra and Geometry, Engineering Mathematics, and Engineering Physics. Hence, a high percentage of modules are shared by all.
- Engineering Analysis: The required competencies are developed evenly throughout all years of study, with comparable contribution from common modules, and shared modules.
- Design: A high percentage of Engineering design outcomes is achieved via the specific design oriented modules at all levels of study. The design stream of the programme is based on the Melbourne model (Smith and Hadgraft, 2007), which adopts a

systems based approach. These modules are shared by some Departments, while differences are accommodated in department specific modules.

- Economic, legal, social, ethical and environmental context: This aspect of education is equally covered by modules common to two or more, and also to all departments. A large level of commonality is present but there are also some discipline specific aspects which must be taken into account, e.g. Electronic Engineering may share with Civil Engineering some aspects related to energy conservation (smart homes); and may share with Automotive and Petroleum Engineering, other aspects – relating for example to air pollution from combustion engines. These topics will be covered in modules shared by some, but not by all departments.
- Engineering practice: Herein the discipline specific modules, with associated workshop practices have a dominant effect. However, students also acquire a substantial amount of engineering practice through the laboratory and workshop sessions, which are shared among two or more departments.
- General Learning Outcomes: From the performed analysis it can be concluded that a majority of contribution to general learning outcomes comes from the Design oriented modules, which are common to all departments. The contribution of non-shared modules is the lowest.

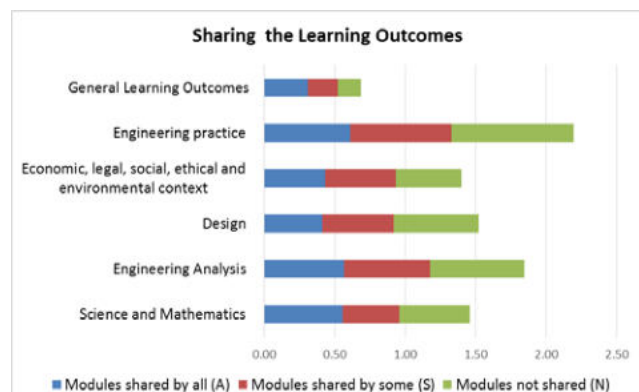


Figure 4. Assessment of the level of contribution to learning outcomes by the modules: shared by all (common) shared by some, and not shared – not scaled to (0:100%)

4. Design and Re-design Engineering Programmes

Students entering the higher education, in most cases, are doing so expecting benefits for themselves and for the society, meaning that their degrees will be recognised and valued on the job market. It is a duty of the education providers to ensure that the students’ expectations, with this respect, are met. It is therefore paramount that the engineering degree programmes are accredited, i.e. they meet all the learning outcomes, as specified, for instance, by ECUK. After fulfilling this

requirement, there is still a degree of flexibility in designing the programmes, to address the needs of local job markets and/or the emerging trends in engineering and technology. Using the fuzzy set approach, described above, can be a useful tool in addressing this goal. Assigning fuzzy membership values to different modules with respect to different learning outcomes would signify the “weight” or importance that is given to any of the learning outcomes. Hence, it will show the bias of the degree (programme of study) towards a particular profile of the graduate.

The analysis presented above would enable the educators to take a holistic view of the programmes of study, to examine how the development of different types of abilities in students progresses in time – by year of study, and in space – by module/unit of study. Furthermore, it could be assessed whether some of the learning outcomes require further expansion in the programmes, or, perhaps contraction. From the performed analysis, the attention can be then directed to specific modules.

If a new or modified degree programme is considered for introduction, to an institution already running accredited programmes, the analysis presented above will be helpful in assessing how such a programme could share modules with other existing programmes. Starting with the desired profile of the graduate, firstly, the technical contents of a programme would be established. This may result in a provisional list of new modules that need to be developed. Next stage would be to map the profile into “weights of contribution” of specific learning outcomes. Further, a function showing contribution to learning outcomes in existing programmes (similar to Figure 4) would be compared with the desired profile of the graduate, hence showing gaps and identifying those learning outcomes which need to be addressed in the newly introduced modules (with their desired fuzzy membership functions). This would also indicate the resource implications. Only after this analysis, one can proceed to designing the actual contents of the modules/units of study.

As an example of this approach, consider a design of a programme of study, which is to be leaned towards practical, workshop, shop floor skills, i.e. discipline specific engineering practice.

4.1 Discipline Specific Engineering Practice

It is the authors’ experience, from their personal career backgrounds, that the usefulness and therefore the attractiveness of engineering degree programmes is proportional to the amount of practical skills, readily deployable in a work-place, which the students acquire in their term of study. For instance, most of UK universities offer so called “sandwich courses”. In those courses, students spend one year working in industry, normally between year 2 and 3 of their degree. Then, they return to University to complete the final year of

bachelor degree. Note that the “sandwich year” is addition to the academic credits acquired during their course. Hence, all the required learning outcomes, for instance related to analytical or design skills are fully covered in the academic programme of study. The “sandwich year” equips students with additional skills, which make them more ready for the work place.

It is well documented (Brooks, 2012; Wickware 2016) that the employability indices for those students who take “sandwich courses” are much higher than for other students. Quite often, the graduates end-up working in the company where they spent their “sandwich year”. During the “sandwich year” the students work in an industrial company in different engineering positions, acquiring practical skills and experience. Those may be called “workshop” or “shop-floor” skills.

At a first glance, it may be seen to contradict earlier argument that the courses should be focused towards transferrable skills. In answer, it should be pointed out that the workshop skills can also be taught as transferrable skills, taking into account the fast changing environment of relating engineering activities. In fact, it has been observed that when the students are confronted with the reality of engineering manufacturing or maintenance, which sometimes lags behind the theoretical state-of-the-art developments, this prompts their better understanding of necessity to be prepared for change management and for continuous professional development.

Hence, the students can also enhance their design skills, by being exposed to industrial constraints and limitations of the production/manufacturing process. This is a well-known issue, and those institutions which take engineering education seriously manage it effectively, either via a module of “industrial placement”, taken for example by students during the summer break; or more extensively, as a “sandwich course” comprising one year of students’ time, fully seconded to an industrial partner. An alternative solution, presented here, is that the industrial practice is incorporated evenly during the academic year, thus being delivered in parallel with academic modules. This may pose a logistical challenge but the advantage is that the development of engineering practical skills can be synchronised with students’ progress in theoretical aspects, delivered in other modules.

Additional motivation in development of this particular approach is in compliance with ECUK requirements for “engineering practice”, as explained earlier. A further factor, in this particular course design example, is to comply with country-specific skill needs; in the knowledge that some students will choose to graduate at Level 5 Diploma in Higher Education and will be seeking employment in a more ‘technician’ oriented role. Hence, the requirements specific to the country of operation must be taken into account.

To illustrate how these requirements are placed within the students' programme of study, one example, of one particular industry specific qualification, which is also called "commercial trade", is presented. The term "trade" is commonly used, e.g. in UK vocational education systems. Here it signifies bridging the gap between academic and vocational qualifications and will be used in the following sections. The trade is Vehicle Mechanics. In its simplified form, the requirements state 14 competencies, which the student must acquire, as follows:

- AS1 To be able to read and draft engineering drawings
- AS2 Have familiarity with basic automotive troubleshooting
- Be able to:
- AS3 Service hydraulic automotive systems
- AS4 Use automotive diagnostic equipment
- AS5 Inspect and service braking systems
- AS6 Remove and install engine components
- AS7 Inspect and repair clutch components
- AS8 Service and repair transmission systems
- AS9 Inspect and service steering systems
- AS10 Inspect and service suspension systems
- AS11 Inspect and service wheels and tyres
- GS1 Understand operational Health and Safety practice
- GS2 Perform planning of workshop activities
- GS3 Understand and implement quality standards in maintenance processes

These trade-related skills have been divided into two groups: general (GS), which are applicable to all trades, and trade specific (AS).

Acquiring of these competencies during the course of study would greatly benefit the students. Those who may complete their education at level of Diploma in Higher Education (DipHE) will be well prepared to demonstrate to future employers their skills in engineering shop-floor practices. Hence, some of the competencies can be assessed by specific, trade approved examinations – demonstrating practical skills, sometimes related to a particular manufacturer, as demanded by the country of operation.

In this example, the objective is to integrate the academic output with a set of practical skills in maintenance, troubleshooting and operation of automotive engineering equipment. From the perspective of ECUK classification, this must be supported by *Underpinning Science and Mathematics, Engineering Analysis and Engineering Design* up to the level of competency commensurate with the DipHE. Also, *General transferrable skills* are required up to the same level, whereas in *Economic, legal, social, ethical and environmental* education some aspects have to be expanded and adopted to the specific requirements. *Considering Engineering Practice*, the workshop skills requirements proposed here substantially exceed the minimum expected from accredited engineering degrees.

When designing the programmes of study, a system based approach was applied in which both the academic requirements and workshop practice requirements were

considered jointly. Hence, the analyses of ECUK Learning Outcomes and of trade needs were combined together when identifying the content and the learning outcomes of appropriate modules (units) of study. Practical skills requirements are fully completed by the end of Level 5 (Engineering Year 3), hence the students graduating with the DipHE will be fully prepared for taking up of their roles with their respective employers.

4.2 Analysis of Trade-related Requirements with Respect to the Academic Programmes of Study

From the perspective of the students, their education and their future career prospects, it is paramount that the degrees offered meet stringent international standards – in this case ECUK accreditation. At the same time, students must be prepared for their immediate future careers in industry. Hence, the students are faced with a challenging task: to combine together two highly demanding requirements; achieving their academic standards and attaining trade-related competency targets. It is our belief that through using the system based approach, by development of interdisciplinary modules, and by exploring a range of common factors in education and training, this had been made possible.

In a vocational education, each trade-related competency would, traditionally, be taught by a combination of theory and practice over a period of several weeks, potentially culminating in a trade-related examination. By applying the system based approach, a large part of the skills required is built into the academic programmes. For this particular trade (Vehicle Mechanic), 12 out of 14 competencies feature in the academic modules. They are not addressed fully in those modules, but the amount of required additional activities is reduced. The academic programme of study up to Level 5 consists of 18 modules. From this number, 15 modules contribute directly to the trade-related competency requirements.

Applying fuzzy classification, a table is generated (see Table 2), showing membership functions in each particular trade related skill for each of the academic modules and for each of the additional (trade related) modules. Allocation of the value of the membership function to each module and each trade is performed by analysing the delivery plan and assessment strategy, in the same way as was illustrated in section 3.1. Here, the programme of study is considered up to Level 5. At level 5 the trade-related programme should be completed.

The analysis is performed using the same fuzzy classification rules, as applied before. For each module, the membership into the trade specific competencies group, general competencies group, and all competencies group is calculated as a maximum (equation (3)). Next, the average is used to calculate the contribution of the academic modules grouped together and non-academic modules grouped together. The results are presented in Figure 5.

5. Conclusions and Future Work

From commencement of the 20th Century engineering practitioners and academics have debated and considered perceived needs for holistic changes in delivery of engineering higher education programmes. This paper presents an implementation of system based curriculum design in a challenging environment. The design is based on meeting the accreditation requirements of the UK Engineering Council, while at the same time emphasising and taking benefit from the multi and interdisciplinary nature of the programmes considered. An additional challenge is posed by the necessity of incorporating particular requirements for practical hand skills, which would enable students to function and to perform well in their future workplace environments.

The paper outlines the specification requirements, presents the design philosophy and discusses the methods adopted to measure the outcome. A fuzzy classification is applied, first - to assess the level of inter-disciplinarity, and, second - to assess the contribution of the academic programmes to the workshop/trade training needs. It is felt that the presented fuzzy classification approach will prove a useful tool, not only for analysis of outcomes and results but also as an ongoing assist to curriculum development and design.

Acknowledgments:

The Authors acknowledge support from National Agency of Academic Exchange (NAWA), "Polish Returns", Grant No: PPN/PPO/2018/1/00063/U/00001.

References:

- Brooks, R. (2012), "Evaluating the impact of placements on employability", *Proceedings of the Employability, Enterprise and Citizenship in Higher Education Conference 2012*, Manchester Metropolitan University, March, pp.?? (or weblink??)
- Bugliarello, G. (1991), "The University and particularly the technological university: Pragmatism and beyond", In: Zinberg, D.S. (Ed), *The Changing University: How Increased Demand for Scientists and Technology is Transforming Education Institutions Internationally*, Kluwer Academic Publishing, The Netherlands, p. 31-37
- ECUK (2014), *The Accreditation of Higher Education Programs*, Third Edition, May.
- Meier, A., Schindler, G., and Werro, N. (2008), "Fuzzy classification on relational database", In: Galindo, M. (Hrsg.), *Handbook of Research on Fuzzy Information Processing in Databases* (Bd. II, S. 586-614), Information Science Reference.
- Rugarcia, A., Felder, R.M., Woods, D.R., and Stice, J.E. (2000), "The future of engineering education, I. Vision for a new century", *Chemical Engineering Education*, Vol.34, No.1, pp.16-25,
- Smith, D.W. and Hadgraft, R.G. (2007), "The 'Melbourne Model' and new Engineering Degrees at the University of Melbourne in 2008", *Proceedings of the 2007 AaeE Conference*, Melbourne. Available from: <https://www.timeshighereducation.com/news/student-experience-survey-2016-creating-new-professionals#survey-answer>, accessed 30/09/2018

- Tadmor, Z. (2006), "Redefining engineering disciplines for the 21st Century, The bridge", *The Journal of the US National Academy of Engineering*, Vol. 36, No.2, pp. 33-37
- Wickware C. (2016), "Why are sandwich courses seeing a resurgence?", *Times Higher Education*, May, on-line access: <https://www.timeshighereducation.com/news/why-are-sandwich-courses-seeing-a-resurgence>
- The Encyclopedia Britannica (1779), *Encyclopædia Britannica* Second Edition, Edinburgh
- UK-SPEC (2014), *UK Standard for Professional Engineering Competence, - Engineering Technician, Incorporated Engineer and Chartered Engineer Standard*, Third Edition. Engineering Council, available from: www.engc.org.uk
- Zimmermann, H.-J. (2000), *Practical Applications of Fuzzy Technologies*, Springer, London

Appendix-1:

Description of Specific Learning outcomes for Engineering degrees to partially meet the educational requirements for Chartered Engineer status, cited from EC UK (2014)

Science and Mathematics (SM)

Engineering is underpinned by science and mathematics, and other associated disciplines, as defined by the relevant professional engineering institution(s). Graduates will need the following knowledge, understanding and abilities:

- SM1.** Knowledge and understanding of scientific principles and methodology necessary to underpin their education in their engineering discipline, to enable appreciation of its scientific and engineering context, and to support their understanding of relevant historical, current and future developments and technologies
- SM2.** Knowledge and understanding of mathematical and statistical methods necessary to underpin their education in their engineering discipline and to enable them to apply mathematical and statistical methods, tools and notations proficiently in the analysis and solution of engineering problems
- SM3.** Ability to apply and integrate knowledge and understanding of other engineering disciplines to support study of their own engineering discipline.

Engineering Analysis

Engineering analysis involves the application of engineering concepts and tools to the solution of engineering problems. Graduates will need:

- E1.** Understanding of engineering principles and the ability to apply them to analyse key engineering processes
- E2.** Ability to identify, classify and describe the performance of systems and components through the use of analytical methods and modelling techniques
- E3.** Ability to apply quantitative and computational methods in order to solve engineering problems and to implement appropriate action
- E4.** Understanding of, and the ability to apply, an integrated or systems approach to solving engineering problems.

Design

Design at this level is the creation and development of an economically viable product, process or system to meet a defined need. It involves significant technical and intellectual challenges and can be used to integrate all engineering understanding, knowledge and skills to the solution of real and

complex problems. Graduates will therefore need the knowledge, understanding and skills to:

- D1.** Understand and evaluate business, customer and user needs, including considerations such as the wider engineering context, public perception and aesthetics
- D2.** Investigate and define the problem, identifying any constraints including environmental and sustainability limitations; ethical, health, safety, security and risk issues; intellectual property; codes of practice and standards
- D3.** Work with information that may be incomplete or uncertain and quantify the effect of this on the design
- D4.** Apply advanced problem-solving skills, technical knowledge and understanding, to establish rigorous and creative solutions that are fit for purpose for all aspects of the problem including production, operation, maintenance and disposal
- D5.** Plan and manage the design process, including cost drivers, and evaluate outcomes
- D6.** Communicate their work to technical and non-technical audiences.

Economic, Legal, Social, Ethical and Environmental Context

Engineering activity can have impacts on the environment, on commerce, on society and on individuals. Graduates therefore need the skills to manage their activities and to be aware of the various legal and ethical constraints under which they are expected to operate, including:

- S1.** Understanding of the need for a high level of professional and ethical conduct in engineering and a knowledge of professional codes of conduct
- S2.** Knowledge and understanding of the commercial, economic and social context of engineering processes
- S3.** Knowledge and understanding of management techniques, including project management, that may be used to achieve engineering objectives
- S4.** Understanding of the requirement for engineering activities to promote sustainable development and ability to apply quantitative techniques where appropriate
- S5.** Awareness of relevant legal requirements governing engineering activities, including personnel, health and safety, contracts, intellectual property rights, product safety and liability issues
- S6.** Knowledge and understanding of risk issues, including health and safety, environmental and commercial risk, and of risk assessment and risk management techniques.

Engineering Practice

This is the practical application of engineering skills, combining theory and experience, and use of other relevant knowledge and skills. This can include:

- P1.** Understanding of contexts in which engineering knowledge can be applied (e.g., operations and management, application, and development of technology)
- P2.** Knowledge of characteristics of particular materials, equipment, processes, or products
- P3.** Ability to apply relevant practical and laboratory skills

- P4.** Understanding of the use of technical literature and other information sources
- P5.** Knowledge of relevant legal and contractual issues
- P6.** Understanding of appropriate codes of practice and industry standards
- P7.** Awareness of quality issues and their application to continuous improvement
- P8.** Ability to work with technical uncertainty
- P11.** Understanding of, and the ability to work in, different roles within an engineering team.

Additional General Skills

Graduates must have developed transferable skills, additional to those set out in the other learning outcomes, that will be of value in a wide range of situations, including the ability to:

- GT1.** Apply their skills in problem solving, communication, working with others, information retrieval and the effective use of general IT facilities
- GT2.** Plan self-learning and improve performance, as the foundation for lifelong learning/CPD
- GT3.** Monitor and adjust a personal programme of work on an on-going basis
- GT4.** Exercise initiative and personal responsibility, which may be as a team member or leader.

Authors' Biographical Notes:

Sarim Al-Zubaidy is the present President of The University of Trinidad and Tobago (UTT). He is an engineer, with over thirty years experiences in both senior academic and administrative positions in a variety of higher education institutions around the world. His expertise ranges from traditional to newly formed universities to those in transition from colleges and polytechnics. Professor Al-Zubaidy is a Fellow of many professional bodies as well as a Chartered Engineer, European engineer, APEC engineer and a Chartered Environmentalist. He is also Principal Fellow of the Higher Education Academy, and is a registered consultant who has spent several years advising industry.

Andrew Ordys is Professor at the Warsaw University of Technology, Poland, and Electronic Engineer with experience in education, management and research in universities in Europe and in Middle East. He is author or co-author of approximately 100 publications. Professor Ordys is Chartered Engineer and Fellow of the Institution of Engineering and Technology (IET). Professor Ordys is also Senior Fellow of the Higher Education Academy and Senior Member of the Institute of Electronic and Electrical Engineers (IEEE).

Eugene D. Coyle is an Electrical Engineer with experience in research, teaching and senior management of courses and programmes of study in Europe, the USA and the Middle East. He has contributed to management of change and accreditation for engineering courses from Technician to Master level. Professor Coyle is Chartered Engineer and Fellow of several professional institutions in Ireland and the UK.

■

A Review of Caribbean Geothermal Energy Resource Potential

Randy Koon Koon^{a,Ψ}, Sheldon Marshall^b, Dawin Morna^c, Randy McCallum^d, and Masaō Ashtine^e

Department of Physics, The University of the West Indies, Mona Campus, Jamaica, West Indies;

^aE-mail: randy.koonkoon@uwimona.edu.jm

^bE-mail: sheldon.marshall@mymona.uwi.edu

^cE-mail: dawin.morna@mymona.uwi.edu

^dE-mail: randy.mccallum@mymona.uwi.edu

^eE-mail: masao.ashtine@cantab.net

^Ψ Corresponding Author

(Received 11 March 2018; Revised 20 September 2019; Accepted 04 November 2019)

Abstract: The Caribbean Community (CARICOM) is comprised of fifteen-member states each exhibiting geographic, cultural and economic diversity. Six of these CARICOM member states along the Eastern Caribbean chain of islands display high-enthalpy systems for geothermal energy exploitation. This paper aims to provide a review into the geothermal energy resource potential across the Caribbean and presents quantitative findings as to the potential power production, economic and environmental savings through which geothermal energy development can bring to each respective nation. Notable findings for a 2027 scenario project an estimated 184.49 MW of geothermal capacity that can be absorbed into the national energy mix, displacing 855,600 barrels of oil (bbls) importation, resulting in approximately 1.1 million tonnes of carbon dioxide (tCO₂) emissions being avoided per year. An inter-island grid connection approach is presented to tackle large-scale energy projects to attract financial investors in an effort to combat the upfront challenges associated with geothermal energy development.

Keywords: Geothermal energy; Eastern Caribbean islands; Inter-island grid connection; Caribbean geothermal landscape, renewable energy

1. Introduction

1.1 The Caribbean Energy Situation

The Eastern Caribbean islands within the Caribbean Community exhibit many geopolitical and socio-economic diversities. The fifteen-member island states encompassing CARICOM have all experienced the extent of the fluctuations of the cost of fossil fuel-based products. The existing dependence on the importation of petroleum products affects all CARICOM nations and as such there is a growing need for the transition to renewable forms of energy. The pursuit of enhanced energy security regionally can be obtained through higher penetration rates of renewables. Furthermore, a reduction in the price of electricity is expected through this foreseeable outcome. The averaged domestic retail cost of electricity within the Caribbean stands at around USD \$0.35/kWh (Energy Chamber, 2017).

However, the region has progressed over the years in tackling this shared problem, and as such has yielded a regional Energy-policy in 2013 (Ochs et al., 2015). Policy frameworks complement and provide enhanced opportunities and energy diversifications for the continued transition towards greater penetration rates of renewables.

1.2 Building Climate Resilience

The Caribbean has recently been a strong advocate on the world stage for greater reductions in greenhouse gas emissions globally. Recent research, published in the Intergovernmental Panel on Climate Change (IPCC) Special Report on warming of 1.5°C above pre-industrial levels, saw over 90 Caribbean and Latin American authors contributing to a body of data for increasing climate security for the vulnerable regional small island developing states (SIDS) (IPCC, 2018). The word “resilience” has been hotly debated within the Caribbean, as many scientists call for strengthening energy resources as a means to mitigate climate change impacts in the region (Gay et al., 2019; Chen and Stephens, 2018; Angeles et al., 2018; Shirley and Kammen, 2015). The Caribbean’s energy infrastructure is aging and severely limited in its distribution across larger islands. Many islands rely on centralised forms of energy distribution which are further limited by crippling fossil fuel imports (Surroop et al., 2018). Climate resilience is thus built through modernising and restructuring the region’s energy and transportation sectors to not only mitigate but adapt to already changing climate regimes.

The hurricane season of 2017 was a clear indication of work to be done. Eastern Caribbean islands such as Dominica and Antigua and Barbuda were devastated after the passage of Hurricanes María and Irma respectively. An increased intensity of hurricanes is

expected through near- and long-term simulations for deep-convective tropical regions (Bhatia et al., 2019), and many Caribbean SIDS are waking up to energy resilience to combat climate change. Popke and Harrison (2018) provide a critique of Dominica's energy systems, both through a historical and current perspective, proposing that recent (and successful) ventures in geothermal power will bring much greater energy security to the island.

1.3 Geothermal Energy Impact

Geothermal Energy is also of interest due to its relatively minuscule carbon emissions whilst being able to supply massive amounts of energy due to high capacity factors (in excess of 90%). This allows for the plants to run non-stop, hence being a good producer of a more governable and consistent supply of baseload energy and heat as opposed to other renewable sources such as solar and wind (Dickson and Fanelli, 2005). Geothermal energy exploitation among Caribbean nations can play a key role in realising targets in energy security, economic development and mitigating the effects of climate change.

Through harnessing the stored thermal energy trapped within rocks, this resource can be utilised in generating electricity and direct applications. The paper aims to provide an update on geothermal energy within the Caribbean, especially within the Eastern Caribbean islands as these nations possess the indigenous resource. Furthermore, reanalysed data are presented for national energy targets, avoided costs associated with fossil fuel importation, beneficial contributions toward national energy grids, climate sensitivity and existing ideas on inter-island grid connections.

2. Caribbean Geothermal Landscape

2.1 Geothermal Energy - Hydrothermal Systems

Geothermal energy is a clean and renewable form of energy naturally occurring within the Earth as well as the primordial heat of planetary formation (Turcotte and Schubert, 2014). This form of energy can be thought of as heat mining. It is a result of the heat flow from the unhurried decay of naturally occurring radioisotopes, namely: Uranium 235, Potassium 40, Uranium 238 and Thorium 232 having half-lives of 0.7, 1.25, 4.5 and 14 billion years respectively (Adams et al., 2015; Kale, 2015), thus making this heat source almost inexhaustible and sustainable - at least on a human scale.

A naturally occurring geothermal resource (hydrothermal resource) has three major facets, a heat source (hot rock system, magmatic intrusion), fluid (fluid-filled reservoirs, subsurface interconnections to fluid pockets – the resulting fluid is generally the result of contributions from different sources such as surface/meteoric water, seawater, and magmatic volatiles) (Nicholson, 1993), and a permeability network (the reservoir must be conducive to allow fluid flow).

The increase of temperature per unit depth within the Earth (crustal region specific for geothermal energy exploration purposes) is defined as the geothermal gradient. This gradient can vary from one location to the other; however, it averages 25-30 °C/km in most regions (Haraksingh and Koon Koon, 2011).

The Eastern Caribbean comprises of a chain of geologically young volcanic islands where the thermal gradient is even higher than average. Some notable volcanic systems across the islands are, Mt. Liamuigua in St. Kitts, Nevis Peak in Nevis, Soufrière Hills in Montserrat, La Soufrière in Guadeloupe, Soufrière Volcanic Centre in St. Lucia, The Soufrière in St. Vincent, and Kick 'em Jenny (submarine), Ronde/Caille and Mt. St. Catherine all of Grenada (Stewart I 2000).

Coupled with a complex tectonically active region (exhibited by the Caribbean plate as seen in Figure 1) this presents many naturally occurring hydrothermal systems within the Caribbean, as such making certain islands prime for geothermal energy exploitation. Thermal manifestations such as fumaroles, hot springs, dormant and active volcanoes across the Caribbean islands are predominantly associated with the subduction of the North Atlantic crustal plate beneath the Caribbean plate and also being a seismically active region (Huttrer and LaFleur, 2015). A tectonically active regime creates a more advantageous subsurface profile, enhancing permeability at depth, allowing a greater extent of fluid transfer, and can also aid in magma intrusion.



Figure 1: The tectonic plates seen across the Caribbean islands.
Source: Google Earth (2018)

Amongst the fifteen CARICOM member states, the six islands of Dominica, Grenada, Montserrat, St. Lucia, St. Kitts and Nevis, and St. Vincent and the Grenadines all exhibit immense untapped geothermal energy potential. With an exception for the 15 MW geothermal electricity production power plant in Guadeloupe, there is no other established power plant among the CARICOM member states. The geothermal potential for these six islands of interest can be seen in Figure 2, all along the Eastern Caribbean chain of islands (Ochs et al., 2015). Further details into these six islands of interest as

to the resource potential, location, depth of exploratory wells and temperatures are tabulated in Table 1.



Figure 2: Exploitable potential geothermal energy for ECIs of interest

2.2 Energy Security Through Geothermal Exploits

Through carefully controlled conditions an extraction well is positioned into the reservoir to obtain high-enthalpy fluid trapped within the crustal region. The stored energy within the hot geofluid (naturally occurring fluid found in rock formations) in a pressurised form is extracted through steam turbines, rotating a mechanical shaft connected to a generator which produces electricity. It must be noted that the fluid obtained from condensation (energy extracted from the

steam, hence a phase shift to the liquid form) is reinjected back into the reservoir at a calculated depths and radial distances from the extraction well. Hence, injection wells supply fluid back into the reservoir to maintain a sustainable balance, and as a result, this avoids depletion of the resource.

Geothermal sources are classified by their temperature into two main categories: High-enthalpy (exceeding 150 °C) or low-enthalpy (less than 85 °C) (Nicholson, 1993). Regions of high tectonic activity are usually analogous to high-enthalpy sources which can be used for the generation of power and heat, whereas the production of heat is the main use of low-enthalpy sources; all these are in more tectonically indolent regions (Matek, 2014). All six ECIs of interest possess high-enthalpy geothermal resources with temperatures exceeding 150 °C as seen in Table 1. The ECIs have an opportunity to truly become energy independent from conventional fossil fuel importations.

Through the Caribbean Sustainable Energy Roadmap and Strategy (C-SERMS) data are obtained in regard to these six islands national renewable energy targets as a percentage share of the total generation to meet CARICOM’s target of 47 % by 2027, and the respective annual fossil fuel importation costs (for 2015). Apart from St. Vincent, all others can have a 100 % transition to achieve their national target. Furthermore, approximately US\$529 million accounts for fossil fuel importation collectively among the six ECIs as seen in Table 1. The implementation of geothermal power plants can provide reliable baseload power into the energy mix and satisfy energy demands. Section 3.3 of the paper further explores the extent of energy demand and production and the reduction of power required to be transmitted along the grid.

3. Geothermal Resource and Potential

This section delves into matters that will address the issue of possible cases of geothermal energy installations solely across the six ECIs. Therefore, it examines

Table 1. National energy targets, fossil fuel importation and resource potential for the six ECIs

Country	National Target (%) ^a	Annual Fossil Fuel Import Costs ^a	Comments on resource potential ^{b,c,d,e}
Dominica	100	5 % GDP ~ USD 27 million	Wotten Waven area, temperatures above 235 °C were recorded around 1500 m in depth ^b
Grenada	100	18 % GDP ~ USD 159 million	A small solfatara has been revealed through pre-feasibility studies on Mt. St Katherine ^b
Montserrat	100	29 % GDP ~ USD 12 million	The highest recorded temperatures were in well MON-2. This was 265 °C at 2870 m ^c
St. Lucia	100	16 % GDP ~ USD 225 million	Hot resource of 230 °C at moderate depths; hot dry rock up to depths of ~ 2 km ^b
St. Kitts and Nevis	100	4 % GDP ~ USD 33 million	At Nevis, 3 exploratory wells were drilled to depths of 782 m - 1,134 m. All 3 wells encountered temperatures in excess of 225 °C. Reservoir temperature is projected at least 260 °C ^e
St. Vincent and the Grenadines	81	10 % GDP ~ USD 73 million	Exploratory drilling reached depths of 1 km - 3 km, within the presence of temperatures up to 230 °C within the geothermal reservoir ^d

Sources: Compiled from, ^a Ochs et al. (2015), ^b Hutterer and LaFleur (2015), ^c Ryan et al. (2019), ^d Environmental Resource Management (2016), and ^e LaFleur and Hoag (2010)

Table 2. Reconstructed data for geothermal energy installation, generation, avoided fuel imports and greenhouse gas emissions for the six ECIs

Eastern Caribbean Island	Estimated geothermal installed capacity, 2027 (MW) ^a	Estimated annual geothermal electricity generation (GWh/year) ^b	Estimated savings from avoided fuel imports (US\$million/year) ^c	Estimated annual avoided greenhouse gas emissions (million tCO ₂ e/year) ^d
Dominica	19.32	152.32	4.48-8.96	0.12
Grenada	40.48	319.14	9.39-18.77	0.24
Montserrat	2.68	21.13	0.62-1.24	0.02
St. Lucia	50.00	394.20	11.59-23.19	0.30
St. Kitts and Nevis	49.87	393.18	11.56-17.35	0.30
St. Vincent and the Grenadines	22.14*	174.60	5.13-10.27	0.13

b - A 90 % capacity factor is assumed for the geothermal power plants.

c - A conversion factor of 1700 kWh = 1 barrel of oil equivalent (boe) was utilised (SPE 2019), after which an oil price range of US\$ (50 - 100)/bbl was investigated as a minimum and maximum range.

d - An emission factor of 760 gCO₂e/kWh is utilised (Honorio et al., 2003).

*50 % of the oil imports are assumed to be displaced through geothermal energy as a benchmark.

Sources: Compiled from, ^a Ochs et al. (2015), ^c SPE (2019), and ^d Honorio et al. (2003)

future installations in 2027, this is consistent with data obtained from the C-SERMS report. Table 2 is reconstructed data that immediately provides a keen insight into the immense untapped power geothermal energy possesses. The aforementioned of fossil fuel importation collectively among the six ECIs accounted for US\$529 million. This daunting financial burden is shared by all members; however, this can be alleviated through higher penetration rates of renewables. Collectively, there exists an estimated geothermal energy potential of 6280 MW (Ochs et al., 2015).

The manner in which this huge resource is exploited and managed can chart a new financially, climatic and societal course for each nation. Further, details to note in the reconstruction of Table 2 are the reanalysed conversion factors to obtain the number of barrels of oil (bbl) from the calculated MWh/year (SPE, 2019). In addition, the ECIs mainly employ the use of low-speed diesel engines to generate electricity. This results in emissions factors of some 760 gCO₂e/kWh (Honorio et al., 2003).

Realising the potential for geothermal energy integration through distributed generations into the utility across each respective nation presents a major opportunity to increase energy security, whilst improving the balance of trade by reducing oil importation. Furthermore, three crucial advantages are addressed through a higher penetration rate of renewable and geothermal in particular. These three areas are:

1. The economic aspect, in terms of avoided costs, implies saving as a result of the reduction and dependence on fossil fuel-based products.
2. The environmental and climatic aspects in terms of the reduction in the number of barrels of oil imported per year resulting in a beneficial decline in the number of tonnes of carbon dioxide emission avoided.
3. The utility and more so the enhanced grid flexibility of having geothermal energy integration into the national grid.

3.1 Economic Analysis

The possibility of the CARICOM to attain the renewable energy target of 47% by 2027 is ambitious, however, highly probable given the intervention to aggressively pursue geothermal energy implementation. It can be noted from Table 2 that an estimated 184.49 MW of geothermal capacity can be absorbed into the energy mix across invaluable base-load power. A major economic alleviation is certainly realised if the national energy targets are attained as stated in Table 1. The findings clearly show that the reliance on the importation of fossil fuel products for electricity generation can be drastically reduced. It is calculated that an estimated 855,600 bbls through importation can be displaced collectively across all ECIs. A breakdown into the estimated number of bbls per island displaced is illustrated through the label callouts as seen in Figure 3.

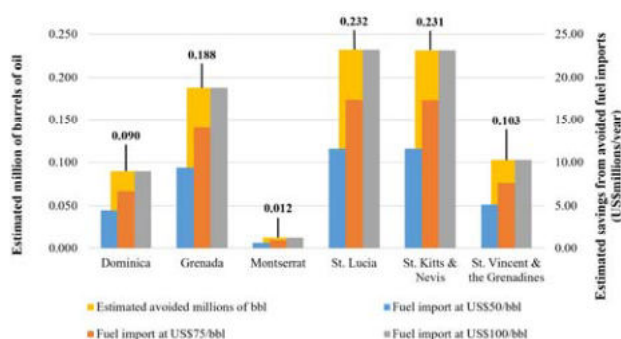


Figure 3: Estimated avoided importation of bbl and perturbed cases of the price per bbl

Three cases are used to further display the idea of the variation of the price per bbl at US\$50.00, US\$75.00 and US\$100.00 accounting for roughly, US\$42.78 M/year, US\$64.17 M/year and US\$85.56 M/year, respectively. It can be noted that Dominica possesses

that largest exploitable potential geothermal resource of 1390 MW, followed by St. Kitts and Nevis (1280 MW) and Grenada (1100 MW), however, this does not necessarily translate to the same order of potential implementation.

3.2 Towards a More Climate-Sensitive Region

The Caribbean islands are geographically positioned at lower latitudes and in direct relation to the vast Atlantic Ocean. The lessons of the 2017 hurricane season and a changing climate regime have clearly illustrated to Caribbean island governments the impacts of extreme events, particularly on energy resilience and security (Klotzbach *et al.*, 2018; Popke and Harrison, 2018). The enhanced drive for higher penetration rates of distributed generations are key to aid in the reduction of greenhouse gases (carbon dioxide in particular) being released into the atmosphere.

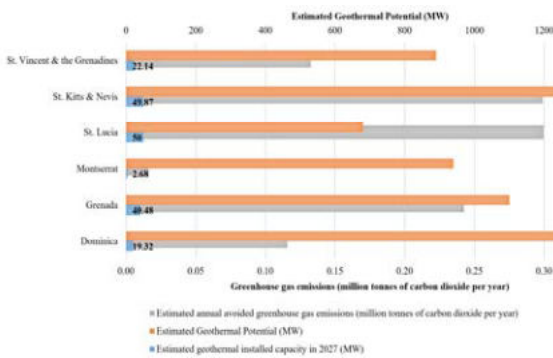


Figure 4: Estimated geothermal potential and installation capacity to displace avoided CO₂ emissions

Potential geothermal generation is estimated at 1.1 million tCO₂e/year collectively across all six ECIs, with a further breakdown per island as seen in Figure 4. Both St. Lucia and St. Kitts and Nevis each exhibits the largest quantities of avoided carbon emission, roughly 0.3 million tCO₂e/year, resulting primarily from each also leading in estimated 2027 installed capacities of 50 MW and 49.87 MW respectively. In addition, geothermal power plants neither releases nitrogen oxide nor particulate matter thus promotes a cleaner environmental impact positively on sustainable tourism as a key driver in many nations.

3.3 Promoting a More Resilient Grid Network

In addition to the installation of geothermal energy among the nations of interest other forms of renewables are being pursued. Solar and wind energy industries are leading the charge in terms of installation and power provided to the national grid. However, the intermittent nature of solar and wind energy adds complexity and variability to the grid. Hence with an increase in the penetration rate of renewables, the national grid must

enhance its flexibility. Grid flexibility is required to incorporate fluctuations in demand throughout the day. Unexpected situations such as malfunctions or climatic conditions can affect the power supply (as with the cases of wind and solar energy). However, geothermal energy provides base-load power, a more reliable form of power. It has a high capacity factor of up to 90 % and is not affected by climatic conditions. Hence a constant power supply can be provided to the grid, without additional costs to enhance its flexibility.

More importantly, the reconstructed data from Table 2, indicates at a capacity factor of 90 %, having a full installation of geothermal power plants by all nations will account for 184.49 MW (1454.52 GWh/year) in 2027, of an averaged peak demand of 335 MW. The dearth and dependence on hydrocarbon resources for most ECIs have resulted in a high importation of fossil fuel to meet their energy demands and thus high rates of electricity. This realisation is clearly illustrated in Figure 5 with nations such as Grenada, Dominica, and St. Lucia having higher than average prices of electricity of US\$0.43/kWh, US\$0.38/kWh and US\$0.34/kWh respectively. However, Grenada, Dominica and St. Lucia are projected to have roughly 60%, 70%, and 45%, respectively of their power to be supplied by geothermal energy in 2027. This will hugely impact their economies providing a much cheaper form of indigenous readily available power.

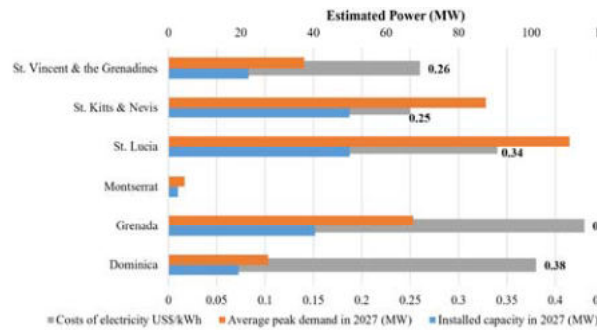


Figure 5: Estimated average peak demand, installed capacity and cost of electricity per island

4. Inter-Island Grid Connections

There have been two inter-island grid connection ideas previously published by Maynard-Date (2015). These two possibilities are the *Dominica-Guadeloupe-Martinique* and *St. Kitts and Nevis* inter-island connection plans. The approximate distance to cover via submarine cables for electrical transmission of high-voltage is about (45-50) km both ways between Guadeloupe - Dominica, and Dominica - Martinique. Clearly, these islands are relatively within proximity to each other to make this plan quite viable. Guadeloupe’s 15 MW geothermal electricity production power plant in

Bouillante is the only such plant currently in the Caribbean. Dominica stands out among the Caribbean islands in terms of geothermal potential. Even the 2027 forecast has Dominica at roughly 1.4 % installed capacity out of its total resource. Such a small percentage of 1.4 % is enough to satisfy approximately 70 % of its power demand in 2027.

Hence Dominica can become a leader within the inter-island grid connection scheme and also across the Caribbean. The other proposed inter-island grid connection scheme is that of *St. Kitts- Nevis*. The distance between these two islands is about 3.5 km (from coast to coast) making the installation of submarine cables even more attractive. Once more roughly 3.9 % of the total resource potential is utilised in the proposed plans at 2027, clearly reiterating the immense potential for power production inherent with geothermal energy exploits.

The realisation of the potential for these inter-island grid connections and for geothermal installation throughout the islands have been hindered by shared challenges. A lack of energy diversification, uncertainty in energy prices (as most energy schemes are based on oil and gas industry prices) are among a few hindrances encountered throughout the Caribbean for the transition to renewables. Geothermal energy inherently possesses a much larger upfront, initial costs when compared to other renewables.

In addition, geothermal energy exploitation and implementation are categorised as a large-scale renewable energy project, and as such many of these ECIs lack the size to self-sufficiently challenge such projects in an attempt to attract volume-oriented international financial markets (Ochs et al., 2015). Therefore, a collaborative stance by groups of nations such as the inter-island plans can prove beneficial to attract and establish financial opportunities on a regional scale and as such is an alternative approach in tackling geothermal energy projects.

5. Conclusion

The Eastern Caribbean islands possess a profound opportunity through the integration of geothermal energy into their national energy mix to ensure a greater sense of energy security, economic diversification, and growth. These high-enthalpy hydrothermal systems collectively provide an estimated energy potential of 6280 MW, as such provides these islands to distinguishably carve massive socioeconomic, and environmental benefits. Extensive documentation through feasibility studies and reports on exploratory wells have confirmed and localised sites of geothermal reservoirs for all six ECIs.

In 2015, importation of fossil fuels accounted for US\$529 million, with Dominica, St. Lucia and Grenada having the highest price of electricity. As such, the findings indicate an estimated 184.49 MW of geothermal capacity can be absorbed into the national energy mix,

displacing 855,600 bbls imports, resulting in approximately 1.1 million tonnes of carbon dioxide emissions being avoided per year. Geothermal integration leads to reliable base-load power to the grid, ensuring cleaner and cheaper power readily available, resulting in an eventual reduction in the price of electricity well below the Caribbean average of US\$0.35/kWh. Finally, the upfront challenges associated to implement large-scale energy project can be tackled through an inter-island grid connection approach to allure financial investors.

References:

- Adams, C., Auld, A., Gluyas, J., and Hogg, S. (2015), "Geothermal energy: The global opportunity", *Proceedings IMechE Part A: Journal of Power and Energy*, Vol.229, No.7; pp.747-754.
- Angeles, M.E., González, J.E., and Ramírez, N. (2018), "Impacts of climate change on building energy demands in the intra-Americas region", *Theoretical and Applied Climatology*, Vol.133, No.1-2, pp.59-72.
- Bhatia, K.T., Vecchi, G.A., Knutson, T.R., Murakami, H., Kossin, J., Dixon, K.W., and Whitlock, C.N. (2019), "Recent increases in tropical cyclone intensification rates", *Nature Communications*, Vol.10, No.1, pp. 635.
- Chen, A. A., and Stephens, A.J. (2018), "Mitigation using solar, wind and batteries in the Caribbean", *Caribbean Quarterly*, Vol.64, No.1, pp.100-113.
- Dickson, M.H., and Fanelli, M. (2005), *Geothermal Energy: Utilisation and Technology*, Earthscan, London, UK.
- Energy Chamber (2017), "Understanding the electricity subsidy in T&T", Accessed on 10th February, 2019. Available at <https://energynow.tt/blog/understanding-the-electricity-subsidy-in-tt>
- Environmental Resource Management (2016), *St. Vincent Geothermal Project Phase I Exploratory Drilling Environmental and Social Impact Assessment (ESIA) Draft Report*, Environmental Resource Management, Washington, April
- Gay, D., Rogers, T., and Shirley, R. (2019), "Small island developing states and their suitability for electric vehicles and vehicle-to-grid services", *Utilities Policy*, Vol.55, pp. 69-78.
- Haraksingh, I. and Koon Koon, R. (2011), "Conceptual model for geothermal energy investigation with emphasis on the Caribbean", *Proceedings of the Thirty-Sixth Workshop on Geothermal Reservoir Engineering*, Stanford University, SGP-TR-191, Stanford, CA, Accessed on, September 29, 2019, Available from : <https://pangea.stanford.edu/ERE/pdf/IGAstandard/SGW/2011/haraksingh.pdf>
- Honorio, L., Bartaire, J., Bauerschmidt, R., Ohman, T., Tihanyi, Z., Zeinhofer, H., Scowcroft, J., and De Janeiro, V. (2003), "Efficiency in Electricity Generation", Accessed on, March 10, 2019, Available from: <http://studylib.net/doc/18037921/efficiency-in-electricitygeneration>
- Huttrer, G., and Joseph, L. (2015), "2015 country update for Eastern Caribbean Nations", *Proceedings World Geothermal Congress*, Melbourne, Accessed on, September 29, 2019, Available from: <https://pangea.stanford.edu/ERE/db/WGC/papers/WGC/2015/01015.pdf>
- IPCC (2018), "Summary for Policymakers", In: Masson-Delmotte, V., Zhai, P., Pörtner, H-O, Roberts, D., Skea, J., Shukla, P.R., Pirani, A., Moufouma-Okia, A., Péan, C., Pidcock, R., Connors, S., Matthews, J.B.R., Chen, Y., Zhou, X., Gomis, M.I., Lonnoy, E., Maycock, E., Tignor, M., and Waterfield, T. (eds.), *Global*

- Warming of 1.5°C. An IPCC Special Report on the impacts of global warming of 1.5°C above pre-industrial levels and related global greenhouse gas emission pathways, in the context of strengthening the global response to the threat of climate change, sustainable development, and efforts to eradicate poverty, World Meteorological Organisation, Geneva, Switzerland, 32 pp.
- Kale, D. (2015), "Geothermal energy", *Proceedings of the Indian National Science Academy*, Vol.81, No.4, pp.993-999. DOI: 10.16943/ptinsa/2015/v81i4/48307
- Klotzbach, P. J., Schreck III, C. J., Collins, J. M., Bell, M. M., Blake, E. S., and Roache, D. (2018), "The extremely active 2017 North Atlantic hurricane season", *Monthly Weather Review*, Vol.146, No.10, pp.3425-3443
- LaFleur, J. and Hoag, R. (2010), "Geothermal exploration on Nevis: A Caribbean success story", *Transactions of the Geothermal Resources Council*, Vol. 34, pp 585-593.
- Matek B. (2014), *Annual U.S. and Global Geothermal Power Production Report*. Geothermal Energy Association, April.
- Maynard-Date, A. (2015), "The Eastern Caribbean Geothermal Energy Interconnection Grid Feasibility Study," *Proceeding the World Geothermal Congress, Melbourne*, Accessed on September 29, 2019, Available from https://pangea.stanford.edu/ERE/db/WGC/papers/WGC/2015/06_047.pdf
- Nicholson, K. (1993), *Geothermal Fluids: Chemistry and Exploration Techniques*, Springer, Berlin
- Ochs, A., Konold, M., Auth, K., Mosolino E., and Killen, P. (2015), *Caribbean Sustainable Energy Roadmap and Strategy (C-SERMS): Baseline Report and Assessment*, Worldwatch Institute, Washington, DC
- Popke, J., and Harrison, C. (2018), "Energy, resilience, and responsibility in post-hurricane Maria Dominica: Ethical and historical perspectives on 'Building Back Better'", *Journal of Extreme Events*, Vol.5, No.4: 1840003.
- Ryan, G.A., and Shalev, E. (2014), "Seismic velocity/temperature correlations and a possible new geothermometer: Insights from exploration of a high-temperature geothermal system on Montserrat, West Indies", *Energies*, Vol.7, No.10, 6689-6720.
- Shirley, R., and Kammen, D. (2015), "Renewable energy sector development in the Caribbean: Current trends and lessons from history", *Energy Policy*, Vol.57, pp.244-252.
- SPE (2019), "Unit conversion factors", Society of Petroleum Engineering, Accessed on, 10th March, 2019. Available at <https://www.spe.org/industry/unit-conversion-factors.php>
- Stewart, I. (2019), "Shuttle radar topography mission, Caribbean volcanoes", Accessed on, March 09, 2019. Available at: www.caribbeanvolcanoes.com/srtm.htm
- Surroop, D., Raghoo, P., and Bundhoo, Z.M.A. (2018), "Comparison of energy systems in Small Island Developing States", *Utilities Policy*, Vol.54, pp.46-54.
- Turcotte, D., and Schubert, G. (2014), *Geodynamics*, 3rd edition, Cambridge University Press, Cambridge, U.K.

Authors' Biographical Notes:

Randy Koon Koon is currently a lecturer in renewable energy at the Department of Physics, The University of the West Indies (UWI), Mona campus. His desire for enhanced renewable energy integration throughout the Caribbean coupled with active research in renewable technologies and energy efficiency methods positions him as an avid renewable energy advocate.

Sheldon Marshall is a postgraduate student pursuing an MSc Renewable Energy Management with special interest in renewable energy technologies and solutions. He is a certified Photovoltaic Associate through the North America Board of Certified Energy Practitioners, thus solidifying his keen interest in renewables.

Dawin Morna is a postgraduate research student in the Department of Physics, UWI, Mona, who is currently pursuing a full-time MPhil degree in Physics. He has a particular interest in Fire Dynamics, Material Science, Optics as well as modelling and simulations of aspects of Raman spectroscopic systems using COMSOL Multiphysics.

Randy McCallum is currently a Secondary School Teacher in Physics who attained a BSc. in Medical Physics at UWI Mona. He has interests in Material Science such as red mud as pozzolan for Portland cement, skid resistance testing using glass and most importantly renewable energy applications particularly because of his time spent at the University.

Masaō Ashtine is Lecturer at The University of the West Indies and has recently completed his doctorate at the University of Cambridge in Geography (climate change implications for the wind energy sector). This follows 6 years at York University in Toronto where he gained his Undergraduate and Masters Degrees in Environmental Sciences and Geography (Climate Science) respectively. With two academic publications (pending submissions as well), Dr. Ashtine is an experienced young academic and professional. His new Lectureship appointment to lead the Alternative Energy Group at The University of the West Indies, Mona (Jamaica), demonstrates his commitment to research within the Caribbean region.

■

An Analysis of the Use of Hydraulic Jet Pumps, Progressive Cavity Pumps and Gas Lift as Suitable Artificial Lift Methods for Heavy Oil Production in East Soldado Reservoirs, Offshore the Southwest Coast of Trinidad

Raffie Hosein^{a,ψ}, and Amrit S. Balgobin^b

Department of Chemical Engineering, Faculty of Engineering, The University of the West Indies, St Augustine, Trinidad and Tobago, West Indies;

^aE-mail: Raffie.Hosein@sta.uwi.edu; Chemical.Engineering@sta.uwi.edu

^bE-mail: amrit.balgobin@bakerhughes.com

^ψ Corresponding Author

(Received 11 November 2018; Revised 12 November 2019; Accepted 21 December 2019)

Abstract: Artificial lift refers to the use of artificial means to increase the flow of oil from a production well when there is insufficient pressure in the reservoir to lift the oil to surface, or in flowing wells to obtain a desired production rate. Generally, this is achieved by the use of a mechanical pump inside the well or by decreasing the weight of the oil column by injecting gas some distance down the well. On platform X in the Soldado field offshore the Southwest coast of Trinidad, gas-lift and to a lesser extent, progressive cavity pumps (PCP), are installed in wells to sustain the desired oil production targets. More recently, hydraulic jet pumps have been installed. However, a performance analysis of these lift systems has never been conducted to determine which one is most suitable for this reservoir. In this study the software PipeSim was used to develop models for the currently installed gas lift and PCP configurations and then optimised to determine the best oil lifting capabilities for these two systems. Similar models were developed for the hydraulic jet pumping system using the SNAPTM software. Data from a pilot well indicate that the optimised installations for gas lift, PCP, and hydraulic jet pumps when sequentially applied are capable of lifting 90, 325, and 450 barrels of fluid per day (bfpd) respectively. These results indicate that hydraulic jet pumps are capable of lifting 40 % more fluids than PCP and 400 % more than gas lift. A lift score analysis between PCP pumps and hydraulic jet pumps was then conducted by comparing lifting potential, installation cost and time, rig vs. non-rig intervention for the installation; and ease of operation and optimisation. The results from this analysis indicate- that the average lift score for hydraulic jet pumps was 4.5 and 2.5 for PCP pumps. These results indicate that in addition to having the highest lifting capability, hydraulic jet pumps are cheaper and easier to install, operate and maintain. It is also a more cost-effective oil lift system compared to PCP pumps. This lift score can also be used as a guide to effectively optimise artificial lift systems for other oil wells from this field.

Keywords: Artificial lift; jet pumps; performance evaluation; increase flow; oil well; Trinidad

1. Introduction

Artificial lift may be defined as the addition of energy to the column of fluid within the wellbore to obtain a higher production rate from the well (Clegg, 1985). This addition of energy is usually applied when the reservoir pressure is declining and the desired production rates cannot be sustained (Hesham and Addou, 2006). The energy addition is by two primary mechanisms:

1. Reduction in column hydrostatic pressure by gas injection
2. The addition of a displacement type device by down-hole pump installation

Both mechanisms increase oil production by reducing the back pressure on the formation allowing for longer economic production periods.

Artificial lift systems can be classified into three primary categories; gas lift; rod pumps/progressive cavity pumps (PCP); hydraulic jet pumps

1.1 Gas Lift

This operation involves the injection of a high pressure gas stream into the production tubing to reduce the fluid column density (see Figure 1). This causes an upward movement of the wellbore fluid to surface as well as greater inflow from the reservoir. This type of lift can be either continuous or intermittent (Vincent et al., 1953). Gas lift is used extensively around the world. A central gas-lift system can easily be used to service many wells or an entire field and lower total capital cost. It is the best artificial lift method for sand or solid materials. The produced sand causes few mechanical problem in the gas-lift system; whereas, only a little sand plays havoc with other pumping methods, except the progressive cavity pumps (PCP). Deviated or crooked holes can be lifted easily with gas lift. This is especially important for offshore platform wells that are usually drilled directionally. Gas lift permits the concurrent use of

wireline equipment, and such downhole equipment is easily and economically serviced. This flexibility allows for routine repairs through the tubing.

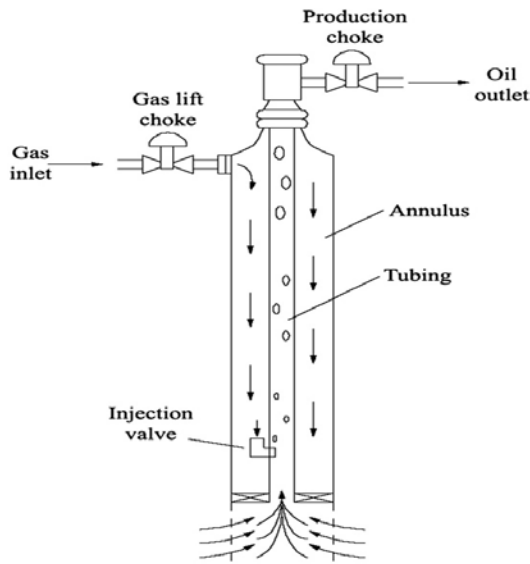


Figure 1. Gas Lift

1.2 Rod Pumps/Progressive Cavity Pumps (PCP)

Rod pumps (see Figure 2) or progressive cavity pumps (PCP) (see Figure 3) assist the flow of fluid from the well bore to surface. Reservoir deliverability is increased as the back pressure on the formation is reduced during the operation (Wang et al., 2010). Rod pumping bottomhole assemblies (BHA) comprise of a plunger, fullbore barrel, flow valve and inflow valve. The up and down reciprocating motion of the plunger produces fluid from the wellbore to surface (Wang et al. 2010).

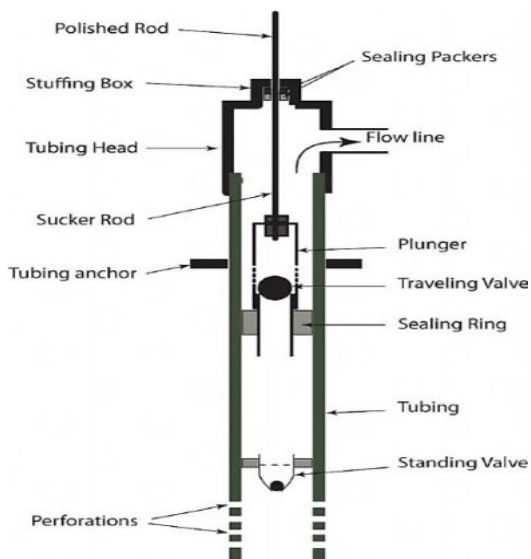


Figure 2. Rod Pump

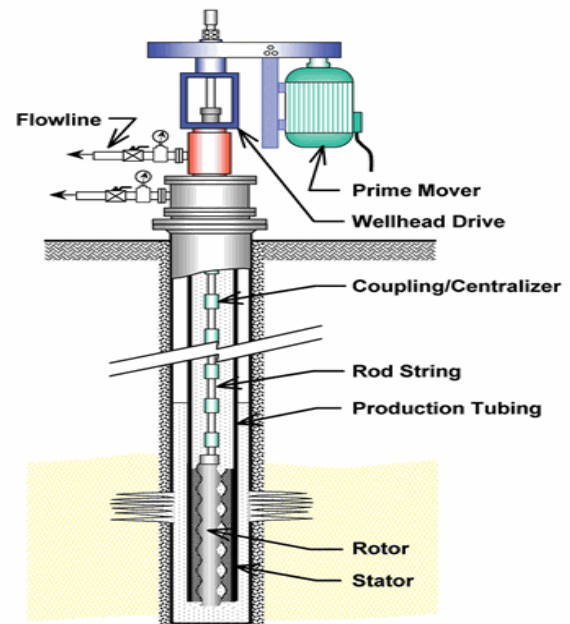


Figure 3. Progressive Cavity Pump (PCP)

Introduced in 1936, the PCP has a simple design and rugged construction. Its low operating speeds (300 to 600 rev/min) enable the pump to maintain long periods of downhole operation, if not subjected to chemical attack or excessive wear or it is not installed at depths greater than 4,000 to 6,000 ft. The pump has only one moving part downhole with no valves to stick, clog, or wear out. The pump will not gas lock and can easily handle viscous heavy oil, sand production. It is not normally plugged by paraffin or scales. PCP BHAs comprise of a rotor and stator. The rotation of the spiral-shaped rotor within the stationary elastomeric stator displaces fluid out of the stator into the production tubing.

1.3 Hydraulic Pump Systems

Jet pumps (see Figure 4) and reciprocating positive-displacement pumps are the two primary hydraulic pumps. The hydraulic jet pump was designed based on the Venturi lift principle (Petrie, 1987). The Venturi effect is created when high pressure/low velocity power fluid (refined oil or produced fluid) is pumped through a nozzle in the pump. Power fluid exiting the nozzle is at high velocity/low pressure. The pressure drop draws in reservoir fluid which mixes with the power fluid in the expansion tube or throat. The mixture fluid changes in the diffuser back to high pressure/low velocity which exit the jet pump housing and travel up the annulus to surface.

Hydraulic pumping is a proven artificial-lift method that has been used since the early 1930s. Successful applications have included setting depths ranging from 500 to 19,000 ft and production rates varying from less than 100 to 20,000 B/D. Hydraulic pumping systems are suitable for wells with deviated or crooked holes that can

cause problems for other types of artificial lift. The surface facilities can have a low profile and may be clustered into a central battery to service numerous wells. The significant feature of jet pumps is being able to easily run the pump in and out of the well. It is especially attractive on offshore platforms and remote locations. Jet pumps can even be used through flowline installations. By changing the power-fluid rate to the pumps, production can be varied from 10 to 100% of pump capacity. It can easily handle viscous heavy oil and sand production.

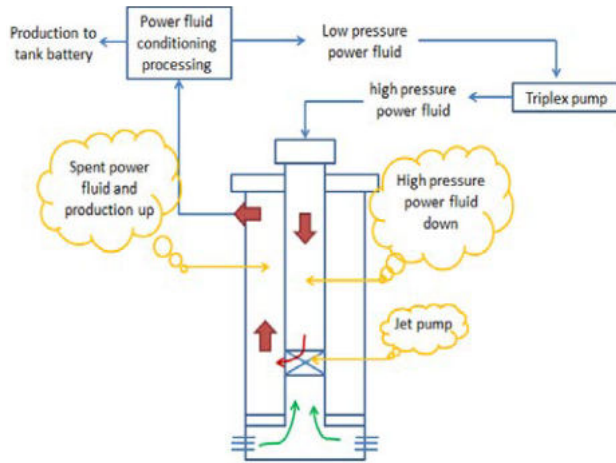


Figure 4. Jet Pump

2. Artificial Lift Monitoring and the Soldado Artificial Lift Experience

Artificial lift systems require continuous monitoring and updating of operating conditions, so as to obtain optimal well productivity. Well and reservoir data are used to model the well potential or inflow performance relationships (IPR) for continuous monitoring of the lift system. IPR curves can be constructed using the relationship between pressure and flow rate described by

Vogel (1968) as:

$$Q_o = (Q_o)_{max} [1 - 0.2(P_{wf} / \bar{p}) - 0.8(P_{wf} / \bar{p})^2]$$

where,

Q_o = oil rate at P_{wf} (STB/day)

$(Q_o)_{max}$ = maximum oil flow rate at zero wellbore pressure, i.e., AOF (STB/day)

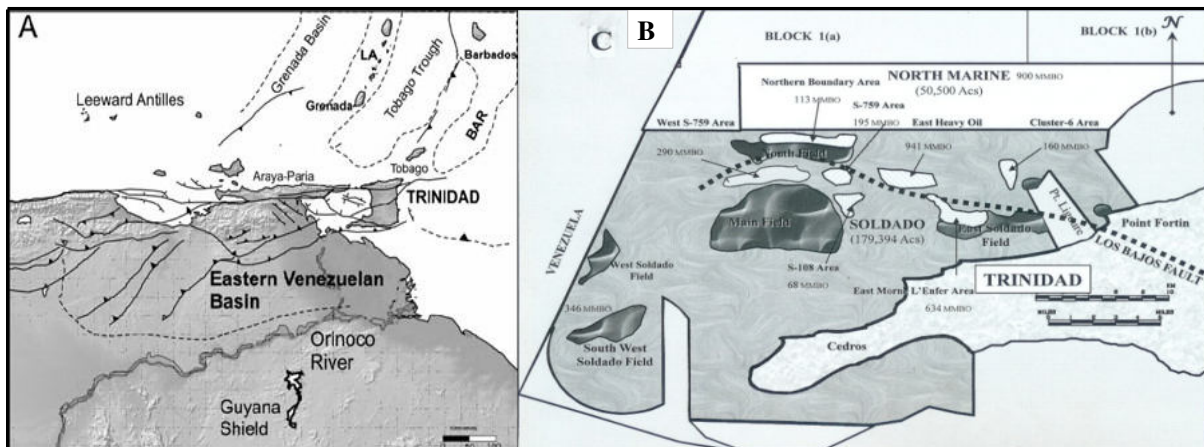
\bar{p} = current average reservoir pressure, psig

P_{wf} = bottom-hole flowing pressure, psig

To use this relationship, the oil production rate; flowing bottom-hole pressure from a production test; and an estimate of the average reservoir pressure at the time of the test must be obtained. With this information, the maximum oil production rate can be estimated and used to estimate the production rates for other flowing bottom-hole pressures, P_{wf} at the current average reservoir pressure, \bar{p} , (Larry and Clegg, 2007). An IPR curve is then generated by plotting surface production rate (STB/d) versus flowing bottom-hole pressure (P_{wf} in psi) on cartesian coordinates. This plot is very useful in estimating well capacity, designing tubing string, and scheduling an artificial lift method.

Trinidad is located East of the Eastern Venezuelan basin; and the Soldado acreage, which had its first oil discovery in 1953, is located offshore the Southwest Coast of Trinidad (see Figure 5). Oil production began in 1957 from the North, Main and East Soldado Fields. Gas lifting operations were implemented in many wells within the North and Main Soldado areas which have low viscosity oil with relatively low GOR's. As deeper reservoirs became pressure depleted, wells were recompleted in shallower horizons with significantly higher oil viscosities. Higher crude viscosities and increased solids production made gas lift a less effective means of sustaining production. Hydraulic pumping was implemented on some wells in the East Field due to high oil viscosities, low reservoir pressures and flow assurance requirements due to wax content. Hydraulic pumping had many challenges which were maintenance related.

Figure 5. Location of Soldado Acreage Offshore the Southwest Coast of Trinidad



Progressive cavity pumping (PCP) was initiated in the Main Soldado Field. The effectiveness of this technology for producing high viscosity oil and formation fines would lead to field wide implementation to boost production in areas that were not amenable to gas lifting operations. This technology requires a rod string to transfer rotational energy down-hole to the rotor – posing a restriction in wells where the inclination exceeds 40° (Wang et al., 2010). Due to platform integrity issues PCP’s are installed on wells across the East Field that is accessible by work-over rigs. This is a major limitation of the existing East Field platform infrastructure limiting the installation of PCP’s to free standing wells.

3. Study Objective and Methodology

The objective of this study was to analyse three artificial lift methods currently applied in the Soldado acreage and to demonstrate which artificial method is most suitable for the Soldado East field heavy oil reservoirs using data from a pilot test well. Installation and operational cost and parameters were then applied to develop a matrix for future selection of suitable artificial lift method for heavy oil application.

Figure 6 shows a workflow of the methodology used. The workflow was divided into three tiers to model the optimum production that can be attained for a pilot well designed to produce oil either under gas lift, PCP or jet pump from platform X for the East Soldado Field.

3.1 Tier-1 Modelling

1. Completion IPR Model (Vogel, 1968)
2. Fluid Viscosity Model (Hossain et al., 2005)

The commercial software PipeSim was used to develop the tier-1 models mentioned above, for determining the deliverability for the pilot well under natural flow and at the deepest artificial lift installation point. The data required for the models are shown in Table 1. These

models were then used as the base for tier-2 models.

Table 1. Reservoir and Wellbore Parameters for Tier-1 Modelling

Reservoir/Wellbore Parameter	Pilot Well
Estimated Reservoir Pressure (psi)	1025
Reservoir Temperature (°F)	125
Reservoir Permeability (mD)	1460
API Oil Gravity (° API)	19
Formation Watercut (%)	72
Gas Oil Ratio (scf/stb)	83
Production Tubing ID (inches)	1.969
Power Tubing ID (inches)	2.441
Last Well Test Rate (blpd)	300
Power Fluid Liquid	Water
Power Fluid Specific Gravity	1.01
Jet Pump Nozzle Diameter (inches)	0.125

Due to the low gas to liquid ratio (GLR) the Pseudo Steady State (PSS) completion model was used. The PSS/Darcy equation (shown below) assumes that the fluid is single phase, laminar flow exists and the fluid is essentially incompressible. A Vogel (1968) correction was applied for liquid flow below the bubble point.

3.1.1 Pseudo-Steady State Flow

$$\bar{p} - P_{wf} = \frac{141.2 q \mu B_o}{kh} [\ln(r_e / r_w) - 0.75]$$

where,

\bar{p} = current average reservoir pressure, psig

P_{wf} = bottom-hole flowing pressure, psig

q = flow rate STB/d

μ = viscosity, cp

B_o = oil formation volume factor, rb/STB

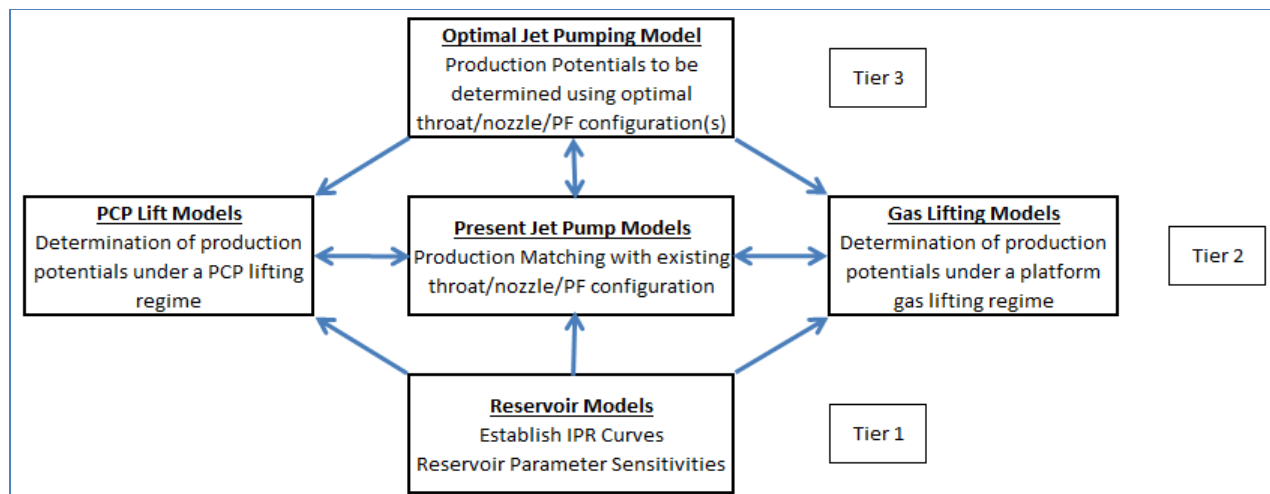
r_e = external (drainage) radius, ft

r_w = well-bore radius, ft

k = permeability, md

h = reservoir thickness, ft

Figure 6. Workflow to Determine a Suitable Artificial Lift Method for the East Soldado Field



3.1.2 Viscosity Model

The Hossain et al. (2005) correlation provide the best prediction for oil viscosity for the East Soldado field. This correlation is valid for heavy oils (10 < API < 22.3) and was used in this study:

$$\mu_{od} = 10^A(T^B)$$

where,

$$A = -0.71523g_{API} + 22.13766$$

$$B = 0.269024g_{API} - 8.268047$$

g_{API} is the API gravity of stock tank oil

3.2 Tier-2 Modelling

The tier-1 models developed for the pilot well were applied in tier-2 modelling for the development of lifting models under gas lift and PCP type regimes, as well as the development of a model for the existing jet pumping configurations. The models were validated using the surface parameters and from production matching (see Appendix 1, Tables A1 and A2). Tier-2 modelling involved:

1. Design and modelling a gas lift type lifting regime to establish a production potential under gas lift conditions using the PipeSim software.
2. Design and modelling a PCP type lifting regime to establish a production potential under PCP conditions using the PipeSm software.
3. Design and modelling a jet pump lifting regime which is representative of the present production conditions and productivity of the pilot well using the SNAP software.

3.3 Tier-3 Modelling

Tier-3 modelling was conducted using the SNAP jet model to determine the production configuration for optimal productivity using the available surface equipment. The production rates from each artificial lift regime were compared to determine the most appropriate lifting regime.

4. Data Analysis and Results

4.1 Tier-1 Model and Results

Static pressure surveys were not available for the pilot well. To confirm the bottom-hole pressure, the following calculation was done using the known fluid column characteristics and wellbore geometry.

Oil Gravity – 18° API

$$\begin{aligned} \text{Oil Specific Gravity} &= 141.5 / \text{Oil API Gravity} + 131.5 \\ &= 141.5 / (18 + 131.5) \\ &= 0.946 \end{aligned}$$

Pilot well watercut – 72%

East Field Water Pressure Gradient – 0.442 psi/ft

Wellbore fluid gradient:

$$= (0.72 * 0.442) + (0.28 * 0.946 * 0.442) = 0.435 \text{ psi/ft}''$$

Mid Perforation Depth – 3,663’ MD; 3,264’ TVD

Well Static Fluid Level from Surface – 884’ MD; 848’ TVD (Perforation Submergence 2416’ TVD)

The wellbore static fluid level correlates directly to the reservoir pressure at the sand-face.

Estimated Reservoir Pressure:

$$\begin{aligned} \text{Reservoir Pressure} &= \text{Pressure Gradient} \times \text{Perforation TVD} \\ &= 0.435 \text{ psi/ft} \times 2416 \text{ft} = 1,050 \text{ psi} \end{aligned}$$

Table 2 shows the reservoir pressures obtained from the calculations.

Table 2. Calculated Reservoir Pressure

Well	Pilot Well
Formation Water Cut (%)	72.0
Well Fluid Gradient (psi/ft)	0.435
Reservoir Pressure (psi)	1,050

The pilot well can produce under natural flow (see Figure 7). This is determined by the intersection of the blue (IPR) curve by the pink (vertical lift performance) curve. Once these two curves intersect at a satisfactory value then artificial lift is not required. If the curves do not intersect or intersect at an undesirable low values, then artificial lift should be considered to improve production rates. Evidence shows the basis for determining feasible production rates for the reservoir/well system (see Figures 7 and 8). Table 3 shows the results of tier-1 model.

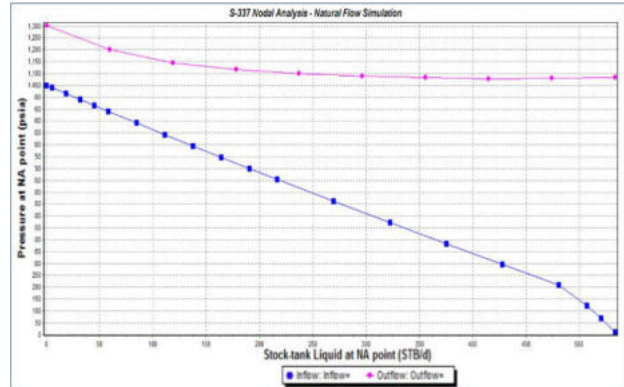


Figure 7. IPR and VLP Curves for Pilot Well

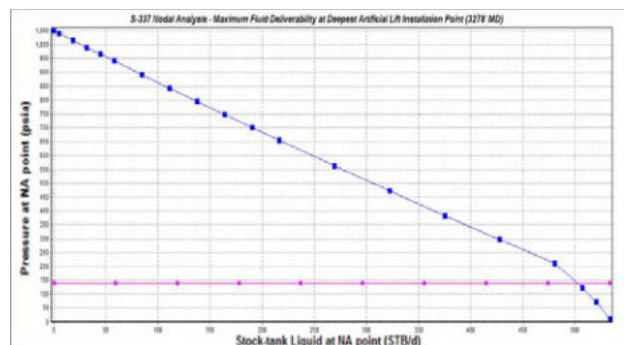


Figure 8. Artificial Lift Confirmation Plot for Pilot Well

Table 3. Tier-1 Model Results

Well	Pilot Well
Artificial Lift Needed	Yes
IPR-VLP Intersection	No
Maximum Potential	510 STB/d

4.2 Tier-2 Model and Results

Tier-2 modelling involved further development of the tier-1 model for the pilot well. Each artificial lift method utilised on platform X (gas lift, PCP and jet pump) was simulated to determine production potential for each lift model for comparison.

4.2.1 Artificial Lift Method 1 – Gas Lift

Considerations:

1. Production tubing size: 2-7/8” 6.5 lb/ft (ID – 2.441”)
2. Gas Lift System details:
 - a. 1200 psi system
 - b. SLB Camco BK-1 Series Valves

Available Injection Gas per well: 0.1 – 0.2 MMscf/d.

Gas lift models were designed using the existing equipment and conditions on platform X. The designs were then applied to the tier-1 model to simulate the production rates under gas lift. The efficiency of this lift regime was analysed using a lift performance plot to determine the maximum production which can be obtained using gas lift and the quantity of gas required for injection for this production.

4.2.2 Pilot Well Gas Lift Potential

Figure 9 shows the results from nodal analyses conducted using platform X gas lift operating conditions and the production potentials (shown in column 3 of Table 4). Figure 10 shows the sensitivities investigated to determine the optimal injection/ production configuration. The maximum potential of the gas lifting regime is shown in columns 5 and 6 of Table 4.

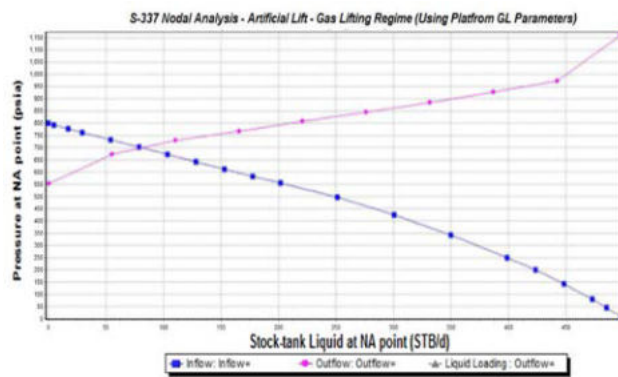


Figure 9. Pilot Well Gas Lift Potential

Table 4. Results from Tier-2 Gas Lift Models

Well	Pilot Well
Design Feasibility at Present Conditions	No
Lift Potential (blpd)	80
Required Injection Gas (MMscf/d)	0.28
Maximum Lift Potential (blpd)	94
Required Injection Gas (MMscf/d)	0.75

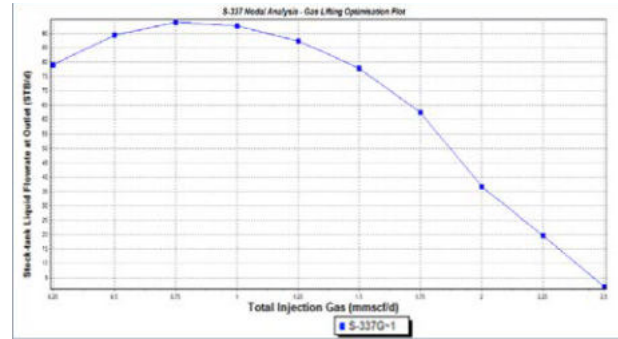


Figure 10. Pilot Well Gas Lift Optimisation Plot

Based on gas lifting operations, the total expected gain is 224 blpd with a required gas injection pressure of 1,200 psi and gas rate of 2.23 MMscf/d.

4.2.3 Artificial Lift Method 2 – Progressive Cavity Pumping

Four assumptions were made to develop the PCP lift model in PipeSim. These are:

1. Pump setting depths (PSD) were estimated to be placed approximately fifty (50’) above the liner top. This would allow for ease in pumping spacing as well as promote higher gas expulsion rates.
2. Standard PCP submergence operating practices were 500’ to 900’ of fluid submergence. This allows for maximum drawdown whilst ensuring the PCP maintains constant fluid contact (for cooling and lubrication).
3. Zero frictional pressure drop within production tubulars.
4. Pump volumetric efficiency of 100% though not possible due to entrained gas in the production stream.

Design Basis for PCP Modelling (S-337):

$$PSD = 3,303' \text{ (TOL)} - 50' = 3,253'$$

Equation 1: PSD Calculation

Determination of FBHP for Scenario 1 – PSD 3,253’ with 900’ submergence:

Mid perforation depth – 3,264’ (TVD)
 Pump depth – 3,253’ MD (2,824’ TVD)

$$BHP \text{ at Pump Depth} = 1,050 \text{ psi} - [(3,264 - 2,824) \times 0.435] = 859.6 \text{ psi}$$

Resultant BHP with a 900’ fluid column:

BHP of system
 = 859.6 psi – (900ft x 0.435 psi/ft) = 533.1 psi

The calculations were repeated for 500’, 700’ and 900’ submergence configurations. Table 5 shows the derived flowing bottom-hole pressures for the aforementioned conditions.

Table 5. PCP FBHP for Submergence at 500, 700 and 900 Feet

Submergence	Flowing Bottom Hole Pressures (psi)
	S-337
500’	380
700’	466
900’	533

The values in Table 5 were applied to the PCP model to replicate the maximum production potentials under a PCP-type regime. This was achieved by determining the inflow into the wellbore by using a drawdown pressure, defined as follows:

Drawdown =
 Reservoir Pressure (P_r) – Flowing Bottom Hole Pressure (FBHP)

4.2.4 Pilot Well PCP Potential

Figure 11 and Table 6 show the results from modelling and installing the resultant PCP design at FBH pressures of 380, 466 and 533 psi, respectively, into the respective tier-1 model.

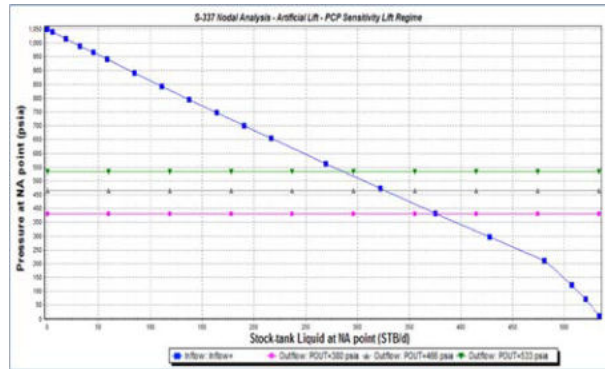


Figure 11. Pilot Well PCP Production Potentials

Table 6. PCP Performance Data for Submergence at 500, 700 and 900 Feet

Well	Pilot	
Design Feasibility at Present Conditions	Yes	
Production Potential for Submergence Specified (BLPD)	500 ft	375
	700ft	325
	900ft	278

Based on empirical data from PCP operations within the East Soldado acreage, a minimum of 700’ of fluid submergence is the optimum trade-off between pump submergence and fluid drawdown. The expected

production from PCP lifting operations (assuming absolute pump volumetric efficiency and ignoring frictional pressure drops) is 325 BLPD. This production is an overestimate of the potential and simulations should be done with PCP modelling software to determine a more accurate production potential.

4.2.5 Artificial Lift Method 3 – Jet Pumping Operations

The objective of tier-2 jet pumping modelling was to develop an accurate model of the existing conditions with the presently installed nozzle-throat configurations in the pilot well. This would be the basis for the first level of jet lift performance comparison and the base model for tier-3 modelling. Figure 12 represents the present potential for the pilot well under the current throat/nozzle/injection pressure regime. A summary of the production potential derived from the jet pump design installed into the tier-1 model is shown in Table 7.

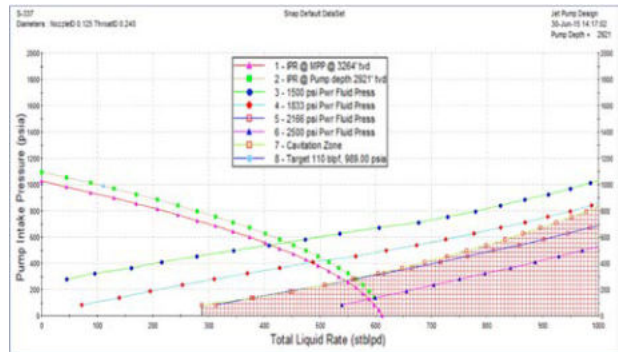


Figure 12. Pilot Well Present Jet Pumping Model

Table 7. Summary of Existing Jet Pump Models

Well	Pilot Well
Production Target, bfpd	410
Injection Pressure, psi	1,560
Power Fluid Required, bfpd	1,300
Throat/Nozzle Size	0.125/0.240

Note: Injection rates were at 900 – 1,100 psi during initial test – October, 2013.

Based on the present designs, the expected production is 410 bfpd. It should be noted that based on simulation sensitivities, the present model have not been optimised. Thus, the jet pumping model developed in tier-2 was then used as the base for tier-3 modelling. Tier-3 was designed to develop optimal jet pumping models to determine the true production capability of the jet pumping system.

4.3 Tier-3 Model and Results

Tier 3 involved the manipulation of tier-2 jet pumping model to obtain an optimal model whilst remaining within the confines of the surface equipment (maximum

pumping pressure of 2,700 psi). It should be noted that three power fluid pumps are available for the delivery of power fluid down-hole. Thus, the operating restriction would be the injection pressure whilst allowing for large volumes of injection fluid to be transmitted. Figure 13 shows the optimised Tier-2 Jet Pumping Model.

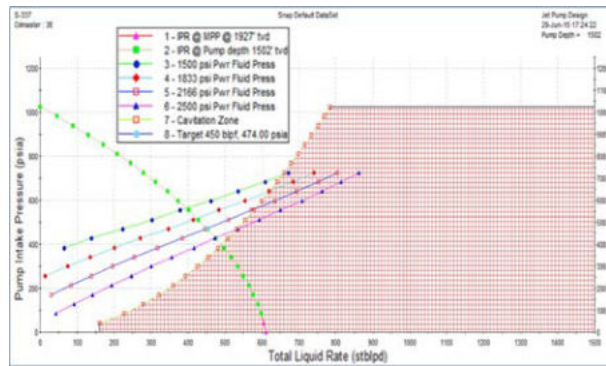


Figure 13. Pilot Well Optimised Jet Pumping Model

Table 8 shows the optimum condition and production potential for the jet pump model determined from this study for the pilot well. The incremental increase in production based on the revised models is 500 bfpd requiring an additional 176 blpd of injection fluid, amounting to a total production of 1,500 bfpd.

Table 8. Optimised Jet Pump Model Parameters

Well	Pilot Well
Production Target, bfpd	450
Injection Pressure, psi	2,166
Power Fluid Required, bfpd	1,150
Throat/Nozzle Size	3E

5. Discussion

The objective of this performance analysis was to determine which artificial lift method is most suitable for heavy oil using the East Soldado field as an example. Based on current well conditions of low GOR's and high water cut, the gas available for injection for gas lift is 0.28 MMscf/d which allows a production rate of 80 bfpd as shown in Figure 10 and Tables 4 and 9.

Figure 11 shows the results from modelling the PCP design at three submergence depths and the corresponding FBH pressures. Under a PCP type regime, a minimum of 700 feet of fluid submergence is the optimum trade-off between pump submergence and fluid drawdown. The expected production from PCP lifting operations (assuming absolute pump volumetric efficiency and ignoring frictional pressure drops) is 325 blpd. Figure 13 and Table 8 show the required injection

pressure and fluid for an optimised jet pump model to produce 450 bfpd using the current well configuration.

Table 9 shows that from these three artificial lift models, hydraulic jet pumps are capable of lifting 40 % more fluids than PCP and 400 % more than gas lift for this heavy oil field. Other reasons contributing to the attractiveness of hydraulic jet pumps are the low installation cost and little set-up time; the existing infrastructure requires minimal surface work; and there is no need for rig intervention.

Table 9. Production Potential Comparison for Artificial Lift Studied

Well Studied		Pilot
Deepest Lifting Point		3,278 ft
Maximum Potential (bfpd)		505
Production via Artificial Lift Method (bfpd)	PCP	325
	Jet Pump	450
	Gas Lift	80

The tier-2 jet pump models were modified for increased production and for the prevention of pump cavitation. A matrix was developed to compare and rank each lifting method: 1 – Poor/Undesirable, 2 – Tolerable, 3 – Fair, 4 – Excellent, and 5 – Ideal. Cost evaluations were done relative to the method with the lowest criteria cost. Based on Table 10, using hydraulic jet pumps is the most efficient and cost-effective artificial lift method for the Soldado East Field with a total score of 4.5.

The limitations to this study were identified as:

1. Pressure surveys for the reservoirs under study were not available. Thus, reservoir pressure had to be calculated using static fluid stream existing in the wellbore.
2. Individual well tests data were unavailable due to test trap system on the platform. Platform X testing system utilises a test separator (operating at 50 psi) with all fluids from the separator proceeding to a 3 bbl metering vessel. Testing jet pumping well resulted in flooding the separator due to the high GLR of the system and volume of liquid being tested.

6. Conclusions

Based on the analysis, it can be concluded that jet pumps are capable of lifting 40% more fluids than PCP and 400% more than gas lift for the East Soldado Field. A lift score analysis was developed in this study between PCP pumps, hydraulic jet pumps and gas lift.

The results indicate that hydraulic jet pumps are cheaper and easier to install, operate and maintain. Moreover, this lift score analysis can be applied to determine the most suitable artificial lift method for other fields in the Soldado acreage.

Table 10. Artificial Lift Comparison Matrix

Criterion	Progressive Cavity Pumping	Hydraulic Jet Pumping	Gas Lifting
Production Potential	325 bfpd requiring electric power Production Potential – Optimistic PCP simulations done ignoring frictional pressure from and assuming 100% pump efficiency. Score: 3	450 bfpd requiring 1,150 bfpd PF Production Potential – Realistic Low resource cost as water is utilised as power fluid and the PF is fully recycled through continuous operations. Score: 5 (1,150 bfpd – stream recycled)	80 bfpd requiring 0.28 MMscf/d Production Potential – Realistic High resource demands as produced low GOR's and watercut impose gas demands on field. Score: 1 (1.25 Mscf/bfpd - poor)
Installation Cost	High Investment Cost required for PCP installation as Winch work (Rig) is required for pump installation. High costs for PCP pumps. High surface equipment cost for PCP Drivehead, Power generation equipment and transmission system. Score: 1	Low Investment Cost required for Jet Pump Installation. No rig intervention required – wireline operations only. Minimal Jet Pump Cost Moderate Surface equipment (PF pump and PF Tank) cost. Score: 4	High Investment Cost required for Gas Lift installation. Rig intervention required for placement of gas lifting string. Costly GL Mandrels and Valves required. Moderate surface equipment (Nat. Gas Compressor) costs. Score: 2
Installation Time	Lengthy Installation time as complete installation requires two tubular trips (Tubing String with stator + Rod String with rotor), wellhead and drivehead placement and electrical connection required. Score: 1	Low installation time as components can be transferred and installed using wireline. Trips required 2 – tubing stop profile and jet pump assembly. Moderate time required for PF transmission lines (if not in place). Score: 4	Lengthy installation time required for the makeup and placement of a gas lifting string with gas lift mandrels and valves. Moderate time required for Gas transmission lines (if not in place). Score: 3
Start-up Time (First Oil)	Moderate start-up time. Process requires power system hook-up and completion fluid offloading. Score: 4	Minimal start-up time. No offloading required as well control is not required. PF pump start-up = first oil Score: 5	Moderate start-up time. Process requires Gas system hook-up and completion fluid offloading. Score: 3
Ease Of Optimisation/ System Change-out	Optimisation resources minimal but range is limited (if VED is present). Drastic optimisation efforts require rig intervention for pump change out. Score: 2	Initial Optimisation resources required – minimal (PF pump pressure/rate adjustment). Drastic optimisation efforts requires wireline operations for pump replacement Score: 4	Initial Optimisation resources required – requires wireline operations for valve replacement. Drastic optimisation efforts require rig intervention. Score: 1
Chemical Injection Complexity/Cost	Injection requires chemical injection mandrel, valve and transmission line for downhole placement. Score: 3	Chemical can be injected and placement downhole by mixing with injection fluid within fluid reservoir/PF transmission line. Score: 5	Injection requires chemical injection mandrel, valve and transmission line for downhole placement. Score: 3
Average Lift Score	2.3	4.5	2.2

Source: Abstracted from Balgobin (2015)

Appendix 1: Well Test Data

Table A1 shows the production test data used to production match modelling parameters in Tier 1. Table A2 shows the tank test data used for production matching Tier-2 Jet Pumping Models.

Table A1. Jet Pumping Test Data for Pilot Well

Date	Test Oil (bpd)	Test Water (bpd)	Gross Fluid (bpd)	Watercut (%)
23/05/13	51.62	105.38	157	71.7
24/05/13	45.58	115.42	161	71.7
25/05/13	37.37	94.63	132	71.7

Table A2. Well Test Data after Jet Pumps were Installed

Date	Rate (bbl/hr)	Rate (bbl/day)
Oct, 2013	24.6	590.4
Nov, 2013	23.2	556.8
Dec, 2013	20.0	480.0
Jan, 2014	15.0	360.0
Feb, 2014	10.0	240.0
Mar, 2014	8.0	192.0
April, 2014	5.5	132.0
June, 2014 – Jan, 2015	0.0 – 1.4	0 – 33.6
Feb, 2015	23.3	599.2
April, 2105	25.1	602.4

References:

- Balgobin, A. (2015), *An Evaluation of the Use of Hydraulic Jet Pumps as an Efficient and Economic Means of Artificial Lift in East Soldado Reservoirs*, MSc Project Report, The University of the West Indies, St. Augustine, Trinidad and Tobago.
- Clegg, J.D., Bucaram, S.M., and Hein, N.M., Jr. (1993), "Recommendations and comparisons for selecting artificial-lift methods", *Journal of Petroleum Technology*, December, pp.1128-1167
- Hesham, A.M. and Addou, A. (2006), "Jet pump performance with secondary fluids differ in density and viscosity from primary fluid", Paper presented at *The SPE's Annual Technical Conference and Exhibition*, Abu Dhabi, UAE, November 5-8
- Hossain, M.S., Sarica, C., Zhang, H.Q., Rhyne, L. and Greenhill, K. (2005), "Assessment and development of heavy-oil viscosity correlations" (SPE 97907), Paper presented at *The SPE International Thermal Operations and Heavy Oil Symposium*, , November, Calgary
- Larry, W.L. and Clegg, D.J. (2007), *Petroleum Engineering Handbook: Production Operations Engineering*, Vol IV, Society of Petroleum Engineers, Richardson, TX 75080-2040, USA
- Petrie, H.W. (1987), *Hydraulic Pumping*, (Chapter 6), Society of Petroleum Engineers
- Vincent, R.P. and Wilder, L.B. (1953), "A new gas lift system", Paper Presented at *The Fall Meeting of the Petroleum Branch of AIME*, Dallas, Texas, October, 19-21
- Vogel, J.V. (1968), "Inflow performance relationships for solution gas drive wells", *Journal of Petroleum Technology*, Vol.20 January, pp 83-89.

- Wang, H., and Yang, D. (2010), "Reliability improvement of progressive cavity pump in a deep heavy oil reservoir", Society of Petroleum Engineers, doi:10.2118/137271-MS

Authors' Biographical Notes:

Raffie Hosein is Senior Lecturer and the Head of the Department of Chemical Engineering and Coordinator of the MSc Reservoir Engineering Programme at The University of the West Indies (UWI), Trinidad and Tobago. Previously, he worked as a Petroleum Engineer with the Ministry of Energy and Energy Industries in Trinidad and later, as Senior Associate Professor in the Department of Petroleum Engineering at Texas A&M University at Qatar. Dr. Hosein received his B.Sc., M.Phil., and Ph.D. degrees in Petroleum Engineering from The UWI. He holds a CEng status, a MEI Chartered Petroleum Engineer with the Energy Institute of London and a Fellow with the Institute of Materials, Minerals and Mining (FIMMM) also of London. In 2018, Dr. Hosein received from the Society of Petroleum Engineers (SPE) the Regional Distinguished Achievement Award for Petroleum Engineering Faculty - Latin America and Caribbean Region.

Amrit S. Balgobin is a Technical Support Engineer with Baker Hughes, Gulf of Mexico region, Trinidad Operations. He received his B.Sc. in Chemical and Process Engineering and then his MSc in Petroleum Engineering from The University of the West Indies, Trinidad and Tobago.

■

Physicochemical and Functional Properties of Starch from Ackee (*Blighia sapida*) Seeds

O'Neil Falloon^a, Saheeda Mujaffar^{b,ψ}, and Donna Minott^c

^aFood Science and Technology Unit, Department of Chemical Engineering, The University of the West Indies, St. Augustine, Trinidad and Tobago, West Indies; E-mail: ofalloon@hotmail.com

^bFood Science and Technology Unit, Department of Chemical Engineering, The University of the West Indies, St. Augustine, Trinidad and Tobago, West Indies; E-mail: saheeda.mujaffar@sta.uwi.edu

^cDepartment of Chemistry, The University of the West Indies, Mona, Kingston 7, Jamaica, West Indies; E-mail: donna.minott@uwimona.edu.jm

^ψ Corresponding Author

(Received 26 July 2019; Revised 18 November 2019; Accepted 10 December 2019)

Abstract: Seeds of the ackee fruit are high in starch content and are a major waste product of the ackee aril canning industry. The objective of this study was to investigate the physicochemical and functional properties of isolated ackee seed starch. De-hulled seeds were dried and milled into 'flour' which was defatted by Soxhlet extraction using petroleum ether. Starch extraction was carried out using 0.2% w/v NaOH solution (24°C, 6 h) and the starch residue soaked in aqueous NaOH (0.05% w/v) for 12 h to remove soluble impurities and then subjected to a bleaching treatment (HCl, 0.01 N). Solubility, swelling power, water absorption, oil absorption and extent of syneresis of the starch were measured and hypoglycin content was determined by reversed phase HPLC. Pasting, thermal properties, crystalline pattern, granule morphology and gel texture were determined, and the gelatinised starch used to prepare retrograded resistant starch. Ackee seed starch comprised small granules which exhibit a C-type diffraction pattern. The starch showed restricted swelling, moderate peak viscosity, and low breakdown compared with commercial corn and potato starches, while the water absorption and oil absorption values were similar to the commercial starches. Ackee starch had a high setback, high syneresis, produced opaque pastes and formed a hard gel texture. Apparent amylose content and the content of retrograded starch were high. Based on the properties, the starch may be suitable in manufacturing of noodles and to produce retrograded resistant starch and may have applications in fat replacers, dusting/face powders and bioplastics.

Keywords: Ackee seed, starch, properties, physicochemical, functional

1. Introduction

The ackee plant is a tropical to sub-tropical tree, originated from West Africa, and it can be found in most islands of the West Indies, Central America and Southern Florida. When the fruit is mature, the red or yellow pod splits open to reveal cream-coloured or light-yellow arils attached to a glossy, spherical black seed (see Figure 1).

Only the mature arils are edible as the immature fruits contain the toxic cyclopropyl non-protein amino acid hypoglycin A (HGA). The seeds of the fruit contain HGA as well as hypoglycin B (HGB), a glutamyl conjugate of HGA (Hassall and Reyle, 1955).

Canned mature ackee arils are produced in Jamaica, Haiti and Belize, and exported to the United States of America (USA), Canada and the United Kingdom (UK). The value of ackee exports from Jamaica averaged 15.6K USD in 2018 (Statistical Institute of Jamaica (STATIN), 2019). Unlike ackee arils, the seeds have no commercial value and are often discarded as a waste

residue of the ackee canning industry (Hyatt, 2006). The seeds are, however, rich in starch (44.2%), protein (22.4%) and fat (21.6%) (Djenontin et al., 2009). Ackee seeds comprise a shiny black protective outer shell that strongly adheres to the cream-coloured cotyledons (Morton, 1987) (see Figure 2).

A few pioneering works have investigated the properties of the ackee seed 'flour' (from whole and de-hulled seeds) and the extraction of starch from the ackee seeds (Abiodun et al., 2015a, 2015b; 2018). Abiodun et al. (2015a) reported on several properties of ackee seed starch isolated from de-hulled seed flour, including amylose content, granules size, swelling properties and paste clarity and viscosity. They reported that ackee seed starch has a relatively high amylose content ($41.5 \pm 1.0\%$), small granules ($6.5 \mu\text{m}$), restricted swelling ($9.68 \text{ g gel/ g starch at } 90^\circ\text{C}$) and produced opaque pastes (light transmission $0.70 \pm 0.11\%$). Additionally, the starch was found to have a low viscosity breakdown (1978 cP), but setback was high (4664 cP).



Figure 1. Mature Ackee Fruit (left) and Immature Ackee Fruit (right)



Figure 2. Ackee Seed (a) whole (b) cotyledon and shell

Abiodun et al. (2015b) reported the whole seed flour to have a carbohydrate content of 59.2% and a swelling power of 8.3 g gel/g flour at 90°C. Additionally, the flour was found to have a lower setback (157.6 cP) compared with the corresponding starch.

In a further study, Abiodun et al. (2018) studied the effect of chemical modification (acid, alkali, acetylation and oxidation) and physical modification (pre-gelatinisation) on the properties of ackee seed starch isolated from de-hulled seed flour. Paste clarity was improved by pre-gelatinisation; however, none of the chemical modifications resulted in increased light transmittance of the starch paste nor improved the freeze-thaw stability of the starch. The starch treated with alkali (2.5% NaOH, pH 10.5) was found to have a higher peak viscosity than the native starch, and the starch was more stable towards heat and shear when treated with acid or alkali, oxidised or pre-gelatinised. All the modifications investigated resulted in an improvement (reduction) in the setback values of the starch.

Previous works on starch isolation were based on an extraction method used for yams and starchy tubers, which do not contain significant quantities of lipids and proteins. Ackee seeds, however, have high lipid and protein contents (up to 20% dry weight each) (Djenontin et al., 2009; Esuoso and Odetokun, 1995). Previous works did not report on the protein content of the isolated ackee seed starch and did not include a defatting step to remove lipids. Lipids are reported to restrict swelling and solubility of granules, and reduce light transmission of starch pastes, hence resulting in opaque

pastes (Alcazar-Alay and Meireles, 2015; Chinma et al., 2012).

The objective of this study was to deepen the characterisation studies of native ackee seed starch through the isolation of starch from defatted seed flour and assessment of physicochemical and functional properties of the starch. Based on the results of the characterisation of the ackee seed starch, possible applications are presented. All analyses (physicochemical and functional properties) were repeated using commercial corn and potato starches for comparison purposes.

2. Materials and Methods

Ackee seeds were collected directly from canned ackee processors. Seeds were manually de-hulled and dried (60°C, 24h) in a forced draft convection oven (Environette, Lab Line Instruments Inc., Illinois). Dried seeds were milled (Model 4-E Quaker City Mill, The Straub Company, Philadelphia) to pass through a sieve (pore size 0.5 mm) and the flour was defatted by Soxhlet extraction using petroleum ether (b.p. 60-80°C).

Starch was isolated from ackee seeds according to a method developed by Falloon (2019, unpublished) to determine an optimum steeping condition in terms of starch recovery and colour. Starch extraction consisted of steeping the defatted flour in an extracting solution of 0.2% sodium hydroxide (NaOH, 1:10 w/v, 24°C, 6 h), soaking in aqueous NaOH (0.05% w/v, 12 h) to remove contaminating proteins, hypoglycin toxins and other soluble impurities, and washing the starch residue in hydrochloric acid (0.01 N) to improve starch whiteness. The starch slurry was dried in a convection oven (37°C ± 2°C, 48 h), ground to a powder (0.5 mm) and stored in re-sealable LDPE bags at 4°C. The process steps are shown in Figure 3.

Chemical composition (g/100 g starch wet weight basis) of ackee seed starch and commercial corn and potato starches was determined using standard analytical methods: moisture (AOAC (2012) Official Method 930.15), total starch (AOAC (2012) Official Method 996.11), crude protein (AOAC (2012) Official Method 2001.11), crude fat (AOAC (2012) Official Method 945.16), damaged starch (AOAC (2012) Official Method 942.05), and apparent amylose (AACC (1999) Method 61-03). Hypoglycin A (HGA) and Hypoglycin B (HGB) contents of starch from ackee seeds were determined by reversed phase HPLC as described by Sarwar and Botting (1994). The analyses were done using four replicates.

Granule size and morphology of ackee seed, corn and potato starch granules were determined using a light microscope and a scanning electron microscope (SEM) according to the method of Pérez et al. (2011). For light microscope, a 2% aqueous starch suspension was stained using iodine solution (3.5 x 10⁻³ N). The granules were viewed on a light microscope at x 40 and x 100

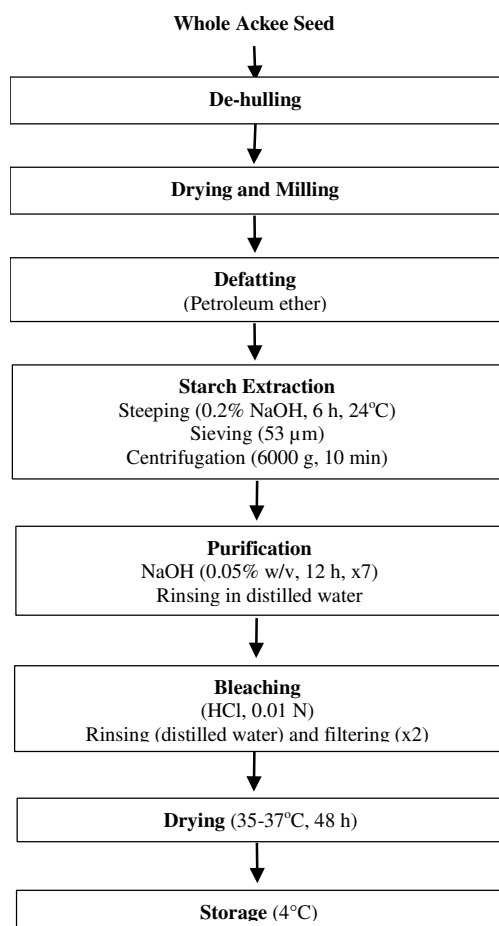


Figure 3. Starch Isolation from Ackee Seed Defatted Flour

magnifications. In the case of SEM (Phillips SEM 515, Denton), starch samples were placed on an electrically ground adhesive tape and coated (EM Sputter Coater) with a thin layer (15 - 40 nm) of gold in an argon atmosphere. The starch granules were viewed at a magnification of x 2500 at 30 kV. Granular diameters were measured using a Gatan Microscopy Suite (GMS 3) software (Gatan, Inc., Pleasanton, CA 94588).

X-Ray diffraction pattern of ackee seeds, corn and potato starches was determined based on the method described by Nwokocha and Williams (2011). Starch samples were heated in a convection oven (Thelco Laboratory Oven, Thermo Electron Corporation, Winchester, Virginia) at 50°C for 24 h. Step-scanned X-ray diffraction patterns for starches were collected on a diffractometer (D2 Phaser, Bruker Corporation, Billerica, Massachusetts) using the DIFFRAC.SUITE V. 3.0 software (Bruker Corporation). The X-Ray source operated at 40 keV and 20 mA with a Cu target and graphite - monochromator radiation $K\alpha$ radiation ($\lambda = 1.5406$). Data were collected by a step-scanned method between 2° to 40° in 2 θ angle (1.2°/min).

Thermal properties of ackee seed, corn and potato starches were determined according to Hussain (2015)

using a Differential Scanning Calorimeter (DSC) (Setaram Micro DSC III). A 1:3 starch/water slurry was prepared, equilibrated to ambient temperature and heated in the DSC from 5°C to 110°C at 2°C/min. Distilled water was used as reference and data analysed using Setsoft 2000 software V. 3.0.6 (Setaram Inc, Cranbury, NJ 08512). Melting enthalpy and temperature axis were calibrated with standard metals. Onset of gelatinisation temperature (°C), peak temperature (°C), conclusion gelatinisation temperature (°C), and gelatinisation enthalpy (J/g) were determined from the resulting thermograms.

Water absorption capacity (WAC) of starches was determined according to the method described by Yadav et al. (2016). Aqueous starch suspensions (1:10 w/v) were stirred for 30 minutes at 25°C on a magnetic stirring plate and the mixtures centrifuged at 2000g for 10 min. WAC (g H₂O/g starch) was calculated according to Equation (1). Oil Absorption Capacity (OAC) was calculated in the same manner except that oil was used instead of water.

$$WAC = \frac{\text{Weight Starch } g_{\text{final}} - \text{Weight Starch } g_{\text{initial}}}{\text{Weight Starch } g_{\text{initial}}} \quad (1)$$

Swelling power (g gel/g starch) and solubility (%) of the starches were based on the method described by Torruco-Uco and Betancur-Ancona (2007). Aqueous starch suspensions (1:10 w/v) were heated in a water bath at 30°C ± 1°C for 30 minutes with constant agitation, centrifuged (12,000 g, 10 minutes) and the supernatants dried in a convection oven at 120°C for 4 h. The weight (g) of the water-saturated starch sediment and the dried soluble starch were recorded. The experiment was repeated at temperatures of 40°C, 50°C, 60°C, 70°C, 80°C, 90°C and 95°C. Solubility and swelling power were calculated using equations (2) and (3) respectively, using four replicates.

$$\% \text{ Solubility } (S) = \left[\frac{\text{Weight Dried Solubilised Starch } g}{\text{Weight Starch Initial } g} \right] \times 100 \quad (2)$$

$$\text{Swelling Power } (g \text{ gel/g Starch}) = \frac{\text{Weight swollen starch granules } g}{\text{Weight Starch Initial } g - [(\% \text{ Solubility}/100) \times \text{Weight Starch Initial } g]} \quad (3)$$

Pasting properties (peak viscosity (cP), breakdown (cP), set back (cP) and pasting temperature (°C) of the starches were determined, in triplicates, using a Rapid Visco Analyser, RVA 4 Stand-alone (Newport Scientific, Warriewood, Australia) according to Method 76-21 STD1 of the American Association of Cereal Chemists (AACC) (1999). The effects of pH on pasting properties were also investigated. The pH of the mixture was adjusted to 3.0, 5.0, 7.0 or 9.0 by dropwise addition of HCl (0.1N) or NaOH (0.1N).

Paste clarity (% transmission) was determined according to the method described by Hassan et al. (2013). Aqueous starch suspensions (1% w/v) from ackee seed, corn and potato were prepared in triplicate and heated (95°C, 1 h) and cooled to 25°C. Initial paste

clarity was determined by measuring the percentage light transmission of the pastes at 640 nm using a UV-VIS spectrophotometer (Evolution 60S, Thermo Scientific, Madison, WI). Starch pastes were stored at 4°C, and light transmittance measured every 24 h for 6 days.

Starch syneresis (%) was determined based on the method described by Torruco-Uco and Betancur-Ancona (2007). Aqueous starch suspensions (6% w/v) were first heated to 95°C for 15 min, held at 50°C for 15 min, then cooled to 25°C. The starch pastes were centrifuged (8000g, 10 minutes). The starch gels were stored at 4°C, and the extent of syneresis determined after 48 h, 72 h, 96 h and 120 h. Percentage syneresis was calculated according to equation (4). Freeze-thaw stability (% syneresis at -18°C) was assessed using the procedure described for syneresis except that gels were stored at -18°C.

$\% \text{ Syneresis} =$

$$\frac{(\text{Weight gel initial g} - \text{Weight gel after storage g}) \times 100}{\text{Weight gel Initial g}} \quad (4)$$

Gel Texture was assessed using the method described by Sun et al. (2014). Aqueous starch suspensions (10% w/v) were heated in the Rapid Visco Analyser (RVA) according to Method 76-21 STD1 of the AACC (1999) to produce starch pastes. The pastes were cooled to ambient temperature and sealed with paraffin film and stored at 4°C for 8 h. Texture parameters were analysed using the Brookfield QTS-25 Texture Analyser using a cylindrical probe (dia 12 mm) at a penetration depth of 10 mm (0.5 mm/s). Hardness (N), adhesiveness (gs), chewiness (gs), springiness (mm), cohesiveness and gumminess (g) were calculated using the TexturePro Version 2.0 software (CNS Farnell, Borehamwood WD61RX, UK). The experiment was repeated by storing the starch pastes at 25°C for 8 h. Analyses were done using three replicates.

Retrograded starch was prepared according to the method described by Sajilata et al. (2006). A 10% starch suspension was heated in a water bath at 95°C for 30 minutes with constant agitation. The resulting starch pastes were further heated in an autoclave at 121°C for 20 minutes, cooled to 25°C and immediately stored at -18°C for 24 h. A portion of the starch paste (15g) was thawed at 25°C for 2 h, dried at 50°C (24 h) in a Precision convection oven (J'Quan Inc., Winchester, Virginia), milled and stored at 4°C. The remaining starch paste was used for two additional autoclave/freezing-thaw cycles. The resistant starch content of the retrograded starches (% dry weight) was determined according to the AOAC (2012) Official Method 2002.02. The experiment was done in triplicate.

Statistical analyses were performed using IBM SPSS Statistics Version 21 (2015) (IBM Corporation, Armonk, New York) and Microsoft Office Excel 2013 (Microsoft Corporation, Redmond, Washington).

3. Results and Discussion

3.1 Chemical Composition

The starch and moisture contents (% wb) of whole and de-hulled seeds and defatted flour are presented in Table 1. The moisture content of de-hulled seeds averaged 50.46 % (wb) or 1.23 g H₂O/g dm. The starch content of whole seeds, de-hulled seeds and defatted flour ranged from 15.42 to 56.31% (wb) or 0.34 to 0.60 g/g DM, respectively. The dry matter content of de-hulled ackee seed flour reported by Abiodun et al. (2015a) was 32.94% (wb).

Table 1. Starch and Moisture Content of Ackee Seed

Component	Ackee Sample		
	Whole Seeds	De-hulled Seeds	Defatted flour
Moisture %wb	55.24 ± 0.89 ^c	50.46 ± 1.11 ^b	5.99 ± 0.55 ^a
Starch %wb	15.42 ± 0.27 ^a	21.74 ± 0.58 ^b	56.31 ± 1.51 ^c

Values represent mean ± standard deviation, N = 3;

^{a-c} Values sharing at least one letter in a row are not significantly different (95% CI)

In this study, the starch yield (%) from the defatted flour averaged 45.13 ± 1.75% which is higher than the 14.31% reported by Abiodun et al. (2015a) for de-hulled seed flour, possibly because the seed flour used in that study was not defatted. In this study, the starch yield (%) from the whole seeds with shell averaged 13.47 ± 0.51%.

The chemical composition of the isolated ackee seed starch and commercial starches is given in Table 2. The moisture content of the isolated starch averaged 12.03% (wb) or 0.14 g H₂O/g dm and was within the normal range expected for starches (Thomas and Atwell, 1999). For all starches, crude fat and protein was less than 0.1% (wb). The process used to isolate starch from ackee seeds was therefore very effective in removing both fat and protein.

Table 2. Chemical Composition of Starches

Component (% wb)	Ackee Sample		
	Ackee Seed	Corn	Potato
Moisture	12.03 ± 0.55 ^b	9.51 ± 0.19 ^a	13.19 ± 0.27 ^c
Crude Protein	0.08 ± 0.01	0.09 ± 0.015	0.10 ± 0.01
Crude Fat	0.07 ± 0.01	0.09 ± 0.021	0.08 ± 0.01
Ash	0.13 ± 0.01 ^a	0.12 ± 0.010 ^a	0.28 ± 0.03 ^b
Total Starch (Purity)	82.59 ± 2.09	82.54 ± 2.31	82.90 ± 1.49
Apparent Amylose	34.26 ± 0.20 ^b	27.62 ± 0.60 ^a	34.25 ± 0.40 ^b
Damaged Starch	1.59 ± 0.09 ^c	1.23 ± 0.22 ^b	0.40 ± 0.07 ^a

Values represent mean ± standard deviation, N = 3

^{a-c} Values sharing at least one letter in a row are not significantly different (95% CI)

Minute quantities of proteins and lipids are chemically bonded to starch granules and are difficult to remove (Thomas and Atwell, 1999). Starch from ackee seed and commercial corn starch had a similar ash content of 0.13% (wb), but the quantity was more than twice as high for potato starch. This may be due to higher quantities of phosphorous in potato starches (Singh et al., 2003).

The purity of starch from the ackee seed averaged 82.59% (wb) (or 0.94 g/g dm) which was similar to values obtained for commercial corn and potato starches. The quantity of damaged starch granules in ackee seed starch was found to be 1.59%, which is within the range reported by Pérez et al. (2011) for waxy yam varieties (0.41-2.95%) and Simsek et al. (2009) for different pea varieties (1.54-1.80%). Lower values were obtained for commercial corn and potato starches. Starch granules may become damaged as a result of milling during starch isolation, or degradation by endogenous amylases in the starting material (Tran et al., 2011; Williams, 1967).

The apparent amylose contents of ackee seed starch and commercial potato starch were similar, but apparent amylose content of commercial corn starch was lower ($p > 0.05$). Abiodun et al. (2015a) reported an amylose content of 41.47% for ackee seed starch extracted from de-hulled seed flour, similar to the findings of this study. However, in a subsequent study, they reported a much lower amylose content of 22.1% for the native starch isolated from de-hulled seed flour, and even lower quantities (18.3 - 21.2%) for the acetylated, alkaline treated and pre-gelatinised starch (Abiodun et al., 2018).

Jane et al. (1999) reported that the apparent amylose content of potato starch was much higher than its absolute amylose content (36% vs 19%); for corn starch, there was a 7% difference between apparent amylose and absolute amylose (29% vs 22%). The disparity between apparent and absolute amylose for potato starch could be as a result of amylopectin chains with relatively fewer branches and intermediate materials; these are known to bind iodine resulting in an overestimation of amylose (Jane et al., 1999). High amylose starches are known to have restricted swelling properties and tend to retrograde rapidly resulting in opaque pastes, hard gels, high syneresis and high setback (Alcazar-Alay and Meireles, 2015).

In this study, no hypoglycin toxins were detected in the ackee seed starch samples. Both compounds are water-soluble (Sarwar and Botting, 1994; Hassall and Reyle, 1955) and would have been leached into solution by repeated washing of the starch residue during isolation. Abiodun et al. (2018) reported HGA and HGB content of native and modified starch obtained from de-hulled ackee seed flour ranged from 38.8 - 57.5 ppm and 71.8 - 84.8 ppm, respectively. In all cases, the values were below the regulatory limits of 150 ppm and 100 ppm set by the Bureau of Standards, Jamaica (BSJ) and the United States Food and Drug Administration (USFDA) (Gordon et al., 2015).

3.2 Size and Shape of Starch Granules

Ackee seed starch granules had a round shape, and some were truncated (see Figure 4a). Regions of darker stains indicated higher amylose content and therefore represented amorphous sections of the granules (Thomas and Atwell, 1999). When viewed under a scanning

electron microscope (SEM), some granules appeared round, truncated or dome-shaped (see Figure 4b).

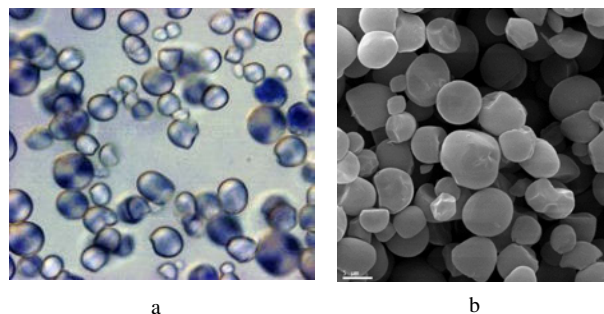


Figure 4. Ackee Seed Starch Granules; a: x 100; b: x 2500

Granule diameter was smaller ($6.89 \pm 1.89 \mu\text{m}$, $N = 407$) compared with corn ($10.74 \pm 2.24 \mu\text{m}$, $N = 90$) and potato starches ($28.56 \pm 14.52 \mu\text{m}$, $N = 90$). Size distribution pattern revealed that approximately 95% of ackee starch granules have a diameter less than $10 \mu\text{m}$. Abiodun et al. (2015a) reported similar morphologies and size distribution for granules of ackee seed starch. Abiodun et al. (2018) further reported that chemical modification by acetylation resulted in granules with deformed shapes, while in the case of the pre-gelatinised starch, the granules appeared as fragments. These modifications thus resulted in damaged starch granules which tend to have a higher water absorption capacity and are more susceptible to attack by amylases (Hossen et al., 2011).

Small granule starches are suitable for use in foods requiring creamy smooth texture and may serve as fat replacers and are desirable for use in biodegradable plastic films (Lindeboom et al., 2004). High amylose starch-based films have higher tensile and impact strengths as well as higher modulus and are less likely to absorb moisture compared with films from waxy starches (Wittaya, 2012). Jane et al. (1992) stated that small-granule starches are suitable for use in dusting, face and baking powders, and as a laundry stiffening agent.

3.3 X-Ray Diffraction Pattern

Starches produce characteristic peaks when subjected to X-ray diffraction because of their semi-crystalline properties (Singh et al., 2003). Starch granules in which chains are closely packed and accommodate relatively few water molecules produce an A-type diffraction pattern while B-type starches have a more open structure accommodating more water molecules (Hizukuri et al., 2006). Starches of the C-type are considered intermediate, comprising granules of both A and B types (Hizukuri et al., 2006). A, B, and C-Type starches are typical of cereal, tuber and legume starches respectively.

The X-Ray diffraction pattern for ackee seed starch,

not previously reported, is shown in Figure 5. A strong peak was observed at 17° (2θ), moderate peaks were observed at 15° and 22.5° in 2θ , and weak peaks were observed at 6° , 10.5° , 20° and 26° in 2θ . These peaks are characteristic of the C-Type crystalline structure (Nwokocha and Williams, 2011). In the case of the commercial corn starch, strong peaks (in 2θ) were observed at 15° , 17° , 18° and 22° , while weak peaks were observed at 11° , 20° , and 26° . This is characteristic of an A-type diffraction pattern (Nwokocha and Williams, 2011). For the commercial potato starch, a strong peak was observed at 17° , a moderate peak at 22° and weak peaks at 15° and 20° suggested that this is a B-Type starch (Nwokocha and Williams, 2011).

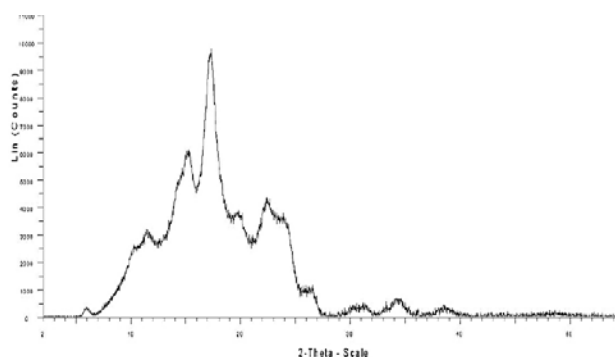


Figure 5. X-Ray Diffraction Pattern for Ackee Seed Starch

3.4 Thermal Properties

The DSC thermogram of ackee seed starch is presented in Figure 6. Ackee seed starch had highest onset of gelatinisation (T_o) ($66.67 \pm 0.09^\circ\text{C}$), peak gelatinisation temperature (T_p) ($71.45 \pm 0.03^\circ\text{C}$) and conclusion gelatinisation temperature (T_c) ($77.62 \pm 0.10^\circ\text{C}$) ($p < 0.05$), slightly lower values were recorded for commercial corn starch ($T_o = 65.75 \pm 0.08^\circ\text{C}$; $T_p = 70.09 \pm 0.09^\circ\text{C}$ and $T_c = 77.18 \pm 0.18^\circ\text{C}$, respectively) and even lower values for commercial potato starch ($T_o = 59.19 \pm 0.05^\circ\text{C}$, $T_p = 63.63 \pm 0.05^\circ\text{C}$ and $T_c = 72.63 \pm 0.13^\circ\text{C}$, respectively). Thermal properties of ackee seed starch using DSC have not been previously reported.

A similar gelatinisation temperature of 71.50°C for ackee seed starch based on microscopic analyses of the granules was reported by Abiodun et al. (2015a). Yuan et al., (2007) stated that starches with higher melting temperatures have a higher level of crystallinity. Additionally, the gelatinisation temperature of a starch is further influenced by the “molecular architecture” of crystalline regions rather than simply the proportion of crystalline and amorphous regions (Huang et al., 2007).

Enthalpy of gelatinisation (Δ_{gel}) was highest for potato starch ($15.98 \pm 0.43 \text{ J/g}$) followed by ackee seed starch ($13.65 \pm 0.12 \text{ J/g}$) and corn starch ($12.34 \pm 0.60 \text{ J/g}$). Variation in Δ_{gel} represents differences in bonding forces between double helices that form amylopectin

crystallites and relates to loss of double helical structures rather than crystalline order (Bhupender et al., 2013). Aggarwal et al. (2004) stated that high Δ_{gel} of starches implies the presence of many large size and irregular granules, while lower Δ_{gel} is indicative of small-sized oval granules. In this study, potato starch granules were found to be larger than ackee seed and corn starches and had highest Δ_{gel} . Simsek et al. (2009) stated that starches having mainly B-poly morph have higher gelatinisation enthalpy than those comprising A-poly morph; this was consistent with findings of this study where potato starch had higher Δ_{gel} compared with corn starch.

Peak Height Index (PHI), the ratio of enthalpy of gelatinisation to gelatinisation temperature range (R), is a measure of uniformity in gelatinisation (Aggarwal et al., 2004). PHI appears to increase as the size of starch granules increases (Aggarwal et al., 2004; Bhupender et al., 2013). There was no significant difference in PHI for ackee seed ($2.86 \pm 0.08 \text{ J/g}^{-1}^\circ\text{C}^{-1}$) and corn starches ($2.85 \pm 0.17 \text{ J/g}^{-1}^\circ\text{C}^{-1}$) but the value was significantly higher ($p < 0.05$) for potato starch ($3.60 \pm 0.10 \text{ J/g}^{-1}^\circ\text{C}^{-1}$), possibly due to larger granular diameter.

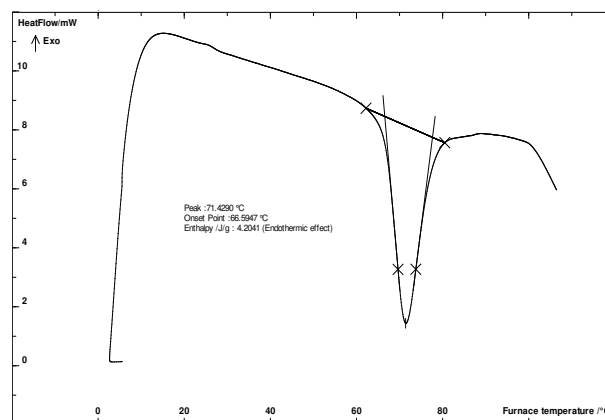


Figure 6. Differential Scanning Calorimeter (DSC) thermogram of ackee seed starch

3.5 Physical Properties

There was no significant difference in water absorption capacity (WAC) at 25°C between ackee seed starch ($1.09 \text{ g H}_2\text{O/g starch}$) and potato starch ($1.10 \text{ g H}_2\text{O/g starch}$), but corn starch had a significantly lower ($p < 0.05$) WAC ($0.84 \text{ g H}_2\text{O/g starch}$). Reasons for this are not clear but could be as a result of differences in granule structure, steric factors, hydrophilic-hydrophobic balance and extent of association between amylose and amylopectin chains (Henríquez et al., 2008). Oil absorption capacity (OAC) for ackee seed starch ($0.75 \text{ g oil/g starch}$) was similar ($p > 0.05$) to those recorded for corn ($0.75 \text{ g oil/g starch}$) and potato starches ($0.72 \text{ g oil/g starch}$). WAC and OAC of ackee seed starch have not been previously reported in the literature.

The swelling power of ackee seed starch at 95°C

was 19.49 ± 0.59 g gel/g starch; this implied a restrictive swelling property. The swelling powers of starches at 95°C can be classified as high (> 30), moderate (20 - 30), restricted (16 - 20) and highly restricted (< 16) (Shimelis et al., 2006). The commercial corn and potato starches were found to have moderate (25.91 ± 0.37 g gel/g starch) and high (40.57 ± 0.92 g gel/g starch) swelling properties respectively at 95°C . For all three starches, swelling power increased exponentially beyond their respective gelatinisation temperatures (see Figure 7). Starches with relatively low amylose content, large granule size and low gelatinisation temperature tend to have high swelling power (Alcázar-Alay and Meireles, 2015; Singh et al., 2003). Swelling occurs primarily as a result of hydration of amylopectin chains; amylose chains reduce swelling because they form insoluble complexes with lipids and proteins (Singh et al., 2003; Shimelis et al., 2006).

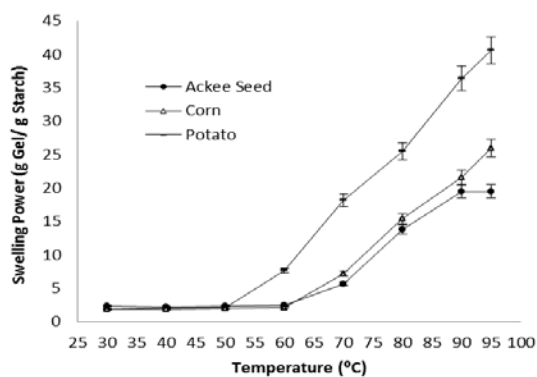


Figure 7. Swelling Power of Ackee Seed Starch and Commercial Corn and Potato Starches

Abiodun et al. (2015a) reported a swelling power of 9.68 at 90°C for ackee seed starch which is lower than the 19.41 ± 0.12 g gel/g starch reported in this study at that temperature. In a further study, Abiodun et al. (2018) reported an increase in swelling power of the ackee starch by chemical modification (acetylation, oxidation, alkali-treated, acid treated) as well as pre-gelatinisation. However, the increase was only marginal, and in all cases, the swelling of the starch was still highly

restricted. The starch extraction method reported by Abiodun et al. (2015a) did not involve a defatting process. Thus, the isolated starch might have had a higher lipid content thus reducing granule swelling (Alcázar-Alay and Meireles, 2015). Starches with restricted swelling properties are suitable for use in foods such as noodles where much swelling is not desired (Shimelis et al., 2006).

At 95°C , solubility of ackee seed starch was significantly lower ($p < 0.05$) ($12.24 \pm 0.60\%$), when compared with potato starch ($15.62 \pm 0.30\%$) and corn starch ($29.34 \pm 0.09\%$). The solubility of the starches increased rapidly beyond their gelatinisation temperature. Like swelling power, solubility is reduced by the presence of bound lipids in starch (Shimelis et al., 2006; Singh et al., 2003). No prior works have been published on the solubility of ackee seed starch.

3.6 Pasting Properties

The pasting curve of ackee seed starch is presented in Figure 8. Ackee seed starch was found to have lower breakdown values and higher setback compared with commercial corn and potato starches (see Table 3). Pasting temperature was also higher for ackee seed starch perhaps due to higher gelatinisation temperatures (see Section 3.3).

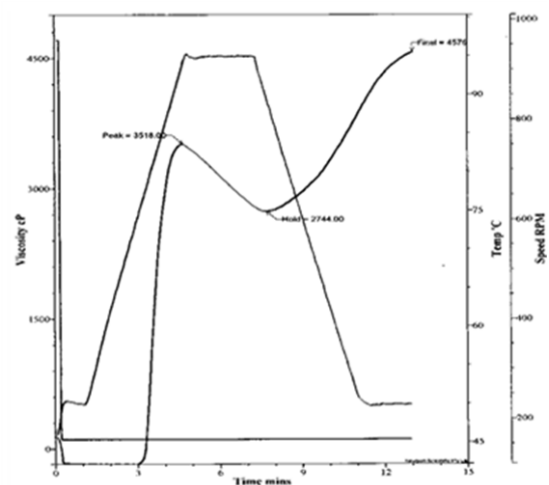


Figure 8. Pasting Curve of Ackee Seed Starch

Table 3. Pasting Properties of Ackee Seed Starch and Commercial Corn and Potato Starches

Pasting Property	Starch Sample		
	Ackee Seed	Corn	Potato
Pasting Temperature ($^\circ\text{C}$)	75.10 ± 0.05^c	74.22 ± 0.08^b	66.20 ± 0.05^a
Peak Viscosity (cP)	3760 ± 142^b	1937 ± 33^a	8348 ± 113^c
Hot Paste Viscosity (cP)	3038 ± 136^c	625 ± 7^a	2727 ± 123^b
Breakdown (cP)	721 ± 53^a	1312 ± 31^b	5621 ± 53^c
Relative Breakdown (% of Peak Viscosity)	19.19 ± 1.39^a	67.73 ± 0.50^b	67.34 ± 1.09^b
Cool Paste Viscosity (cP)	5230 ± 113^c	1265.33 ± 20.82^a	3297 ± 88^b
Setback (cP)	2191 ± 46^b	640 ± 18^a	570 ± 51^a
Relative Setback (% of Peak Viscosity)	58.37 ± 3.31^c	33.05 ± 0.41^b	6.84 ± 0.65^a
Pasting Time (min)	4.55 ± 0.04^c	4.05 ± 0.04^b	3.33 ± 0.00^a

Values represent mean \pm standard deviation, $N = 3$; ^{a-c}Values sharing at least one letter in a row are not significantly different (95% CI)

The lower breakdown of ackee seed starch suggests that it may be suitable as a thickening agent in foods processed at high temperature such as gravies and soups. However, a high setback means that ackee starch has a high tendency to retrograde. The consequences of starch retrogradation include exudation of water from gels and staling of bread (Alcázar-Alay and Meireles, 2015). A high setback and low breakdown of ackee starch were also reported by Abiodun et al. (2015a), although peak viscosity was higher (i.e., 501.25 RVU or approximately 6015 cP). Highest peak viscosity was recorded for potato starch, but breakdown was also the highest suggesting that this starch paste is not stable towards heat and shear.

With regards to chemical modification of ackee seed starch, Abiodun et al. (2018) found that peak viscosity was significantly higher for the alkali treated starch (3973 cP) compared with the native starch (3685 cP). However, peak viscosity was lower (2970 - 3259 cP) for the acid-treated, acetylated and oxidised starches. As expected, peak viscosity was the lowest for the pre-gelatinised starch (543 cP). The authors found that acetylation increased the tendency of the starch to breakdown; however, the thermal stability of the starch improved significantly when modified with alkali or acid, oxidised, or pre-gelatinised. Abiodun et al. (2018) reported a setback of 1139 cP for native ackee starch; with acid and alkali treatments resulting in lower setback (204 cP and 235 cP, respectively), thus reducing the tendency of the starch to retrograde.

When the effects of pH (3.0, 5.0, 7.0 and 9.0) on the pasting properties were investigated, ackee seed starch paste appeared more stable towards acidic conditions compared with corn and potato starches. Peak viscosity of ackee seed starch was largely unaffected by pH changes (see Figure 9), though relative breakdown (33.68 ± 0.67% of peak viscosity, or 1133.67 ± 26.08 cP) was slightly higher at pH 3.0 (see Figure 10).

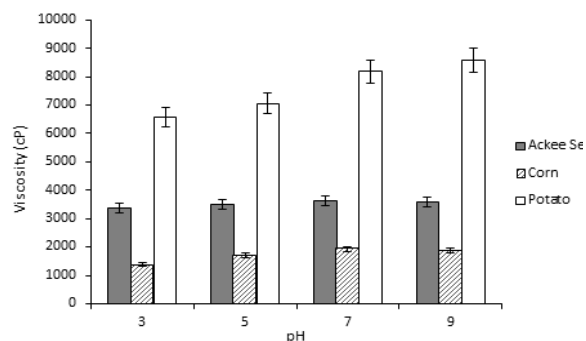


Figure 9. Effect of pH on Peak Viscosity of Starch Paste from Ackee Seed, Corn and Potato

Ackee seed starch relative setback was significantly lower at pH 3.0 (40.16 ± 1.39 % of peak viscosity, or 1351.33 ± 37.10 cP) compared with that at higher pH values (56.58 - 66.58 % of peak viscosity). These results

imply that ackee seed starch might be more suitable for use in acidic foods compared with corn and potato starches. No previous studies have been reported concerning the effects of pH on pasting properties of ackee seed starch.

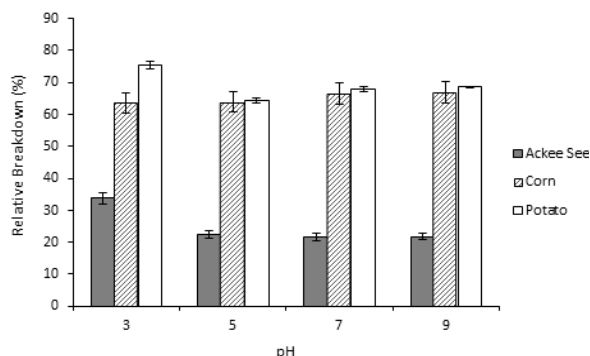


Figure 10. Effect of pH on Relative Paste Viscosity Breakdown

3.7 Paste Clarity

The changes in paste clarity of the starches with storage time are shown in Figure 11. Ackee seed starch formed an opaque paste; recording an initial light transmission (T) of 11.10 ± 1.00%. For corn starch, a translucent paste was produced (T = 29.88 ± 0.88%) while potato starch formed a clear paste (T = 74.80 ± 6.46%). The clarity of the pastes from ackee seed and potato starches decreased rapidly during the first three to four days of refrigerated storage and tapered off thereafter. In the case of corn starch, paste clarity decreased slowly during the first three days of storage at 4°C (from 29.88 to 23.76%) but showed very little change after that.

Lower light transmittance of ackee seed starch paste was reported by Abiodun et al. (2015a), averaging 0.70 (after 24 h), 0.62 (48 h) and 0.53 (72 h), possibly due to a higher lipid content of the starch. In a subsequent study in 2018, the authors found that chemical modifications of the starch did not result in any increase in paste clarity. However, the percentage transmittance of the pre-gelatinised starch increased to 9-14% within 24 h of storage but decreased on further storage.

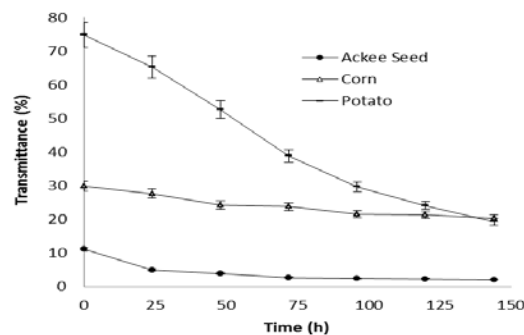


Figure 11. Effect of Storage Time (at 4°C) on % Transmittance of starches from Ackee Seed, Corn and Potato

Starches that produce opaque pastes have relatively high amounts of phospholipids that form insoluble complexes with amylose and long chain amylopectin, which reduce light transmittance (Alcázar-Alay and Meireles, 2015; Singh et al., 2003). Potato starches are known to contain phosphate-amylopectin monoesters which are responsible for the high paste clarity (Alcázar-Alay and Meireles, 2015; Singh et al., 2003). An implication of these findings is that ackee seed starch pastes would be more useful in dark-coloured products such as sauces, salad dressings and puddings (Alcázar-Alay and Meireles, 2015; Torruco-Uco and Betancur-Ancona, 2007).

3.8 Starch Gel Syneresis

Water loss (syneresis) of starch gels from ackee seed, corn and potato at 4°C and -18°C is illustrated in Figure 12 and 13, respectively. A high level of syneresis for ackee starch was observed at 4°C (see Figure 12), with values ranging from 31.35 (g H₂O/100 g gel) within 24 h to 49.18 after storage for 120 h. The starch gels would, therefore, be unsuitable for use in foods typically stored at refrigerated temperature. A lower syneresis was observed with gels from corn and potato starches. The realignment of amylose chains on cooling of starch gels results in exudation of water molecules; this process is accelerated when gels are stored at refrigerated or frozen temperatures (Lee et al., 2002). Syneresis of ackee seed starch gels has not been previously reported.

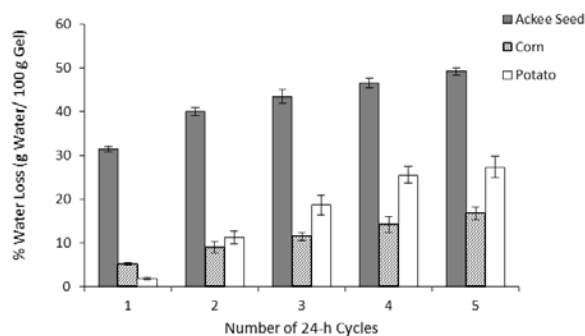


Figure 12. Syneresis of Starch Gels from Ackee Seed, Corn and Potato at 4°C

When the starch gels were stored at frozen temperature (-18°C) and subjected to five freeze-thaw cycles, high syneresis was observed for all starches (see Figure 13). Several authors have reported poor freeze-thaw stability of gels from native starches including corn, amaranth, plantain, banana, rice, potato, and cassava (Torruco-Uco and Betancur-Ancona, 2007; Bello-Pérez et al., 1999). Abiodun et al. (2018) attempted to improve the freeze-thaw stability of ackee starch by chemical modification (acid-treated, alkali-treated, acetylation and oxidation) and pre-gelatinisation. However, all the modifications failed to improve the

freeze-thaw stability of the starch paste.

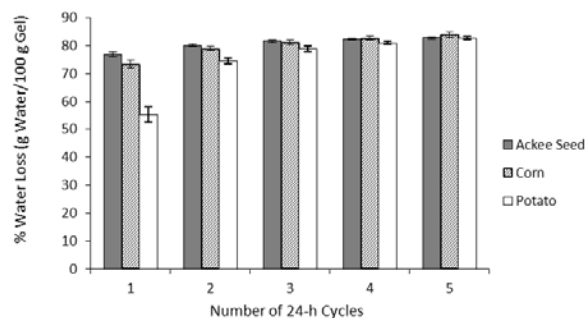


Figure 13. Syneresis of Starch Gels from Ackee Seed, Corn and Potato at -18°C

3.9 Starch Gel Texture

The textural properties of the starch gels are given in Table 4. Starch gels from ackee seed had a significantly harder texture compared to gels from corn and potato starches. Hardness values (N) were higher when the gels were stored at 4°C compared with 25°C. Starches that produce hard gel texture have a high tendency to retrograde, and this effect is more pronounced at refrigerated and frozen temperatures (Herceg et al., 2010).

Cohesiveness describes the strength of internal bonds within the gel (Trinh and Glasgow, 2012). It was not significantly different among the starch gels when incubation was done at 25°C. However, when ackee seed starch gels were stored at 4°C, cohesiveness was significantly lower (0.48, $p < 0.05$) compared with storage at 25°C (0.64). Springiness, which describes the elasticity of a food sample (Trinh and Glasgow, 2012), ranged from 7.00 to 8.44 mm and was generally similar regardless of starch source or incubation temperature.

The values suggest that gels from ackee seed and potato starches that were set at the ambient temperature will require more energy to chew compared with gels set at 4°C. A reverse in this trend was observed for corn starch gels. Overall, chewiness (gs) was lowest for corn starch gels due mainly to lower hardness. Gels from ackee seed starch had significantly higher gumminess than gels from corn and potato starches incubated at 25°C. Potato starch gel incubated at 4°C showed similar gumminess to gels from ackee seed starch. Higher gumminess suggests that ackee starch could be used in the manufacturing of gummy candies.

Adhesiveness, the work required to overcome sticky forces between the samples and probe (Trinh and Glasgow, 2012), was significantly higher for ackee seed starch gels, incubated at 25°C, compared with other starch gels. Ackee seed starch may, therefore, be suitable for use in the manufacturing of adhesives. No prior works have been reported regarding the textural properties of ackee seed starch gel.

Table 4. Effect of Storage Temperature on Texture Properties of Gels of Ackee Seed, Corn and Potato Starches

Property	Starch Sample					
	Ackee Seed		Corn		Potato	
	4°C	25°C	4°C	25°C	4°C	25°C
Hardness (N)	109.67 ± 5.13 ^d	91.00 ± 2.65 ^c	42.67 ± 5.03 ^a	36.67 ± 1.15 ^a	94.00 ± 4.36 ^c	61.00 ± 1.00 ^b
Cohesiveness	0.48 ± 0.02 ^a	0.64 ± 0.04 ^b	0.64 ± 0.05 ^b	0.65 ± 0.03 ^b	0.60 ± 0.01 ^b	0.65 ± 0.02 ^b
Springiness (mm)	7.68 ± 0.68 ^{a,b}	8.44 ± 0.19 ^b	8.20 ± 0.19 ^b	7.98 ± 0.25 ^{a,b}	7.64 ± 0.24 ^{a,b}	7.00 ± 0.56 ^a
Chewiness (gs)	398.76 ± 49.40 ^c	486.95 ± 18.99 ^d	255.40 ± 42.29 ^{a,b}	191.34 ± 18.28 ^a	436.45 ± 29.55 ^{cd}	278.45 ± 24.94 ^b
Gumminess (g)	51.82 ± 1.82 ^c	57.67 ± 1.85 ^c	27.47 ± 4.96 ^a	23.95 ± 1.73 ^a	57.12 ± 2.50 ^c	37.41 ± 4.50 ^b
Adhesiveness (gs)	-92.15 ± 2.54 ^b	-166.94 ± 15.34 ^c	-104.05 ± 25.93 ^b	-92.91 ± 20.99 ^b	-38.28 ± 6.13 ^a	-0.17 ± 0.30 ^a

Values represent mean ± standard deviation, N = 3; Values sharing at least one letter in a row are not significantly different (95% CI)

3.10 Retrograded (Resistant) Starch

Resistant starches are not broken down by human digestive enzymes and can be used as a more palatable source of dietary fibre compared with traditional sources (Öztürk and Köksel, 2014; Sharma et al., 2008). These starches are thus used to fortify products such as cereals, and baked and fried goods, while maintaining or even improving sensory attributes such as taste, crispiness, texture and mouthfeel (Fuentes-Zaragoza et al., 2010; Raigond et al., 2015). The production of retrograded resistant starch from ackee seed starch is being reported for the first time.

The native starches of ackee, corn and potato were found to have a resistant starch content of 44.42, 8.81 and 77.31 % (dry weight basis), respectively. The types of resistant starch found in native starches are RS1 (physically inaccessible starches locked within cell walls) and RS2 (starches having rigid crystalline structures), both of which become completely digestible when freshly cooked (Raigond et al., 2015; Sharma et al., 2008). Such starches are therefore not suitable as a functional ingredient in baked or cooked products. Retrograded resistant starch (RS3) is stable to gelatinisation up to 150°C and hence ideal for use in thermally processed foods (Raigond et al., 2015; Leszczyński, 2004). The resistant starch contents of retrograded starches (RS3) (up to three autoclave/freezethaw cycles) from ackee, corn and potato are shown in Figure 14. The process used to produce the retrograded starches would have completely destroyed the native RS1 and RS2 starches.

The highest amount of RS3 (11.61% db) was produced from ackee retrograded starch at cycle 3. Additionally, in the case of ackee and corn retrograded starches, the amount of RS3 formed increased as the number of autoclave/freezethaw cycles increased, but more so for corn. However, for potato, the quantity of RS3 decreased as the number of cycles increased. The quantity of RS in ackee seed retrograded starch was higher than values reported for waxy maize (2.5% db), potato starch (4.4% db), maize starch (7.0% db) and wheat starch (7.8% db) (Sievert and Pomeranz, 1989). Similar resistant starch content was reported for pea retrograded starch (10.5% db) (Sievert and Pomeranz, 1989) and a slightly higher value was reported for rice (13.9% wb) (Ha et al., 2012). Higher yields of RS3

might have been possible through modifications of process variables such as autoclave temperature and time, starch/water ratio, freezing temperature/time, amylose content and the number of heating/cooling cycles (Ha et al., 2012; Calixto and Abia, 1991).

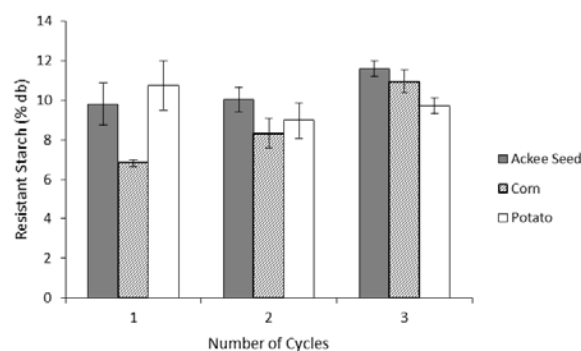


Figure 14. Resistant Starch Content of Retrograded Starches from Ackee Seed, Corn and Potato

4. Conclusions

High purity starch was successfully isolated from defatted ackee seed flour. Isolated starch was characterised as having small-sized granules, high apparent amylose content, C-type crystalline structure, high gelatinisation and pasting temperatures, restricted swelling, moderate peak viscosity, low breakdown and a high tendency to retrograde. Because of its tendency to readily retrograde, ackee seed starch could be used to produce retrograded resistant starch (RS3).

The low breakdown of ackee seed starch suggests that it could be used as a thickening agent in foods processed at high temperatures such as gravies and soups. The restricted swelling of the starch makes it suitable for use in the manufacturing of noodles. Because of its small granular size, ackee seed starch could be used as fat replacers in foods and other products such as dusting powders and baking powders. The starch may be suitable in the production of biodegradable plastic films because of its high apparent amylose content and small granule size. Further research is recommended to investigate the actual behaviour of the starch in these specific applications.

References:

- AACC International (1999), *Approved Methods of Analysis*, 11th edition, AACC International, St. Paul, Minnesota, USA.
- Abiodun, O.A., Adepeju, A.B., Dauda, A.O., and Adebisi, T.T. (2015a), "Potentials of under-utilized *Blighia sapida* seed as a source of starch for industrial utilization", *American Journal of Food Science and Nutrition*, Vol 2, No. 6, pp. 108-112.
- Abiodun, O.A., Adepeju, A.B., and Olosunde, O.O. (2015b), "Influence of cooking on the compositions of under-utilized *Blighia sapida* seed flour", *Proceedings of the OAU Faculty of Technology Conference, 2015*, Obafemi Awolowo University, Nigeria, 20-25th September, pp. 12-16.
- Abiodun, O.A., Dauda, A.O., Ojo, A., Adepeju, A.B., Odenibi, D.E., and Mudi F.O. (2018), "Physicochemical properties of modified *Blighia sapida* seed starch", *Proceedings of the 4th Regional Food Science and Technology Summit (ReFoSTS) of NIFST East Central Chapter*, Nigerian Institute of Food Science and Technology, Oshodi, Nigeria, June, pp.365-372.
- Aggarwal, V., Singh, N., Kamboj, S.S., and Brar, P.S. (2004), "Some properties of seeds and starches separated from different Indian pea cultivars", *Food Chemistry*, Vol .5, No.4, pp.585-590.
- Alcázar-Alay, S.C., and Meireles, M.A.A. (2015), "Physicochemical properties, modifications and applications of starches from different botanical sources", *Food Science and Technology (Campinas)*, Vol.35 No.2, pp.215-236.
- AOAC (2012), *Official Methods of Analysis of AOAC International*, 19th Edition, AOAC International, Gaithersburg, Maryland, USA.
- Bello-Pérez, L.A., Agama-Acevedo, E., Sánchez-Hernández, L., and Paredes-López, O. (1999), "Isolation and partial characterisation of banana starches", *Journal of Agricultural and Food Chemistry*, Vol.47, No.3, pp.854-857.
- Bhupender, S.K., Rajneesh, B., and Baljeet, S.Y. (2013), "Physicochemical, functional, thermal and pasting properties of starches isolated from pearl millet cultivars", *International Food Research Journal*, Vol.20, No.4, pp.1555-1561.
- Calixto, F.S. and Abia, R. (1991), "Resistant starch: an indigestible fraction of foods", *Grasas y Aceites*, Vol 42, pp. 239-242.
- Chinma, C.E., Abu, J.O., James, S., and Iheanacho, M. (2012), "Chemical, functional and pasting properties of defatted starches from cowpea and soybean and application in stiff porridge preparation", *Nigerian Food Journal*, Vol 30, No. 2, pp. 80-88.
- Djenontin, S.T., Wotto, V.D., Lozano, P., Pioch, D., and Sohounhloué, D.K. (2009), "Characterisation of *Blighia sapida* (Sapindaceae) seed oil and defatted cake from Benin", *Natural Product Research*, Vol. 23, No. 6, pp. 549-560.
- Esuoso, K.O. and Odetokun, S.O. (1995), "Proximate composition and possible industrial utilization of *Blighia sapida* seed and seed oils", *L. Riv. Ital. Grasse*, Vol. 72, pp. 311-313.
- Falloon, O.C. (2019), *Isolation and Physicochemical Properties of Starch and Proteins from the Seeds of the Ackee (Blighia sapida) Fruit*, PhD Thesis (Unpublished), Department of Chemical Engineering, The University of the West Indies, Trinidad and Tobago.
- Fuentes-Zaragoza, E., Riquelme-Navarrete, M., Sánchez-Zapata, E., and Pérez-Álvarez, J. (2010), "Resistant starch as functional ingredient: A review", *Food Research International*, Vol 43, No. 4, pp. 931-942.
- Gordon, A., Saltsman, J., Ware, G., and Kerr, J. (2015), "Re-Entering the US Market with Jamaican Ackees: A Case Study", In: Gordon, A. (ed.), *Food Safety and Quality Systems in Developing Countries*, Elsevier Academic Press, Amsterdam, Netherlands, pp.91-114.
- Ha, A.W., Han, G.J., and Kim, W.K. (2012), "Effect of retrograded rice on weight control, gut function, and lipid concentrations in rats", *Nutrition Research and Practice*, Vol 6, No.1, pp.16-20.
- Hassall, C.H., and Reyle, K. (1955), "Hypoglycin A and B, two biologically active polypeptides from *Blighia sapida*", *Biochemical Journal*, Vol.60, No.2, pp.334-339.
- Hassan, L.G., Muhammad, A.B., Aliyu, R.U., Idris, Z.M., Izuagie, T., Umar, K.J., and Sani, N.A. (2013), "Extraction and characterisation of starches from four varieties of *Mangifera indica* seeds", *IOSR Journal of Applied Chemistry*, Vol.3, No.6, pp.16-23.
- Henríquez, C., Escobar, B., Figuerola, F., Chiffelle, I., Speisky, H., and Estévez, A.M. (2008), "Characterisation of piñon seed (*Araucaria araucana* (Mol) K. Koch) and the isolated starch from the seed", *Food Chemistry*, Vol.107, No.2, pp. 592-601.
- Herczeg, I.L., Jambrak, A.R., Šubarić, D., Brnčić, M., Brnčić, S.R., Badanjak, M., Tripalo, B., Ježek, D., Novotni, D. and Herczeg, Z. (2010), "Texture and pasting properties of ultrasonically treated corn starch", *Czech Journal of Food Science*, Vol.28, No.2, pp. 83-93.
- Hizukuri, S., Abe, J.I., and Hanashiro, I. (2006), "Starch: Analytical aspects", In: Eliasson, A.-C. (ed.), *Carbohydrates in Foods*, CRC Press, Boca Raton, FL, pp. 305-390.
- Hossen, M.S., Sotome, I., Takenaka, M., Isobe, S., Nakajima, M., and Okadome, H. (2011), "Effect of particle size of different crop starches and their flours on pasting properties", *Japan Journal of Food Engineering*, Vol.12, No.1, pp. 29-35.
- Huang, J., Schols, H.A., van Soest, J.J., Jin, Z., Sulmann, E., and Voragen, A.G. (2007), "Physicochemical properties and amylopectin chain profiles of cowpea, chickpea and yellow pea starches", *Food Chemistry*, Vol.101, No.4, pp.1338-1345.
- Hussain, S. (2015), "Native rice starch and linseed gum blends: Effect on pasting, thermal and rheological properties", *Czech Journal of Food Science*, Vol. 33, No. 6, pp. 556-563.
- Hyatt, K. (2006), "Assessing the competitiveness of Jamaican ackee in light of the challenges faced by sugar and bananas", *Proceedings of the 26th West Indies Agricultural Economics Conference*, Caribbean Agro-Economic Society, San Juan, Puerto Rico, July 2006, pp. 25-35.
- Jane, J., Chen, Y.Y., Lee, L.F., McPherson, A.E., Wong, K.S., Radosavljevic, M., and Kasemsuwan, T. (1999), "Effects of amylopectin branch chain length and amylose content on the gelatinization and pasting properties of starch", *Cereal Chemistry*, Vol. 76, No. 5, pp. 629-637.
- Jane, J.-L., Shen, L., Wang, L. and Manningat, C. (1992), "Preparation and properties of small-particle corn starch", *Cereal Chemistry*, Vol. 69, pp. 280-283.
- Lee, M.H., Baek, M.H., Cha, D.S., Park, H.J., and Lim, S.T. (2002), "Freeze-thaw stabilisation of sweet potato starch gel by polysaccharide gums", *Food Hydrocolloids*, Vol.16, No.4, pp. 345-352.
- Leszczyński, W.A. (2004), "Resistant starch: Classification, structure, production", *Polish Journal of Food and Nutrition Sciences*, Vol.13, No. 54, pp. 37-50.
- Lindeboom, N., Chang, P.R., and Tyler, R.T. (2004), "Analytical, biochemical and physicochemical aspects of starch granule size, with emphasis on small granule starches: A review", *Starch-Starke*, Vol.56, No.3-4, pp.89-99.
- Morton, J.F. (1987), "Ackee", In: Dawling, C.F., (ed), *Fruits of Warm Climates*, J.F. Morton, Miami, Florida, p. 269-271.
- Nwokocha, L.M., and Williams, P.A. (2011), "Structure and properties of *Treculia africana*, (Decne) seed starch", *Carbohydrate Polymers*, Vol. 84, No. 1, pp. 395-401.
- Öztürk, S., and Köksel, H. (2014), "Production and characterisation of resistant starch and its utilisation as food ingredient: A review", *Quality Assurance and Safety of Crops and Foods*, Vol 6, No. 3, pp. 335-346.
- Pérez, E., Gibert, O., Rolland-Sabaté, A., Jiménez, Y., Sánchez, T., Giraldo, A., Pontoire, B., Guilois, S., Lahon, M.C., Reynes, M., Dufour, D. (2011), "Physicochemical, functional, and

- macromolecular properties of waxy yam starches discovered from 'Mapuey' (*Dioscorea trifida*) genotypes in the Venezuelan Amazon", *Journal of Agricultural and Food Chemistry*, Vol.59, No.1, pp.263-273.
- Raigond, P., Ezekiel, R., and Raigond, B. (2015), "Resistant starch in food: A review", *Journal of the Science of Food and Agriculture*, Vol.95, No.10, pp.1968-1978.
- Sajilata, M.G., Singhal, R.S., and Kulkarni, P.R. (2006), "Resistant starch: A review", *Comprehensive Reviews in Food Science and Food Safety*, Vol.5, No.1, pp.1-17.
- Sarwar, G., and Botting, H.G. (1994), "Reversed-phase liquid chromatography determination of hypoglycin A (HG-A) in canned ackee fruit samples", *Journal of AOAC International*, Vol. 77, No. 5, pp. 1175-1179.
- Sharma, A., Yadav, B., and Yadav, R.B.(2008), "Resistant starch: Physiological roles and food applications", *Food Reviews International*, Vol. 24, No. 2, pp. 193-234.
- Shimelis, E.A., Meaza, M., and Rakshit, S.K. (2006), "Physicochemical properties, pasting behaviour and functional characteristics of flours and starches from improved bean (*Phaseolus vulgaris* L.) varieties grown in East Africa", *Agricultural Engineering International: CIGR E-Journal*, Vol.8, Manuscript FP 05 015.
- Sievert, D., and Pomeranz, Y. (1989), "Enzyme-resistant starch - I. Characterisation and evaluation by enzymatic, thermoanalytical, and microscopic methods", *Cereal Chemistry*, Vol.66, No.4, pp.342-347.
- Simsek, S., Tulbek, M. C., Yao, Y., and Schatz, B. (2009), "Starch characteristics of dry peas (*Pisum sativum* L.) grown in the USA", *Food Chemistry*, Vol.115, No.3, pp.832-838.
- Singh, N., Singh, J., Kaur, L., Sodhi, N.S., and Gill, B.S. (2003), "Morphological, thermal and rheological properties of starches from different botanical sources", *Food Chemistry*, Vol.81, No.2, pp.219-231.
- Statistical Institute of Jamaica (STATIN) (2019), "Traditional and Non-Traditional Exports Annual" [Online]. Available at <http://statinja.gov.jm/Trade-Econ%20Statistics/InternationalMerchandiseTrade/Ne%20trademore.aspx> (Updated: 24 March 2019).
- Sun, Q., Xing, Y., Qiu, C., and Xiong, L. (2014), "The pasting and gel textural properties of corn starch in glucose, fructose and maltose syrup", *Plos One*, Vol. 9, No. 4, e95862, doi: 10.1371/journal.pone.0095862.
- Thomas, D.J., and Atwell, W.A. (1999), *Starches*, Eagan Press, St. Paul, Minnesota, USA.
- Torruco-Uco, J., and Betancur-Ancona, D. (2007), "Physicochemical and functional properties of makal (*Xanthosoma yucatanensis*) starch", *Food Chemistry*, Vol.101, No.4, pp.1319-1326.
- Tran, T.T., Shelat, K.J., Tang, D., Li, E., Gilbert, R.G., and Hasjim, J. (2011), "Milling of rice grains. The degradation on three structural levels of starch in rice flour can be independently controlled during grinding", *Journal of Agricultural and Food Chemistry*, Vol.59, No.8, pp.3964-3973.
- Trinh, K. T., and Glasgow, S. (2012), "On the texture profile analysis test", *Proceedings of Chemeca Conference 2012: Analyzing the Impact of Chemical Engineering on Environment*, Wellington, New Zealand, September, pp.749-761.
- Williams, P. (1967), "Relation of starch damage and related characteristics to kernel hardness in Australian wheat varieties", *Cereal Chemistry*, Vol.44, No.4, pp.383-391.
- Wittaya, T. (2012), "Rice starch-based biodegradable films: Properties enhancement", In: Eissa, A.A. (ed.), *Structure and Function of Food Engineering*, InTech, London, UK, p.103-134.
- Yadav, R.B., Kumar, N., Yadav, B.S. and Yildiz, F. (2016), "Characterisation of banana, potato, and rice starch blends for their physicochemical and pasting properties", *Cogent Food and Agriculture*, Vol. 2, No.1, doi: 10.1080/23311932.2015.1127873
- Yuan, Y., Zhang, L., Dai, Y., and Yu, J. (2007), "Physicochemical properties of starch obtained from *Dioscorea nipponica* Makino comparison with other tuber starches", *Journal of Food Engineering*, Vol.82, No.4, pp.436-442.

Authors' Biographical Notes:

O'Neil Falloon is a Lecturer at the College of Agriculture, Science and Education in Jamaica. He graduated with a Ph.D in Food Science and Technology (UWI, Saint Augustine) in 2019, with High Commendation. He holds an MSc in Food Science and Technology (UWI, St. Augustine) and a BSc (UWI, Mona) with double majors in Chemistry and Food Chemistry. Dr. Falloon worked as a Research Assistant (2013-2018) and as an Engineering Technician from January to August 2019, in the Food Science and Technology Unit, The UWI - Department of Chemical Engineering, UWI. His research interests are in areas of food chemistry and processing.

Saheeda Mujaffar is a Lecturer in the Department of Chemical Engineering at The University of the West Indies (UWI), Saint Augustine Campus. Dr. Mujaffar holds a BSc. Degree in Natural Sciences and an MPhil and PhD Degree in Agricultural Engineering (UWI), and has worked as a Food Technologist in industry. She served as the Coordinator of the Food Science and Technology Programme (2017-2019), and is actively involved in both teaching and research at the postgraduate level. Dr. Mujaffar's specific areas of research interest include Drying of Agricultural Commodities, Mathematical Modelling, Food Waste Utilization and Product Development. She is an active Reviewer for local and international Food Science Journals. Dr. Mujaffar has served as the Deputy Dean, Outreach and Enterprise Development in the Faculty of Engineering and as a Director in the Livestock and Livestock Products Board.

Donna Minott is a Senior Lecturer and Head of the Food Chemistry Section in the Department of Chemistry at The University of the West Indies, Mona Campus. Her research interests have focused on the characterisation of nutrients and anti-nutrients (toxicants, carcinogens, etc.), process contaminants and flavour profile of local foods. She has supervised/co-supervised two PhD, eight MPhil and two MSc candidates. Besides being a reviewer for several international journals, she has also served on several Technical Committees of the Bureau of Standards Jamaica in relation to development of local and regional food standards, as well as on a government task force and state advisory bodies. Dr. Minott has a BSc in Chemistry and a PhD in Organic Chemistry (UWI, Mona).



Investigating the Impact of Deformation on a 3D-printed Antenna in Biomedical Systems

Jeevan Persad^a and Sean Roche^{b,Ψ}

Department of Electrical and Computer Engineering, The University of the West Indies, St. Augustine, Trinidad and Tobago, West Indies;

^aEmail: jeevan.persad.sta.uwi.edu

^bEmail: sean.roche@sta.uwi.edu

^Ψ Corresponding Author

(Received 29 April 2019; Revised 26 November 2019; Accepted 07 January 2020)

Abstract: Recently, there has been increasing interest in using wearable sensors with flexible antennas. The antenna structures, which may be used for communications or for sensory elements, can possibly change their characteristics due to mechanical deformations. In this work, Radio frequency (RF) characteristics of a flexible Planar Inverted-F Antenna (PIFA) antenna intended for biomedical applications are explored. In the investigation, a traditional PIFA antenna structure on a Nylon substrate is considered. Using simulation studies, the flexible structure is subjected to various realistic mechanical deformations. Simulations facilitated investigation of the impact of the mechanical deformations on antenna performance, through consideration of the impact of flexibility on the reflection coefficient, transmission frequency and radiation patterns between 700MHz and 4GHz. Results demonstrated good stability on the antennas resonant frequency and physical resilience. However, increases in the reflection coefficient and the reach of the far-field as well as changes in the directionality of the antenna radiation pattern were observed as the antenna structure was pressed into the underlying tissue. These results provide valuable insights for those interested in deploying flexible antenna structures for wearable antenna and RF sensor applications.

Keywords: 3D printing, antenna analysis, biosensor, body area networks, wearables

1. Introduction

In recent years there has been an increased integration of technology into everyday aspects of our lives (Case, Burwick, Volpp, and Patel, 2015; Pantelopoulos and Bourbakis, 2010; Rais et al., 2009). As an example, this increased integration has resulted in devices becoming increasingly present in users' personal space, worn on the body of the user and integrated into the body of the user. As a consequence, there is a greater need to improve traditional electronics manufacturing to create devices that can adapt to a user's anatomy both internally and externally and also a need to examine the health effects of device usage. However, despite the challenges presented in the manufacturing of flexible electronic structures (Bandonkar, Jeerapan, and Wang, 2016) and ensuring their safe operation (Mertz, 2016), they present tremendous opportunities in the area of biomedical applications. In particular, monitoring human physiological function is becoming increasingly prevalent with devices emerging in the form of discrete sensors and complete systems (Pantelopoulos and Bourbakis, 2010).

Wearable devices in biomedical monitoring applications present significant opportunities for the continued monitoring of various physiological phenomena. Added benefit is gained when the

information gathered through the devices can be analysed and visualised using remote applications (e.g., on the user's smart phone or on a medical practitioner's dashboard) (Pantelopoulos and Bourbakis, 2010; Salonen, Sydanheimo, Keskilammi, and Kivikoski, 1999). This exchange of information is facilitated through some form of communication system. For a great number of the remote applications the communication system is a form of wireless technology and a key component of the wireless communication system is the antenna. The design of the antenna for these wireless applications poses a significant challenge since there are concerns about antenna robustness, human safety and deterioration of the antenna performance as the wearer moves (Casula et al., 2017; Hall and Hao, 2006).

Considerable work has been undertaken to inform the construction and testing of antenna structures using flexible materials (e.g., Bai and Langley (2009, 2012), Bai, Rigelsford, and Langley (2013), Elias et al. (2013), and Sundarsingh et al. (2014)). The authors note that these studies have been limited in terms of the degree of distortion examined and the consideration given to the underlying tissue. Consequently, in this work, the impact of various induced deformations on the electromagnetic characteristics of antenna structures is examined. In

particular, the authors investigate the performance of a traditional Planar Inverted-F Antenna (PIFA) which has been adapted to a flexible substrate that can be produced using 3D printing manufacturing technologies.

It is noted that the analysis can be extended to other antenna structures. Investigations are performed via simulation studies using COMSOL Multiphysics software. The substrate material chosen was Nylon which is a readily available 3D printing material and has been frequently adapted to antenna structures (Hertleer et al., 2007; Matthews and Pettitt, 2009; Shakhirul et al., 2014). Deformation of the structure is examined for forces pressed into the skin surface and for forces acting up out of the skin surface due to for example, a bending joint. The investigations provide valuable insights for factoring into the design and use of wearable Very Low Frequency (VLF) to Ultra High Frequency (UHF) devices.

The paper is structured as follows. A brief literature review is presented along with the motivation behind the work. This is followed by the methodology and a description of the modelling work. Finally, the simulated results are presented and discussed.

2. Related Work

The examination of the antenna performance under instances of deformation is important when one considers that the modification of the antenna structure caused by the deformation can result in changes in antenna performance including shifting of resonant frequencies, varying radiation patterns and varying S-parameters (Rais et al., 2009). When these variations in antenna characteristics occur the ability of the antenna to function is compromised which can lead to significant performance degradation and/or unsafe operational conditions (Rogier, 2015; Soh et al., 2012).

Several studies have been undertaken which focus specifically on the deformation of wearable antennas. In much of the existing body of work, researchers have examined simple deformation patterns of the antenna structure with an emphasis on deformations in a single plane. In Bai and Langley (2009), the behaviour of a dual band Coplanar Waveguide Fed (CPW) antenna was examined under bending and crumpling conditions where deformations were examined on a single plane and no body model was considered. In Bai and Langley (2012), the performance of a PIFA antenna, centre frequency 2.4GHz, was observed under crumpling conditions and a simple human body model (HBM) was used to examine human interaction.

However, the crumpling pattern was examined on a single plane and the antenna structure was modelled as being 5 mm above the HBM. The electromagnetic structure considered in Bai et al. (2013) was a microstrip patch array which was subjected to crumpling and a phantom was used for human body simulations. As with the previous studies, the crumpling pattern was

examined on a single plane and the antenna structure was not placed against the model surface but was suspended 3mm above. Elias et al. (2013) examined the crumpling of a dipole antenna, centre frequency 2.4GHz, a body model was used to consider the impact of human tissue. The crumpling pattern was examined on a single plane and the antenna was not placed on the surface of the body model but was suspended 1 mm above. Finally, in Sundarsingh et al. (2014), a GSM-900 and 1800 dual-band patch antenna was studied under bending and crumpling conditions and a rectangular 3 layer body model was used for the human study. The bends and crumpling were examined on a single plane and the deformed antenna structure was not considered with the body model.

Additionally, in the literature, there has not been considerable investigation of the surrounding antenna environment. For the specific case of human tissue interaction, researchers utilised simulation models and phantoms but no study considered the effect of the antenna directly on the body. Finally, to the authors' knowledge, no body of work has examined the behaviour of such antenna structures while considering complex multi-planar deformations due to the body tissue and muscle movement where the underlying body tissue is also deformed.

To address these gaps, in this study a PIFA antenna structure was considered as being worn on the user's skin. The deformation of the antenna structure was investigated for forces pressed into the skin surface and for forces acting up out of the skin surface due to for example a bending joint. The impact of these deformations on antenna characteristics was then investigated.

3. Methodology

For the study an existing Planar Inverted-F Antenna (PIFA) design as proposed in Bai and Langley (2012) with a resonant frequency of 2.4GHz was considered under two distinct deformation conditions across the frequency range of 700MHz–4GHz. The deformation conditions were application of external forces acting on the wearer's skin (i.e., pressing forces) and forces from within the wearer's body (e.g., bicep bulging, skin folding and elbow joint bending body forces). The study was conducted using simulation tools due to the complexity of the antenna geometry and the expected irregularity of the distorted antenna structure. In this study the antenna is considered to be directly secured to the tissue surface (epidermis). For the purpose of the study the reflection coefficient, transmission frequency and radiation pattern of the PIFA were examined before and after distortion due to the application of pressing and body forces. The general antenna features, simulation modelling assumptions and model setup are described in the following sections.

3.1. Theory of Operation

The Planar Inverted-F Antenna (PIFA) is one of the most popular antenna structures used in mobile devices Bevelacqua (2016). The PIFA achieves resonance at roughly a quarter wavelength, which allows it to have a significantly smaller footprint. The specific Planar Inverted-F Antenna (PIFA) used in this study was adapted from the work described in Bai and Langley (2012). The previous PIFA design was intended for a textile adaptation with centre frequency of 2.4GHz which is suitable for wireless applications. Therefore, the design was selected due to its desirable resonant frequency and previous evaluation on a flexible substrate intended for a body worn applications. Since the goal of the extended work is to ultimately manufacture the antenna and support electronics using 3D printing techniques, the substrate was chosen to be Nylon. Nylon as a material is compatible with many 3D printing processes and is readily available from multiple suppliers. The material has also been frequently adapted as a substrate for antenna structures (Andreuccetti, Fossi, and Petrucci, 1997; Hertleer et al., 2007; Liang and Boppart, 2010; Matthews and Pettitt, 2009; Shakhirul et al., 2014).

Figure 1 shows the basic PIFA antenna structure. The impedance of the antenna is controlled by $D3$, the distance between the short pin and the feed point.

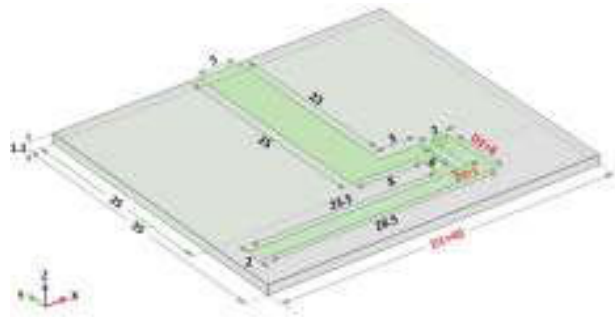


Figure 1. PIFA antenna structure

If one were to consider the radiation pattern of the antenna structure to be along its edge then the resonant length of the PIFA would be given by Bevelacqua (2016):

$$D1 + D2 = \frac{\lambda}{4} \quad (1)$$

where λ is the wavelength of the resonant frequency f . The resonant frequency would be given by:

$$f = \frac{c}{(4\sqrt{\epsilon_r}(D1+D2))} \quad (2)$$

where c is the speed of light in a vacuum and ϵ_r is the relative permittivity of the antenna substrate.

Antenna performance can be affected by changes in geometry due to deformations (e.g., substrate stretching and folding) which can affect distances such as the

distance between the feed point and short pin, (i.e., $D3$) as well as changes in material properties such as effective permittivity due to the operating environment (e.g., moisture/humidity) and effects of human tissue Rogier (2015). In this work the emphasis is on the impact of deformations and as such the effects of other factors are not studied.

3.2. Model details

An antenna structure serves to couple currents to electromagnetic waves to facilitate either radiation or reception. The behaviour of the associated electric and magnetic waves is governed by complicated solutions of Maxwell's equations for applied boundary conditions Balanis (1992):

$$\vec{E} \cdot d\vec{l} = -\frac{d}{dt} \int_S B \cdot d\vec{S} \quad (3)$$

$$\vec{H} \cdot d\vec{l} = \int_S J \cdot d\vec{S} + \frac{d}{dt} \int_S D \cdot d\vec{S} \quad (4)$$

While paper-based analysis using antenna theory is possible this approach is not suitable to the analysis of the current distribution in an irregularly distorted antenna structure. Thus, due to the complexity of the antenna distortions a 3D simulation model of the antenna was created.

Similarly, for the mechanical deformation of the human tissue there are several factors which would impact the behaviour of the tissue layers. For example, in the work undertaken by Liang and Boppart (2010) an expression was proposed for displacement in a single plane (z-axis) based on the harmonic excitation of skin tissue as an infinite elastic homogenous layer:

$$u_z = R_e \left\{ \frac{\partial \phi}{\partial z} + \frac{\partial H_z}{\partial x} \right\} = (Ae^{-qz} - 2sqe^{-sz}) \cos(k_R x - \omega t) \quad (5)$$

where ϕ and H_z are potentials, k_R is the wavenumber of the surface wave propagating on the skin, ω is the driving angular frequency and A , s and q are parameters to be computed. Due to the computational complexity of calculating the deformations across more than one plane, simulation tools were utilised. The simulation software utilized was the COMSOL Multiphysics tool. The COMSOL software allows crosscutting studies integrating different disciplines, in this case, Mechanical and Electrical facilitating the simultaneous examination of the physical and electromagnetic behaviour of models. The simulation model used for the study is shown in Figure 2.

The dimensional and material details which were used in building the model are captured in Table 1 Andreuccetti et al. (1997), where P is material density, E is Young's modulus, ν is Poissons ratio, ϵ_r is material permittivity, σ is material conductivity. For the purposes of this study the frequency range of 700MHz - 4GHz was used. The body model as presented in the simulation

represents a blood vessel which is located close to the skin surface on the forearm.

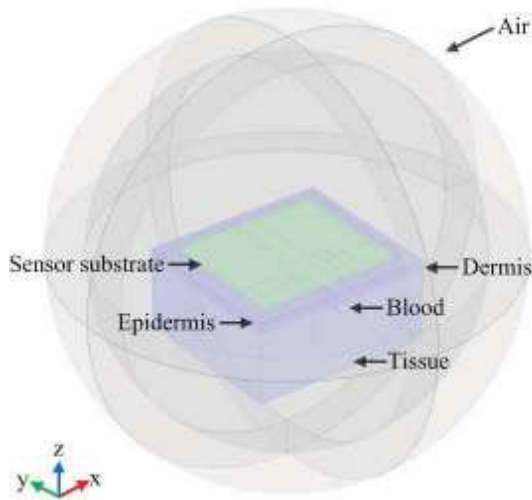


Figure 2. PIFA Antenna and body model used for the study

Table 1. Dimensional and material details used in the model

Dimensions (L,W,H)	Mechanical Parameters	Electrical Parameters
<i>Air</i>		
dia. 60.0mm, 50.0mm		
<i>Substrate (Nylon)</i>		
40.0mm 35.0mm 1.1mm	$P = 1150[\text{kg/m}^3]$ $E = 2e9[\text{Pa}]$ $\nu = 0.4$	$\sigma = 1.0e - 11[\text{S/m}]$ $\epsilon_r = 4.0$
<i>Epidermis</i>		
50.0mm 45.0mm 1.1mm	$P = 1190[\text{kg/m}^3]$ $E = 102e6[\text{Pa}]$ $\nu = 0.47$	$\sigma = 1.8e - 2[\text{S/m}]$ $\epsilon_r = 31$
<i>Dermis</i>		
50.0mm 45.0mm 1.5mm	$P = 1116[\text{kg/m}^3]$ $E = 102e5[\text{Pa}]$ $\nu = 0.47$	$\sigma = 4.3e - 1[\text{S/m}]$ $\epsilon_r = 40$
<i>Tissue</i>		
50.0mm 45.0mm 20.0mm	$P = 971[\text{kg/m}^3]$ $E = 102e2[\text{Pa}]$ $\nu = 0.48$	$\sigma = 1.5e - 1[\text{S/m}]$ $\epsilon_r = 17$
<i>Blood Vessel</i>		
dia. 3.2mm, 45mm	$P = 1060[\text{kg/m}^3]$ $E = 6e4[\text{Pa}]$ $\nu = 0.4$	$\sigma = 4.3e - 1[\text{S/m}]$ $\epsilon_r = 65$

3.3. Test Cases

The antenna and body model was considered under conditions of external forces acting on the antenna (pressing forces) and forces from within the wearers body (body forces). For both distortion scenarios the surface of the antenna face was divided into nine overlapping regions as shown in Figure 3. The pressing and body forces were then applied to each region.

In considering the pressing force the specific scenario of an index finger pressing downward was examined. The pressing force created would vary based

on an individual's age, sex and other demographics Peebles and Norris (2003) and for this work a uniform loading of 40N was used. The average finger dimension of 25 mm as found in Murai et al. (1997) was used. In considering the body acting forces the specific scenario of a bicep muscle contracting was considered. The contraction is a function of the movement of the forearm in which the bulging of the bicep muscle transmits a force through the layers of tissue. The force produced varies based on several factors including the degree of exertion and various individual demographic factors such as age, sex, level of fitness (Cameron et al., 1993) and for this work a uniform loading of 30N was used (Shima et al., 2009). The zoning of the body acting forces was developed based on the antenna being placed in varying positions above the bicep region.

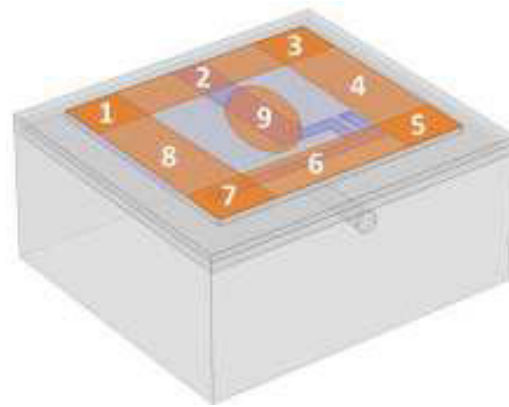


Figure 3. Nine (9) regions of force application onto the antenna face

For each simulation scenario the radiation pattern in the x-y, x-z, y-z planes, resonant frequency f_r and reflection coefficient S_{11} of the undistorted and distorted model were calculated and compared for the frequency range of 700MHz-4GHz in 50MHz steps.

4. Results

Figures 4 and 5 show examples of the 3D displacement plots generated in COMSOL for forces applied to the regions identified in Figure 3, due to the action of the body forces and press forces, respectively. The plots also record the maximum displacement (mm) for each of the distortion scenarios. The figures also illustrate the radiation plots in the x-y, x-z and y-z planes for three selected frequencies: 1GHz, 3GHz, 4GHz before and after the application of the respective forces.

For the displacement plots of the pressing forces, it was observed that the antenna structure was pressed into the underlying epidermis and dermis at each of the affected regions. For the pressing forces the average maximum displacement was approximately 2.74 mm with the greatest displacement of 3.16 mm being observed at regions 4 and 8. A significantly smaller

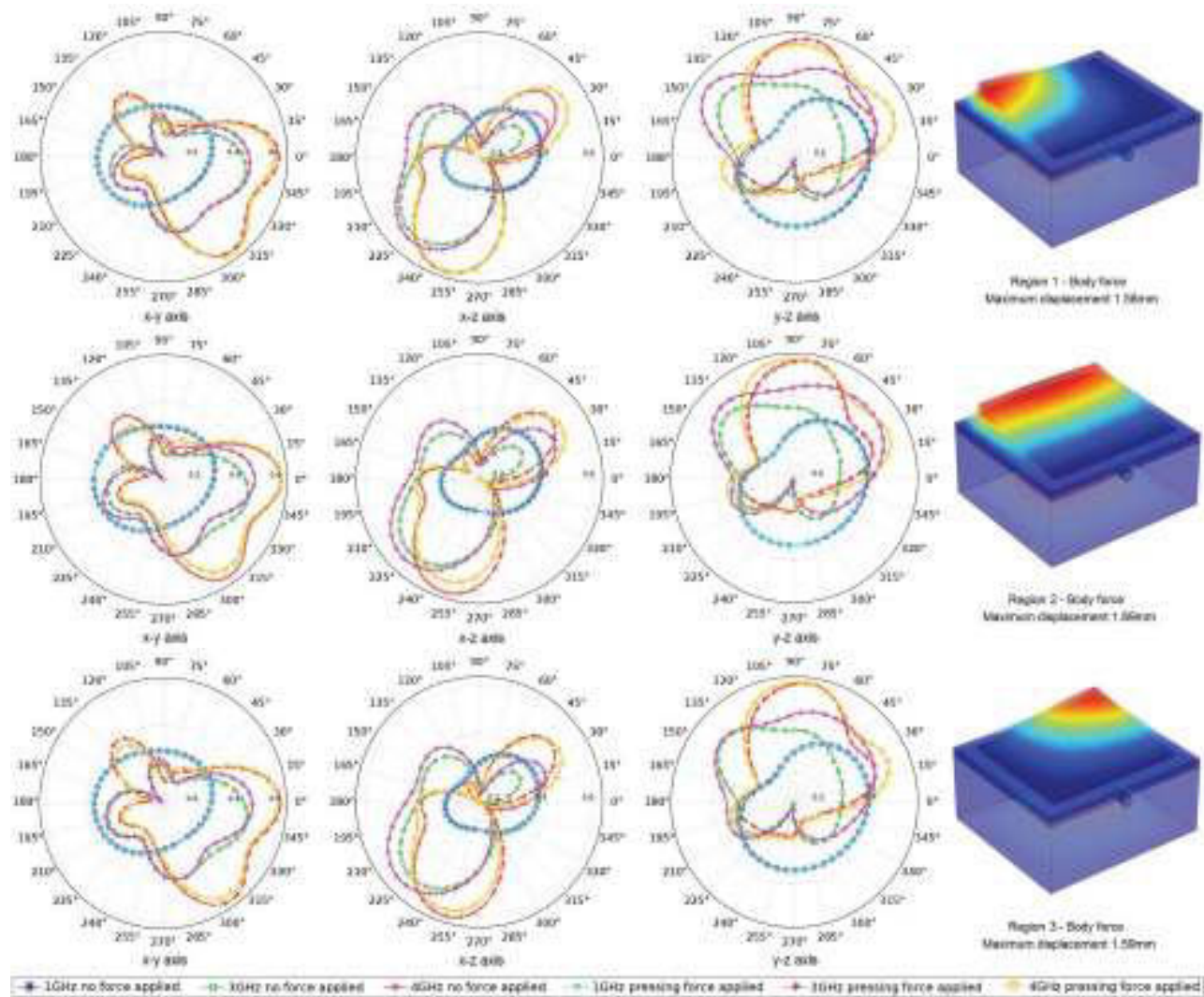


Figure 4. Plots of the antenna radiation pattern in the x-y, x-z, y-z planes and maximum displacement for the action of body forces, applied to Regions 1-3

displacement of 0.20mm was observed for region 9 of the antenna surface. For the displacement plots of the body forces, it was observed that the antenna structure was bent outward at the point of action of the force. For the body forces the average maximum displacement was approximately 1.77mm with the greatest displacement of 2.00mm being observed at regions 4 and 8. The minimum displacement observed was 0.57 mm at region 9.

Significant change in the radiation pattern for the three planes was observed at the higher frequencies of 3GHz and 4GHz due to the application of the pressing force. For the radiation plots at 1GHz involving the application of the pressing force, it was observed that the radiation pattern in all three planes was relatively symmetric. Furthermore, no significant deviation in the radiation pattern was observed due to the bending of the antenna and distortion of the underlying tissue caused by

the application of the pressing force. In contrast, for the radiation plots at 3GHz and 4GHz respectively, it was observed that the patterns grew increasingly distorted and extended further afield as the frequency increased.

For the radiation plots at 1GHz involving the application of the body force, the radiation pattern in all three planes was observed to be relatively symmetric. Furthermore, at 1GHz, no significant deviation in the radiation pattern was observed due to the action of the body force on the antenna and the underlying tissue. For the higher frequency plots at 3GHz and 4GHz respectively, the radiation pattern was observed to be significantly less symmetric as compared to the lower frequency and extended further afield. Furthermore, it was observed that the radiation pattern plots at 3GHz and 4GHz showed significant variation as a result of the tissue motion and antenna bending caused by the applied body force.

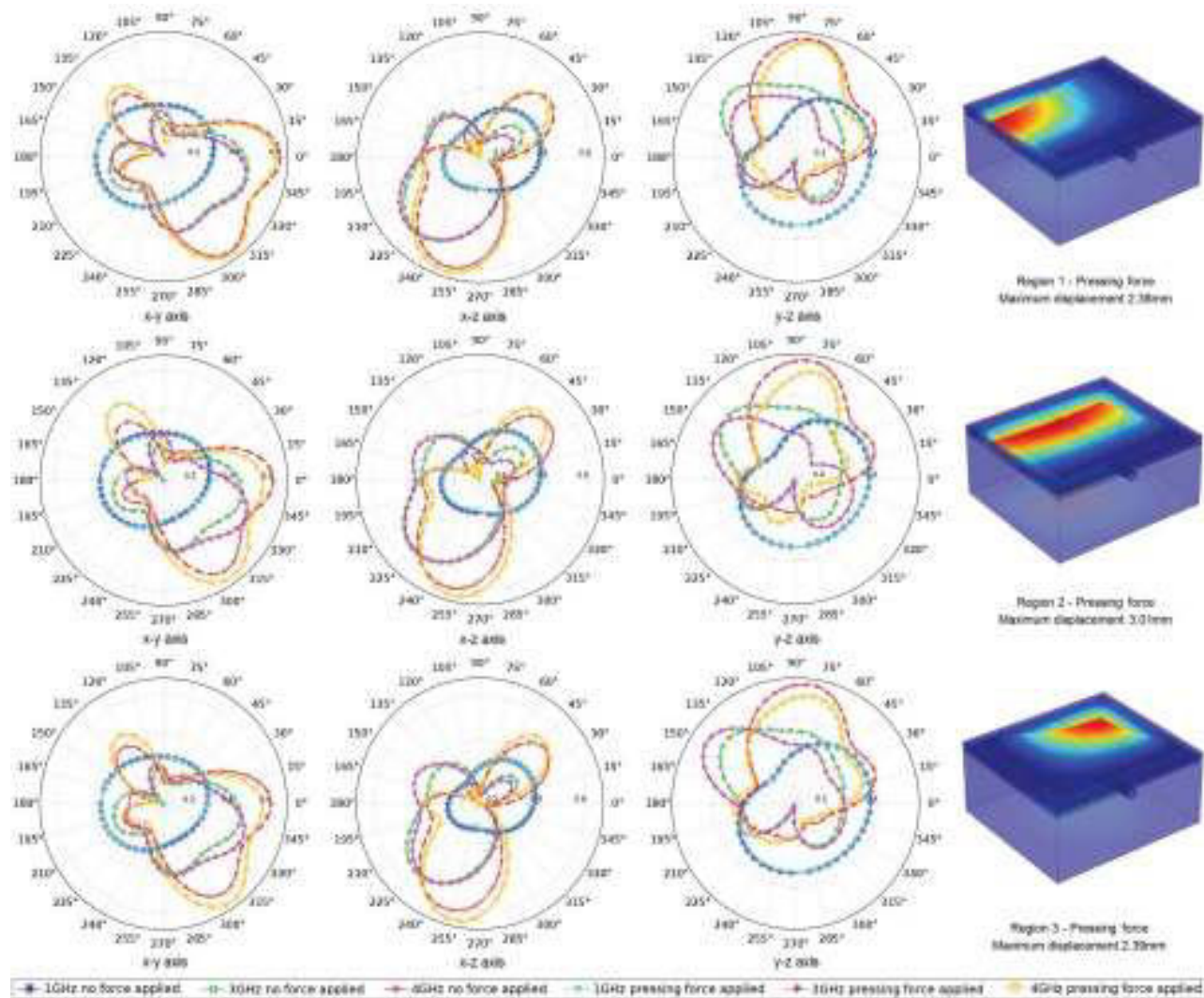


Figure 5. Plots of the antenna radiation pattern in the x-y, x-z, y-z planes and maximum displacement for the action of pressing forces, applied to Regions 1-3

Tables 2-4 summarise the Mean Square Error (MSE) calculations for the normalized far-field radiations plots for the press force (x-y, x-z, y-z planes) and the body force (x-y, x-z, y-z planes) as well as for the 3-dimension volume. The MSE was chosen to give a quantitative measure of the degree to which the radiation patterns deviate from the undisturbed antenna structure

(i.e. with no applied forces) as a result of deformations induced by the applied forces. The calculated MSE values (for both the planes as well as the 3D volume) showed an increase as the signal frequency was increased. The increase in the MSE values was noted for application of the press force as well as for the body force.

Table 2. MSE values for the normalised far-field in the x-y, x-z, y-z planes for the press force. D_{press} denotes the displacement in mm

Region	D_{press}	MSE Far-field norm 1GHz, x-y plane	MSE Far-field norm 3GHz, x-y plane	MSE Far-field norm 4GHz, x-y plane	MSE Far-field norm 1GHz, x-z plane	MSE Far-field norm 3GHz, x-z plane	MSE Far-field norm 4GHz, x-z plane	MSE Far-field norm 1GHz, y-z plane	MSE Far-field norm 3GHz, y-z plane	MSE Far-field norm 4GHz, y-z plane
1	2.38	3.61E-05	1.19E-03	6.76E-04	2.79E-05	6.88E-04	9.74E-04	3.49E-05	1.33E-03	1.07E-03
2	3.01	3.54E-05	2.71E-03	1.90E-03	3.14E-05	1.59E-03	2.85E-03	4.85E-05	2.39E-03	2.44E-03
3	2.39	6.35E-06	6.07E-04	8.94E-04	3.74E-05	7.92E-04	1.31E-03	9.79E-06	5.46E-04	9.12E-04
4	3.16	2.19E-05	6.94E-04	2.81E-03	5.12E-05	8.63E-04	4.80E-03	8.82E-06	6.22E-04	3.04E-03
5	2.39	1.34E-05	2.73E-04	5.13E-04	9.43E-06	6.14E-04	1.40E-03	6.32E-06	5.29E-04	7.91E-04
6	3.01	2.80E-04	6.60E-03	5.82E-03	3.82E-05	3.98E-03	4.10E-03	3.66E-05	7.29E-03	3.48E-03
7	2.40	1.85E-04	2.98E-03	3.20E-03	1.02E-05	1.69E-03	2.75E-03	1.55E-05	2.87E-03	2.05E-03
8	3.16	3.48E-04	6.94E-03	9.73E-03	6.60E-05	3.79E-03	5.28E-03	1.06E-04	5.41E-03	6.72E-03
9	0.20	8.01E-07	5.73E-06	1.48E-05	1.16E-06	1.12E-05	1.87E-05	1.14E-06	1.21E-05	1.19E-05

Table 3. MSE values for the normalised far-field in the x-y, x-z, y-z planes for the body force. D_{body} denotes the displacement in mm

Region	D_{body}	MSE Far-field norm 1GHz, x-y plane	MSE Far-field norm 3GHz, x-y plane	MSE Far-field norm 4GHz, x-y plane	MSE Far-field norm 1GHz, x-z plane	MSE Far-field norm 3GHz, x-z plane	MSE Far-field norm 4GHz, x-z plane	MSE Far-field norm 1GHz, y-z plane	MSE Far-field norm 3GHz, y-z plane	MSE Far-field norm 4GHz, y-z plane
1	1.58	9.79E-06	1.86E-03	4.38E-04	1.75E-05	3.29E-03	8.62E-04	1.44E-05	2.91E-03	7.08E-04
2	1.89	8.69E-06	2.55E-03	8.32E-04	1.32E-05	5.64E-03	1.51E-03	1.54E-05	4.21E-03	1.23E-03
3	1.59	2.85E-06	1.22E-03	2.36E-04	1.03E-05	3.50E-03	8.13E-04	4.80E-06	1.98E-03	4.75E-04
4	2.00	1.44E-05	1.01E-03	7.56E-04	1.65E-05	2.08E-03	2.06E-03	1.31E-05	1.31E-03	8.37E-04
5	1.59	1.70E-05	6.48E-04	4.51E-04	4.09E-06	1.47E-03	1.07E-03	1.73E-05	9.25E-04	4.68E-04
6	1.89	3.91E-04	3.96E-03	7.98E-03	8.27E-05	1.72E-03	3.16E-03	5.87E-05	2.00E-03	2.59E-03
7	1.59	6.23E-05	1.60E-03	1.78E-03	4.97E-06	1.16E-03	1.74E-03	2.37E-05	1.40E-03	1.23E-03
8	2.00	1.11E-04	4.80E-03	3.22E-03	3.03E-05	2.51E-03	2.99E-03	6.15E-05	4.22E-03	2.32E-03
9	0.57	4.52E-06	7.31E-04	2.06E-04	3.16E-06	1.98E-03	5.42E-04	7.66E-06	1.21E-03	3.05E-04

Table 4. MSE values for the normalised far-field of the 3d volume

Region	D_{press}	D_{body}	Press force			Body force		
			MSE Far-field norm 1GHz	MSE Far-field norm 3GHz	MSE Far-field norm 4GHz	MSE Far-field norm 1GHz	MSE Far-field norm 3GHz	MSE Far-field norm 4GHz
1	2.38	1.58	4.30E-05	9.87E-04	9.51E-04	1.34E-05	1.76E-03	4.55E-04
2	3.01	1.89	5.60E-05	1.95E-03	2.41E-03	1.38E-05	2.53E-03	1.14E-03
3	2.39	1.59	9.95E-06	5.12E-04	1.11E-03	3.44E-06	1.11E-03	4.54E-04
4	3.16	2.00	1.65E-05	7.58E-04	3.26E-03	1.42E-05	7.63E-04	1.08E-03
5	2.39	1.59	8.24E-06	5.06E-04	7.91E-04	1.77E-05	5.15E-04	4.83E-04
6	3.01	1.89	5.96E-05	7.89E-03	4.17E-03	2.43E-04	3.26E-03	4.59E-03
7	2.40	1.59	4.00E-05	3.36E-03	2.30E-03	4.18E-05	1.34E-03	1.26E-03
8	3.16	2.00	1.51E-04	6.38E-03	6.96E-03	8.36E-05	4.05E-03	2.23E-03
9	0.20	0.57	1.19E-06	9.40E-06	1.40E-05	6.54E-06	6.46E-04	2.10E-04

For the 1GHz signal frequency, the MSE value was significantly smaller than at the higher frequencies for all force application scenarios. For the body force, the highest MSE values were observed for the 3GHz signal in all regions except 4 and 6. For the press force, the highest MSE values were observed for the 4GHz signal in all regions except 1, 6 and 7.

Figures 6 and 7 show the plots of the reflection coefficient S_{11} vs the applied signal frequency obtained from the frequency sweep for both before and after a press force and body force were applied to all nine regions on the antenna surface. For all scenarios the resonant frequency of the antenna was observed at 1.1GHz. The resonant frequency was not seen to shift for any of the tested scenarios when the force was applied. However, small variations in the value of the reflection coefficient were observed at the resonant frequency. These changes are captured in Figure 8.

Figure 8 shows the change in the reflection coefficient S_{11} for each of the nine regions for the press force (a) and body force (b). For the press force, there was an increase in the reflected power for regions 2-4 and 7-9. The greatest increase in reflected power of 1.05dB was seen for region 4 and the smallest increase in power of 0.10dB for region 8. For regions 1, 5-6, there was a decrease in the reflected power. The greatest decrease of 0.13dB was observed for region 6 and the smallest decrease of 0.09dB was seen at region 5. For the application of the body force, all regions showed a decrease in the reflected power due to the bending of the antenna and underlying tissue. The greatest decrease of

0.84dB was observed for region 4. For region 1, there was little to no change in the reflected power with a decrease of 0.02dB being produced.

5. Analysis

Based on the information obtained for each of the force application scenarios the antenna structure was seen to have undergone significant flexing with various bending forms observed and displacement as much as 3.16mm produced. All of the observed deformations of the antenna structure and underlying tissue were not confined to a single plane but were complex multi-planar changes in shape. For the bending of the antenna structure, it was noted that the greatest displacement was achieved when the acting force (press or body force) was along the vertical or horizontal axis as compared to application at the diagonals. The observed trend in the deforming and displacement of the antenna structure and underlying tissue can be attributed to the fact that application of the press or body force to the ends of the antenna structure (regions 2, 4, 6 and 8) allow for the body of the antenna to act as a fulcrum and amplify the effect of the applied force.

Finally, action of the press and body force through the centre of the body of the antenna and underlying tissue (region 9) was seen to produce the smallest variations in displacement (0.20mm and 0.57mm, respectively). The significantly smaller changes in displacement may be due to the body of the antenna having resisted being bent and stretched through its centre.

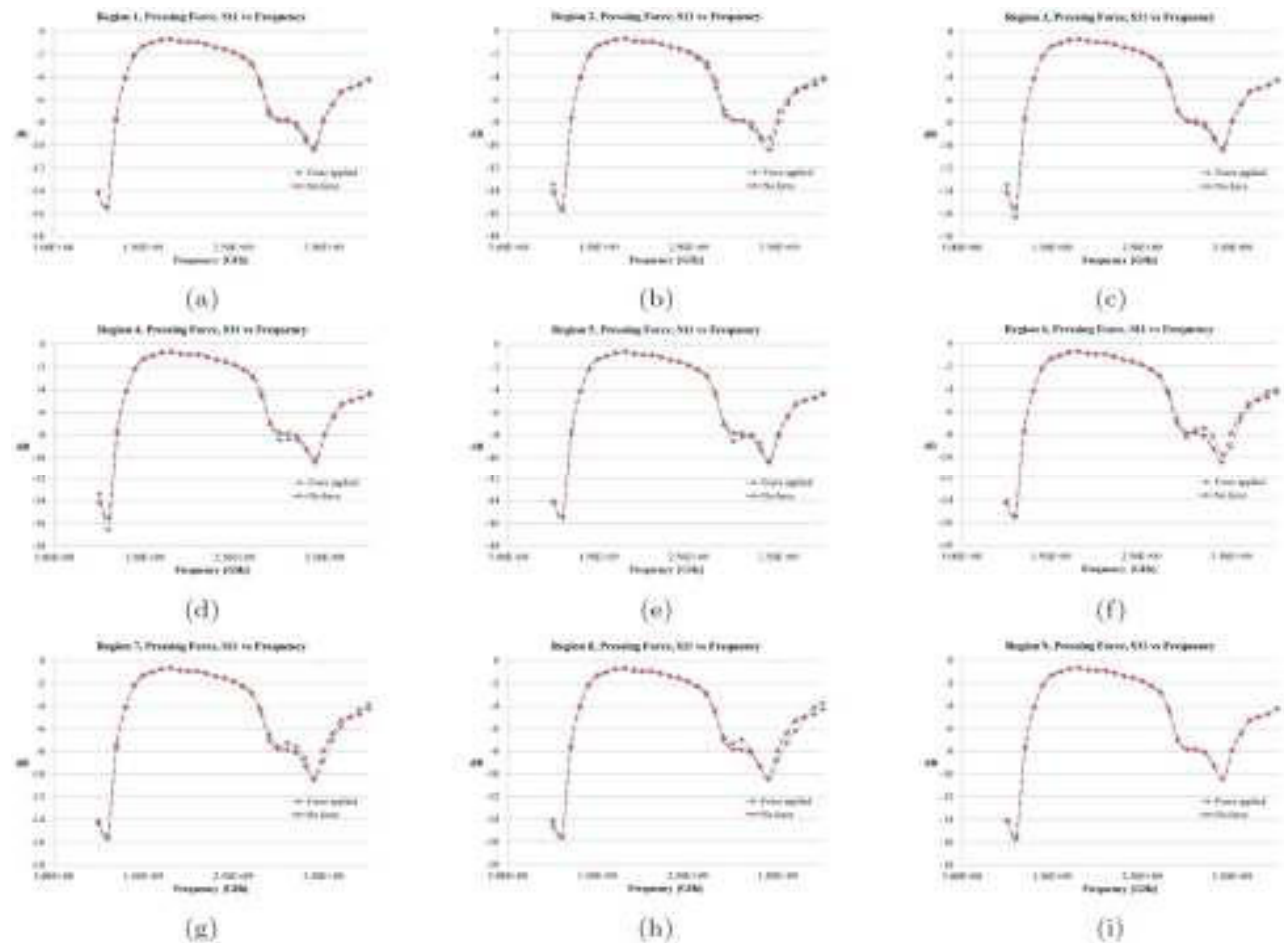


Figure 6. Plot of the reflection coefficient S11 vs frequency for before and after application to all nine regions of the action of pressing forces

It is worth noting that for all test scenarios the antenna structure was not seen to undergo destructive deformation (resulting in a rupture and/or tear) but was able to bend and conform to the movement of the underlying body tissue. This observed behaviour of the antenna structure lends support to the use of Nylon as a flexible substrate material for the antenna.

For the antenna performance, the antenna structure and body model prior to the application of a body or press force was seen to achieve resonance at 1.1GHz with a lesser resonant point at 3.4GHz. For all instances of force application (body and press force) it was noted that the resonant frequency points did not shift. Thus, the antenna resonant frequency showed good stability under deformation due to both press and body forces acting over its surface. This stability may be due to the fact that although the antenna structure underwent deformation due to the force, the deformation did not result in a significant change in the antenna geometry and/or dimensions.

While good stability was achieved for the antenna resonant frequency, variations were noted in the reflection coefficient S11. For the body force acting on

all regions of the antenna there was a resultant reduction in the transmission power. The reduction in the transmission power can be considered as a result of the net movement and deforming of the antenna and the underlying tissue. In particular, the movement of the tissue layers and blood vessel would create a change in the resultant permittivity below the antenna surface and therefore would affect the antenna performance. Another key contributor to the reduction in the reflection coefficient S11 would be which section of the antenna's surface was shifted. It was noted that motion and deformation which most impacted the geometry of the antenna's conductive pattern and the microstrip line resulted in the greatest reduction in the transmission power.

For the press force testing, a reduction in the reflection coefficient S11 was observed for only three regions (region 1, 5 and 6). For all other regions of force application, an increased in S11 was observed. It was noted that the regions which produced the increase in the transmission power were regions where the applied force resulted in the microstrip line being pressed into the epidermis and dermis of the user.

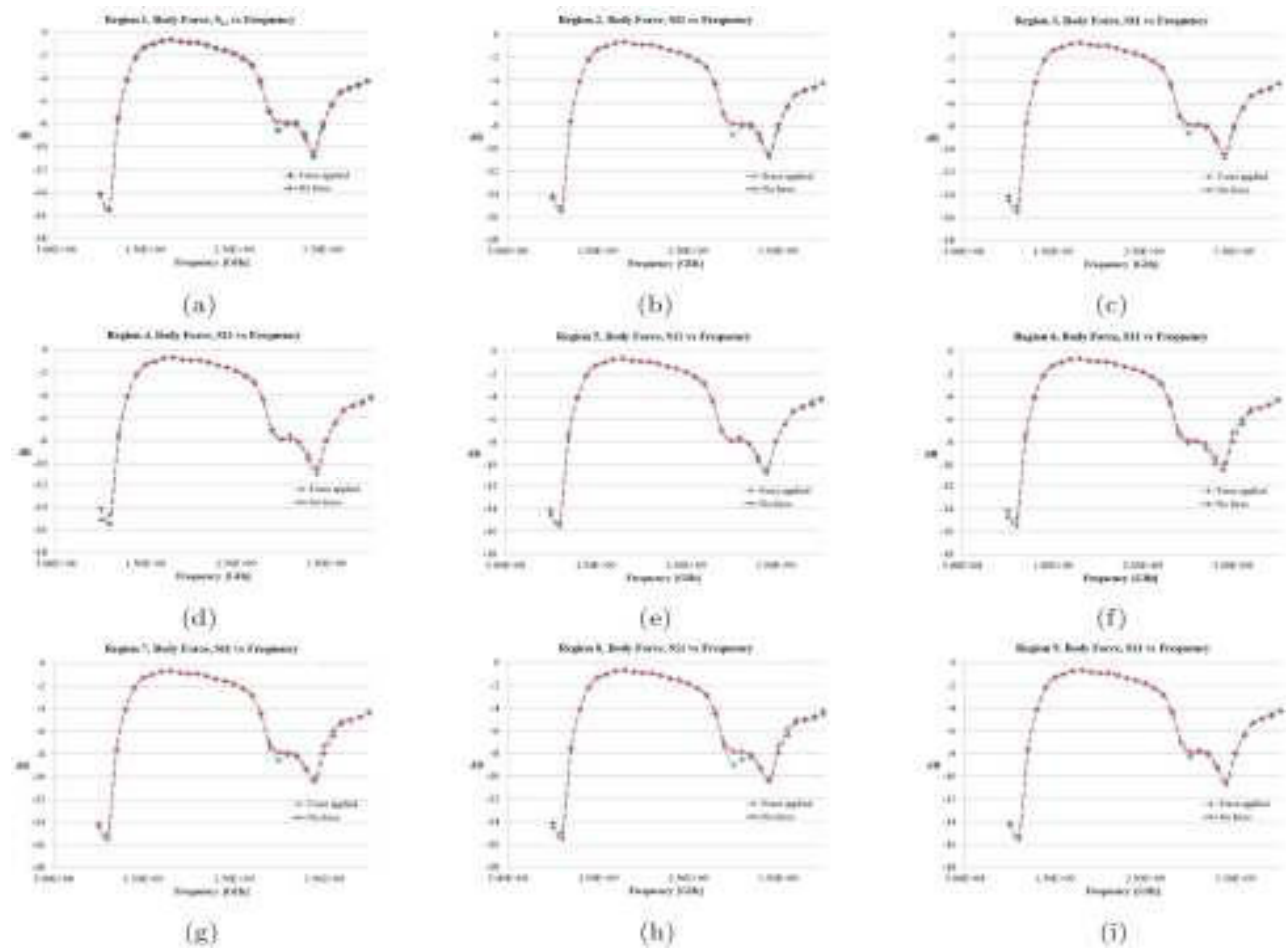


Figure 7. Plot of the reflection coefficient S11 vs frequency for before and after application to all nine regions of the action of body forces

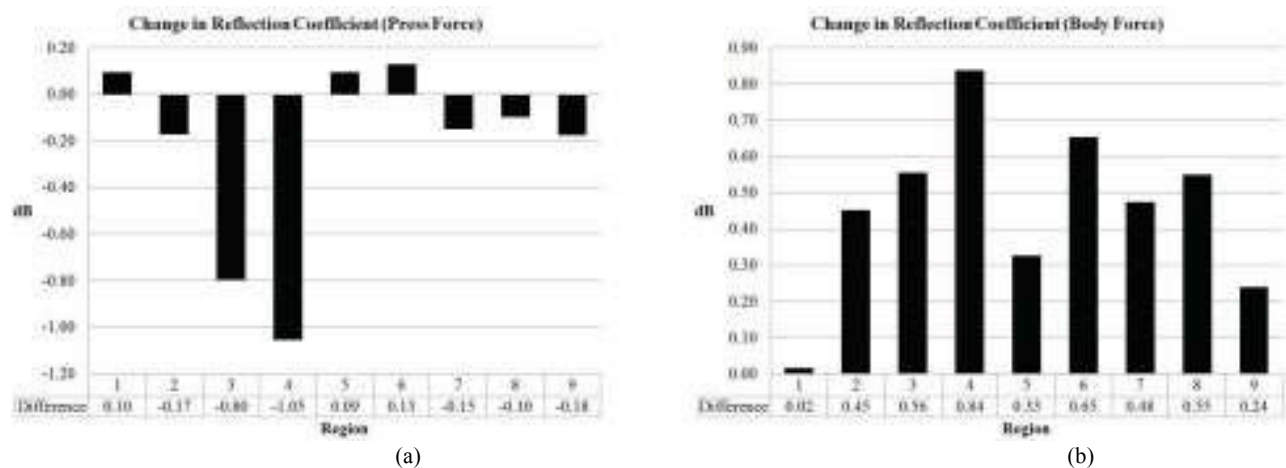


Figure 8. Plots of the change in reflection coefficient vs region (a) pressing forces (b) body forces

This observation is particularly significant since it illustrates that the underlying skin layers are contributing to an increase in the transmission power of the antenna. This behaviour can have possible consequences for the safe operation of such antenna structures.

The radiation pattern of the antenna was found to be largely unaffected at 1GHz due to the action of the press and body force. The radiation pattern at 1GHz was also found to be very symmetric in all planes and this symmetry was seen to be unaffected by the action of the applied forces (press and body force).

This characterisation shows that the antenna structure is resilient to the application of forces acting on it. The radiation patterns at the higher frequencies (3GHz, 4GHz), with no force applied to the antenna showed an increased in distortion and fell further afield for increased signal frequency. It was also observed that as the test frequency was increased the radiated signal was seen to become increasingly directional allowing the signal to penetrate further into the underlying tissue layers and surrounding air domain. The application of the force to the structure was seen to further increase the distortion of the radiated pattern. The signal was observed to fall even further afield, reaching deeper into the tissue layers and surrounding air domain. This result was of particular significance since the action of the force on the antenna and tissue layers resulted in the radiated signal penetrating further into the tissue as compared to when no force was acting.

The variation of the radiation pattern at the higher frequencies in response to the press and body forces can be attributed to the resultant displacement. The greatest displacement recorded was 3.16mm which would be equivalent to the wavelength of a frequency of approximate order of magnitude of GHz. As the applied signal frequency is increased and approaches multiples of the equivalent frequency (of the displacement) the distortion and spread of the radiation pattern would be more pronounced. The behaviour of the antenna structure at the higher frequencies can allow the structure to be adopted for sensing applications which require signal penetration further into the underlying tissue. However, the responsiveness of the antenna structure to deformations would require that some form of signal compensation is undertaken to allow for signal changes due to the deformation of the underlying tissue. The responsiveness of the antenna structure to the application of the force and the resultant deformation can allow the antenna to be used as a means to potentially monitor for press and body forces to the tissue.

The results from this work would suggest that the antenna structure as designed using the Nylon substrate would demonstrate good performance stability as regards the reflection coefficient S11, resonant frequency and general mechanical strength. The observed increased in transmission power for the scenarios involving the structure pressed into the flesh represents another area of interest for further investigation. The results obtained vis-a-vis the directionality and increased field penetration at higher frequencies presents possible opportunities for applying the antenna structure as a sensor targeting deeper tissue layers. Further investigation of the work would be conducted through more detailed simulation studies which are reinforced by building the antenna structure using the proposed materials and 3D printing processes and testing of the antenna structures in the identified frequency range of 700MHz-4GHz.

6. Conclusions

The simulation work conducted allowed for the examination of a PIFA antenna structure which was constructed using a Nylon substrate and which was subjected to various forces applied to nine different zones of the antenna surface. In addition, the antenna behaviour was considered in the context of it being present on the surface of a user's skin. The skin surface and underlying tissue were suitably represented both geometrically and with their assigned mechanical and electrical properties. The examination highlighted the extent of physical deformation possible when simple forces are applied to the antenna structure.

The stability of the antenna structure when subjected to forces was also demonstrated in terms of its reflection coefficient S11, resonant frequency and physical resilience. The work also revealed the interesting behaviour of the antenna when pressed into the body of the user, namely an increase in the reflection coefficient. The variation of the antenna radiation pattern both directionally as well as the increase in its far-field reach as the applied signal frequency was increased was noted. Also, of interest was the change in the radiation pattern at higher frequencies due to the deformation of the antenna and tissue when press and body forces were applied. This characterisation of the antenna behaviour at higher frequencies may present opportunities for the antenna structure to be adopted as a sensor.

Further work is proposed to examine the impact of the antenna structure on the underlying skin layers when varying levels of indentation into the skin are achieved. Work is also proposed to examine a more realistic representation of a 3D printed substrate (which considers for e.g. the existence of print-line boundaries and surface undulations). This work will be conducted through the creation of more detailed simulation models and the creation of prototype antenna structures.

References:

- Andreuccetti, D., Fossi, R., and Petrucci, C. (1997), "An internet resource for the calculation of the dielectric properties of body tissues in the frequency range 10 Hz-100 GHz", Retrieved from <http://niremf.ifac.cnr.it/tissprop>
- Bai, Q., and Langley, R. (2009), "Wearable ebg antenna bending and crumpling", *Proceedings of the Antennas and Propagation Conference, 2009*, Loughborough, November 16, pp. 201-204.
- Bai, Q., and Langley, R. (2012), "Crumpling of pifa textile antenna", *IEEE Transactions on Antennas and Propagation*, Vol.60, No.1, pp.63-70.
- Bai, Q., Rigelsford, J., and Langley, R. (2013), "Crumpling of microstrip antenna array", *IEEE Transactions on Antennas and Propagation*, Vol.61, No.9, pp.4567-4576.
- Balanis, C.A. (1992), "Antenna theory: A review", *Proceedings of the IEEE*, Vol.80, No.1, pp.7-23.
- Bandodkar, A.J., Jeerapan, I., and Wang, J. (2016), "Wearable chemical sensors: Present challenges and future prospects", *ACS Sensors*, Vol.1, No.5, pp.464-482.
- Bevelacqua, P.J. (2016), *PIFA - The Planar Inverted-F Antenna*. Retrieved from <http://www.antenna-theory.com/antennas/patches/pifa.php>

- Cameron, J.R., Skofronick, J.G., Grant, R.M., and Siegel, E. (1993), "Medical physics: Physics of the body", *American Journal of Physics*, Vol.61, No.12, pp.1156-1156.
- Case, M.A., Burwick, H.A., Volpp, K.G., and Patel, M.S. (2015), "Accuracy of smartphone applications and wearable devices for tracking physical activity data", *Journal of the American Medical Association*, Vol.313, No.6, pp.625-626.
- Casula, G.A., Michel, A., Montisci, G., Nepa, P., and Valente, G. (2017), "Energy-based considerations for ungrounded wearable uhf antenna design", *IEEE Sensors Journal*, Vol.17, No.3, pp.687-694.
- Elias, N., Samsuri, N., Rahim, M., and Othman, N. (2013), "Investigation of crumpling effects on em absorption and antenna performance at 2.4 ghz", *Proceedings of the RF and Microwave Conference, 2013*, (IEEE International), Penang, December 9, pp. 395-399.
- Hall, P.S., and Hao, Y. (2006), "Antennas and propagation for body centric communications", *Proceedings of the first European Conference on Antennas and Propagation, 2006*. Nice, November 6, pp.1-7.
- Hertleer, C., Tronquo, A., Rogier, H., Vallozzi, L., and van Langenhove, L. (2007), "Aperture-coupled patch antenna for integration into wearable textile systems", *IEEE Antennas and Wireless Propagation Letters*, Vol.6, pp.392-395.
- Liang, X., and Boppart, S.A. (2010), "Biomechanical properties of in vivo human skin from dynamic optical coherence elastography", *IEEE Transactions on Biomedical Engineering*, Vol.57, No.4, pp.953-959.
- Matthews, J., and Pettitt, G. (2009), "Development of flexible, wearable antennas", *Proceedings of the 3rd European Conference on Antennas and Propagation*, Berlin, March 23, pp. 273-277.
- Mertz, L. (2016), "Are wearables safe?: We carry our smart devices with us everywhere-even to bed-but have we been sleeping with the enemy, or are cautionary tales overinflated?" *IEEE Pulse*, Vol.7, No.1, pp.39-43.
- Murai, M., Lau, H.-K., Pereira, B.P., and Pho, R.W. (1997), "A cadaver study on volume and surface area of the fingertip", *The Journal of Hand Surgery*, Vol.22, No.5, pp.935-941.
- Pantelopoulos, A., and Bourbakis, N.G. (2010), "A survey on wearable sensor-based systems for health monitoring and prognosis", *IEEE Transactions on Systems, Man, and Cybernetics, Part C (Applications and Reviews)*, Vol.40, No.1, pp.1-12.
- Peebles, L., and Norris, B. (2003), "Filling gaps in strength data for design", *Applied Ergonomics*, Vol.34, No.1, pp.73-88.
- Rais, N., Soh, P.J., Malek, F., Ahmad, S., Hashim, N., and Hall, P. (2009), "A review of wearable antenna", *Proceedings of the Antennas and Propagation Conference*, Loughborough, November 16, pp.225-228.
- Rogier, H. (2015), "Textile antenna systems: design, fabrication, and characterisation", In: Tao, X. (ed), *Handbook of Smart Textiles*, Springer, Switzerland, pp.433-458.
- Salonen, P., Sydanheimo, L., Keskilampi, M., and Kivikoski, M. (1999), "A small planar inverted-f antenna for wearable applications", *Digest of Papers (Proceedings of) the third international symposium on Wearable Computers*, San Francisco, Oct ober18, pp.95-100.
- Shakhirul, M., Jusoh, M., Sahadah, A., Nor, C., and Rahim, H.A. (2014), "Embroidered wearable textile antenna on bending and wet performances for uwb reception", *Microwave and Optical Technology Letters*, Vol.56, No.9, pp.2158-2163.
- Shima, K., Tamura, Y., Tsuji, T., Kandori, A., Yokoe, M., and Sakoda, S. (2009), "Estimation of human finger tapping forces based on a finger pad-stiffness model", *Proceedings of the Annual International Conference of the IEEE on Engineering in Medicine and Biology Society*, Minneapolis, September 3, pp.2663-2667.
- Soh, P.J., Vandenbosch, G.A., Ooi, S.L., and Rais, N.H.M. (2012), "Design of a broadband all-textile slotted pifa", *IEEE Transactions on Antennas and Propagation*, Vol.60, No.1, pp.379-384.
- Sundarsingh, E.F., Velan, S., Kanagasabai, M., Sarma, A.K., Raviteja, C., and Alsath, M.G.N. (2014), "Polygon-shaped slotted dual-band antenna for wearable applications", *IEEE Antennas and Wireless Propagation Letters*, Vol.13, pp.611-614.

Authors' Biographical Notes:

Jeevan Persad received his B.Sc. degree in Electrical and Computer Engineering at The University of the West Indies in 2003 and his Masters in Electronic Product Development from The University of Bolton in 2012. His areas of interest include the application of 3D printing to the manufacture of electronic assemblies.

Sean Rocke received his BSc in Electrical and Computer Engineering from The University of the West Indies in 2002, his Masters in Communications Management and Operational Communications from Coventry University in 2004, and his Ph.D. in Electrical and Computer Engineering from Worcester Polytechnic Institute in 2013. His areas of interest include signal processing and optimisation techniques relating to wireless communications management application and biosensor development and biological data mining, as well as and emergency communication systems.

■

Driver Gap Acceptance Behaviour at Roundabouts in Trinidad and Tobago

Khary Leighton Campbell^a and Trevor A. Townsend^{b, Ψ}

^a Urban Development Corporation of Trinidad and Tobago (UDeCOTT), Trinidad and Tobago, West Indies;
Email: kharycampbell2@gmail.com

^b Department of Civil and Environmental Engineering, The University of the West Indies, St. Augustine, Trinidad and Tobago, West Indies; Email: trevor.townsend@sta.uwi.edu

^{Ψ} Corresponding Author

(Received 19 January 2019; Revised 01 December 2019; Accepted 14 January 2020)

Abstract: One important node used to manage conflicting traffic at intersections is the roundabout. Roundabouts operate based on the gap acceptance behavior of drivers, with a major flow in the circulatory lane of the roundabout and minor flows on the approaches which enter the roundabout when there is a gap the driver decides to accept. This study investigates the gap acceptance behaviour of motorists to determine the critical gap in Trinidad and Tobago (T&T). The research found that, for the roundabouts selected, critical gap estimates do not differ significantly based on either time of day or location. The estimated critical gaps were compared with values commonly used in the Highway Capacity Manual (HCM), so as to determine the effect on estimated intersection capacity. The results indicate that the critical gap values differ significantly from the United States (US) default values (which is one of the standards adopted by T&T), which therefore affects the estimated capacity of the roundabouts. The published values from the HCM are significantly higher than the values obtained, which means that the estimated capacities using the default US values underestimate the existing capacities in T&T.

Keywords: Roundabout, driver behaviour, critical gap, gap acceptance, capacity

1. Introduction

Roundabout capacity is dependent on various factors, which include the traffic flow rate from the numerous legs, geometry, vehicle mix and driver behaviour (Kusama and Koutsopoulos, 2011, p.710). Capacities, delays and queue lengths are interdependent and are all used in determining the Level of Service (LOS) of the roundabout intersection. Since the LOS is used during the feasibility stage in determining whether a traffic mitigation proposal is a viable option, it is important to refine the analysis by using site specific data to yield results which would bring about the most feasible solution for implementation. This highlights the importance of determining accurate gap acceptance behaviour of drivers who attempt to merge from an approach road into the traffic stream already in the roundabout.

In Trinidad and Tobago (T&T), the Ministry of Works and Transport usually mandates that international codes, mainly the American Association of State Highway Transportation Officials (AASHTO), are to be used as the basis for design of highways and main roads. The AASHTO geometric design policy was developed from extensive research conducted in the United States of America. The use of these international standards in T&T may result in geometric designs that are inappropriate since they do not take into account local data.

There are two theories of incorporating driver behavioural characteristics in traffic analysis, namely 1) the gap acceptance method (exponential model) as described in the Highway Capacity Manual (HCM) 2010 (TRB, 2010), and 2) the linear regression method of the Transport Research Laboratory (TRL). Both are endorsed by the major transportation research bodies.

In the design of roundabouts using the Highway Capacity Manual 2010 (TRB, 2010), default values in programs and average values from tables are assumed and used to determine the Level of Service and safety. There is a need for a design parameter to incorporate gap acceptance behavioural characteristics in modelling the flow of traffic and designing roadways for safety in T&T. The paper reports a study to determine the critical gaps of drivers at selected roundabouts in T&T. It seeks to determine if there are significant differences between the critical gaps for roundabouts in T&T and that of international references, and to compare the estimated capacities of the roundabouts based on the HCM 2010 model using the local critical gap versus the default values.

2. Literature Review

2.1 Factors Affecting the Critical Gap

The critical gap is the minimum time gap in the priority stream that a minor street driver is ready to accept for

crossing or entering the major stream conflict zone (Brilon et al., 1999, p.71). Figure 1 illustrates the critical gap spatially.

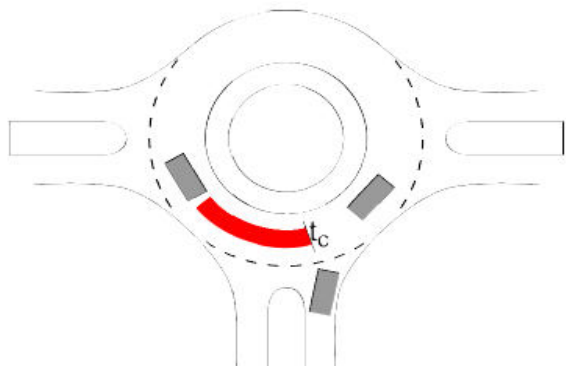


Figure 1. Spatial critical gap
Source: Abstracted from Barry (2012, p.21)

There have been various studies which indicate that the critical gap varies by region and is also heavily influenced by the behavioural characteristics of drivers (Gazzarri, et al., 2012). Gap acceptance models are strongly affected by driver behaviour and local habits. Therefore, the HCM 2010 capacity model should be calibrated to local conditions.” Based on these studies, the average critical headway is significantly lower than the values recommended by international references. Some factors that affect the critical gap are differing driver behaviours, the type of intersection and movement. Additionally, according to Shiftan et al. (2005), waiting time and queuing may also have an effect on the critical gap.

Mensah et al. (2009) hypothesised that the critical gap could be affected by local conditions such as the waiting time for drivers, queue lengths, aggression of local drivers and lastly, seasonal variation. They postulated that critical gaps would decrease as drivers became more familiar with local conditions and that could result in a decrease of the 95th percentile queue length by almost 50%. Moreover, from research conducted by Tupper (2011, 12-13, 60-75), Xu and Tian (2008, 122) and Shiftan et al. (2005, p.1), the other factors that affect the critical gap include weaving, vehicle performance characteristics, geometry of the intersection, number of lanes on minor street, design speed, traffic volumes on the minor and major streets and time of day.

There is some conflicting research about the effect of geometric design on the critical gap. Xu and Tian (2008, p.117) contended that geometric design was insignificant. This is not surprising since within a country, the design standard is assumed to be uniform and should cause minimal changes to the critical gap. This assumption was supported by research conducted by Gazzarri et al. (2012, p.318), which showed that

standard deviations in critical gap measurements of the various multi-lane roundabout sites measured were less than one tenth of a second. In such context, the current study was designed to mitigate the effects of some of these confounding variables by examining roundabouts with typical geometric and traffic flow characteristics for T&T. The HCM 2010 roundabout capacity model will be used.

2.2 Importance of Critical Gap to Capacity

Fundamentally, three methodologies can be used to assess the capacity of roundabouts. These methodologies are: 1) interweave theory model, 2) gap acceptance theory, and 3) regression analysis theory (Wanga and Yang, 2012, p.3)

Miller (1972, p.216) conducted thorough methods for the estimation of critical gaps and their impact on the capacities of roundabouts using the gap acceptance theory, whereas others (Tian et al., 2000, p.407) did research using the regression analysis theory. Research conducted into the capacities of roundabouts in Beijing has shown that roundabout capacities should be measured in terms of the entry capacity, rather than weaving section capacity (Wanga and Yang, 2012, p.159). This notion was further supported by analysis of the HCM gap acceptance theory which calculates the capacity by using information about entry vehicles. The Tanner (1997) formula is considered to be typically representative of this model. It should also be noted that the capacity formula is suggested for a single lane, and completely symmetrical roundabout.

In support of the importance of the critical gap effect on capacities, Gazzarri et al. (2012, p.310) stated that two parameters that may be changed to reflect local driving behaviour are the critical headway and follow-up headway (referred to as critical gap and follow-up time in earlier studies). These factors affect the critical gap which in turn affects the operational factors of the highway system (Mensah et al., 2009, p.8). Additionally the critical gap is used to incorporate the behavioural aspect of the analysis of capacity for intersections in models for determining the expected capacity and delays.

According to Akçelik (2011) and Akçelik and Associates Pty Ltd (2012), SIDRA is a modelling software used by traffic engineers that incorporates the critical gap into the design and analysis of the performance of roundabouts. Moreover, the critical gap is used, along with the follow up headway, in sensitivity analyses of the effects of (a) the driver behaviour and traffic characteristics, and (b) the intersection geometry. The critical gap together with the follow up headway is usually 60% of the critical gap (Akcelike and Associates Pty Ltd, 2012, p.116). It is used to determine the capacities of roundabouts. Therefore, based on the critical gap information used in the analysis, the capacity of roundabouts can be under- or over-estimated (Barry, 2012, pp.31-33).

2.3 Critical Gap Estimation Methods

One of the fundamental methods of estimating the critical gap was developed by Raff in the 1950s (Raff and Hart, 1983, p. 255-258). The method states that the critical gap can be obtained from the intersection between the graphical plot of the cumulative functions of accepted gaps and rejected gaps (see Figure 2). The equation can be represented as:

$$1 - F_r(t) = F_a(t) \tag{1}$$

where,

- t = headway of major stream;
- $F_a(t)$ = cumulative probability of accepted gap; and
- $F_r(t)$ = cumulative probability of rejected gap.

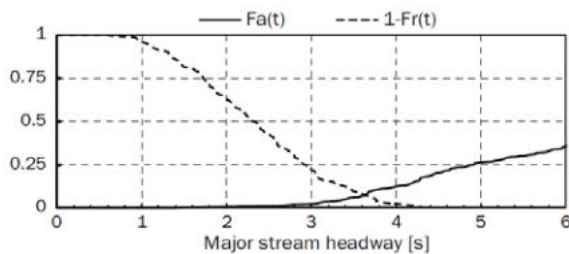


Figure 2. Graphical representation of the intersection
Source: Adopted from Vasconcelos (2012)

Table 1 shows a summary of various methods for the determination of the critical gap and their suitability. Raff’s method has been deemed to be a very good estimator of the critical gap once all the gaps are used. It was decided to use the simple approach that gives similar quality results as the more complex methods.

Table 1. Benefits of the different method of analysis for critical gaps

Methods	Variation	Estimates Critical Gap	Ease of Use	Use of Data
Average Accepted Gap	All accepted gaps	No	Very Good	Poor
	Accepted gaps < 12 seconds			Very Poor
Raff Method	All gaps	Yes	Very Good	Very Good
	All accepted gaps and maximum rejected gaps			Good
Cumulative Acceptance	All accepted gaps	Yes	Very Good	Poor
	Accepted gaps < 12 seconds			Very Poor
Equilibrium of Probabilities	All accepted gaps and rejected gaps	Yes	Poor	Very Good
	All accepted gaps and maximum rejected gaps			Good
Fit Maximization	All accepted gaps and rejected gaps	Yes	Good	Very Good
	All accepted gaps and maximum rejected gaps			Good

Source: Abstracted from Tupper (2011, p. 45)

3. Data Collection and Processing

The research monitored the real world gap acceptance behaviour, and was carried out without the drivers being aware. The studied roundabouts were selected, taking into consideration the different conditions that would affect the measured critical gap, such as different geometries, flows, approach conditions and times of day.

Only one lane of each multi-lane roundabout was measured and the longitudinal gap was not considered. The first step was to identify the suitable sites for data retrieval. This was done by listing the possible sites at which data could be collected and then eliminating unsuitable sites. Factors that affected the suitability are:

1. Establishing an effective camera position;
2. Located in Trinidad;
3. Two-lane geometry;
4. Standard circular geometry;
5. Limited to no interruptions by pedestrians, traffic lights, vending or bicycles.
6. Defect free pavement surface.

Nine (9) major roundabouts throughout Trinidad were considered, as follows:

- Roxy Roundabout (Irregular oval shape),
- Arthur Lok Jack Roundabout at Mt. Hope,
- Trincity Mall Roundabout,
- Couva Interchange Roundabouts (West and East),
- Tarouba Link Road and South Trunk Road Roundabout (always saturated and has a deficient pavement surface),
- Maritime Roundabout,
- Grand Bazaar Roundabout (Single lane),
- Price Plaza Roundabout (Vending activity affects the usage), and
- Aranguez Overpass Roundabouts (North and South).

These roundabouts were evaluated to determine their suitability for the study. Those roundabouts were eliminated from consideration if there were extraneous elements which would tend to affect the driver’s gap acceptance behaviour such as high levels of saturation, vending occurring near the circular roadway, and pavements with undulating surfaces of the roundabout lanes. As a result, three roundabouts namely, the Arthur Lok Jack roundabout in Mt. Hope, the Maritime roundabout in Barataria and the Aranguez Overpass South roundabout, were selected. These roundabouts had differing geometric layouts but shared a similar standard design with respect to their layouts.

Field data was collected using video recordings of traffic at the roundabouts for a typical weekday. No notices or announcements were made public to indicate that the recordings would be taking place, so as to avoid any alteration in the behavioural characteristics of the drivers. The cameras were discretely placed on signage of the roundabouts and were not easily seen by the drivers. Video playback software - LUT version 3 player - was used to decode the information required.

The critical and follow-up gaps were estimated for each roundabout (see Table 2). In total, 1,206 gaps in traffic were observed at these three roundabouts. The video observations took into consideration varied site and traffic conditions. The recordings started at 6 AM and were stopped at 6 PM. Temporary markers were painted onto the roadway to help measure the duration of the accepted and rejected gaps.

Table 2. Summary of Roundabout Data Collection

Town/Location	Roundabout	Inscribed Circle Diameter (m)	Entry Lanes	Leg	Lane Analysed	Date and Time
Mt Hope	Arthur Lok Jack	60	2	South	Inner	Wednesday 29/04/2015 06:00 - 8:00 AM and 2:00 - 4:00PM
Barataria	Maritime	45	2	East	Outer	Tuesday 28/04/2015 06:00 - 8:00 AM and 2:00 - 4:00PM
Aranguez	Aranguez Overpass South	52	2	South	Outer	Thursday 28/05/2015 6:00 - 7:00 AM and 2:00 - 4:00PM

4. Results

4.1 The Maritime (Barataria) Roundabout

The Maritime (Barataria) roundabout is located at the intersection of 10th Avenue and Lady Young south roadway (see Figure 3). Data was analysed during the peak flow periods in both the AM and PM. Figures 4 and 5 show the cumulative accepted versus rejected gaps for the Maritime Roundabout in AM and PM, respectively.

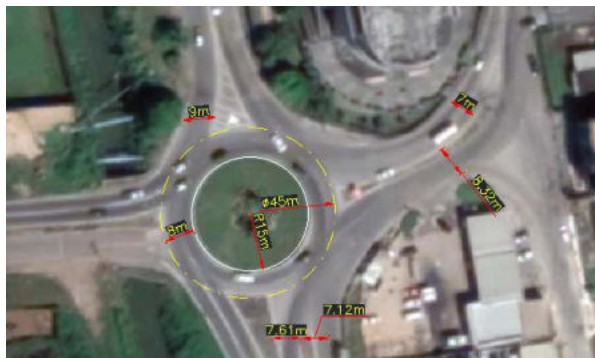


Figure 3. An aerial photograph of the Maritime roundabout
Source: Google Earth, accessed 25/09/2019)

maximum rejected gap was near to 9 seconds which came from a large truck manoeuvring around the roundabout. The capacities were calculated and compared using the HCM 2010 model with the default gap parameters and the measured critical gaps (see Figures 6 and 7).

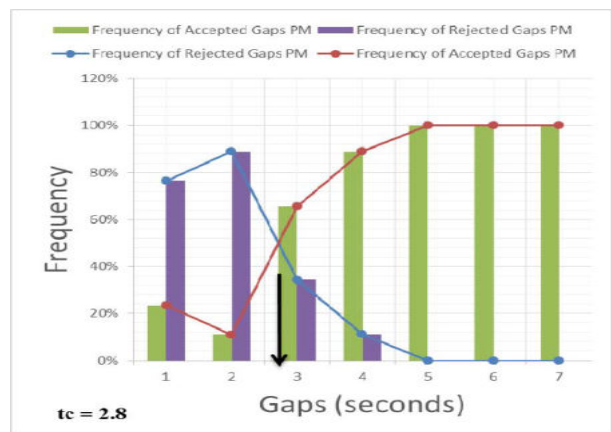


Figure 5. Plot of the Cumulative Accepted vs Rejected Gaps for the Maritime Roundabout PM

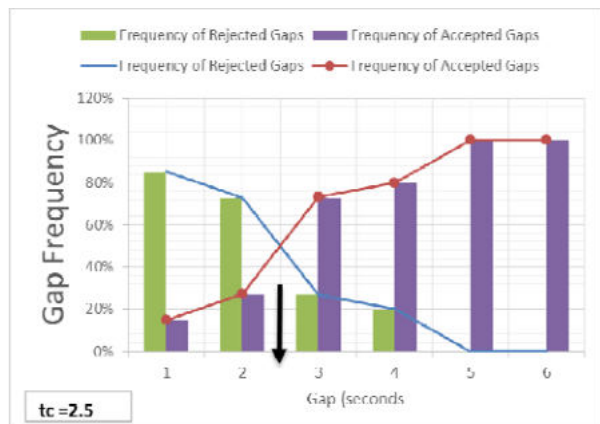


Figure 4. Plot of the Cumulative Accepted vs Rejected Gaps for the Maritime Roundabout AM

As shown in Table 3, the critical gap variation between the morning and afternoon estimations yielded a difference of 19.14%. It should be noted that the minimum accepted gap measured for the AM and PM time periods were 0.56 and 0.6 seconds respectively. The

Table 3. Summary of Gaps at the Maritime Roundabout

Gaps	Mean (sec)	Standard Deviation (sec)	Minimum (sec)	Maximum (Lag) (sec)
Accepted AM	2.9	2.5	0.6	17.4
Rejected AM	1.5	0.7	0.7	9.0
Accepted PM	2.2	1.3	0.6	6.7
Rejected PM	1.7	0.6	0.8	10.1

Gaps	Seconds
t_c AM	2.35
t_c PM	2.8
Δ AM vs PM	0.45
Δ %	19.14%
Maritime t_c	2.6
Δ Lane Capacity of Approach	170
Δ Capacity %	19%
Δ Degree of Sat	0.076
Δ Degree of Sat%	20%

The critical gap value used in the SIDRA model to determine the capacity corresponds to the maximum volumes observed. The maximum volumes were measured in the morning periods, therefore the AM critical gaps were used in the calculations of the capacities. A change in the critical gap value from the

default HCM 2010 to the value measured in this study results in an increased estimated capacity of 170 vehicles per hour.

the cumulative accepted versus rejected gaps for the Arthur Lok Jack Roundabout in AM and PM, respectively.

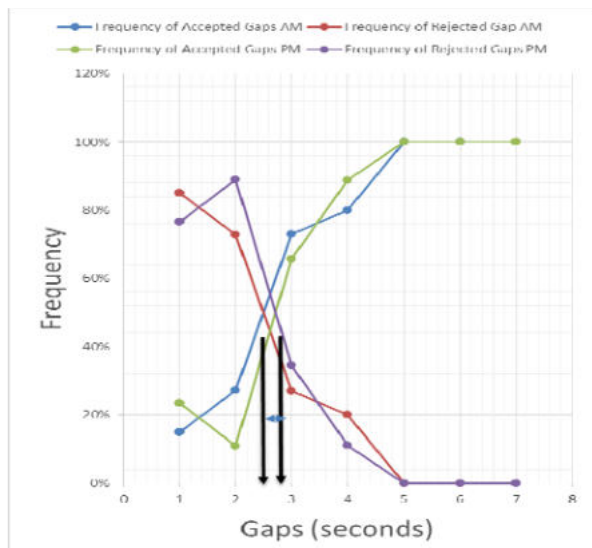


Figure 6. Plot of the Cumulative Accepted vs Rejected Gaps for Maritime Roundabout AM vs PM

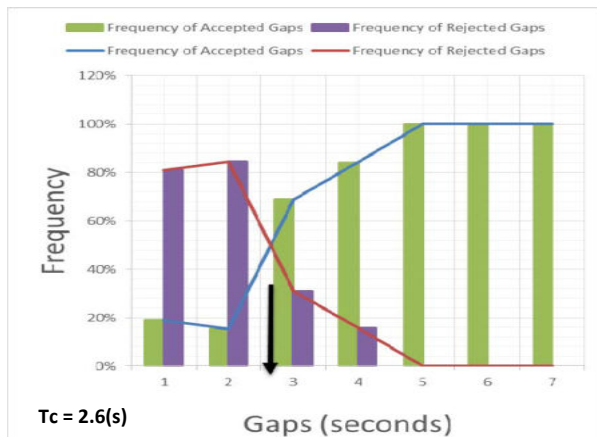


Figure 7. Plot of the Cumulative Accepted vs Rejected Gaps for Maritime Roundabout AM and PM Combined

4.2 The Arthur Lok Jack (Mt Hope) Roundabout

The Arthur Lok Jack Roundabout is located at the intersection of the Uriah Butler Highway (northern section), the entrances to Arthur Lok Jack and the southern entrance to The University of the West Indies (see Figure 8). This is a four-leg roundabout that has predominant flows in the north and south bound directions. These north and south approaches are fed with traffic from the Eastern Main Road and the Churchill Roosevelt Highway respectively Data from the southern approach was analysed during the peak flow periods in both the AM and PM. Figures 9 and 10 show

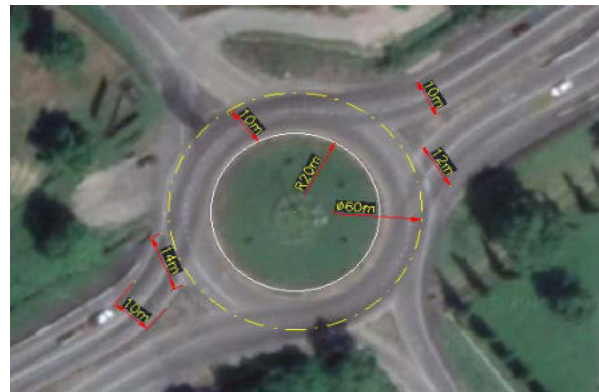


Figure 8. An aerial photograph of the Arthur Lok Jack (Mt Hope) roundabout
Source: Google Earth, accessed 25/09/2019

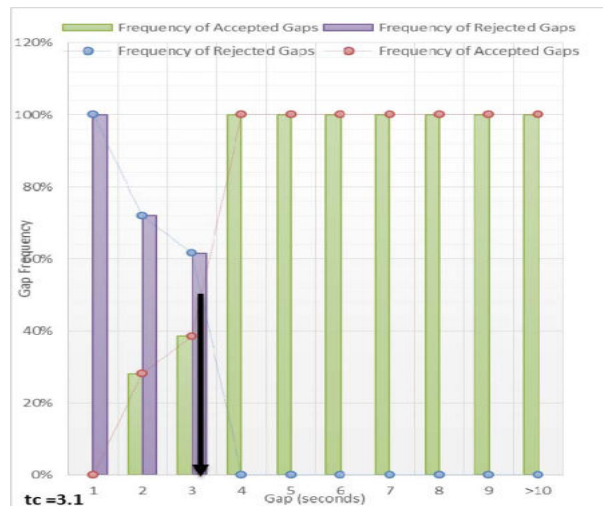


Figure 9. Plot of the Cumulative Accepted vs Rejected Gaps for the Arthur Lok Jack Roundabout AM

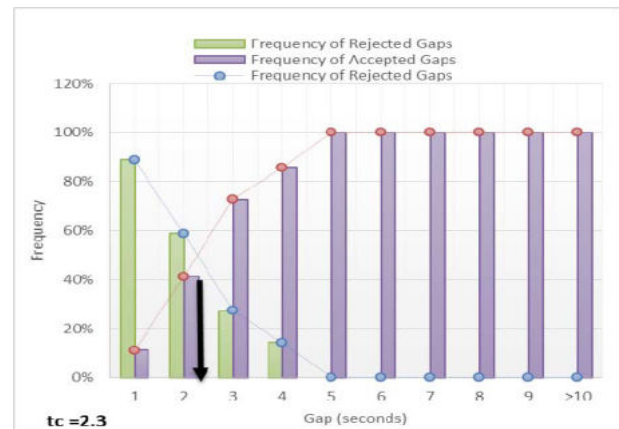


Figure 10. Plot of the Cumulative Accepted vs Rejected Gaps for the Arthur Lok Jack Roundabout PM

Table 4 shows a summary of gaps at the Arthur Lok Jack roundabout. There was a larger difference between the critical gap values for the morning and afternoon as compared to Maritime. The variation between the AM and the PM for this roundabout was comparable to the difference obtained for the Aranguez South roundabout. In addition, the lowest critical gap measured at Arthur Lok Jack roundabout was in the afternoon period. The minimum accepted and rejected gaps were around 1 second for both morning and afternoon periods. This may suggest that on the day of the observation, that similarly small gaps were both accepted and rejected at this roundabout (see Figures 11 and 12).

Table 4. Summary of Gaps at the Arthur Lok Jack Roundabout

Gaps	Mean (sec)	Standard Deviation (sec)	Minimum (sec)	Maximum (Lag) (sec)
Accepted AM	5.1	3.2	1.5	14.3
Rejected AM	2.0	0.6	1.1	3.4
Accepted PM	4.4	2.9	1.2	14.3
Rejected PM	1.9	0.8	1.0	3.9

Gaps	Seconds
t_c AM	3.1
t_c PM	2.3
Δ AM vs PM	0.8
Δ %	2.8
Arthur Lok Jack t_c	34.78%
Δ Lane Capacity of Approach	13
Δ Capacity %	1%
Δ Degree of Sat	0.004
Δ Degree of Sat%	2%

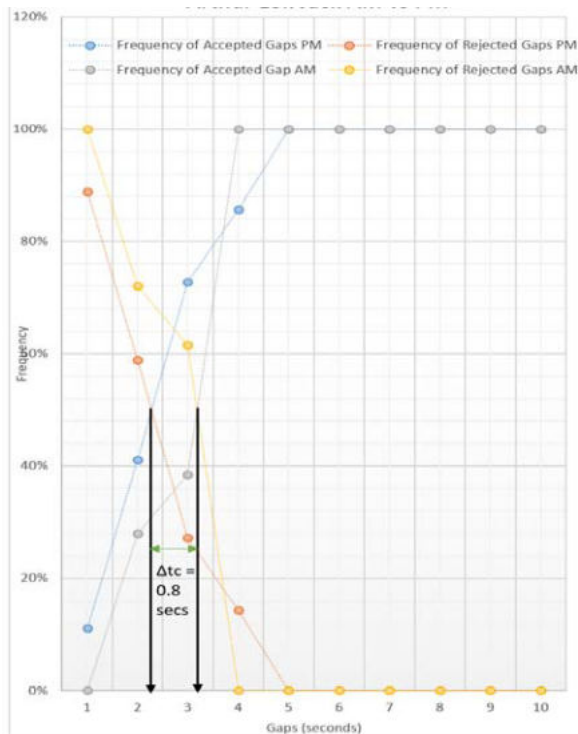


Figure 11. Plot of the Cumulative Accepted vs Rejected gaps for the Arthur Lok Jack Roundabout AM vs PM

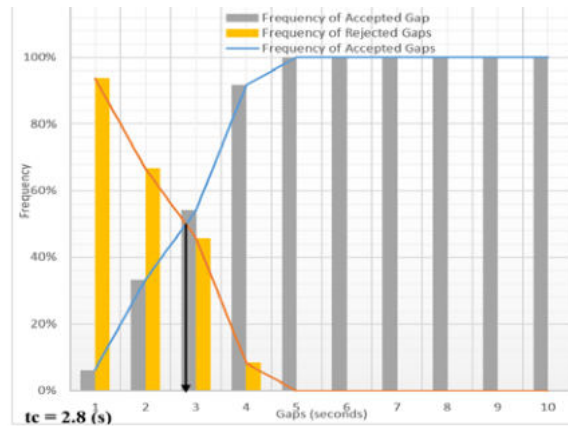


Figure 12. Plot of the Cumulative Accepted vs Rejected gaps for the Arthur Lok Jack Roundabout AM vs PM combined

The difference between the critical gaps measured in the morning and afternoon was 0.8 seconds. This difference was an increase as compared to the difference observed at the Maritime roundabout. The associated increase in capacity using the different critical gaps in the SIDRA HCM 2010 analysis was 13 vehicles per hour, a 1% percent increase, and therefore much lower than the increase in the observed inner lane capacity at Maritime.

4.3 The Aranguez South Roundabout

This roundabout is located at the intersection of Garden Road and the Aranguez South Link Road. This is a three-leg roundabout that has predominant flows in the south bound direction. The south approach receives its traffic from the westbound side of the Churchill Roosevelt Highway. Data was analysed during the peak flow periods in both the AM and PM. Figures 14 and 15 show the cumulative accepted versus rejected gaps for Aranguez South Roundabout in AM and PM, respectively.



Figure 13. Aerial photograph of the Aranguez South roundabout
Source: Google Earth, accessed 25/09/2019

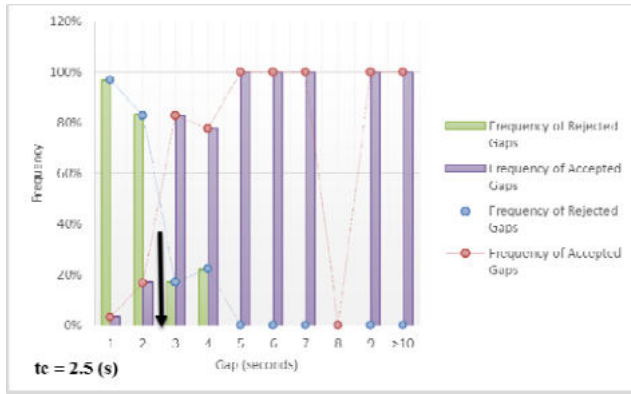


Figure 14. Plot of the Cumulative Accepted vs Rejected Gaps for the Aranguez South roundabout, AM

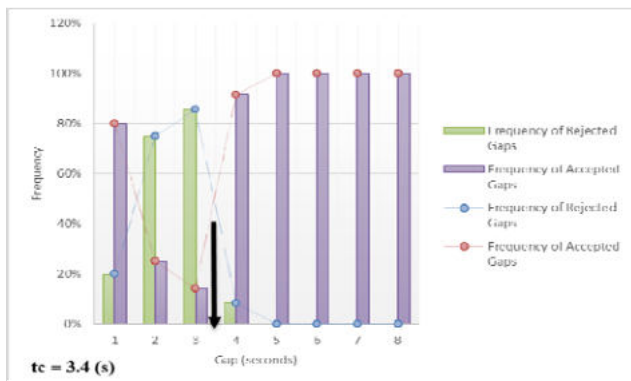


Figure 15. Plot of the Cumulative Accepted vs Rejected Gaps for the Aranguez South roundabout, PM

Table 5 shows a summary of the critical gap variation between the morning and afternoon estimations, yielding a difference of 36%. This difference was the highest variation between the morning and afternoon of all the observed roundabouts. Furthermore, the critical gap in the afternoon period was the highest critical gap measured amongst the roundabouts. It should also be noted that the minimum accepted gap measured for the AM and PM time periods was 1 second. The critical gap used to calculate the capacity was 2.5 seconds which resulted in a 62% difference in capacity as compared with those obtained with the default HCM 2010 values (see Figures 16 and 17). This was the highest increase in capacity among all of the three roundabouts under study.

The population critical gap was determined assuming driver behavioural characteristics are consistent across the selected roundabouts in Trinidad. This assumption is tested with the null hypothesis that the three roundabout samples belong to the same population (see t-test 2). Then, if the mean does not significantly differ, it can be used to represent the population as its variations would be random errors. Figure 18 shows the cumulative accepted versus rejected gaps for the population.

Table 5. Summary of Gaps at the Aranguez South Roundabout

Gaps	Mean (sec)	Standard Deviation (sec)	Minimum (sec)	Maximum (Lag) (sec)
Accepted AM	3.1	1.7	0.6	9.9
Rejected AM	1.8	0.5	0.9	4.1
Accepted PM	3.7	1.8	0.9	7.5
Rejected PM	2.3	0.6	1.4	3.6

Gaps	Seconds
t_c AM	2.5
t_c PM	3.4
Δ AM vs PM	0.9
Δ %	36.0%
Aranguez South t_c	2.6
Δ Lane Capacity of Approach	655
Δ Capacity %	62%
Δ Degree of Sat	0.068
Δ Degree of Sat%	28%

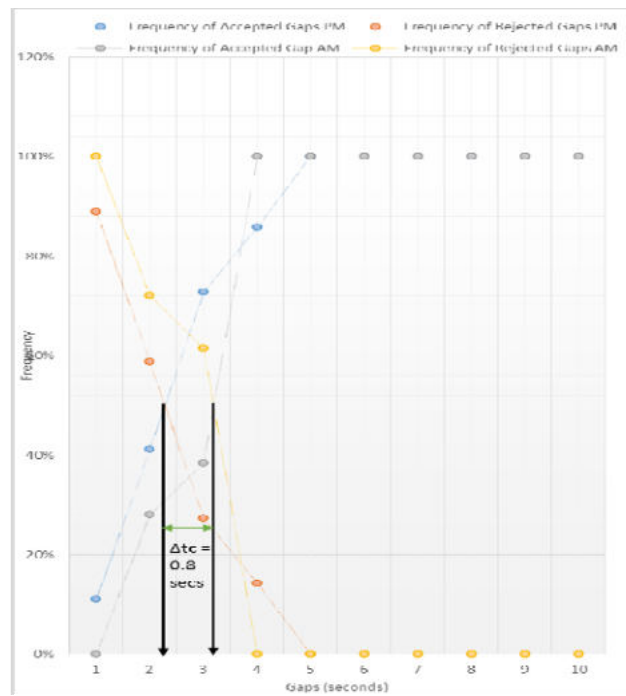


Figure 16. Plot of the Cumulative Accepted vs Rejected Gaps for the Aranguez South Roundabout AM vs PM

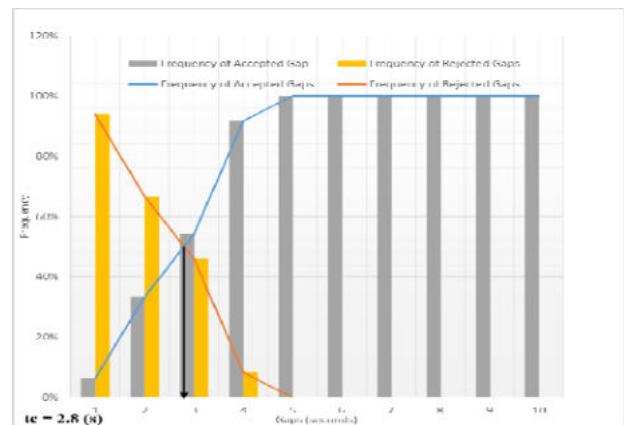


Figure 17. Plot of the Cumulative Accepted vs Rejected Gaps for the Aranguez South Roundabout AM and PM combined

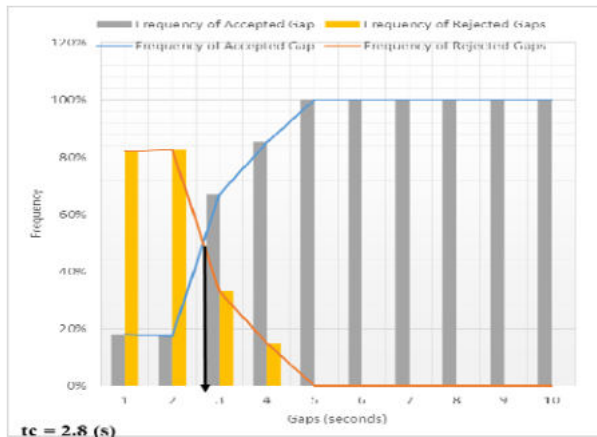


Figure 18. Plot of the Cumulative Accepted vs Rejected Gaps for the Population

5. Data Analysis

5.1 Testing Framework

A number of paired comparisons were undertaken. It is hypothesised that:

1. The critical gap would vary significantly between the morning and afternoon periods,
2. The combined sample of the critical gap for all sites will vary significantly from the population critical gap, and
3. The sample mean critical gap will significantly differ from those stated in the HCM 2010.

Figure 19 shows a flow chart of the significance testing framework. Null hypotheses 1 and 2 were tested using the students t-test. The significance level (α), i.e. the probability of the occurrence of wrongfully rejecting the null hypothesis, was set at 5%. For hypothesis 3, this was quantified by the use of differences as they were calculated values and not observed.

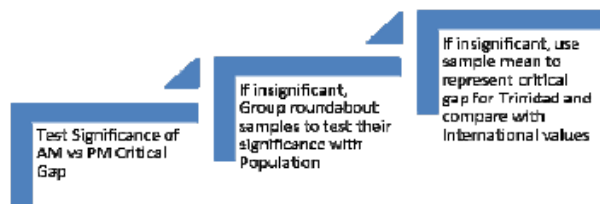


Figure 19. A Flow Chart of the Significance Testing Framework

Using the t-test in this study, it was assumed that:

- The data is distributed along a normal distribution (it can be verified by the checking for skew),
- A two-sided test is to be more suitable,
- Each observation in the study had an equal chance of participating in the study,
- Drivers were not aware of their driving patterns being recorded, and
- The critical gap holds for both inner and outer lanes and tested separately.

5.2 Testing of Hypotheses

Three hypotheses were tested. These are listed below and records of respective the computations are summarised in Tables 6, 7, and 8, respectively.

- t-test 1: Measured Gap AM versus PM,
- t-test 2: Samples represents the Population, and
- t-test 3: Combined Measured Gap vs HCM gap.

Table 6. Test for Significance of Hypothesis 1

Variables	Overall observed Outer Lane	Overall Observed Inner Lane
Expected Value	2.83	2.65
Mean AM	2.65	2.65
Mean PM	2.83	2.83
Standard Deviation AM	0.40	0.40
Standard Deviation PM	0.55	0.55
Level of Probability	0.05	0.05
Number of data points	3.00	3.00
Standard Error AM	0.23	0.23
Standard Error PM	0.32	0.32
Actual t value AM	0.80	-
Actual t value PM	-	0.58
Critical t value	4.30	4.30
Significance t-Test 1	Accept Null Hypothesis	Accept Null Hypothesis
	With accepting the Null Hypothesis, there is an insignificant difference of measured critical gap in the AM	With accepting the Null Hypothesis, there is an insignificant difference of measured critical gap in the PM

Table 7. Test for Significance of Hypothesis 2

Variables	Overall observed
Expected Value	2.80
Mean Critical Gap	2.67
Standard Deviation of samples	0.12
Level of Probability	0.05
Number of data points	3.00
Standard Error	0.07
Actual t value	2.00
Critical t value	4.30
Significance t-Test 2	Accept Null Hypothesis
	With accepting the Null Hypothesis, there is no significant difference between the sample mean and population

Table 8. Test for Skew and Significance Testing of Hypothesis 3

Variables	Overall observed Outer Lane	Overall Observed Inner Lane
Expected Value	4.30	4.11
Population Mean	2.67	2.67
Standard Deviation	0.12	0.12
Level of Probability	0.05	0.05
Number of data points	3.00	3.00
Standard Error	0.07	0.07
Actual t value	24.50	21.65
Critical t value	4.30	4.30
Significance t-Test 3	Reject Null Hypothesis	Reject Null Hypothesis
	With rejecting the Null Hypothesis, there is a 95% chance that the measured critical gap differs from the HCM 2010 critical gap	With rejecting the Null Hypothesis, there is a 95% chance that the measured critical gap differs from the HCM 2010 critical gap

Several limitations of the *t*-test are identified. Firstly, the *t*-test gives correlation and does not imply causation. Secondly, the expected values published in the HCM 2010 are a range, and the mean values were used. Also, these mean values were consistent with the value used in the SIDRA analysis.

6. Discussions and Interpretation of the Results

The results of the hypothesis testing showed 1) that there was no significant difference between the measured critical gaps in the morning and afternoon, 2) that there was no significant difference between the population mean and the grouped sample mean, and 3) that there was a significant difference of the group sample mean and the critical gap values referenced in the HCM 2010.

The summary of findings is given in Table 9. The associated increases in the capacities were minimal except in the case of Aranguez South where there was a 62% difference. The majority of the gaps were estimated between 2 to 3 seconds. Only two estimations were over 3 seconds but all were under the stated values of the HCM 2000, HCM 2010 and NCHRP 572.

Table 9. Summary of the Critical Gaps and Capacities of Three Roundabouts in Trinidad

Gaps	Arthur Lok Jack	Maritime	Aranguez South
tc AM (s)	3.1	2.35	2.5
tc PM (s)	2.3	2.8	3.4
Δ AM vs PM %	34.78%	19.07%	36.00%
tc Combined AM and PM	2.8	2.6	2.6
Δ Capacity %	1%	19%	62%
Δ Degree of Sat%	2%	20%	28%

The comparisons of the critical gaps determined at selected roundabouts Trinidad are in Table 10 which shows that the gaps determined were lower than most of the international values. Critical gap values were determined for each roundabout for both the morning and afternoon periods and overall, so the variability of time and its effect on the gap values could be investigated. The overall results showed a variation of the critical gaps observed at all three roundabouts under study. This variation was due to the flow conditions, as well as the varying geometries at different roundabouts. There were also insignificant differences observed between the critical gaps for each of the roundabouts according to the time of day.

The population critical gap was determined assuming driver behavioural characteristics are consistent across Trinidad. The three different roundabout samples were determined to belong to the same population. The mean does not significantly differ, and it was used to represent the population as its variations would be random errors. Moreover, lack of traffic law enforcement in Trinidad may result in road users not following the operational rules of a roundabout.

Table 10. International Critical Gap References

Country	Mean Critical Gap (sec)	Observation
Australia		
2 lane	2.9	Model based on conflicting flow and number of lanes, diameter and entry width
Denmark		
2 lane, rural	4	Parameters by Regression
Poland		
Medium 2 lane (L)	4.3	Parameters by Regression
Medium 2 lane (R)	4.6	
Portugal		
2 lane	3.7	Maximum Likelihood method and Raff
Sweden		
2 lane roundabouts (L)	4.5	Maximum Likelihood method
2 lane roundabouts (R)	4.15	
United States (HCM 2010)		
2 lane roundabouts (L)	4.3	Maximum Likelihood method
2 lane roundabouts (R)	4.11	Maximum Likelihood method
United States (NCHRP 572)		
2 lane roundabouts (L)	4.85	Maximum Likelihood method
2 lane roundabouts (R)	4.15	
Trinidad		
2 lane roundabout (L)	3.1	Raff at Arthur Lok Jack
2 lane roundabout (R)	2.35	Raff at Maritime
2 lane roundabout (L)	2.5	Raff at Aranguez South

For example, road users drive on the shoulder lane of the roundabout which introduces an additional parameter to the capacity which theoretically comprises of the circulatory lanes, entry lanes and the exit lanes. Also noteworthy is the fact that, due to the improper use and incorrect education on the use of a roundabout, many users do not enter into the correct lanes and weave dangerously within the circulatory lanes of the roundabout. Alternatively, some road users merge into the circulatory stream dangerously, therefore accepting very small gaps.

A comparison and a capacity analysis were performed using the standard values of the Highway Capacity Manual 2010. The analysis used the maximum volumes as the best model of the expected capacities at the roundabout sites. The calculated values were compared to the HCM values and it was determined that the estimations for Aranguez South in the afternoon (3.4 seconds) and Arthur Lok Jack in the morning period (3.1 seconds) were those closest to the guided values of the HCM 2010 values of 4.3 and 4.11 seconds. The Arthur Lok Jack roundabout gap estimate for the afternoon was the furthest from the HCM 2010 value (80 percent lower). Hence, the Aranguez South roundabout had the lowest critical gap for all the morning periods and therefore was used for the capacity analysis at this site. This resulted in a value 72 percent higher than the expected HCM 2010.

There was a statistically significant difference between the critical gaps measured in the morning and those published in the HCM 2010 for the sub dominant (outer) lane. This was not the case for the mean of the afternoon gaps when compared to the dominant (inner) lane HCM 2010 standard.

7. Conclusion

The objectives of this study were 1) to determine the critical gaps for drivers at selected roundabouts in Trinidad, 2) to determine if they differed significantly from international values, and 3) to use the measured values to determine the differences in capacities from that of the HCM default values. With the use of video technology the critical gaps as defined by Raff and Hart (1983) were determined at the three roundabouts under study. Comparisons were made between different times of day and their effects on the predicted and actual capacities of the roundabouts. It was discovered from the samples taken in this study that the time of day did not result in a significant variation of the critical gap. Furthermore, it was shown that the estimated critical gaps at the three roundabouts were not statistically significantly different.

The results of the research showed significant differences between the critical gaps in T&T and those from international sources included the default gaps used in the Highway Capacity Manual 2010. The differences determined resulted in increases of the calculated capacities at the three roundabouts by as much as 72% when the locally derived critical gaps were used. The results showed the importance of using locally derived measures, as far as possible in designing and determining the performance of roundabouts.

References:

- AASHTO (2004), *Geometric Design of Highways and Streets*, American Associated of State Highway Transportation Officials, Washington, DC.
- Barry, C. (2012), *Calibration of the HCM 2010 Roundabout Capacity Equations for Georgia Conditions*, Master's Thesis. Georgia Institute of Technology, USA.
- Brilon, W., Koenig, R., and Troutbeck, R. (1997), "Useful estimation procedures for critical gaps", *Proceedings of the Third International Symposium on Intersections without Traffic Signals*, Washington, July, pp.71-87 (Transportation Research Board)
- FHA (2000), *Roundabouts: An Informational Guide*, Federal Highway Administration, Portland
- Gazzarri, A., Martello, M.T., Pratelli, A., and Souleyrette, R.R. (2012), "Estimation of gap acceptance parameters for HCM 2010 roundabout capacity model applications", *Proceedings of the Eighteenth International Conference on Urban Transport and the Environment*, Southampton (WIT Press)
- Kusuma, A., and Koutsopoulos, H.N. (2011), "Critical gap analysis of dual lane roundabouts", *Procedia - Social and Behavioural Sciences*, Vol.16, pp.709-717.
- Mensah, S., Eshragh, S., and Faghri, A. (2009), *A Critical Gap Analyses of Modern Roundabouts*, University of Delaware, Delaware
- Miller, J.A. (1972), "Nine estimators of gap acceptance parameters", In: Newell, G.G.F. (ed.), *Traffic Flow and Transportation: Proceedings*, Elsevier, New York, pp.215-235
- Raff, M.S. and Hart, J.W.A. (1983), "A volume warrant for urban stop sign", *Traffic Engineering and Control*, Vol.24, No.5, May, pp.255-258.
- Shifftan, Y., Shmueli-Lazar, S., and Polus, A. (2005), "Evaluation of the waiting-time effect on critical gaps at roundabouts by a logit model", *European Journal of Transport and Infrastructure Research*, Vol. 5, No.1, pp.1-12.
- Tian, Z., Troutbeck, R., Kyte, M., Brilon, W., Vandehey, M., Kittelson, W., and Robinson, B. (2000), "A further investigation on critical gap and follow-up time", *Proceedings of the 4th International Symposium on Highway Capacity*, Maui/Hawaii, pp.409-421 (Transportation Research Circular E-C018)
- Tian, Z., Vandehey, M., Robinson, B.W., Kittelson, W., Kyte, M., Troutbeck, R., Brilon, W., and Wu, N. (1999), "Implementing the maximum likelihood methodology to measure a driver's critical gap", *Transportation Research Part-A: Policy and Practice*, Vol.33, No.3, pp.187-197.
- TRB (2010), *Highway Capacity Manual 2010*, Transportation Research Board, 5th Edition, Washington, DC
- Tupper, S.M. (2011), *Safety and Operational Assessment of Gap Acceptance through Large-Scale Field Evaluation*, Master's Thesis, University of Massachusetts, Amherst, USA
- Vasconcelos, A.L.P. (2012), "Comparison of procedures to estimate critical headways at roundabouts", *PROMET – Traffic and Transportation*, Vol. 25, pp.43-53.
- Wanga, W., and Yang, X. (2012), "Research on capacity of roundabouts in Beijing", *Procedia - Social and Behavioural Sciences*, Vol.43, pp.157-168.
- Xu, F., and Tian, Z.T. (2008), "Driver behaviour and gap-acceptance characteristics at roundabouts in California", *Journal of the Transportation Research Board*, Vol.2071, pp.117-124

Authors' Biographical Notes:

Khary Leighton Campbell is a Project Manager at the Urban Development Corporation of Trinidad and Tobago. A MSc in Civil Engineering from The University of the West Indies (UWI) in 2016, he is a Member of Association of Professional Engineers of Trinidad and Tobago, a Project Management Professional (PMP), and a Registered Civil Engineer with the Board of Engineering Trinidad and Tobago. His past work experience as Project Engineer at the Ministry of Works and Transport (MOWT), Programme for Upgrading Road Efficiency (PURE) entails road infrastructure design. Mr. Campbell research interest includes geometric design, and traffic mitigation.

Trevor A. Townsend is a Senior Lecturer in Transportation Engineering, Department of Civil and Environmental Engineering, Faculty of Engineering, The University of The West Indies, St. Augustine, Trinidad. A Ph.D. in Civil Engineering specialising in Transportation Systems Analysis from Northwestern University in 1987, he is a Fellow of Association of Professional Engineers of Trinidad and Tobago, the Institute of Transportation Engineers and the Chartered Institution of Highways and Transport. His work experience includes appointments as the Chief Traffic Engineer, Traffic Management Branch of the Ministry of Public Utilities and National Transportation, General Manager of the Public Transport Service Corporation, CEO of Caribbean Steel Mills Ltd., and CEO of Trinidad Aggregate Products Ltd. Dr. Townsend's research interests include travel behaviour, transportation policy and transportation systems operations.



Microwave Drying of West Indian Bay Leaf (*Pimenta racemosa*)

Saheeda Mujaffar^{a,Ψ}, and Shari Bynoe^bFood Science and Technology Unit, Department of Chemical Engineering, The University of the West Indies,
St. Augustine, Trinidad and Tobago, West Indies;^aEmail: saheeda.mujaffar@sta.uwi.edu^bEmail: shatoni26@msn.com^Ψ Corresponding Author

(Received 31 July 2019; Revised 26 December 2019; Accepted 07 January 2020)

Abstract: The effect of microwave power (200, 500, 700 and 1000W) on the drying behaviour of West Indian Bay leaf (*Pimenta racemosa*) was investigated. Leaves were dried in a commercial digital microwave oven until there was virtually no change in weight. The initial moisture content and water activity (a_w) values of fresh leaves averaged 0.85 g H₂O/g DM (46.0 % wb) and 0.912, respectively. Although a decrease in moisture content, water activity and drying time increased with microwave power level, the most noticeable changes were seen as microwave power increased from 200 to 500W. Overall, drying time to equilibrium moisture values decreased from 48.8 to 5.2 minutes for leaves dried at 200-1000W, respectively. The final moisture content values of leaves dried at 200, 500, 700 and 1000W averaged 0.22, 0.05, 0.04 and 0.02 g H₂O/g DM (18.7 to 2.0 % wb), respectively. Corresponding water activity values for microwave-dried leaves averaged 0.756 for leaves dried at 200W power and 0.326 for leaves dried at 1000W. Drying rates at the start of drying averaged 0.02 g H₂O/g DM/min for leaves dried at 200W power, compared with 0.63 g H₂O/g DM/min for leaves dried at 1000W. Drying of all leaves occurred in the falling rate period. Drying rate constants (k) ranged from 0.0410 to 1.0930 1/min, with the corresponding diffusivity values averaging 0.62 and 16.69 x 10⁻⁹ m²/s, for leaves dried at 200-1000W, respectively. Rehydration ratios were found to increase with rehydration temperature ($p \leq 0.05$). Significantly lower rehydration ratios were seen in leaves dried at 200W when rehydration was carried out at ambient temperature. Leaves experienced changes in colour and texture during drying, with undesirable changes occurring during drying at 200W and 1000W power levels. Drying at 500W and 700W was favourable and found to be similar with respect to the colour attributes and equilibrium moisture content of dried leaves, as well as energy consumption. The chlorophyll content was higher in leaves dried at 500W while the odour of leaves dried at 700W was stronger. Of the nineteen thin layer models applied to the MR data, the Verma model best fit the data for leaves dried at 500W power level and the Jena and Das model best fit the data for leaves dried at 700W. The results show the clear potential for microwave drying as a rapid drying method of drying bay leaves.

Keywords: Microwave drying, West Indian Bay leaf, thin layer modelling

Nomenclature

A	Drying constant	MR	Moisture Ratio $(M-M_e)/(M_o-M_e)$
a_w	Water activity	P	Microwave power (W)
D_{eff}	Diffusion coefficient (m ² /s)	R^2	Coefficient of determination
DM	Dry matter (g)	RMSE	Root Mean Square Error
E_t	Energy consumption (W.h)	RR	Rehydration Ratio
k	Drying rate constant (1/min)	W	Watts
L	Half thickness of leaf (m)	$K, K_p, K_1, a, b, c, g, n$	Model constants
L^*, a^*, b^*	Colour attributes	t	Time (min)
M	Moisture content (g H ₂ O/g DM) at time = t	wb	Wet basis (g H ₂ O/100g FW)
M_o	Initial Moisture Content (g H ₂ O/g DM)	χ^2	Chi-Square
M_e	Equilibrium Moisture Content (g H ₂ O/g DM)		

1. Introduction

West Indian bay leaves (*Pimenta racemosa*) are dark green, shiny, evergreen leaves that emit a potent spicy aroma that is also comparable with the smell of lemon (Paula *et al.*, 2010; Ogundajo *et al.*, 2011). The leaves derive from a large tree (15-25 metres), are also known as West Indian Bay, Bay Leaf, Bay Tree, Bay Cherry, Bois d'Inde, Matagueta and Wild Cinnamon (Seaforth

and Tikasingh, 2008). The tree is native throughout the Caribbean region, but is predominantly grown in the West Indies, Mexico, Indonesia, Guyana, Puerto Rico, Venezuela, Jamaica and Africa (Seaforth and Tikasingh, 2008; Ogundajo *et al.*, 2011). Traditionally, West Indian bay leaves (*Pimenta racemosa*) are used in the production of bay rum which is made by distillation of the leaves with rum, and these leaves are purported to

have soothing and antiseptic properties (Seaforth and Tikasingh, 2008). The essential oil, commonly known as “bay oil” or “Myrcia oil” is obtained by steam distillation (McGaw *et al.*, 2016). Bay oil is used in aftershaves, hair growth and hair loss lotions, perfumes and as a commercial flavouring in food. In Caribbean folk medicine, bay oil is used to treat rheumatism and toothaches and for its painkilling and anti-inflammatory effects (Jirovetz *et al.*, 2007; Alitonou *et al.*, 2012).

West Indian bay leaves are used as a spice and share equivalent culinary uses as *Laurus nobilis*, also called “bay leaves” and bay laurel leaves, but which is a completely unrelated species and differs botanically from the West Indian bay (McHale *et al.*, 1977; Alitonou *et al.*, 2012). *Laurus nobilis* is mainly produced in Turkey and prepared for market by process of drying; usually sun drying (Demir *et al.*, 2004). Drying is usually fully achieved over a period of up to ten days in optimal climatic conditions, however, due to the external exposure to the environment, losses in quality as well as contamination result (Demir *et al.*, 2004).

The drying of leafy herbs is an important operation in value addition and extending the shelf life. Herbs are dried prior to extraction of essential oils and other compounds, and dried herbs are also used extensively in many food preparations. Because of the importance of the drying step, the oven-drying behaviour (40-70°C) of *Laurus nobilis* leaves has been investigated by some researchers (Demir *et al.*, 2004; Gunhan *et al.*, 2005; Doymaz, 2014; Cakmak *et al.*, 2013). The oven drying behaviour of the West Indian bay leaf was investigated by the authors of this work (Mujaffar and Bynoe, 2019). Leaves were dried in a single layer for 300 min in a cabinet oven set at 60°C and the moisture content of the leaves declined from 45.9% (wb) to an equilibrium moisture content value of 5.7%. There was a corresponding decline in water activity value from 0.912 to 0.496. Drying was found to occur in the falling rate period only and the effective moisture diffusivity averaged $0.32 \times 10^{-9} \text{ m}^2/\text{s}$. The drying data was best described using the Logistic model. Rehydration ratios for oven-dried leaves averaged 1.10 and 1.44 for leaves rehydrated at 30°C and 60°C, respectively.

There has been an interest in the microwave drying of herbs such as mint, basil, parsley and celery leaves as a viable alternative to the conventional hot air oven-drying method (Di Cesare *et al.*, 2003; Soysal, 2004; Ozbek and Dadali, 2007; Demirhan and Ozbek, 2011; Seyedabadi, 2015). Microwaves are a form of electromagnetic radiation that effect heating of foods by a process of dielectric heating (Decareau, 1985; Zhang *et al.*, 2006). While conventional heating occurs by convection followed by conduction where heat must diffuse into the material, materials can absorb microwave energy directly and internally convert this energy to heat (Vadivambal and Jayas, 2007). The advantages of microwave drying are reduced drying time, less energy

use with less impact on product quality (Zhang *et al.*, 2006).

The microwave-drying kinetics of bay laurel (*Laurus nobilis*) leaves was explored by Cakmak *et al.* (2013) at a power level of 180W, with favourable results with regard to drying time and quality attributes. Sellami *et al.* (2011) noted that drying method impacted on the yield of essential oil from *Laurus nobilis* leaves and reported that microwave drying (500W) gave an oil yield similar to that of fresh leaves, while oven drying at 45°C and 65°C resulted in the lowest essential oil recovery. Previous work by the authors (Mujaffar and Bynoe, 2019) showed the potential for microwave drying at 500W power as a rapid drying method for West Indian bay leaves. Compared with oven (hot-air drying) at 60°C, drying time was reduced from 300 min to 15.6 min with minimum negative effects on the colour and odour of leaves, compared with oven drying.

This study was undertaken to further explore the microwave drying of the West Indian bay leaf, specifically to investigate the effect of microwave power level (200-1000W) on the thin-layer drying behaviour and selected quality attributes.

2. Materials and Methods

Fresh West Indian bay (*Pimenta racemosa*) leaves were harvested from a single large bay tree. Unblemished leaves were gently wiped with paper towels to remove any adhering dust before drying and drying done on the same day as harvesting. The length, width and thickness of leaves averaged $0.065 \pm 0.005 \text{ m}$, $0.044 \pm 0.004 \text{ m}$ and $0.0030 \pm 0.000 \text{ m}$, respectively. Preliminary experiments revealed that blanching of leaves, as recommended by Ahmed *et al.* (2001) for coriander leaves, did not result in any noticeable improvements in quality of microwave-dried leaves.

Microwave drying was carried out using a 34L oven capacity Amana MCS10TS MenuMaster Commercial digital microwave oven (Accelerated Cooking Products (ACP), Cedar Rapids, IA, USA) with the following technical features: 3.5kV, 1000W, 120V, 60 Hertz. Microwave power levels used were based on the four pre-set levels (200W, 500W, 700W, 1000W). A sample size of 10g of leaves was selected as the amount could be spread in a single layer onto the sample plate. The total weight of the plate with the leaves was recorded before placing into the oven. At 30s intervals the plate with the leaves was removed from the oven, quickly weighed and returned to the oven. Drying was continued until there was no further change in weight. At the end of drying, leaves were allowed to cool, packaged in re-sealable plastic storage bags and stored in laboratory desiccators until analysis. A total of five (5) drying runs were conducted at each power level.

The rehydration characteristics of dried bay leaves were investigated at ambient temperature (30-35°C) and 60°C using a 26.5L capacity, Precision Reciprocating

Shaker Water Bath (Model 2872, Thermo-Scientific, Ohio, USA) with a stainless-steel chamber and temperature range of ambient to $99.9^{\circ}\text{C} \pm 0.1^{\circ}\text{C}$. Dried samples (2g each) were placed into beakers containing 200ml of distilled water, then placed into the water bath for 4h (Cakmak *et al.*, 2013). The rehydration behaviour of a commercially available sample of dried bay leaf (*Laurus nobilis*) was also checked for comparison.

Procedures and instruments used for measuring sample weight, water activity (a_w) and colour were described previously by Mujaffar and Lee Loy (2016), with the following variations: the moisture content of the fresh and dried leaves was measured at 160°C and the dried leaves were blended to create a homogenous sample before colour assessment (Cakmak *et al.*, 2013). Chlorophyll determination was carried out spectrophotometrically based on the procedure of Rai *et al.* (2011) and the results expressed in mg/g DM based on the dilution factor and mass of sample used (Looi *et al.*, 2019) as well as the sample moisture content. Energy consumption for microwave drying was obtained using Equation 4 (Hebbar *et al.*, 2004).

$$E_t = P.t \quad (1)$$

Drying data was analysed using the standard approach to drying studies, that is, the generation of drying curves and drying rate curves as described in detail previously (Mujaffar and Sankat, 2005; 2014; Mujaffar and Lee Loy, 2016). The final moisture content values were used together with the sample weight data to back-calculate the moisture changes in the leaves during the drying process. Moisture Ratio (MR) was calculated based on the analytical solution of Fick's Law for an infinite slab assuming uniform initial moisture distribution and negligible external resistances (Crank, 1975), which reduces to the straight-line equation given in Equation (2). The drying rate constant (k) was obtained from the slope of the plot of $\ln MR$ versus time (t) and effective moisture diffusivity (D_{eff}) values were calculated using 0.003 m as the leaf thickness (Equation 3).

$$MR = \frac{M - M_e}{M_0 - M_e} = \frac{8}{\pi^2} \exp\left(\frac{-\pi^2 D t}{4L^2}\right) \quad (2)$$

$$k = \frac{\pi^2 D}{4L^2} \quad (3)$$

Rehydration Ratio was calculated using the following equation (Cakmak *et al.*, 2013):

$$\text{Rehydration Ratio} = \frac{\text{Weight of rehydrated bay leaf sample (g)}}{\text{Weight of dried bay leaf sample (g)}} \quad (4)$$

For this study, a total of nineteen (19) empirical and semi-empirical thin layer models (see Table 1) most commonly used in curve fitting studies were applied to the MR data (Erbay and Icier, 2010, Ertekin and Firat, 2017). Curve fitting was carried out using Curve Expert Professional software (Version 2.3, Hyams, 2016) and fit assessed through the use of the coefficient of

determination (R^2), root mean square error ($RMSE$) and the chi-square statistic (χ^2) (Mujaffar and Lee Loy, 2016). ANOVA was carried out using Minitab 17 Statistics Software (Minitab Inc., PA, USA) (Minitab 2016) and post hoc analysis carried out using "Rapid publication-ready MS-Word tables for one-way ANOVA" (Assaad *et al.*, 2015).

Table 1. Thin Layer Drying Models

Model name	Equation
Newton	$MR = \exp(-Kt)$
Page	$MR = \exp(-Kt^n)$
Modified Page	$MR = \exp(-Kt)^n$
Henderson and Pabis	$MR = a \exp(-Kt)$
Modified Henderson and Pabis	$MR = a \exp(-Kt) + b \exp(-gt) + c \exp(-ht)$
Logarithmic	$MR = a \exp(-Kt) + c$
Two-Term	$MR = a \exp(-K_0 t) + b \exp(-K_1 t)$
Two-Term Exponential	$MR = a \exp(-Kt) + (1-a) \exp(-Kat)$
Wang and Singh	$MR = 1 + at + bt^2$
Verma	$MR = a \exp(-Kt) + (1-a) \exp(-gt)$
Hii	$MR = a \exp(-Kt^n) + c \exp(-gt^n)$
Midilli	$MR = a \exp(-Kt^n) + b t$
Weibull distribution	$MR = a - b \exp(-Kt^n)$
Diffusion approach	$MR = a \exp(-Kt) + (1-a) \exp(-Kbt)$
Aghbashlo <i>et al.</i>	$MR = -K_1 t / (1 + K_2 t)$
Logistic	$MR = a_0 / ((1 + a \exp(Kt)))$
Jena and Das	$MR = a \exp(-t + b t^{1/2}) + c$
Demir <i>et al.</i>	$MR = a \exp(-Kt^n) + c$
Alibas	$MR = a \exp(-Kt^n + b t) + g$

3. Results and Discussion

3.1 General Observations and Colour

Leaves were initially shiny, dark green in colour and pliable in texture. The aroma of the fresh whole leaves was mild, which became more pronounced when the leaves were torn. Noticeable changes in appearance and texture occurred during the drying process (see Figure 1). Leaves dried at 500 to 1000W power levels became very brittle and were susceptible to tearing during post-drying handling.

During the drying process, moisture was observed on the surface of the leaves which then evaporated. The higher the power level, the faster this process occurred. Leaves dried at 200W power level developed a damp appearance with the centre of the leaves turning yellow after approximately 4 min of drying. After 12 min, leaves appeared discoloured, with areas of dark green, brown and yellow. After 25 min the leaves were fully yellow/ brown. It is possible that due to the low drying potential at this power level, leaves dried at 200W became "cooked". It took approximately 40 min for the leaves to start losing the moisture and become more brittle.

Undesirable changes were also observed in leaves dried at 1000W. The leaves became severely distorted and curled at the edges after 2 min of drying. After 6 min, the edges of some of the leaves turned brown and



Figure 1. Appearance of fresh (a) and dried (b) 200W (c) 500W (d) 700W (e) 1000W West Indian bay leaves

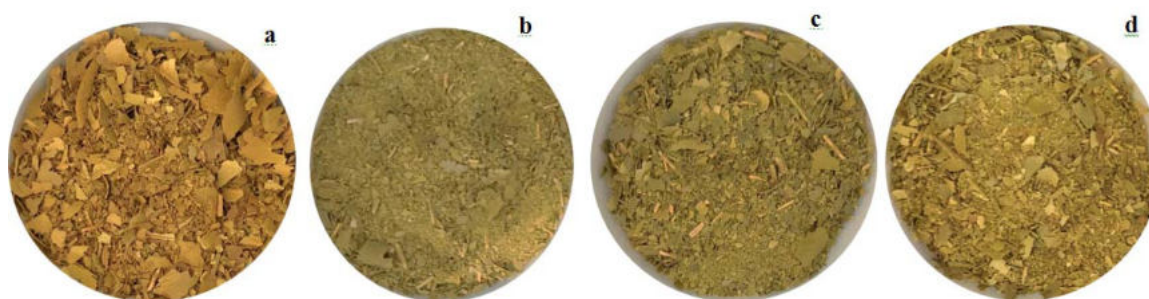


Figure 2. Appearance of ground, dried West Indian bay leaves (a) 200W (b) 500W (c) 700W (d) 1000W

Table 2. Colour attributes and Total chlorophyll content of fresh and dried West Indian bay leaves.

Quality Attribute	Bay Leaf Sample				
	Fresh	200W	500W	700W	1000W
<i>L*</i>	49.58 ± 1.75 ^b	38.65 ± 0.73 ^c	63.97 ± 0.26 ^a	62.64 ± 0.13 ^a	64.36 ± 0.05 ^a
<i>a*</i>	-7.07 ± 0.50 ^b	8.44 ± 0.08 ^a	-8.56 ± 0.07 ^c	-8.48 ± 0.09 ^c	-8.66 ± 0.07 ^c
<i>b*</i>	8.32 ± 0.55 ^d	20.12 ± 0.4594 ^c	37.32 ± 0.26 ^a	35.10 ± 0.33 ^b	36.95 ± 0.10 ^a
Hue (°)	-49.67 ± 0.37 ^b	67.23 ± 0.6468 ^a	-77.07 ± 0.046 ^c	-76.42 ± 0.04 ^c	-76.81 ± 0.08 ^c
Total Chlorophyll (mg/g DM)	5.81 ± 0.09 ^a	3.46 ± 0.02 ^b	1.46 ± 0.02 ^c	0.99 ± 0.002 ^d	0.82 ± 0.04 ^d

Values are means ± SEM. n = 3

^{a-c} Means in a row without a common superscript letter differ ($P < 0.05$) as analysed by one-way ANOVA and the LSD test.

were very brittle. These undesirable changes could have been the result of overheating and uneven heating in the microwave oven (Zhang et al. 2006). The leaves dried at 200 and 1000W power levels lost their shine.

During microwave drying, the leaves emitted a moderate odour which became stronger near the end and after drying; especially when the leaves were torn or crushed. The odour of the torn, dried leaves was weaker in leaves dried at 500 and 1000W power levels. Leaves dried at 500 and 700W power levels were the most attractive, with the typical bay leaf odour being stronger in leaves dried at 700W. Leaves dried at 700W power level appeared to be visibly greener than the leaves dried at 500W.

The dried leaves were ground prior to colour analysis (see Figure 2). Compared with the leaves dried at 200W, leaves dried at the higher power levels were easier to grind as the leaves were more brittle. Velu et al. (2006) reported that microwave drying improved the grinding of maize, with microwave-dried maize showing a decreased Bond's work index, which is a measure of

grinding energy. The colour attributes and chlorophyll content (mg/g DM) of the fresh and dried leaves are given in Table 2.

Higher *L** values indicated the lightening of leaves dried at 500-1000W power levels, while darkening of the leaves occurred at 200W. Leaves dried at the higher power levels maintained a dark green colour, as reflected in high negative *a** values, while a positive value of +8.44 was found for leaves dried at 200W power level, indicating reddening/browning. The high positive *b** values indicated the increase in yellowing of all leaves after drying, increasing at the higher microwave power levels. Increasing microwave power from 200 to 500W resulted in a large decline in the chlorophyll content of the leaves.

Mujaffar and Bynoe (2019) found that microwave-dried West Indian bay leaves were greener in appearance with correspondingly lower *a** values than oven-dried (60°C) leaves, which were brown in colour. Cakmak et al. (2013) found that microwave-dried (180W) *Laurus nobilis* leaves were greener but with higher *b** values

compared with oven-dried leaves. Microwave-dried leaves also showed a smaller colour difference when compared with fresh leaves. Demir *et al.* (2004) found that while the colour attributes of dried *Laurus nobilis* were significantly different from the fresh leaves, the impact of drying method (oven, sun and shade drying) was not significant. Vadivambal and Jayas (2007) noted that microwave-dried products are generally less brown than conventional air-dried products. From the present study, the lowest chlorophyll content (0.82 mg/g DM) was observed in leaves dried at 1000W power level, however, this was higher than the 0.68 mg/g DM reported for leaves dried at 60°C (Mujaffar and Bynoe, 2019).

3.2 Drying Curves

During drying, all leaves experienced a change in weight. The maximum weight loss (% over original weight) experienced by microwave-dried leaves at 500-1000W was approximately 43%, with most of the change in weight occurring at the early stages of the process. The maximum weight loss for leaves dried at 200W was 34%.

The initial moisture content and water activity of fresh leaves averaged 0.85 g H₂O/g DM (46% wb) and 0.912, respectively. The decline in moisture content of the leaves as a function of microwave power is given in Figure 3. Moisture content was significantly affected by drying time and microwave power level, as well as a time-power interaction ($p \leq 0.001$). Increasing the power level from 200 to 1000W resulted in an increase in moisture reduction, with the greatest effect was observed as the power level increased from 200 to 500W. Equilibrium moisture and water activity of dried leaves are given in Table 3. The final moisture content values of leaves dried at 200, 500, 700 and 1000W averaged 0.22, 0.05, 0.04 and 0.02 g H₂O/g DM, respectively (18.7, 5.2, 3.8, 2.0 %wb). The higher the power level, the shorter the drying time to achieve equilibrium moisture content.

The increase in moisture decline and drying time with increasing microwave power has been described for many leafy materials, including celery, basil, parsley, spinach and amaranth (Soysal, 2004; Alibas 2014; Demirhan and Ozbek, 2011; Seyedabadi, 2015; Mujaffar and LeeLoy, 2016). Increasing microwave power increases the rate of energy supply (J/s) to the material, which leads to faster heating. Evaporation of moisture is therefore increased and the movement of internal moisture to the surface of the material occurs at a faster rate.

Mujaffar and Bynoe (2019) reported that oven-dried (60°C) West Indian bay leaves took 300 min to reach equilibrium moisture content. Cakmak *et al.* (2013) found that microwave drying of *Laurus nobilis* leaves at 180W resulted in a four-fold reduction in drying time, compared with leaves dried in an oven at 50-70°C, and

that drying could be completed within 25 min. Demir *et al.* (2004) reported that *Laurus nobilis* leaves could be dried to 10-12% moisture in 2.5 to 9h in a convection oven at 40-60°C, respectively. Doymaz (2014) found that drying time for *Laurus nobilis* leaves could be reduced from 170 to 60 min when the drying temperature increased from 50 to 70°C.

The drying energy consumption (W/h) for 10g samples of bay leaves is given in Figure 4. Energy consumption decreased from 9670 to 5200 W/h as microwave power increased from 200 to 1000W. Energy consumption values were not significantly different ($p \leq 0.05$) between 500 and 700W power levels, or 700 and 1000W power levels. Alibas Ozkan *et al.* (2007) also reported higher energy consumption values of leaves dried at lower power levels of 90 to 160W microwave power levels, with similar values at 350 to 1000W power levels.

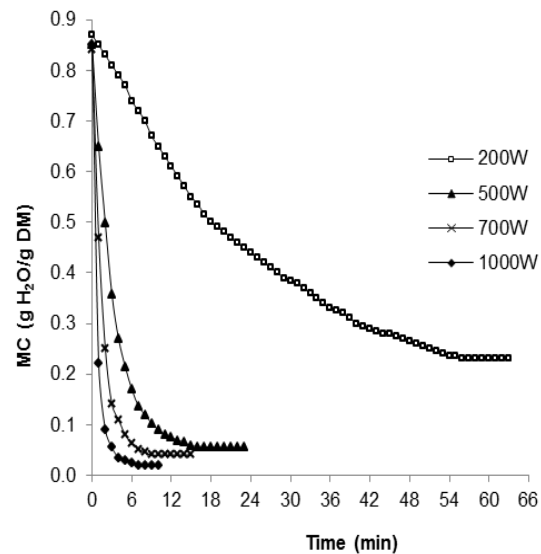


Figure 3. Effect of microwave power level on the moisture content of West Indian bay leaves

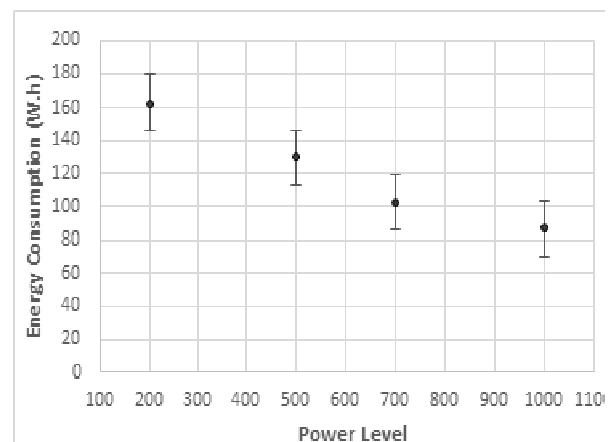


Figure 4. Energy Consumption for microwave drying of West Indian bay leaves at different power levels

Table 3: Moisture and water activity values of fresh and dried leaves

Quality Attribute	Bay Leaf Sample				
	Fresh	200W	500W	700W	1000W
MC (g H ₂ O/g DM)	0.87 ± 0.06 ^a	0.22 ± 0.022 ^b	0.05 ± 0.005 ^c	0.04 ± 0.004 ^c	0.02 ± 0.002 ^c
a _w	0.912 ± 0.006 ^a	0.756 ± 0.016 ^b	0.406 ± 0.007 ^c	0.331 ± 0.014 ^d	0.326 ± 0.008 ^d
Time to Equilibrium (min)	NA	48.8 ± 3.5 ^a	15.6 ± 0.93 ^b	8.8 ± 0.97 ^c	5.2 ± 0.58 ^c

Values are means ± SEM, n = 5 per treatment group.

^{a-d} Means in a row without a common superscript letter differ (P<0.05) as analysed by one-way ANOVA and the LSD test.

3.3 Drying Rate Curves

Drying rates of microwave-dried bay leaves as a function of average moisture content are shown in Figure 5. The higher the power level, the higher the drying rates for most of the drying process. Initial drying rates averaged 0.02, 0.20, 0.37 and 0.63 g H₂O/g DM/min, for leaves dried at 200, 500, 700 and 1000W, respectively. Drying at 200W power level occurred in the constant rate and falling rate period, with the falling rate period beginning at a moisture value of 0.65 g H₂O/g DM (40% wb). Drying at the higher power levels occurred in the falling rate period only, which means that drying was controlled by diffusion of moisture.

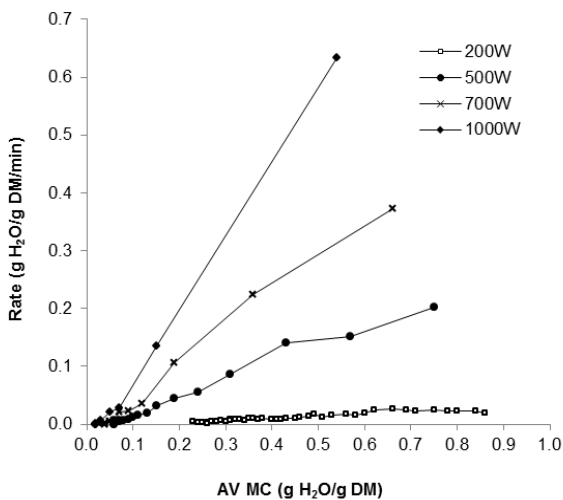


Figure 5. Drying rate curves for West Indian bay leaves at various microwave power levels

With respect to the drying of bay leaves, specifically, Gunhan *et al.* (2005) presented curves of drying rate as a function of drying time for oven-dried *Laurus nobilis L.* leaves dried at 40-50°C. They noted that drying rates were impacted by drying temperature, but not by the humidity of the air, with approximate initial values of 0.18 to 0.80 g H₂O/g DM/min for leaves dried at 40-50°C, respectively. Doymaz (2014) presented curves of drying rate versus Moisture Ratio (*MR*) to support that drying of bay leaves at 50-70°C occurs in the falling rate period only.

Similar changes in drying rate with time and with increasing microwave power levels were reported for celery, mint, parsley, spinach and amaranth leaves (Soysal, 2004; Alibas Ozkan *et al.*, 2007; Ozbek and Dadali, 2007; Demirhan and Ozbek, 2011; Sharada, 2013, Mujaffar and Lee Loy, 2016). According to those authors, high moisture values of leaves at the initial stages of drying result in higher absorption of microwave power and higher drying rates due to higher moisture diffusion. Decrease in moisture as drying progresses results in a decrease in absorption of microwaves and a drop in temperature, with a resulting decrease in drying rate. Other authors have reported drying during the falling rate only for the drying of spinach and celery leaves (Alibas Ozkan *et al.*, 2007; Demirham and Ozbek, 2011). Demirham and Ozbek (2011) added that the critical moisture content was equal to the initial moisture content of celery leaves which meant that the microwave drying process at 180 to 900W power levels was entirely controlled by mass transfer resistance. It has been suggested that microwave drying is most effective at product moisture contents below 20% (wb), which usually corresponds to drying in the falling rate period (Maskan, 2001). The removal of moisture during this time is therefore more rapid than with oven (hot-air) drying.

3.4 Moisture Ratio (*MR*), Drying Rate Constants (*k*) and Diffusion Coefficients (*D_{eff}*)

Plots of Moisture Ratio (*MR*) versus time (min) are given in Figure 6. A similar trend to the drying curves was observed, where increasing the power level from 200W to 1000W resulted in the decline in values, but with the greatest decline occurring when microwave power level was increased from 200 to 500W.

The drying rate constants (*k*) for the initial minutes of microwave drying of bay leaves were determined from plots of the ln free moisture (ln *MR*) as a function of drying time. Drying rate constants (see Table 4) were significantly affected by microwave power level (*p* ≤ 0.05). The increase in drying rate with microwave power level could be described by the following relationship (*R*² = 0.9953):

$$k = 7 \times 10^{-7} \cdot P^{2.0781}$$

Mujaffar and Bynoe (2019) reported *k*-values of 0.0213 1/min and *D_{eff}* values of 0.32 × 10⁻⁹ m²/s for West Indian bay leaves dried in an oven at 60°C.

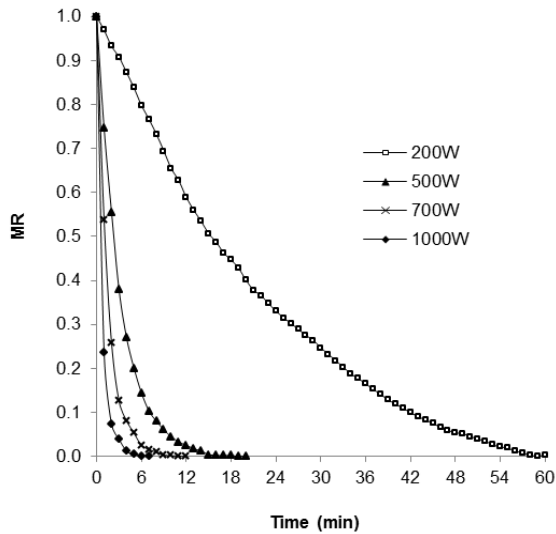


Figure 6. Moisture ratio curves for bay leaves at different microwave power levels

Table 4. Drying rate constants (*k*) and diffusion coefficients (*D_{eff}*) for microwave-dried bay leaves

Microwave power level (W)	<i>k</i> (1/min)	<i>D_{eff}</i> (m ² /s)	<i>R</i> ²
200	0.0410 ± 0.016 ^d	0.62 × 10 ⁻⁹	0.9905
500	0.3115 ± 0.005 ^c	4.73 × 10 ⁻⁹	0.9989
700	0.6397 ± 0.030 ^b	9.72 × 10 ⁻⁹	0.9939
1000	1.0930 ± 0.028 ^a	16.60 × 10 ⁻⁹	0.9706

Values are means ± SEM, n = 5 per treatment group.

^{a-d} Means in a column without a common superscript letter differ (*P*<0.05) as analysed by one-way ANOVA and the LSD test.

^a*D_{eff}* = *k* (4*X*²/π²) where *X* = half thickness 0.0015m

With respect to work done on the microwave-drying of *Laurus nobilis* leaves, Cakmak *et al.* (2013) reported *D_{eff}* values of 1.52 to 3.64 × 10⁻⁹ m²/s for leaves dried in an oven at 50-70°C, and 8.08 × 10⁻⁹ m²/s for microwave-dried leaves. Doymaz (2014) reported lower *D_{eff}* values of 9.38 to 20.70 × 10⁻¹² m²/s for leaves dried in an oven at 50-70°C, demonstrating the rapid drying rates achieved through microwave drying in the present study.

With respect to *D_{eff}* values for other microwave-dried leafy greens and herbs, Demirhan and Ozbek (2011) reported moisture diffusivity values for microwave-dried celery leaves of 0.343 × 10⁻¹⁰ to 1.714 × 10⁻¹⁰ m²/s as microwave power increased from 180 to 900W using 25g celery leaf samples. Alibas (2014) reported *D*-values for microwave-dried celery leaves ranging from 1.595 × 10⁻¹⁰ to 6.377 × 10⁻¹² m²/s at power levels of 90 to 1000W. An increase with microwave

power level has been attributed to the increased activity of water molecules at higher power levels.

3.5 Rehydration Ratio

Rehydration ratios for the dried leaves are given in Table 5. Rehydration ratio increased at the higher temperature (60°C). There were no significant (*p*<0.05) differences between dried leaves at the higher rehydration temperature, but at 30°C, the rehydration ratios of leaves were significantly lower for leaves dried at 200W power level.

Rehydration is an indicator of cellular and structural changes that may have occurred during the dehydration process and Cakmak *et al.* (2013) reported a rehydration ratio of less than 1.2 for microwave-dried (180W) bay laurel leaves. According to Vadivambal and Jayas (2007), enhanced rehydration may be seen in microwave-dried products compared with air-dried samples.

During microwave-drying, the rapid outward flux of water vapour from inside the material can help to prevent shrinkage and collapse of the tissue structure typical of air-drying systems and therefore lead to improved rehydration characteristics (Al-Duri and McIntyre, 1991). Leafy materials such as the bay leaf are very thin (0.003 m), so there may not be noticeable structural differences between oven- and microwave-dried leaves.

3.6 Thin Layer Curve fit

Given that the drying of leaves at 200W and 1000W did not give good results in terms of drying time and/or quality of leaves, the thin layer models were applied only to the data for leaves dried at 500 and 700W. Of the nineteen thin layer models applied to the MR data, the Verma model fits the data best for leaves dried at 500W power level and the Jena and Das model fits the data best for leaves dried at 700W (see Table 6).

The comparison of Predicted versus Experimental MR values for leaves dried at 500 and 700W gave straight lines with high *R*² values (0.9996 and 0.9994, respectively), an indication of good agreement of values.

With respect to the oven drying of West Indian bay leaves, Mujaffar and Bynoe (2019) found the Logistic model to adequately describe the drying data. With respect to modelling work done on *Laurus nobilis* leaves, Cakmak *et al.* (2013) found the Midilli model to adequately describe the drying data for both oven- and microwave-dried leaves, while the Page and Midilli models were reported to best fit the MR data for

Table 5. Rehydration ratios of West Indian bay leaves dried at varying power levels.

Temperature (°C)	Microwave Power			
	200W	500W	700W	1000W
30	1.04 ± 0.008 ^a	1.14 ± 0.004 ^b	1.13 ± 0.004 ^b	1.14 ± 0.017 ^b
60	1.39 ± 0.033	1.50 ± 0.034	1.55 ± 0.006	1.46 ± 0.063

Values are means ± SEM, n = 2 per treatment group.

^{a-b} Means in a row without a common superscript letter differ (*P*<0.05) as analyzed by one-way ANOVA and the LSD test.

Table 6. Thin layer models and constants in order of best fit for West Indian bay leaves dried at different microwave power levels (a) 500W and (b) 700W

Model	(a) 500W - Model constants								R ²	RMSE	χ^2
	K	n	a ₀	a	b	c	g	h			
Verma	0.3362	-	-	1.0707	-	-	1.8524	-	0.9998	0.005436	0.000035
Jena and Das	0.3572	-	-	0.9983	0.0735	0.0019	-	-	0.9998	0.005482	0.000038
Modified Henderson and Pabis	0.6419	-	-	-15.522	15.9587	-	0.6301	0.2783	0.9998	0.005215	0.000039
Alibas	1.1650	1.0179	-	0.9986	0.8739	0.5631	0.0032	-	0.9997	0.005805	0.000045
Logistic	0.3527	-	5.7601	4.7340	-	-	-	-	0.9997	0.006380	0.000048

Model	(b) 700W - Model constants								R ²	RMSE	χ^2
	K	n	a ₀	a	b	c	g	h			
Jena and Das	0.7457	-	-	0.9935	0.1093	0.0070	-	-	0.9997	0.007957	0.000099
Newton	0.6500	-	-	-	-	-	-	-	0.9995	0.009643	0.000102
Page	0.6412	1.0201	-	-	-	-	-	-	0.9995	0.009462	0.000109
Weibull distribution	0.6427	1.0502	-	0.0069	-0.9944	-	-	-	0.9996	0.008444	0.000112
Two-Term Exponential	0.6937	-	-	0.7662	-	-	-	-	0.9995	0.009579	0.000112

oven-dried leaves (Demir *et al.*, 2004; Gunhan *et al.*, 2005; Doymaz, 2014). The Page, Midilli and logarithmic models have all been reported to successfully describe the *MR* data for microwave-dried leafy materials including celery, mint, parsley and basil leaves (Soysal 2004; Ozbek and Dadali, 2007; Demirhan and Ozbek, 2011; Seydabadi, 2015).

4. Conclusions

From the results of this study, microwave drying appears to be a feasible drying method for the rapid drying of West Indian bay leaves. Microwave power level had a significant impact on the drying rates and quality of dried samples. An increase in power level resulted in increased drying rates, with browning and the risk of scorching increasing at 1000W power. Drying at 200W power level was unfavourable in terms of low drying rates and leaf quality.

Drying of leaves at 500W and 700W was favourable and found to be similar with respect to the colour attributes, equilibrium moisture content of dried leaves as well as energy consumption, but with less drying time required at 700W power level (8.8 min versus 16.6 min). Leaves dried at 500W had slightly higher chlorophyll contents while leaves dried at 700W had a stronger bay leaf odour. Leaves dried at 500 and 700W remained intact as whole leaves but could be easily be blended to a powder. Drying at 500 and 700W occurred in the falling rate period only.

The drying data was successfully analysed through the determination of drying rate constants (*k*) and moisture diffusivity values (*D_{eff}*), and the Verma and Jena and Das models best fit the data for leaves dried at 500W and 700W, respectively. Future work on the optimisation of the microwave-drying process will focus on the impact of power level on the essential oil content of the leaves.

References:

Ahmed, J., Shivhare, U.S., and Singh, G. (2001), "Drying characteristics and product quality of coriander leaves", *Food*

and Bioproducts Processing, Vol.79, No.2, pp.103-106, <https://doi.org/10.1205/096030801750286258>

Al-Duri, B., and McIntyre, S. (1991), "Comparison of drying kinetics of foods using a fan-assisted convection oven, a microwave oven and a combined microwave/ convection oven", *Journal of Food Engineering*, Vol. 15, No. 2, pp. 139-155.

Alibas, I. (2014), "Mathematical modelling of microwave-dried celery leaves and determination of effective moisture diffusivities and activation energy", *Food Science and Technology*, Vol. 34, No. 2, pp. 394-401.

Alibas Ozkan, I., Akbudak, B., and Akbudak, N. (2007), "Microwave drying characteristics of spinach", *Journal of Food Engineering*, Vol.78, No.2, pp.577-583. <https://doi.org/10.1016/j.jfoodeng.2005.10.026>

Alitonou, G., Noudogbessi, J.P. Philippe S., Tonouhewa, A.B.N., Avlessi, F., Menut, C. and Sohounhoute, D.C.K. (2012), "Chemical composition and biological activities of essential oils of *Pimenta racemosa* (Mill.) J.W. Moore from Benin", *International Journal of Biosciences*, Vol.2, No.9, pp.1-12.

Assaad, H. I., Hou, Y., Zhou, L., Carroll, R. J., and Wu, G. (2015), "Rapid publication-ready MS-Word tables for two-way ANOVA", *SpringerPlus*, Vol.4, No.1, pp.33.

Cakmak, H., Kumcuoglu, S., and Tavman, S. (2013), "Thin layer drying of bay leaves (*Laurus nobilis L.*) in conventional and microwave oven", *Academic Food Journal*, Vol.11, No.1, pp.20-26.

Crank, J. (1975), *The Mathematics of Diffusion*, 2nd Edition. Oxford University Press, UK.

Decareau, R.V. (1985), *Microwaves in the Food Processing Industry*, Academic Press, Orlando

Demir, V., Gunhan, T., Yagcioglu, A.K., and Degirmencioglu, A. (2004), "Mathematical modelling and the determination of some quality parameters of air-dried bay leaves", *Biosystems Engineering*, Vol. 88, No. 3, pp. 325-335.

Demirhan, E., and Ozbek, B. (2011), "Thin-layer drying characteristics and modeling of celery leaves undergoing microwave treatment", *Chemical Engineering Communications*, Vol.198, No.7, pp.957-975. <https://doi.org/10.1080/00986445.2011.545298>

Di Cesare, L.F., Forni, E., Viscardi, D., and Nani, R.C. (2003), "Changes in the chemical composition of basil caused by different drying procedures", *Journal of Agricultural and Food Chemistry*, Vol.51, pp.3575-3581. <https://doi.org/10.1021/jf021080o>.

Doymaz, I. (2014), "Thin-layer drying of bay laurel leaves (*Laurus nobilis L.*)", *Journal of Food Processing and Preservation*. Vol.38, No.1, pp.449-456.

Erbay, Z., and Icier, F. (2010), "A review of thin layer drying of

- foods: theory, modelling, and experimental results”, *Critical Reviews in Food Science and Nutrition*, Vol.50, No.5, pp.441-64.
- Ertekin, C., and Firat, M.Z. (2017), “A comprehensive review of thin-layer drying models used in agricultural products”, *Critical Reviews in Food Science and Nutrition*, Vol.57, No.4, pp.701-717.
- Gunhan, T., Demir, V., Hancioglu, E., and Hepbasli, A. (2005), “Mathematical modelling of drying of bay leaves”, *Energy Conversion and Management*. Vol.46, No.11-12, pp.1667-1679. <https://doi.org/10.1016/j.enconman.2004.10.001>
- Hebbbar, H.U., Vishwanathan, K., and Ramesh, M., (2004), “Development of combined infrared and hot air dryer for vegetables”, *Journal of Food Engineering*, Vol.65, No.4, pp.557-563, <https://doi.org/10.1016/j.jfoodeng.2004.02.020>.
- Hyams, D.G. (2016), *CurveExpert Professional Software*, Version 2.3. <http://www.curveexpert.net>.
- Jirovetz, L, Buchbauer, G., Stoilova, I., Krastanov, A., Stoyanova, A., and Schmidt, E. (2007), “Spice plants: Chemical composition and antioxidant properties of *Pimenta Lindl.* Essential oils, Part 2: *Pimenta racemosa* (Mill.) J.W. Moore Leaf Oil from Jamaica”, *Ernahrung/Nutrition*, Vol.31, No.2, pp.293-300.
- Looi, Y., Ong, S.P., Julkifle, A., and Alias, M.S. (2019), “Effects of pretreatment and spray drying on the physicochemical properties and probiotics viability of *Moringa (Moringa oleifera Lam)* leaf juice powder”, *Journal of Food Processing and Preservation*, Vol.43, No.4, pp.177-182. <https://doi.org/10.1111/jfpp.13915>
- Maksan, M. (2001), “Drying, shrinkage and rehydration characteristics of kiwifruits during hot air and microwave drying”, *Journal of Food Engineering*, Vol.48, No.2, pp.177-182.
- McGaw, D.R., Clarke, W. and Maharaj, S. (2016), “Comparison of supercritical fluid extraction with steam distillation for the extraction of bay oil from bay (*Pimenta racemosa*) leaves”, *International Journal of Engineering Science Invention*, Vol.5, No.1, pp.51-55.
- McHale, D., Laurie, W.A., and Woof, M.A. (1977), “Composition of West Indian Bay Oils”, *Food Chemistry*, Vol.2, No.1, pp.19-25, [https://doi.org/10.1016/0308-8146\(77\)90004-8](https://doi.org/10.1016/0308-8146(77)90004-8).
- Mujaffar, S., and Sankat, C. K. (2005), “The air drying behaviour of shark fillets”, *Canadian Biosystems Engineering / Le Genie Des Biosystems Au Canada*, Vol.47, pp.11-21.
- Mujaffar, S., and Sankat, C.K. (2014), “Modelling the drying behaviour of unsalted and salted catfish (*Arius sp.*) slabs”, *Journal of Food Processing and Preservation*, Vol.39, No.6, pp.1385-1398. <https://doi.org/10.1111/jfpp.12357>.
- Mujaffar, S., and Lee Loy, A. (2016), “Drying kinetics of microwave-dried vegetable amaranth (*Amaranthus dubius*) leaves”, *Journal of Food Research*, Vol.5, No.6, pp.33-44, <https://doi.org/10.1002/fsn3.406>.
- Mujaffar, S., and Bynoe, S. (2019), “Investigations into hot air and microwave drying of the West Indian bay leaf (*Pimenta racemosa*)”, *Proceedings of the 7th European Drying Conference (Eurodrying 2019)*, Torino, Italy, July 10-12, pp.143-149.
- Ogundajo, A.L., Owolabi, M.S., Oladosu, I.A., Ogunwande, I.A., Flamini, G., and Yusuff, K.O. (2011), “Volatile constituents and potatoes tuber sprout suppressant activity of *Pimenta racemosa* (Mill.) J.W. Moore”, *African Journal of Basic and Applied Sciences*, Vol.3, No.3, pp.92-97.
- Ozbek, B., and Dadali, G. (2007), “Thin-layer drying characteristics and modelling of mint leaves undergoing microwave treatment”, *Journal of Food Engineering*, Vol.83, No.4, pp.541-549, <https://doi.org/10.1016/j.jfoodeng.2007.04.004>
- Paula, J.A.M., Reis, J.B., Ferreira, L.H.M., Menezes, A.C.S., and Paula, J.R. (2010), “Genus *Pimenta*: Botanical aspects, chemical composition and pharmacological potential”, *Journal of Medicinal Plants*, Vol.12, No.3, pp.363-379. <http://dx.doi.org/10.1590/S1516-05722010000300015>
- Rai D.R., Chadha, S., Kaur, M.P., Jaiswal, P., and Patil R.T. (2011), “Biochemical, microbiological and physiological changes in Jamun (*Syzyium cumini L.*) kept for long term storage under modified atmosphere packaging”, *Journal of Food Science and Technology*, Vol.48, No.3, pp.357-365.
- Seaforth, C., and Tikasingh, T. (2008), *A Study for the Development of a Handbook of Selected Caribbean Herbs for Industry*, CTA Technical Publication, Wageningen, The Netherlands.
- Sellami, I.H., Wannas, W.I., Bettaieb, S.B., Chahed, T., Marzouk, B., and Limam, F. (2011), “Qualitative and quantitative changes in the essential oil of *Laurus nobilis L.* leaves as affected by different drying methods”, *Food Chemistry*, Vol.126, No.2, pp.691-697. <https://doi.org/10.1016/j.foodchem.2010.11.022>
- Seyedabadi, E. (2015), “Drying kinetics modelling of basil in microwave dryer”, *Agricultural Communications*, Vol.3, No.4, pp.37-44.
- Sharada, S. (2013), “Microwave drying of *Spinacia oleracea*”, *International Journal of Research in Engineering and Technology* (IJRET), Vol. 2, pp. 481-486.
- Soysal, Y. (2004), “Microwave drying characteristics of parsley”, *Biosystems Engineering*, Vol.89, No.2, pp.167-173, <https://doi.org/10.1016/j.biosystemseng.2004.07.008>
- Vadivambal, R., and Jayas, D.S. (2007), “Changes in quality of microwave-treated agricultural products: A review”, *Biosystems Engineering*, Vol.98, No.1, pp.1-16. <https://doi.org/10.1016/j.biosystemseng.2007.06.006>
- Velu, V., Nagender, A., Prabhakara Rao, P.G., and Rao, D.G., (2006), “Dry milling characteristics of microwave dried maize grains (*Zea mays L.*)”, *Journal of Food Engineering*, Vol.74, No.1, pp.30-36; <https://doi.org/10.1016/j.jfoodeng.2005.02.014>
- Zhang, M., Tang, J., Mujumdar, A. S., and Wang, S. (2006), “Trends in microwave-related drying of fruits and vegetables”, *Trends in Food Science and Technology*, Vol.17, No.10, pp.524-534. <https://doi.org/10.1016/j.tifs.2006.04.011>.

Authors' Biographical Notes:

Saheeda Mujaffar is a Lecturer in the Department of Chemical Engineering at The University of the West Indies (UWI), Saint Augustine Campus. Dr. Mujaffar holds a BSc. Degree in Natural Sciences and an MPhil and PhD Degree in Agricultural Engineering (UWI), and has worked as a Food Technologist in industry. She served as the Coordinator of the Food Science and Technology Programme (2017-2019), and is actively involved in both teaching and research at the postgraduate level. Dr. Mujaffar's specific areas of research interest include Drying of Agricultural Commodities, Mathematical Modelling, Food Waste Utilisation and Product Development. She is an active Reviewer for local and international Food Science Journals. Dr. Mujaffar has served as the Deputy Dean, Outreach and Enterprise Development in the Faculty of Engineering and as a Director in the Livestock and Livestock Products Board.

Shari Bynoe is currently a Quality Control Technician II (Quality Control and Microbiology) at Vemco Limited, Diego Martin, Trinidad. She holds a MSc. Degree (with Distinction) in Food Science and Technology and a BSc. Degree in Chemical and Process Engineering (UWI, St. Augustine). Ms. Bynoe has also worked as a Quality Control Technician (Microbiology Portfolio) at Caribbean Bottlers (T&T) Limited, Tunapuna, Trinidad and as an Intern at Barbados Dairy Industries (Pinehill Dairy) in St. Michael, Barbados. ■

Electrical Engineering and the New SI Definitions

Fasil Muddeen

Department of Electrical and Computer Engineering, The University of the West Indies, St. Augustine,
Trinidad and Tobago, West Indies;
Emails: Fasil.Muddeen@sta.uwi.edu; fmuddeen@gmail.com

(Received 09 July 2019; Revised 28 October 2019; Accepted 20 January 2020)

Abstract: In 2019, the new definitions of the SI system were announced and adopted. These new definitions marked a substantial change from the previous ones and will have a considerable impact on the realisation of the various units and in particular the kilogram. Seven of these units directly relate to the units of measure used in Electrical Engineering. This paper will examine the new definitions, how the fundamental units of electrical engineering are realised from the definitions, the impact of these changes on the uncertainty of measurement of electrical units and the role of the new Volt, Ohm and Ampere in the realisation of the new kilogram.

Keywords: Electrical Engineering, electrical units, SI Definitions

1. Introduction

The behaviour and relationship between magnetic fields \mathbf{B} and electric fields \mathbf{E} in electrical engineering are described by Maxwell's four equations (Hayt and Buck, 2006):

$$\nabla \cdot \mathbf{E} = \frac{\rho_v}{\epsilon_0} \quad (1)$$

$$\nabla \cdot \mathbf{H} = 0 \quad (2)$$

$$\nabla \times \mathbf{E} = -\mu_0 \frac{\partial \mathbf{H}}{\partial t} \quad (3)$$

$$\nabla \times \mathbf{H} = \epsilon_0 \frac{\partial \mathbf{E}}{\partial t} + \sigma \mathbf{E} \quad (4)$$

These four equations form the basis for many calculations in electrical engineering for example in antenna designs. In three of these equations, the constants ϵ_0 , the permittivity of free space, and μ_0 the permeability of free space appear. The value of μ_0 was defined for many years as $4\pi \times 10^{-7} \text{ Hm}^{-1}$ and the value of ϵ_0 was then fixed as $\approx 8.854 \times 10^{-12} \text{ Fm}^{-1}$ via the fixed value of the speed of light, and the Equation $c^2 = 1/\mu_0\epsilon_0$.

In 2019, new definitions of the *Systeme International des Unites*, or the SI system were announced and adopted (CGPM, 2018). These new definitions marked a substantial change from the existing ones and will also have a considerable impact on the realisation of the various SI units. Seven (7) of these units directly relate to the units of measure used in Electrical Engineering. The constants ϵ_0 and μ_0 stable for so long, and such a fundamental part of Maxwell's Equations, will change from their previously fixed values. This paper will examine the new definitions, how the fundamental units of electrical engineering are

realised from the definitions and the impact of these changes on the measurement of electrical units.

2. The *Systeme International des Unites*

The name *Systeme International des Unites* or SI system, was given at the 11th Conférence Générale des Poids et Mesures, (CGPM) in 1960, and is the final attempt (so far) to have an internationally agreed set of measurement standards and units. Its history is long and interesting and well described in the 8th edition of the SI Brochure (BIPM, 2006).

Modern science and engineering measurements and results are quoted almost exclusively in SI units. In trade and manufacture, the SI system is somewhat less exclusive, especially with older plant and equipment where imperial units for example may still be encountered. In fact the existence and contemporaneous use of alternative measurement systems has almost led to tragedy, as with the Gimli Glider incident in 1983 (Witkin, 1983) or has led to the loss of expensive equipment, such as the Mars Climate Orbiter in 1999 (Hotz, 1999).

The SI system is maintained by a system of international metrology, administered by the Bureau International des Poids et Mesures (BIPM), in France. Figure 1 depicts the operational structure of the BIPM, under the authority of the Metre Convention. The BIPM and its various committees, are responsible for defining units of measurement and for publishing the '*mises en pratique*', which are the ways to create the various units. BIPM committees comprise representatives from large national measurement organisations, such as the National Institute of Science and Technology (NIST) in the United States of America (USA), the National Physical Laboratory (NPL) in the United Kingdom (UK), the

Physikalisch-Technische Bundesanstalt (PTB) in Germany, and of course, the BIPM's own laboratories. A full list of the BIPM membership, comprising 60 Members and 42 Associates, including CARICOM, is available from the BIPM's website (BIPM, 2019).

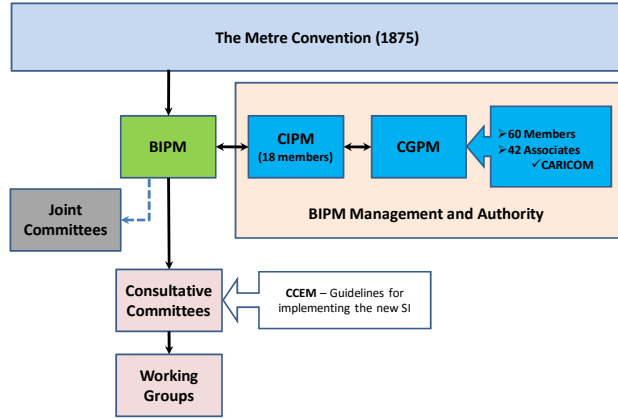


Figure 1. The Structure of the BIPM

Many of the BIPM members create and maintain their own set of measurement standards. These entities are known as Primary Standards Laboratories (PSLs), again including the previously mentioned NIST, NPL, PTB, BIPM and several others. The values of their units are inter-compared through a process organised by the consultative committees of the CIPM. The results of these 'key comparisons' as referred to by the BIPM, are published, together with the experimental uncertainty associated with the published value, in the Key Comparison Database (KCDB). Uncertainty is discussed in section 4 of this paper.

These comparisons form the backbone of *measurement traceability* and is the reason why, for example, a 2.5 mm² British Standard BS6004 electrical conductor manufactured in Trinidad and Tobago will have the same current carrying capacity as one made in Singapore.

As scientific knowledge increases, new methods are discovered to create the various units of measurement. The BIPM and the metrology community are continually seeking methods which will create units (called the realisation) with less uncertainty. When such methods are discovered, they are rigorously examined internationally over many years, compared with existing methods and the existing standards before being published by the BIPM as a new *mise en pratique* (BIPM, 2006).

Discoveries in quantum physics over the last century and vast amounts of validated experimental data, presented the BIPM with an opportunity to revise the existing SI system. The revision is not going to define any new units of measurement or remove any existing units, but rather will improve how the current units are

defined (CGPM, 2018). In particular, the revision redefines four (4) of the existing base units, namely the Kilogram, the Ampere, the Kelvin and the Mole.

3. Fundamental Units of Electrical Engineering

The BIPM defines seven (7) base units quantities, namely, length, mass, time, electric current, thermodynamic temperature, amount of substance and luminous intensity (BIPM, 2019). These quantities are independent of one another. For example, the quantity of electric current does not depend on the quantity of thermodynamic temperature.

To enumerate these quantities, the BIPM defines seven (7) base units, the International System of Units (Liard et al., 2014), called the Metre, Kilogram, Second, Ampere, Kelvin, Mole and Candela respectively. These units are also, by definition, intended to be independent, but in reality are not so in a number of instances. For example, the pre-2019 Ampere's definition is a relationship between the Kilogram, the Second and the Metre as a dimensional analysis would show.

In addition, there are a number of derived units, which are obtained by algebraic combinations (products of powers) of base units. For example, the unit of pressure, the Pascal, can be expressed in terms of the base units as $m^{-1} \cdot kg \cdot s^{-2}$. Where there is no other multiplicative factor other than 1, the derived units are called *coherent derived* units (BIPM, 2019). There is a very large number of derived (and coherent derived) units used to express scientific quantities and the number keeps increasing as scientific knowledge expands and the need to quantify new measured phenomena arises.

Twenty-two derived units (meaning derived and coherent derived units) have been given names for ease of use, for example the previously mentioned Pascal. In addition to the Ampere, Table 1 lists the most frequently encountered coherent derived units encountered in

Table 1. Frequently Encountered Coherent Derived Units Used in Electrical Engineering

Derived Quantity	Derived Unit and Symbol	In terms of other SI units	Base Unit Relationship
Energy	Joule (J)	Nm	$m^2kg s^{-2}$
Power	Watt (W)	Js^{-1}	$m^2kg s^{-3}$
Charge	Coulomb (C)	As	As
Potential Difference	Volt (V)	WA^{-1}	$m^2kg s^{-3} A^{-1}$
Capacitance	Farad (F)	CV^{-1}	$m^{-2}kg^{-1}s^4 A^2$
Resistance	Ohm (Ω)	VA^{-1}	$m^2kg s^{-3} A^{-2}$
Conductance	Siemens (S)	AV^{-1}	$m^{-2}kg^{-1}s^3 A^2$
Magnetic Flux	Weber (Wb)	Vs	$m^2kg s^{-2} A^{-1}$
Magnetic Flux Density	Tesla (T)	Wm^{-2}	$kg s^{-2} A^{-1}$
Inductance	Henry (H)	WA^{-1}	$m^2kg s^{-2} A^{-2}$

electrical engineering practice, their relationships to other SI units (their derivation) and their descriptions in terms of the base units. A more complete listing of derived units can be found in the BIPM document, the *SI Brochure* (BIPM, 2019).

4. Definitions, Realisations and Uncertainty

The previous section used the word "define" in the description of the units. Creating a unit of measurement, for example an Ampere, involves three (3) things:

1. A Definition of the unit;
2. A Realisation of the unit; and
3. A determination of the Uncertainty associated with the realisation of the unit.

The **Definition** of a unit is a written description of what the unit is in terms of scientific principles and physical constants. The Ampere, for example, prior to May 2019, was defined as:

"The constant current which, if maintained in two straight parallel conductors of infinite length, of negligible circular cross-section, and placed one metre apart in vacuum, would produce between those conductors a force equal to 2×10^{-7} Newtons per metre of length." (BIPM, 2006)

All seven base units have such definitions. According to the BIPM (2006), the definition provides "a sound theoretical basis upon which the most accurate and reproducible measurements can be made."

The **Realisation** of a unit is the actual scientific method that will be used to create it while satisfying the requirements of the Definition. Physical sciences and a significant amount of engineering are required to develop a particular realisation. The BIPM publishes its recommended method to create the various units in *mises en pratique*. In addition, there generally is more than one way to realise a particular definition or the Primary Standards Laboratories will each carry out experiments according to the *mises en pratique* or of their own derivation. This creates several 'values' for each unit and this is where the third parameter, the **Uncertainty**, plays an important role.

The **Uncertainty** of the particular realisation is a carefully determined expression of the accuracy (closeness to the definition) and precision (repeatability) of the method used. A scientific result should always be presented together with its uncertainty. For example, according to CODATA (2014), the agreed value of Planck's constant was

$$h = 6.626\,0693(11) \times 10^{-34} \text{ Js } [1.7 \times 10^{-7}]$$

The uncertainty of this value of h , depends on the last two significant figures shown in parentheses and is given by number in square brackets. That is 0.17 parts per million.

The determination of measurement uncertainty is a complex process and generally requires large quantities of historical data to enable the essential statistical

analyses to be done. For measurements, the BIPM document - *Guide to the expression of uncertainty in measurement* (BIPM, 2008) is the internationally accepted standard for determining and describing measurement uncertainty.

Therefore, a realisation that can produce a unit with an uncertainty of 1 part per billion (10^{-9}), would be better than one with an uncertainty of 1 part per million (10^{-6}). The current state of the art in realising some of derived units that is able to achieve a lower degree of uncertainty than the base units from which they emanate (Mills et al., 2006). The Farad, for example, can be realised using a Thompson-Lampard Calculable Capacitor with lower uncertainty that can be achieved in the realisation of the Ampere. This will be described in Section 6 of this paper.

5. The Rationale for Changes to the SI system

The main problems that lead to the revision of the SI system can be identified by a careful examination of the definition of one of the base units as a typical illustrative example, the Ampere, repeated here for convenience:

"The constant current which, if maintained in two straight parallel conductors of infinite length, of negligible circular cross-section, and placed one metre apart in vacuum, would produce between those conductors a force equal to 2×10^{-7} Newtons per metre of length." (BIPM, 2006)

This definition can be translated into an equation according to electromagnetic theory. The force per unit length developed between two parallel current carrying conductors spaced d metres apart, carrying steady currents of I_1 and I_2 , respectively, is given by:

$$\frac{F}{l} = \frac{\mu_0 I_1 I_2}{2\pi d} \quad (5)$$

If both currents are exactly equal to 1 Ampere and the separation distance d , is exactly 1 m, then the force per unit length is exactly 2×10^{-7} N/m.

The definition requires a number of conditions to be inherently satisfied, namely, that:

- i) The wires must be infinitely long;
- ii) Their diameters must be negligibly small compared to d ;
- iii) The currents must be exactly 1 Ampere, identical and constant;
- iv) The experiment has to take place in a vacuum;
- v) That the separation distance, d , is exactly 1m;
- vi) The constant μ_0 in Equation (5) is exactly $4\pi \times 10^{-7}$ N/m; and
- vii) There are instruments available to measure the distances, current and force to the required levels of accuracy and uncertainty.

In practice, conditions (i) and (ii) can be engineered to be very close to these requirements by making the length and separation distance considerably greater than the wire diameter, using for example, coils of very fine

wire. Conditions (iii) and (v) depend on the instrumentation (i.e., Condition (vii)). Condition (iv) can be obtained but at great expense. Condition (v) requires precise measurement of the distance, which in turn depends on specialised instrumentation to achieve this. Condition (vi) is addressed by defining μ_0 to be *exactly* $4\pi \times 10^{-7}$ N/m. In this way knowledge of π to some number of significant digits is avoided. Condition (vii) includes reference to the part of the definition which requires a force measurement, and therefore a relationship to the SI unit *kilogram*. This leads to the first problem with the last SI system.

Problem #1: The kilogram was the only SI base unit which depended on a physical artefact. The actual SI value of the kilogram has been the value of the international prototype kilogram (IPK), a cylinder made of a 90%/10% platinum iridium alloy kept in a vault at the BIPM in France. Its value has changed minutely over time due to handling and micro-deposits of contaminants on the surface of the metal so that it isn't really a standard in the true sense of the word.

The realisation of the Ampere is typical of the realisation of all SI units. The engineering and scientific complexity required to realise any of them is daunting and presents several problems which have to be overcome. In the case of the Ampere, the *quantity* of current is not dependent on any other quantity, however the *unit* of current, that is the realisation of the Ampere, depends on the Kilogram and as we will see, the Volt, the Watt and the Ohm (Chyla, 2012).

There are two (2) accepted ways to realise the Ampere (Mills et al., 2006). The first method uses an apparatus called a Kibble Balance to compare an electrical watt with a mechanical watt. The second method uses realisations of the Volt (V) and Ohm (Ω) and the relationship of Ohms Law, $V = IR$, to calculate a value of the Ampere.

At present, the best realisations of the Ampere use the second method and achieve a better uncertainty than the Kibble Balance method. This is the second problem with the SI system.

Problem #2: The current state of the art in realising some of derived units achieves a better uncertainty than the base units from which they emanate. For example, despite the fact that the Ampere is an SI base unit it is possible to realise other derived units, namely the Volt and the Ampere, with better uncertainties. These realisations are described in the next section.

6. Realisations of the Electrical Units pre-May 2019

6.1 The Volt

Figure 2 shows the Josephson's Junction Schematic. When certain materials are cooled below a very low temperature called the transition temperature, electrons are able to travel throughout the material without resistance, a behaviour called superconductivity. A

particular superconductor can accommodate a maximum flow of electrons, called the critical current, before the flow begins to exhibit resistance. Brian Josephson discovered that when a junction, comprising two (2) thin layers of superconductor material separated by a very thin layer of insulator, was cooled below the transition temperature of the superconductor, a current flowed across the insulator (Wikipedia, 2019).

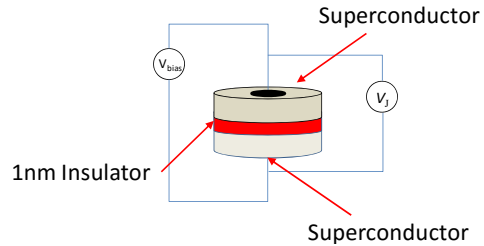


Figure 2. Josephson's Junction Schematic

If the junction was deliberately biased with a dc voltage V_{bias} , as shown in Figure 2, such that a supercurrent greater than the critical current flows across the junction, a very high frequency signal appeared across the junction. This is known as the Josephson's effect (Warburton, 2011), and the frequency of the signal is developed, as given by:

$$f_j = \frac{1}{2\pi} \left(\frac{2e}{h} \right) V \quad (6)$$

In Equation (6), h is Planck's Constant and e is the fundamental charge on an electron. The ratio $2e/h$ is known as the Josephson Constant K_J . Until the redefinition of the SI in 2019, the value, agreed to in 1990 and denoted as K_{J-90} , was $483\,597.9 \text{ GHzV}^{-1}$.

More interesting from an electrical engineering point of view though is that if the junction is irradiated with a magnetic field at harmonic multiples of f_j , then the voltage across the junction develops in precise, highly stable and predictable integer multiples of K_J and is given by:

$$V_J = n \left(\frac{2\pi f_j}{K_J} \right) \quad (7)$$

The voltage V_J , is called the Quantized Josephson's Voltage, n is an integer, f_j is the frequency of the magnetic field radiation. A single junction develops a very small voltage, on the order of a few mV , so that in order to make a practical voltage source, several hundred junctions contained in a cryogenic chamber together with complex instrumentation are required.

6.2 The Ohm

The Lorentz force, $d\mathbf{F}$, exerted on an element of charge, dQ , moving through a magnetic field, \mathbf{B} , with drift velocity \mathbf{v} , is given by:

$$d\mathbf{F} = dQ\mathbf{v} \times \mathbf{B} \quad (8)$$

If a slab of current carrying semiconductor material, is exposed to a magnetic field, the force described by Equation (8), results in displacement of electrons in a direction perpendicular to both the magnetic field and the direction of motion of the charges, indicated by the cross product. This displacement produces a voltage across the semiconductor and is known as the Hall effect.

If the semiconductor is cooled below its critical temperature and the magnetic field is on the order of 10T, the resistance across the current carrying channel in the direction of the developed Hall effect voltage, assumes very stable, discrete values according to the following Equation (9):

$$R_H = n \left(\frac{V_H}{I_{channel}} \right) = n \left(\frac{h}{e^2} \right) \quad (9)$$

This is known as the Quantum Hall effect and leads to the realisation of a very accurate unit of resistance (Taylor and Witt, 1989). The ratio (h/e^2) in Equation (9) is known as the Von Klitzing Constant, R_K . The current agreed value of the Von Klitzing Constant, denoted as R_{K-90} is 25 812.807 Ohm.

Like the Josephson voltage standard, the apparatus to produce this effect in measurable levels is very complex. Besides, like the Josephson voltage standard, the Quantum Hall devices can be used to independently determine accurate values of h and e . These can then be cross compared with those obtained by other methods after which an agreed value of h and e is published (Stock, 2012).

6.3 The Amp

The Ampere can be realised indirectly by a device called a Kibble Balance (or Watt balance in older usage). The device relates electrical power to mechanical power in order to determine Planck's constant, h , in terms of a mass traceable to the international prototype kilogram. From this determination and a primary realisation of the Ohm for example, a very accurate value of the Ampere can be calculated.

A diagram indicating the principles of the Kibble Balance is shown in Figure 3. In essence, the Kibble balance, after Bryan Kibble (Robinson and Schlamminger, 2016) is a mechanical balance with a current carrying coil suspended in a strong magnetic field on one arm and a conventional mass pan on the other.

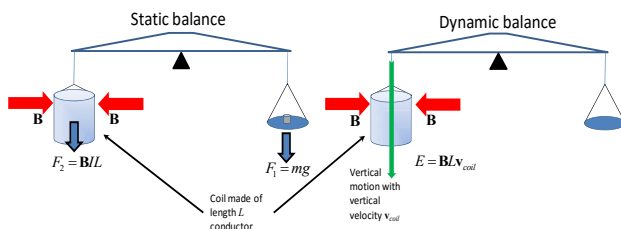


Figure 3. Kibble Balance schematic

The balancing of the arm occurs in two parts: (i) a static balance; and (ii) a dynamic balance. The final relationships do not require the knowledge of the field strength or the length of the coil.

For the static balance, a current is passed through the coil. A Lorentz force is developed on the coil which is carefully counterbalanced by known masses on the other pan. Previously, it was stated that the Lorentz force, $d\mathbf{F}$, exerted on an element of charge, dQ , moving through a magnetic field, \mathbf{B} , with drift velocity \mathbf{v} , is given by Equation (8). Therefore, the total static force \mathbf{F} , on the current carrying coil due to the movement of the charges in it is found by integrating (8) over the length of the coil.

$$\mathbf{F} = \oint dQ\mathbf{v} \times \mathbf{B} \quad (10)$$

Since it can be shown for a current carrying conductor that (Hayt and Buck 2006):

$$dQ\mathbf{v} = Id\mathbf{L} \quad (11)$$

then, substituting into (15)

$$\mathbf{F} = \oint Id\mathbf{L} \times \mathbf{B} \quad (12)$$

For the long conductor in the coil arrangement, it can be shown that (12) reduces to:

$$\mathbf{F} = I\mathbf{L} \times \mathbf{B} \quad (13a)$$

$$\text{and } |\mathbf{F}| = BIL\sin\theta \quad (13b)$$

In Equation (13b), θ refers to the angle between the field and the coil. At static balance and with $\theta = 90^\circ$,

$$mg = \mathbf{B}IL \quad (15)$$

For the dynamic measurement, the coil is made to move through the magnetic field with a constant velocity, \mathbf{v}_{coil} . Because of this, a voltage E , is induced in the coil given by:

$$E = L\mathbf{B}\mathbf{v}_{coil} \quad (16)$$

Since the coil is the same for both experiments, $\mathbf{B}L$ can be eliminated from Equations (15) and (12).

$$L\mathbf{B} = \frac{mg}{I} \quad (17)$$

The final equation for I is then:

$$I = \left(\frac{mg}{E} \right) \mathbf{v}_{coil} \quad (18)$$

The value of E is measured with by a very accurately calibrated voltmeter traceable to a Josephson junction voltage standard. The mass m , is traceable to the international prototype kilogram, g is measured by accurate gravimetry experiments, for example by the National Research Council (Liard et al., 2014), and \mathbf{v}_{coil} by laser interferometers. The Kibble Balance measurements are very complicated and have to include corrections for gravitational variations due to tidal, earth motion and atmospheric effects. They typically run over several weeks (Liard et al., 2014).

Interestingly, the Kibble balance can also be used to realise a mass standard in terms of Planck's constant as follows (Robinson and Schlamminger 2016). In Equation

(17), the current I can be measured by passing it through a known resistance R , and measuring the voltage drop E_1 across it. Thus, Equation (17) can be re-arranged as follows:

$$m = \left(\frac{IE}{gV_{coil}} \right) = \left(\frac{\left(\frac{E_1}{R} \right) E}{gV_{coil}} \right) \quad (19)$$

Both E and E_1 are measured by calibrated voltmeters traceable to the same Josephson junction voltage standard voltage, while R is calibrated to a reference traceable to a Quantum Hall device resistance standard. The mass to Planck's constant relationship is then derived as follows. Since E and E_1 are both traceable to Equation (7) and R is traceable to Equation (9), the factor $(E_1/R) E$ in Equation (18) turns out to be traceable only to integer multiples of h as shown below.

$$\left(\frac{E_1}{R} \right) E = \left(\frac{n_1 h}{e} \right) \left(\frac{n_2 e^2}{h} \right) \left(\frac{n_3 h}{e} \right) = nh \quad (20)$$

where $n = n_1 n_2 n_3$ is an integer.

Therefore, from Equation (18), m in kilograms, will be calculated in terms of Planck's Constant, h , which has an agreed value, the metre and the second, which are both SI base units. Note that the value of h , can itself be independently determined from the realisations of the Volt and the Ohm as described before.

The realisations of the Volt, Ohm and Ampere, at this point in time ultimately depend on having accurate values of h and/or e . This inter-relationship is depicted in Figure 4. The bi-directional arrows indicate that h and/or e can either be used in the realisations of the units, or can themselves be determined from the accepted current values of the units. Whichever of the three (3) units is realisable with the lowest uncertainty can be used to calculate the other two. Also to be noted is the presence of the *Kilogram* in Figure 4.

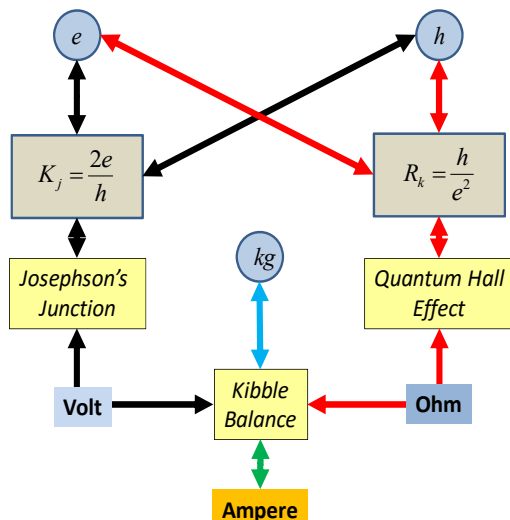


Figure 4. Present Volt-Ohm-Ampere Inter-relationships

6.4 The Farad

Interestingly, the SI electrical unit which offers the lowest realised uncertainty at this time, is the Farad (Mills et al., 2006). This uncertainty is achieved through a device called the Calculable (Thompson-Lampard) Capacitor (Clothier, 1965) and is based on a theorem in electrostatics proposed by Lampard (1957). The theorem proved that it was possible to create a capacitor whose value was directly proportional to the length of the electrodes. In the specific case of a cylindrical capacitor, the theorem states that the capacitance per unit length, C , was given by:

$$C = \frac{\log_e 2}{4\pi^2} \text{ Farads/metre} \quad (21)$$

Equation (20) means that if the electrode length can be accurately measured using equipment traceable to the SI unit of length, then the calculated value of C , will be known to the same degree of uncertainty as the metre, 1×10^{-8}

This low uncertainty has led to the calculable capacitor being used as the most accurate method to realise the Ohm using a technique proposed by Thomson (Thompson, 1968). As discussed before, whichever of the three (3) electrical units is realisable with the lowest uncertainty will be used to calculate the other two (BIPM, 2019).

7. The New Definitions

The solution declared by the BIPM to the problems identified in Section 5 of this paper and other historical issues, is to redefine the SI definitions in terms of declared fixed values of some universal constants (BIPM, 2019). The most significant consequence of the new definitions is to remove any future dependence on the physical kilogram artefact.

The following constants are now exactly defined to the respective stated values. These are:

1. the ground state hyperfine splitting frequency of the caesium 133 atom $\Delta\nu(^{133}\text{Cs})_{\text{hfs}}$ is exactly 9 192 631 770 Hertz (unchanged),
2. the speed of light in vacuum, c , is exactly 299 792 458 metre per second (unchanged),
3. the Planck constant, h , is exactly $6.626\ 060\ 701\ 5 \times 10^{-34}$ Joule second (new),
4. the elementary charge, e , is exactly $1.602\ 176\ 634 \times 10^{-19}$ Coulomb (new),
5. the Boltzmann constant, k_B , is exactly $1.380\ 649 \times 10^{-23}$ Joule per Kelvin (new),
6. the Avogadro constant, N_A , is exactly $6.022\ 140\ 76 \times 10^{23}$ reciprocal mole (new), and
7. the luminous efficacy, K_{cd} , of monochromatic radiation of frequency 540×10^{12} Hz is exactly 683 Lumen per Watt (unchanged).

Note that these values are exact and therefore have no uncertainty. The seven (7) SI base units remain the same, but because of the above definitions, it will be possible

to realise all of them without having to resort to using the physical kilogram. Hence, of specific interest to the electrical engineering profession are the declaration of the elementary charge and Planck's constant as constants. These will now have the effect of defining a fixed value for the Volt, Ohm and in particular, the Ampere as described next.

7.1 The Volt 2019

The Volt, V, will once again be realised using the Josephson effect and the new fixed value of the Josephson constant: $K_J = 483\,587.848\,416\,984\text{ GHzV}^{-1}$, calculated to 15 significant digits according to Equation (1) in the *Mise en pratique* for the definition of the Ampere and other electric units in the SI (BIPM, 2019, Appendix 2). This level of accuracy has been achieved following many years of deriving the values of e and h , for example at NIST (Haddad et al., 2017) and the NRC (Wood, 2017). The 'new' Volt is smaller than the K_{J-90} version by 108.665×10^{-9} (BIPM, 2019, Appendix 2) because of the difference between K_J and K_{J-90} .

7.2 The Ohm 2019

Similar to the Volt, the ohm Ω will be realised using a Quantum Hall device and the following value of the von Klitzing constant $R_K = 25\,812.807\,459\,3045\ \Omega$. Like the value of K_J , this value has been calculated to 15 significant digits according to Equation (2) in the *Mise en pratique* for the definition of the Ampere and other electric units in the SI (BIPM, 2019, Appendix 2). The 'new' Ohm is smaller than the R_{K-90} version by 17.793×10^{-9} (BIPM, 2019, Appendix 2).

7.3 The Ampere 2019

According to BIPM (2019), the new definition of the Ampere is, “*The ampere, symbol A, is the SI unit of electric current. It is defined by taking the fixed numerical value of the elementary charge, e, to be $1.602\,176\,634 \times 10^{-19}$ when expressed in the unit C, which is equal to As, where the second is defined in terms of $\Delta\nu_{Cs}$.*”

This definition will be realised in one of three (3) methods, as follows:

- 1) Via Ohm's Law and the realisations of the 'new' Volt and Ohm;
- 2) Using the relationship $A = C/s$, the fixed value of e and the SI base unit of time, the second; or
- 3) Using the relationships $I = C \cdot dV/dt$, $A = F \cdot V/s$, the 'new' Volt, the Farad and the SI base unit of time, the second.

A consequence of this definition is that primary standards labs, for example, NIST (Robinson and Schlamminger, 2016), can now use the Kibble Balance to create a practical realisation of the kilogram.

8. Implications of the Changes for Electrical Engineering

The BIPM clearly indicated that the new SI definitions “*will be so chosen that at the moment of change the magnitudes of the new units will be indistinguishable from those of the old units.*” (CGPM, 2018)

There should be no discernable impact to normal electrical engineering calculations after the redefinitions are implemented, but there will be change. For example, as discussed in the previous section, the new SI definitions make it possible to have values for the Ampere, Volt and Ohm, calculated to 15 significant figures because of these units' relationships to e and h , which are now exactly defined and fixed. Of significance is that for the first time since it was originally defined, the Ampere is not dependent on the kilogram (BIPM 2019).

From an Electrical Engineering viewpoint, the constants μ_0 , the permeability of free space and ϵ_0 , the permittivity of free space, will change from their current, fixed values to new experimentally determined ones. Because e , h and c will be fixed, the following equations will be used to derive μ_0 and ϵ_0 , respectively:

$$\mu_0 = \frac{2h\alpha}{ce^2} \text{ NA}^{-2} \quad (22)$$

and

$$\epsilon_0 = \frac{1}{\mu_0 c^2} \text{ Fm}^{-1} \quad (23)$$

In Equation (21), the symbol α refers to the fine structure constant, which is a quantum level, dimensionless number, derived from the electromagnetic interaction between elementary charged particles such as the electron and the proton. According to CODATA 2014 values, α has the experimentally determined value of $7.297352566417 \times 10^{-3}$.

Using the proposed values of e , h and c , μ_0 can be calculated using Equation (21). The existing value of μ_0 is $1.2566370614 \times 10^{-6} \text{ NA}^{-2}$ (CODATA 2014). This value differs from the new calculated value of $1.256637062 \times 10^{-6} \text{ NA}^{-2}$ by $|1.809 \times 10^{-9}| \text{ NA}^{-2}$. This supports the BIPM guiding principle that there should not be any drastic change in the defined values of the universal constants. We have shown that the calculated value of μ_0 is not going to be significantly different from the current value as to have a noticeable effect in electrical engineering calculations.

One electrical engineering sector which could certainly feel the most impact is the calibration industry - the manufacturers of standards and calibrators of electrical and electronic equipment. For example, Fluke, a manufacturer of high end calibrators, had to make drastic adjustments to the performance specification of one of their devices, with respect to the newly redefined Volt and Ohm.

According to Gust (2011), the effect of the 1990 volt change was approximately 100% of the one year specification for DC voltage. While the BIPM have gone to great lengths to avoid as drastic a change in going to

the 2019 SI revision, there is going to be an impact at the cutting edge of electrical metrology and other areas.

9. The Kilogram 2019

Perhaps the most dramatic and significant change with the new version of the SI is the removal of the artefact kilogram as the standard of mass. This standard mass, in its various forms, has existed since 1889 and remained the only unit still based on a physical object. According to (BIPM, 2019), the 'new' kilogram is defined as follows:

“The kilogram, symbol kg, is the SI unit of mass. It is defined by taking the fixed numerical value of the Planck constant h to be $6.626\ 060\ 701\ 5 \times 10^{-34}$ when expressed in the unit $J\ s$, which is equal to $kg\ m^2\ s^{-1}$, where the metre and the second are defined in terms of c and $\Delta\nu_{Cs}$.”

The most likely practical realisation of this definition will be via the Kibble Balance and the declared values for e and h and the relationship developed in Equation (18). In fact, in 2012 the BIPM published a possible method for doing exactly this and described in a paper by Stock (2012). Another possibility is through Avogadro's Constant, also declared as fixed in the new SI (Stenger and Göbel, 2012) and (Bartl et al. 2017). The possible techniques which have the required level of uncertainty and repeatability to realise the kilogram are described by the *Mise en pratique* for the definition of the kilogram in the SI, in Appendix 2 of the 9th edition of the SI brochure (BIPM, 2019), but the front runner remains the Kibble Balance realisation.

Figure 5 depicts the New Volt-Ohm-Ampere inter-relationships. There are two major changes from the previous relationship (as illustrated in Figure 4). The first

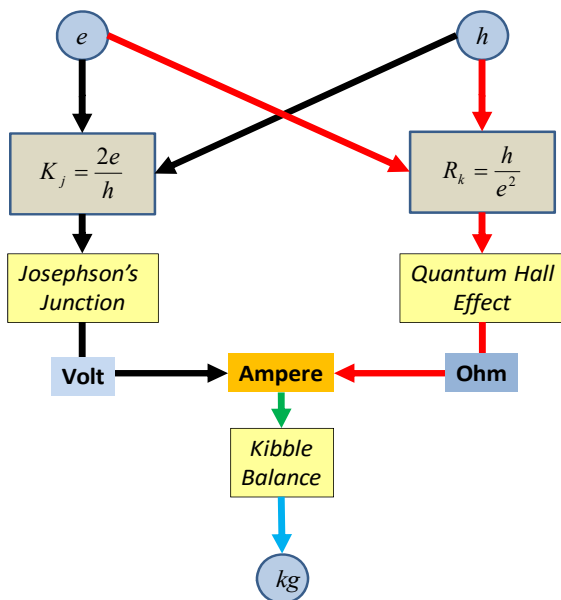


Figure 5. New Volt-Ohm-Ampere Inter-relationships

is the one-way arrows following from the now constant declared values for e and h , straight through to the Ampere. The second is that the kilogram is now defined (the most likely at this time) from the electrical units Volt, Ohm and Ampere via the Kibble balance.

According to the note 5, Appendix 2 of the SI Brochure - 9th edition (BIPM, 2019), the value of the new kilogram will be the currently agreed reference value in order to preserve the international equivalence of calibration certificates.

10. Conclusion

The new SI definitions, which came into effect on May 20th 2019, have the electrical base unit Ampere and the derived units Volt and Ohm, now fixed by declared universal constants and therefore inherently stable. The electrical units themselves have now assumed new importance in that they will be used in at least one method to derive the first non artefact kilogram in 130 years. The BIPM took a deliberate decision to minimise the effects of the redefinitions and for the most part they will succeed. There may be an impact on high end calibration equipment manufacturers.

This paper gave an overview of the previous and new SI system from the perspective of electrical engineering units and in so doing described how units are created, how traceability works, international electrical metrology, measurement uncertainty and the level of scientific and engineering effort required to maintain a system for the units of measurement.

References:

Bartl, G., Becker, P., Beckhoff, B., Bettin, H., Beyer, E., Borys, M., Busch, I., Cibik, L., D’Agostino, G., Darlatt, E., Di Luzio, M., Fujii, K., Fujimoto, H., Fujita, K., Kolbe, M., Krumrey, M., Kuramoto, N., Massa, E., Mecke, M., Mizushima, S., Müller, M., Narukawa, T., Nicolaus, A., Pramann, A., Rauch, D., Rienitz, O., Sasso, C.P., Stopic, A., Stosch, R., Waseda, A., Wundrack, S., Zhang, L., and Zhang, X.W. (2017), “A new 28 Si single crystal: counting the atoms for the new kilogram definition”, *Metrologia*, Vol.54, No.5, pp.693.

BIPM (2006), *SI Brochure: The International System of Units (SI)*, 8th edition, Bureau international des poids et mesures (The International Bureau of Weights and Measures), France (accessed December 2018).

BIPM (2008), *Guide to the Expression of Uncertainty in Measurement*, Bureau international des poids et mesures, France.

BIPM (2019), *SI Brochure: The International System of Units (SI)* 9th edition, Bureau international des poids et mesures, France (accessed 30 June 2019).

CGPM (2018), *The 26th General Conference on Weights and Measures*, Palais des Congrès, Versailles, France, November 13-16 2018.

Christof, G., Bernd, F., Norbert, H., Axel, K., Bettina, T-K., Thorsten, Z., Joachim, F., Otto, J., and Wladimir, S. (2017), “Final determination of the Boltzmann constant by dielectric-constant gas thermometry”, *Metrologia*, Vol. 54, No.3, pp.280.

Chyla, W.T. (2012), “On the structure of the new SI definitions of base units”, *Metrologia*, Vol.49, No.4, pp.L17-L19.

Clothier, W.K. (1965), “A calculable standard of capacitance”, *Metrologia*, Vol.1, No.2, pp.36-55.

- CODATA (2014), *Recommended Values of the Fundamental Physical Constants*, Committee on Data of the International Council for Science, International Council for Science (ICSU), Paris, France.
- Gust, J. (2011), "The impact of the new SI on industry", In: NCSL (2011)(ed), *NCSL International Workshop and Symposium*, National Conference of Standards Laboratories.
- Haddad, D., Seifert, F., Chao, L.S., Possolo, A., Newell, D.B., Pratt, J.R., Williams, C.J., and Schlamminger, S. (2017), "Measurement of the Planck constant at the National Institute of Standards and Technology from 2015 to 2017", *Metrologia*, Vol.54, No.5, pp.633.
- Hayt, W.H., and Buck, J.A (2006), *Engineering Electromagnetics*. 7th edition, McGraw-Hill
- Hotz, R.L. (1999), "Mars probe lost due to simple math error", *Los Angeles Times*, October 1, Retrieved from <http://articles.latimes.com/1999/oct/01/news/mn-17288>
- Lampard, D.G. (1957), *A New Theorem in Electrostatics with Applications to Calculable Standards of Capacitance*, IEEE Monograph.
- Liard, J.O., Sanchez, C.A., Wood, B.M., Inglis, A.D. and Silliker, R.J. (2014), "Gravimetry for watt balance measurements", *Metrologia*, Vol.51, No.2, pp.S32-S41.
- Mills, I.M., Mohr, P.J., Quinn, T.J., Taylor, B.N., and Williams, E.R. (2006), "Redefinition of the kilogram, ampere, kelvin and mole: a proposed approach to implementing CIPM recommendation 1 (CI-2005)", *Metrologia*, Vol.43, No.3, pp.227-246.
- Robinson, I.A., and Schlamminger, S. (2016), "The watt or Kibble balance: a technique for implementing the new SI definition of the unit of mass", *Metrologia*, Vol.53, No.5, pp.A46-A74.
- Stenger, J., and Göbel, E.O. (2012), "The silicon route to a primary realisation of the new kilogram", *Metrologia*, Vol.49, No.6, pp.L25-L27.
- Stock, M. (2012), "Watt balance experiments for the determination of the Planck constant and the redefinition of the kilogram", *Metrologia*, Vol.50, No.1, pp.R1-R16.
- Taylor, B.N., and Witt, T.J. (1989), "New International Electrical Reference Standards based on the Josephson and Quantum Hall Effects", *Metrologia*, Vol.26, No.1, pp.47-62.
- Warburton, P.A. (2011), "The Josephson Effect: 50 years of science and technology", *Physics Education*, Vol.46, No.6, pp.669-675.
- Wikipedia (2019), *Josephson Effect*, October 1, Retrieved from https://en.wikipedia.org/wiki/Josephson_effect
- Witkin, R. (1983), "Jet's fuel ran out after metric conversion errors", *New York Times*, July, <https://www.nytimes.com/1983/07/30/us/jet-s-fuel-ran-out-after-metric-conversion-errors.html>.

Authors' Biographical Notes:

Fasil Muddeen is a Lecturer in the Department of Electrical and Computer Engineering at The University of the West Indies. His areas of research include the acoustics of the steelpan, digital signal processing, electronics, measurement and instrumentation. Dr. Muddeen is a registered engineer with the Board of Engineering of Trinidad and Tobago, a Fellow of the Association of Professional Engineers of Trinidad and Tobago, a Member of the IEEE and a former Chairman of the IEEE Trinidad and Tobago Section.

■

Subscription Order Form

Please enter my **Annual subscription** to the forthcoming Volume (2 Issues).

- US\$15.00 or equivalent in Trinidad and Tobago Dollars (Local subscription)
- US\$25.00 (By airmail)
- Payment enclosed. Amount equivalent TT\$/US\$ (Cheque, Bank draft)
- Send pro-forma invoice for despatch

Please make cheque payable to The West Indian Journal of Engineering.

Name: _____

Profession: _____

Areas of Specialisation: _____

Address: _____

Telephone: _____ Fax: _____ E-mail: _____

(Cut along this line)

Change of Address

Please note that my new postal address is:- _____

instead of:- _____

(Cut along this line)

Send orders and/or change of address forms to: **The Editorial Office**, The West Indian Journal of Engineering, Block #1, Faculty of Engineering, The University of the West Indies, St. Augustine, Trinidad and Tobago, West Indies.

Orders must be accompanied by payment which should be in Trinidad and Tobago (TT) Dollars or its equivalent at the time of order in US Dollars. Despatch of issues will commence only after receipt of payment.

For further information, contact:

Professor Kit Fai Pun, The Editor-in-Chief,
The Editorial Office, West Indian Journal of Engineering, c/o Faculty of Engineering,
The University of the West Indies, St Augustine, Trinidad and Tobago, W.I.
Tel: (868) 662-2002 Exts-83459/82069 • Fax: (868) 662-4414
E-mails: uwije@sta.uwi.edu; KitFai.Pun@sta.uwi.edu

Notes and Guidance to Authors

The West Indian Journal of Engineering, WIJE (ISSN 0511-5728)

Copyright:

Articles submitted to The West Indian Journal of Engineering, WIJE (ISSN 0511-5728) should be original contributions and should not be under consideration for any other publication at the same time. Authors submitting articles for publication warrant that the work is not an infringement of any existing **copyright** and will indemnify the publisher against any breach of such warranty. For ease of dissemination and to ensure proper policing of use, papers and contributions become the legal copyright of the publisher unless otherwise agreed. Submissions should be sent to:

The Editor-in-Chief:

Professor Kit Fai Pun, c/o WIJE, Faculty of Engineering, The University of the West Indies, St Augustine, Trinidad and Tobago, West Indies. Tel: 1-868-662-2002 exts-82069/83459; Fax: 1-868-662-4414; E-mails: KitFai.Pun@sta.uwi.edu; uwije@sta.uwi.edu

Editorial Aim and Policy:

The WIJE is an international journal which has a focus on the Caribbean region. Since its inception in 1967, it is published twice yearly by the Faculty of Engineering at The University of the West Indies and the Council of Caribbean Engineering Organisations in Trinidad and Tobago.

WIJE aims at contributing to the development of viable engineering skills, techniques, management practices and strategies relating to improving the performance of enterprises, community, and the quality of life of human beings at large.

Apart from its international focus, WIJE also addresses itself specifically to the Caribbean development by identifying and supporting emerging research areas and promoting various engineering disciplines and their applications in the region.

WIJE welcomes the submission of papers in various engineering disciplines and related areas. Emphasis is placed on the publication of articles which seek to link theory with application or critically analyse real situations with the objective of identifying good practice cross different engineering and related disciplines.

Articles may be of a theoretical nature, be based on practical experience, report a case study situation or report experimental results. The prime requirement for acceptance of an article will not be its form but rather that it:

- (1) makes a significant original contribution to the field of engineering and the advancement of engineering practices;
- (2) is directly relevant to engineering, engineering management and technology, and related areas;
- (3) contains elements which have general application;
- (4) is within the scope of the journal; and
- (5) has generally not been published previously except in very limited circulation.

The reviewing process:

Each paper is to be reviewed by the Editor-in-Chief and, if it is judged suitable for this publication, it is then sent to two referees for double-blind peer-review. Based on their recommendations, the Editor-in-Chief then decides whether the paper should be accepted as is, revised or rejected.

Manuscript requirements:

Full manuscript should be submitted in double line spacing with wide margins. The names of author(s) and their details-- brief **autobiographical note**, affiliation, e-mail address and full international contact details must appear on a sheet separate from the article. The author(s) should not be identified anywhere else in the article. To facilitate the reviewing processes, submissions via e-mail are advisable.

As a guide, technical/research papers should be between 3,000 and 6,000 words in **length**. Shorter articles (Communications, Discussions, Book Reviews, etc.) should be between 500 and 2,000 words. Please provide the word count on the first page of your paper. A **title** of not more than eight words should be provided.

Authors must supply a **structured abstract**. Maximum is 250 words in total. In addition provide up to six **keywords** which encapsulate the principal topics of the paper and categorise your paper. **Headings** must be short, clearly defined and not numbered. **Notes or Endnotes** should be used only if absolutely necessary and must be identified in the text by

consecutive numbers, enclosed in square brackets and listed at the end of the article.

All **Figures** (charts, diagrams and line drawings) and **Plates** (photographic images) should be submitted in both electronic form and hard-copy originals. Figures should be of clear quality, in black and white and numbered consecutively with Arabic numerals.

Figures created in MS Word, MS PowerPoint, MS Excel, Illustrator and Freehand should be saved in their native formats.

Electronic figures created in other applications should be copied from the origination software and pasted into a blank MS Word document or saved and imported into an MS Word document by choosing "Insert" from the menu bar, "Picture" from the drop-down menu and selecting "From File..." to select the graphic to be imported.

For figures which cannot be supplied in MS Word, acceptable standard image formats are: pdf, ai, wmf and eps. If you are unable to supply graphics in these formats then please ensure they are tif, jpeg, or bmp at a resolution of at least 300dpi and at least 10cm wide.

To prepare screen shots, simultaneously press the "Alt" and "Print screen" keys on the keyboard, open a blank Microsoft Word document and simultaneously press "Ctrl" and "V" to paste the image. (Capture all the contents/windows on the computer screen to paste into MS Word, by simultaneously pressing "Ctrl" and "Print screen".)

For photographic images (plates) good quality original photographs should be submitted. If supplied electronically they should be saved as tif or jpeg files at a resolution of at least 300dpi and at least 10cm wide. Digital camera settings should be set at the highest resolution/quality possible.

In the text of the paper the preferred position of all tables, figures and plates should be indicated by typing on a separate line the words "Take in Figure (No.);" or "Take in Plate (No.)". Tables should be typed and included as part of the manuscript. They should not be submitted as graphic elements. Supply succinct and clear captions for all tables, figures and plates. Ensure that tables and figures are complete with necessary superscripts shown, both next to the relevant items and with the corresponding explanations or levels of significance shown as footnotes in the tables and figures.

References to other publications must be in Harvard style and carefully checked for completeness, accuracy and consistency. This is very important in an electronic environment because it enables your readers to exploit the Reference Linking facility on the database and link back to the works you have cited through CrossRef. You should include **all** author names and initials and give any journal title in full.

You should cite publications in the text: (Adams, 2008) using the first named author's name or (Adams and Brown, 2008) citing both names of two, or (Adams et al., 2008), when there are three or more authors. At the end of the paper, a reference list in alphabetical order should be supplied:

- For **books**: Surname, initials, (year), title of book, publisher, place of publication, e.g., Walesh, S. G. (2012), *Engineering Your Future: The Professional Practice of Engineering*, 3rd Edition, ASCE Press/John Wiley & Sons, New Jersey, NJ.
- For **book chapters**: Surname, initials, (year), "chapter title", editor's surname, initials, title of book, publisher, place of publication, pages, e.g., Liebowitz, J. (2005), "Conceptualising and implementing knowledge management", in Love, P. E. D., Fong, P. S. W. and Irani, Z., (ed.), *Management of Knowledge in Project Environments*, Elsevier, New York, NY, pp. 1-18
- For **journals**: Surname, initials, (year), "title of article", journal name, volume, number, pages, e.g. Tsang, A. H. C. (2012), "A review on trend tests for failure data analysis", *West Indian Journal of Engineering*, Vol. 35, No.1, July, pp.4-9.
- For **electronic sources**: Surname, initials, or institution, (year), name of website, website address, date updated (if any) or date visited, e.g., EFQM (2012), *European Foundation for Quality Management*, available at: <http://www.EFQM.org/> (Dated: 1 January 2012)

Final submission of the article:

Once accepted for publication, the Editor may request the final version as an attached file to an e-mail or to be supplied on a diskette or a CD-ROM labelled with author name(s); title of article; journal title; file name.

The manuscript will be considered to be the definitive version of the article. The author must ensure that it is complete, grammatically correct and without spelling or typographical errors.

The preferred file format is Word. Another acceptable format for technical/mathematics content is Rich text format.